The Pennsylvania State University

The Graduate School

Department of Biochemistry and Molecular Biology

MECHANISMS OF THE SAGA COACTIVATOR COMPLEX IN REGULATION OF GENE TRANSCRIPTION

A Thesis in

Biochemistry and Molecular Biology

by

Decha Sermwittayawong

Submitted in Partial Fulfillment
of the Requirements
for the Degree of

Doctor of Philosophy

August 2006

The thesis of Decha Sermwittayawong was reviewed and approved* by the following:

Song Tan
Associate Professor of Biochemistry and Molecular Biology
Thesis Advisor
Chair of Committee

Jerry L. Workman
Paul Berg Professor of Biochemistry and Molecular Biology

Frank Pugh
Professor of Biochemistry and Molecular Biology

Joseph Reese
Associate Professor of Biochemistry and Molecular Biology

Robert Paulson
Associate Professor of Veterinary and Biomedical Sciences

Juliette T.J. Lecomte
Associate Professor of Chemistry

Robert A. Schlegel
Professor of Biochemistry and Molecular Biology
Head of the Department of Biochemistry and Molecular Biology

*Signatures are on file in the Graduate School

ABSTRACT

The SAGA coactivator complex functions in response to an activator protein to activate gene transcription. This thesis describes my investigations into two major functions of the SAGA complex: 1) its recruitment of the TATA-binding protein (TBP) and 2) its histone acetyl transferase activity (HAT) on a nucleosome substrate. My experiments show that the SAGA complex utilizes the Spt8 and possibly Ada1 subunits to bind the TATA-binding protein (TBP). This is the first time that Ada1 has been identified as a potential SAGA subunit that interacts directly with TBP. In contrast, Spt3, a strong genetic candidate for interacting with TBP, does not bind TBP on its own. However, in the context of the SAGA complex, Spt3 contributes to the overall interaction between TBP and SAGA.

Sequence analysis indicates a putative WD40 domain repeats within the C-terminal region of Spt8. These putative WD40 repeats are apparently sufficient for the interaction with TBP. Unexpectedly, I find that Spt8 or the SAGA complex binding to TBP competes with TBP dimer formation. Furthermore, the association of Spt8 or the SAGA complex with TBP prevents TBP binding to the TATA box DNA, suggesting that Spt8 binds to the concave surface of TBP. Based on these results, I propose a hand off model that can explain why the SAGA complex is able to act alternatively as a corepressor or a coactivator. The hand off model also explains why the SAGA complex is not found localized to the core promoter *in vivo*.

I have also investigated the requirement of the Gcn5 bromodomain for nucleosomal acetylation function by the trimeric Ada3/Ada2/Gcn5 SAGA subcomplex or the intact SAGA complex. My mutational analyses show three basic residues, K415, R419, and K422 that lie on the surface of the bromodomain, are necessary for the nucleosomal acetylation of the Ada3/Ada2/Gcn5 complex. Interestingly, the spatially distinct peptide binding pocket of the bromodomain is not necessary for the HAT function of the trimeric

subcomplex. The Gcn5 bromodomain is also required for the global acetylation of histone H3 in yeast cells.

Spt8, Spt3, and possibly Ada1 SAGA subunits function to regulate interaction with TBP, whereas the Gcn5 bromodomain is required for nucleosomal acetylation of the trimeric Ada3/Ada2/Gcn5 or the SAGA complexes. My results advance our basic understanding of how SAGA regulates gene transcription.

TABLE OF CONTENTS

LIST OF FIGURES

LIST OF TABLES

LIST OF ABBREVATIONS

ADA	Adaptor protein
CAM	Calmodulin affinity matrix
CBP	Calmodulin binding protein
ChIP	Chromatin Immunoprecipitation
GNAT	Gcn5-related *N*-acetyltransferase
HAT	Histone acetyl transferase
HDAC	Histone deacetylase complex
HPLC	Hi-pressure liquid chromatography
HRP	Horseradish peroxidase
LON	Long oligo nucleosomes
MMTV	Mouse mammary tumor virus
MYST	MOZ, Ybf2/Sas3, Sas2, and Tip60
NCP	Nucleosome core particle
Ni-NTA	nickel-nitrilotriacetic acid
PIC	Pre-initiation complex
SAGA	Spt-Ada-Gcn5 Acetyltransferase
SLIK	SAGA-like complex
SPT	Suppressor of Ty
STR	*Strep*-Tactin
TAF	TBP associated factors
TAND	TAF N-terminal domain
TAP	Tandem affinity purification
TBP	TATA-binding protein
TEV	Tobacco etch virus
TFIIA	Transcription factor IIA
UAS	Upstream activating sequence

ACKNOWLEDGEMENTS

I would like to take this opportunity to express sincere thanks to my family, friends, professors, and colleagues who have contributed to my professional skills and to my personal life.

First and foremost, I would like to thank to my advisor, Song, who has always been a role model for an intelligent, efficient, organized, hard working, and dedicated scientist. The philosophies and knowledge I have learned from him will definitely be useful for my future professional career. He always pushes me to the next level of being a better scientist. I thank you Song for being patient and trusting my work. I also appreciate his time, support, advice, guidance, and criticisms throughout all these years of intense training. Without them, none of these works would be possible.

I am also thankful to Drs. Jerry Workman, Joseph Reese, Frank Pugh, David Gilmour, Robert Simpson, Robert Paulson, and Juliette Lecomte for help, advice, and for teaching me the basics. I specially thank to Dr. Jerry L. Workman for his willingness to stay in my committee even after he has moved to the Stowers Institute.

I am grateful for constant supports and comments from our gene regulation community (Tan, Workman, Pugh, Gilmour, Simpson, Reese, and Wang Labs). I received so much help from the Workman Lab, especially for the SAGA complex purification. I appreciated tremendous help and advice from the Reese Lab for all the yeast work. Help and suggestions from the Simpson, Pugh Labs and the rest of the gene regulation community were deeply appreciated.

The Tan lab members (Will Selleck, Ryan Kramer, Adam Barrios, Brian Hnatkovich, Doba Jackson, Christopher Graham, and the undergraduate students) have always been the friends in need. I am thankful for knowing all of them. Without them, my life in Tan

lab would be boring and difficult. Will Selleck, a long-time technician, a skillful scientist, and a good friend taught me a lot of scientific tricks, and got me out of trouble several times. My all time favorite “Soldier,” Ryan Kramer, has always been a fun person to work with. I will always remember “the war,” and the divided territory. That’s right, the SAGA continues, Ryan. Adam Barrios always loves to hear some techno-dance music, to sky dive, and also a fun person to work with. I will look forward to the days Adam and Carrie come visit me in Thailand. Brian is a sport guru and a hard core Penn State, Steelers, and Pirates fan. Thank you for embarrassing me at your wedding. I wish I knew more details about the garter. I truly enjoy working with him in the lab. Doba Jackson, a Postdoctoral scientist, always gets at least 3 phone calls in a day. Thank you for always being a really good friend, taking me to grocery shopping, and almost always keeping me a company in the lab. Chris, a family man and a devout Christian, is always nice and polite to people around him. Thank you for introducing me to a warm and caring family. Lastly, I thank to all the undergraduate students and others former lab members for making the lab a better environment: Rama, Narendra, Heather, Lisa, April, Jamey, Susan, Anna, Austin, Mei, Mike, Jordan (Shaggy), Dan (Dan the man), Deanna, Julia, Druv (40 ml), Omkar, Ron, Chris, Tim, Josh (lab tech), Brian Geary, Nathan, Cynthia, Tom Zikos, and Tom Koerber.

These friends in the department have made my stay in the BMB program special: Sangita Chakraborty, Alessandra Costanzo, Victoria Korneeva, Wei-Jong Shia, Shiva Tyagarajan, Takeshi Shimizu, Jordan Irvin, Melissa Durant, Kate Huisinga, Bob Boor, John Diller, Daeyoup Lee, Bing Li, Vishva Mitra Sharma, Zhengjian Zhang, Christine Brown, Scott Galasinski, Michael Carrozza, Philippe Prochasson, Hemant and Neela Yennawar, Il Minn, Bhramara Tirupati, Lin Cheng (Marris), Dennis Lee, Jay Russell, Priscilla Lee, Alexandra Surcel, Lilun Ho, James Psathas, Jennifer Kruk, Jeong-Seon Kim, Raghuvir Singh Tomar, Hesheng Zhang Technical information and scientific discussion were highly valuable, and their friendships and fun time would always be remembered.

I thank to these people who have read my thesis: Adam Barrios, Brian Hnatkovich, Chuck Balentine, and David and Marcia Beppler. I greatly appreciate their time and their willingness to help correcting some grammar mistakes.

I would also like to thanks all the friends from the Thai club and the International Student Council (ISC) for being part of my life outside the lab. I would also like to thank you all my friends and teachers in the US, Thailand, and other parts of the world. I apologize for not being able to mention all the names, but their friendships will always be cherished.

I have always been grateful to Mrs. Soonthrie Maneenium, my high school teacher who showed me a path to become a scientist, a good scientist. She died before I finished my first year of college. I always think of her and respected her as my own parent. Without her, I would not have come to the US. Last but not least, I am thankful to my family (Ma, Pa, N'Ying, and N'Ae+) for constant love, strength, and courage that get me through all those years of frustration. Without my parents, I would not have come this far.

Chapter 1

Literature review and background

1.1 Chromatin structure and histone modifications

A eukaryotic cell packs several billion base pairs of DNA into a tiny nucleus that is only a few microns in diameter. Those DNA strands must be properly organized to allow condense packaging in nuclei without entangling or breaking during cell division. A roughly equal molecular weight of histone proteins and DNA form a complex to create nucleosomes, the building blocks of chromatin. The structural organization within a nucleosome core particle is well understood but higher-order chromatin structure still requires more investigation.

1.1.1 Core histone proteins

Core histones are basic nuclear proteins, essential for cell viability, formation of nucleosomes, and chromatin structures. There are 4 core histone proteins: H2A, H2B, H3, and H4, whose molecular weights range from 10 to 14 kDa. As illustrated in Figure **1-1** A, each of these histones contains a conserved C-terminal 'histone fold' domain, which is also present in many non-histone proteins such as in the TBP-associated factors (TAFs) (See). The histone fold secondary structure has a combination of 3 α-helices and 2 loops (α1-L1-α2-L2-α3). In addition to the histone fold domain, H3, H2A, and H2B contain "histone fold extensions" on their termini, which are also considered part of the nucleosome core structure (Figure **1-1** A). The N-terminal histone tails of core histones do not participate in the formation of nucleosomes in the crystal structure (Luger et al., 1997). However, they are subjected to post-translational modifications, which have

implications on gene regulation. Interestingly, archaebacterial histones are missing histone tails and histone-fold extensions (Sandman and Reeve, 2005).

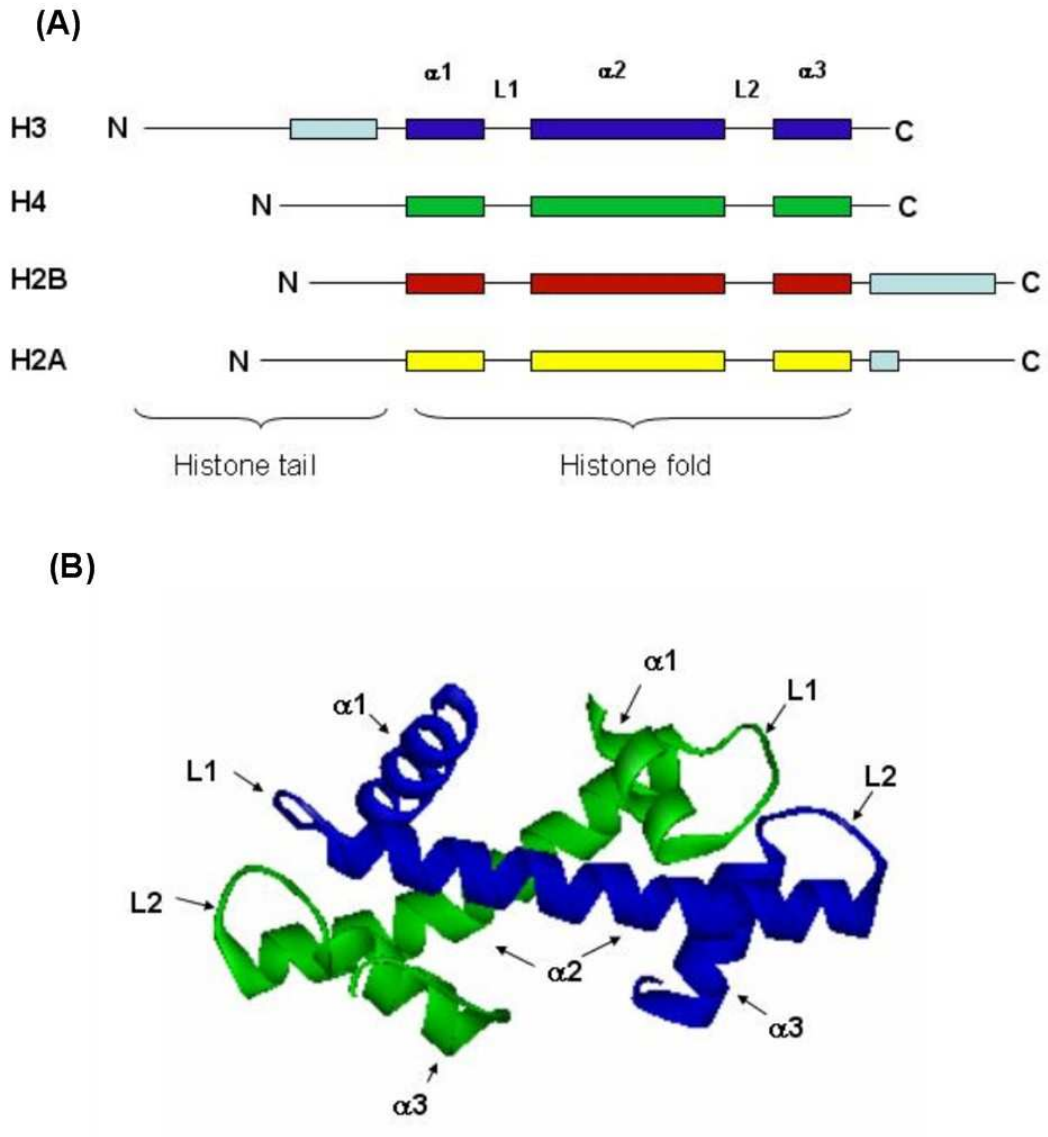

Figure **1-1**: Secondary and ternary structures of core histone proteins

(A) A cartoon shows a secondary structure of each core histone. The 'histone fold extensions' domain is extended N-terminally from the histone-fold domain of H3 and C-terminally from the histone-fold domain of H2A and H2B (in light blue boxes) are also part of the nucleosome core structure. (B) Histone H3 (blue) and H4 (green) histone fold domains form a 'handshake' motif. Histone H2A and H2B also interact the same way

Histone variants play important roles in gene regulation (Kamakaka and Biggins, 2005). For example, macroH2A, which contains an extra domain on the C-terminus compared to histone H2A, associates with inactive X chromosome (Chadwick et al., 2001; Chadwick and Willard, 2001). In yeast, a histone H2A variant, HTZ1, which is preferentially located at the intergenic regions (IGR) in yeast, is associated with both activation and repression (Dhillon et al., 2006; Keogh et al., 2006; Li et al., 2005; Millar et al., 2006; Santisteban et al., 2000; Zhang et al., 2005). H3 has its own variants such as CenH3, which is localized in the centromere region to facilitate the binding of proteins for the formation of a kinetocore structure (Zhong et al., 2002). Interestingly, histone H4 has no known variations

1.1.2 Chromatin structure

A nucleosome is a basic unit of chromatin. The crystal structures of a nucleosome core particle at 2.8 Å and 1.9 Å resolutions, were solved by the group of Richmond (Chasman et al., 1993; Davey et al., 2002; Luger et al., 1997). Figure **1-2** shows the nucleosome core particle at 1.9 Å resolution is comprised of 147 bp DNA that wraps around a histone octamer in 1.65 turns, forming a left-handed superhelix (Davey et al., 2002). There are 10.2 base pairs of DNA per helical turn, as opposed to 10.5 for regular B form DNA, indicating that the histone proteins alter the DNA conformation. The histone proteins contact the inward facing minor grooves. The DNA sequence contributes to flexibility of the DNA and nucleosome formation. For example, AT bases are preferentially located in minor grooves that face outward whereas the GC bases are less flexible and tend to be located within major grooves. This theory could probably explain why some DNA sequences show preference to form a complex with the core histone proteins (Brukner et al., 1995; Lowary and Widom, 1998; Shrader and Crothers, 1989).

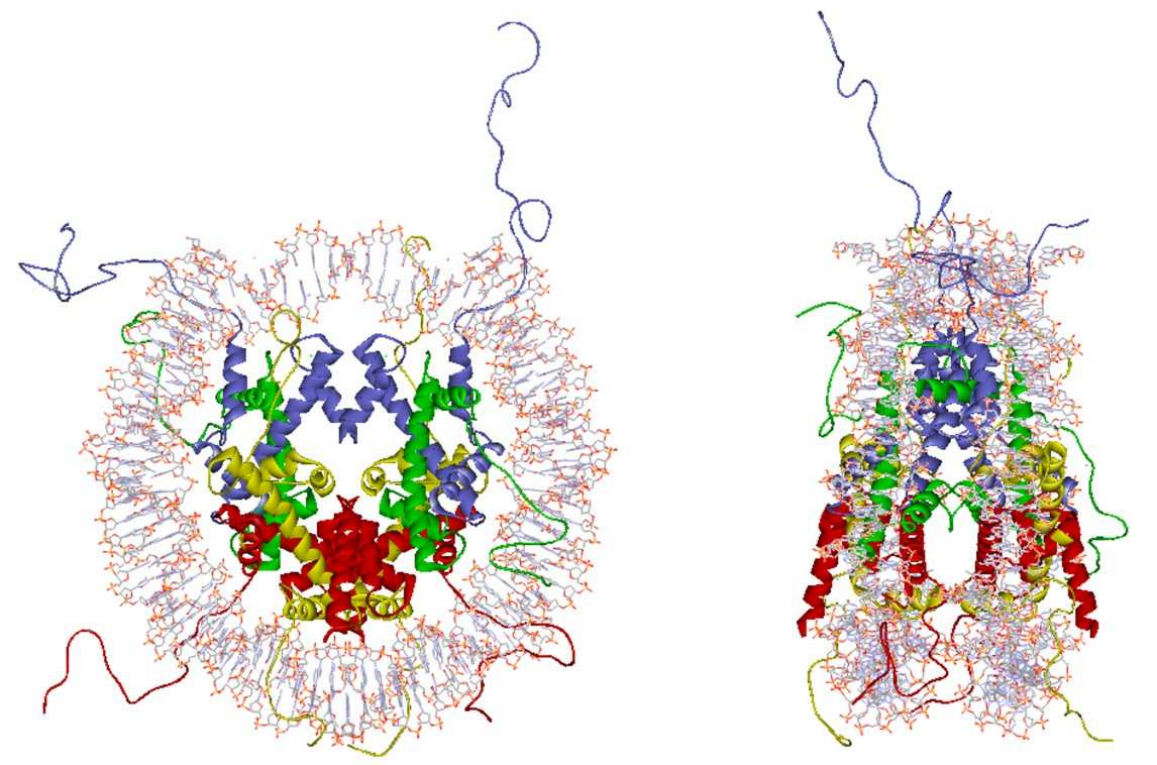

Figure **1-2**: Crystal structure of the nucleosome core particle at 1.9 Å resolution.

Nucleosome core particle with 147 bp DNA (brown and green) wraps around the histone octamer (blue: H3; green: H4; yellow: H2A; red: H2B) (Davey and Richmond, 2002). Left figure is a front view of the nucleosome, and the right picture is a 90˚ rotation. The WebLab ViewerLite program was used to manipulate the structure.

Two copies of each histone are present in the nucleosome core particle. Two histone fold motifs of each core histones form a stable head to tail arrangement: a "handshake" motif as shown in Figure **1-1** B (Arents and Moudrianakis, 1995). Under physiological conditions, histone H3 pairs with histone H4 to create a stable tetramer in which the two H3/H4 dimers stably interact with each other through the hydrogen bonding and hydrophobic interactions (Banks and Gloss, 2004). On the other hand, H2B and H2A form a dimer. Two H2A-H2B dimers and one H3-H4 tetramer can form a stable octamer in the presence of DNA or a monovalent ion such as NaCl at a concentration greater than 1.2 M (Hartman et al., 1998).

Although much is known about the structure of nucleosome core particle at atomic resolution (Davey and Richmond, 2002), less is known about how a higher-order structure of chromatin fiber is organized. Nucleosomes, which appear as 11 nm beads on a string, can be further condensed into the 30 nm fiber, as the first level of chromatin compaction (Igo-Kemenes et al., 1982; Luger and Hansen, 2005; Oudet et al., 1975). Two models for an arrangement of nucleosomes into the 30-nm structure have been proposed. The first model is the one-start solenoidal helix in which a linear array of nucleosome arrangement follows the helical path (Finch and Klug, 1976). The other proposal suggests a two-start model in which nucleosomes are arranged in a zigzag structure and twisted to form the 30-nm structure (Dorigo et al., 2003; Woodcock et al., 1984). A more recent study has shown that the organization of the 30-nm fiber chromatin follows the two-start model (Schalch et al., 2005).

Compaction of nucleosomes requires several factors such as divalent ions and the histone tail. Divalent cations such as Ca^{2+} or Mg^{2+} could induce the formation of the 30 nm fiber (Widom, 1986). Ions bind to DNA to reduce the net charge of DNA, thereby promoting further aggregation of chromatin fibers (Allard et al., 1999). Besides the influence of cations, it has been shown that the tailless nucleosome array is not able to condense into the first level of compaction, suggesting a role of histone tails in the compaction of chromatin (Carruthers and Hansen, 2000). However, a more recent study has shown that only the deletion of histone H4 tail (amino acid 14-19) prevents the 30-nm fiber formation (Dorigo et al., 2003). Also, it has been observed that those amino acid residues of histone H4 tail make intermolecular contacts with H2A/H2B of a neighboring nucleosome (Luger et al., 1997). One could also argue that this observation was due to crystal contact artifacts.

An additional method of creating higher-order chromatin is to introduce a linker histone such as histone H1 since it is important for the mitotic chromosome condensation in *Xenopus laevis* (Maresca et al., 2005). In addition, linker histones might also be involved

in regulatory processes such as genomic stability, gene expression, homologus recombination and signal transduction (Harvey and Downs, 2004).

The structure of the chromatin fiber beyond the 30 nm is less well understood. Condensation of chromosomes in the metaphase requires the cooperation of other non-histone proteins such as condensin and topoisomerase (Porter et al., 2004; Swedlow and Hirano, 2003). Understanding the structural organization of a higher-order chromain still remains a challenging task.

1.1.3 Histone modifications

While core histones are well structured within nucleosomes, histone tails are non-structured, and yet they play important roles in regulation of cellular activities. Histone tails can be post-translationally modified. These modifications include acetylation, phosphorylation, methylation, ubiquitylation, and sumoylation. A specific modification on particular residue can influence other modifications on histone tails. This concept leads to the idea of a histone code hypothesis (Cosgrove and Wolberger, 2005; Jenuwein and Allis, 2001; Strahl and Allis, 2000), in which a combination of different histone modifications dictates a specific outcome of cellular activities such as gene activation and repression, DNA repair, nucleosome assembly, and cell division.

1.1.3.1 Histone Acetylation

Covalent histone acetylation is the best characterized among all histone modifications. Histone acetylation reaction is catalyzed by histone acetyl transferase (HAT) proteins, which transfer an acetyl group to the epsilon amino group of a lysine residue of histone proteins. These enzymes can be divided into two generic classes: type A nuclear HAT and type B cytoplasmic enzymes (Workman and Kingston, 1998). Some cytoplasmic

type B HAT enzymes, such as Hat1, acetylate free histones when they are newly synthesized (Adams and Kamakaka, 1999; Rosaleny et al., 2005). On the other hand, type A HAT enzymes are found in the nucleus and are usually present in multi-subunit coactivator complexes.

HAT activity of nuclear protein was first discovered through an in-gel assay. Using a SDS-PAGE gel that was polymerized with core histone substrates, a 55-kiloDalton protein (p55) from a nuclear extract of *Tetrahymena thermophila,* was found to have HAT activity (Brownell and Allis, 1995). The amino acid sequence of the p55 is very similar to the yeast Gcn5 (Brownell et al., 1996), which is also known as Ada4, a putative transcriptional adaptor that functions together with other adaptor proteins (Ada2 and Ada3) to respond to acidic activators such as Gcn4 and VP16 (Georgakopoulos et al., 1995; Georgakopoulos and Thireos, 1992; Grant et al., 1997; Horiuchi et al., 1995; Marcus et al., 1994). It has been shown that Gcn5 is a HAT enzyme, whose activity is important for the global histone H3 acetylation, transcriptional activation, and cell growth (Howe et al., 2001; Kristjuhan et al., 2002; Marcus et al., 1994; Wang et al., 1998). To date, yeast Gcn5 is the best characterized type A HAT enzyme.

The two main classes of type A HAT enzymes, the GNAT superfamily and the MYST family have a distinct HAT mechanism. Enzymes in the GNAT family, such as the yeast Gcn5 SAGA subunit, acetylate a histone tail by allowing the formation of a ternary complex: (enzyme)-(acetyl-CoA)-(Histone). A lysine residue from the histone tail directly extracts an acetyl group from the bound acetyl Co-A (Tanner et al., 1999). In contrast to this mechanism, enzymes in the MYST family, such as the yeast Esa1, transfer an acetyl group to the enzyme itself before transferring it to a lysine residue on a histone tail (Allard et al., 1999; Yan et al., 2002). A summary of the two HAT mechanisms is illustrated in Figure **1-3** (Berndsen and Denu, 2005).

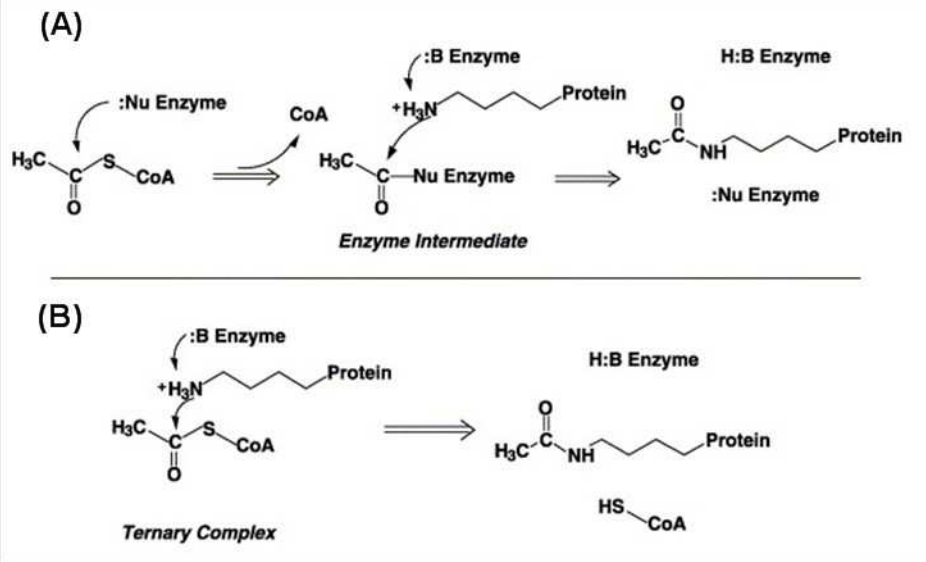

Figure **1-3**: Mechanisms of HAT enzymes

The picture is from a published article (Berndsen and Denu, 2005). (A) A ping-pong mechanism for Esa1 while (B) is a ternary complex formation used by another HAT enzyme such as Gcn5 in the GNAT family.

Histone acetylation affects the interaction between the histones and DNA. An *in vitro* study revealed that histone H4 tail can bind to DNA with high affinity (Hong et al., 1993). However, the binding affinity is dramatically reduced when the tail is acetylated. Thus, histone acetylation is likely to reduce the overall positive charge of the histone and weaken its interaction with DNA. Furthermore, it has been shown that highly pre-acetylated histone octamers inhibit the formation of higher-order chromatin when they are reconstituted into a nucleosomal 5S rRNA array (Tse et al., 1998). Subsequently, this hyperacetylated array increases levels of transcription by RNA polymerase III when it is transcribed by *Xenopus laevis* oocyte nuclear extract. Therefore, not only does histone acetylation alter the nucleosome structure, but it also promotes accessibility of transcription factors that activate genes through changing chromatin structure. In addition, histone acetylation serves as a docking site for many transcription factors. Proteins that contain a bromodomain, such as yeast Gcn5 of the SAGA complex or Swi2/Snf2 of the Swi/Snf chromatin remodeling complex, have the ability to bind to

acetylated histone tails (Hassan et al., 2002; Kasten et al., 2004; Ornaghi et al., 1999). Histone acetylation is usually concentrated at the promoter of actively transcribed genes (Vogelauer et al., 2000), suggesting another connection between acetylation and the association with transcription factors.

Histone acetylation is generally correlated with an active gene transcription. For example, deletion of the yeast Gcn5 not only causes the global loss of histone H3 acetylation, but is accompanied by a global gene repression (Howe et al., 2001; Huisinga and Pugh, 2004; Kristjuhan et al., 2002; Suka et al., 2001; Zhang et al., 1998). Besides transcription, histone acetylation also has other implications such as cell cycle regulation, chromatin assembly and DNA repair. For example, HAT enzymes in the MYST family, such as Esa1 or Sas3, are required for cell growth and cell cycle progression (Howe et al., 2001; Smith et al., 1998). Additionally, a newly synthesized histone H4 is subjected to acetylation on K5, K8 and K12, which are required for nucleosome assembly in yeast (Ma et al., 1998). Lastly, histone H3 K56A—but not K56Q amino acid substitution—confers a sensitivity to DNA damaging agents, linking histone acetylation to a DNA repair pathway (Hyland et al., 2005). Together, these results demonstrate the roles of histone acetylation in several regulatory functions.

1.1.3.2 Histone deacetylation

Histone deacetylation is not a form of covalent modification since it is a removal of acetyl groups and yet it plays significant roles in gene regulation. Acetylation of histones is chemically reversed by Histone Deacetylase enzymes (HDACs), which are generally involved in repression. Besides the role of HDACs in gene repression, yeast HDACs are also involved in DNA repair and replication (Kurdistani et al., 2004).These enzymes can be categorized into 3 main classes: class I, RPD3-like; class II, HAD-1-like; and class III, Sir2-like (Gray and Teh, 2001; Peterson, 2002). A combination of microarrays and ChIP techniques reveals localizations of different HDACs on the yeast genome (Robyr et al.,

2002). For example, the Rdp3-Sin3 complex, which represents the class I HDAC, preferentially functions at most of the intergenic region (IGR) (Carrozza et al., 2005). Unlike Rdp3, Hda1, the class II HDAC, functions at the region 10-25 kb from telomeres, while other class II HDAC enzymes are involved in deacetylating ribosomal DNA and ribosomal genes. Lastly, Sir2 is responsible for the telomeric region, HML, HMR, and rDNA silencing (Cockell et al., 2000; Rine and Herskowitz, 1987). Interestingly, Sir2 is also involved in the aging mechanism in yeast (Kaeberlein et al., 2005a; Kaeberlein et al., 2005b; Lamming et al., 2005).

1.1.3.3 Histone Phosphorylation

Histone phosphoryaltion can lead to many cellular activities including cell cycle progression, mitotic chromosome condensation, apoptosis, and DNA repair (Goto et al., 2002; Peterson and Laniel, 2004). Importantly, histone phosphorylation is also implicated in gene transcription. For instance, it has been shown that Snf1, a histone kinase enzyme in the Snf1/AMPK kinase family that phosphorylates the histone H3 S10, is required for activation of specific genes such as INO1 (Lo et al., 2001). The histone H3 S10 phosphorylation is required for the acetylation function of Gcn5 at the INO1 promoter, providing a connection between different histone modifications (Lo et al., 2001). In fact, S10 phosphorylated histone H3 is a preferred substrate for Gcn5 to acetylate K14 on the same histone (Cheung et al., 2000). Furthermore, the yeast Gcn5 R164A mutation, which is in a close proximity to the histone H3 S10 in the tGcn5/CoA/H3 trimeric complex, reduces the activity of Gcn5 *in vivo* at some Gcn5 dependent promoters (Lo et al., 2000). The same study also showed that the S10A mutation in histone H3 causes a similar effect. Thus, phosphorylation and acetylation work together to regulate gene transcription in cells. A diagram that illustrates a relationship between histone phosphorylation and acetylation is shown in Figure **1-4**.

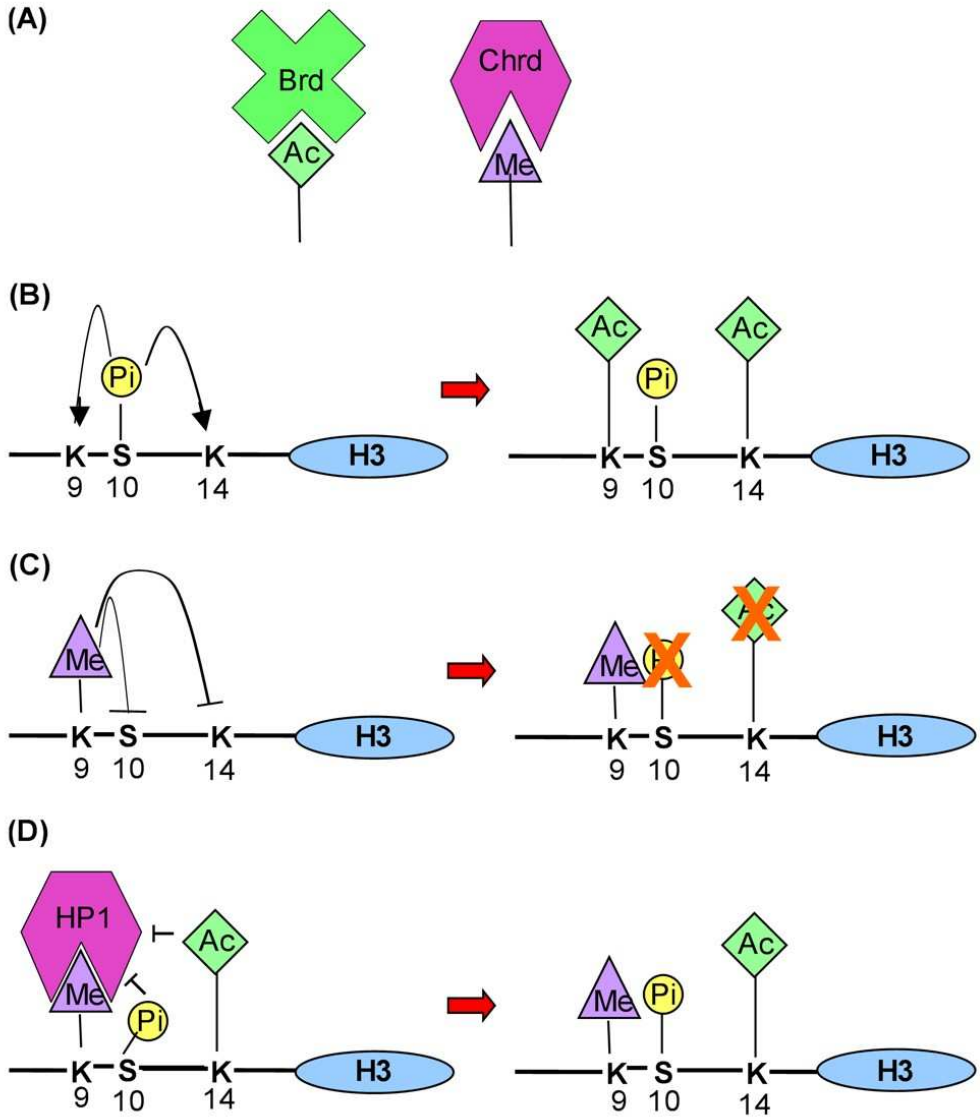

Figure **1-4**: Interplays between different histone modifications

(A) An acetylated histone is recognized by a bromodomain (Brd), whereas a methylated histone is bound by a chromodomain (Chrd). (B) Histone H3 S10 phosphorylation promotes acetylation of H3 K9 and K14 on the same histone tail (Cheung et al., 2000; Lo et al., 2001; Lo et al., 2000). In contrast, (C), methylation of H3 K9 interferes with phosphorylation of H3 S10 and acetylation of H3 K14 (Galarneau et al., 2000). However, different researchers argue that methylated H3 K9 can exist together with phosphorylated H3 S10 (Mateescu et al., 2004).

1.1.3.4 Histone methylation

Different classes of enzymes that methylate lysine or arginine residues have been identified and characterized. The lysine methyl transferases can be classified into two general groups: Set and non-Set families. The Set family consists of several different enzymes such as Suv39, Set1, Set2, Mll, and Riz (Kouzarides, 2002). These enzymes are further classified based on the existence of other domains besides the Set domain. Unlike the Set family, Dot1, which methylates H3 K79 and promotes gene transcription as well as telomere gene silencing, is the only member of the non-Set family identified to date (Min et al., 2003). The Dot1 enzyme is well conserved from yeast to human. In addition to the lysine methyl transferase enzymes, arginine methyl transferase enzymes have also been characterized. PRMT1, PRMT3, PRMT4/CARM1 are examples of enzymes that methylate arginine side chain (Kouzarides, 2002).

Lysines on histone tails could be either mono-, di-, or tri-methylated, and the result of which dictates a different outcome of gene transcription. For example, a tri-methylated histone H3 K9 by Suv39 correlates with transcriptional repression in flies and human (Margueron et al., 2005). Interestingly, yeast does not methylate H3 K9 but might employ a different mechanism to promote transcriptional repression. Another interesting example is methylation on the histone H3 K4. Di-methylated histone H3 K4 are present in both active and inactive transcription regions, but only tri-methylated H3 K4 correlates well with active gene transcription in both yeast and higher eukaryotes (Santos-Rosa et al., 2002; Schneider et al., 2004).

Just as the bromodomain recognizes an acetylated lysine, the chromodomain binds to a methylated lysine (Figure **1-4** A). Different chromodomain containing proteins recognizes different methylated histones. For example, the di-methylated histone H3 K4 is bound by the Chd1 subunit of the SAGA coactivator complex, linking methylation to acetylation and active gene transcription (Pray-Grant et al., 2005). In contrast, the tri-methylated histone H3 K9 can be recognized by HP1 protein. However, not all

chromodomains recognize methylated histone tails. For instance, chromodomain of yeast Esa1 does not bind to methylated histone H3 K9; however, it prefers binding to unmodified histone H3 tail (Jacobs et al., 2001).

As illustrated in Figure **1-4** C, methylation of histone H3 K9 has been shown to interfere with phosphorylation of histone H3 S10 because of steric hindrance (Galarneau et al., 2000). However, it has also been shown that HP1, which is a marker for methylated H3 K9, remains bound to the same histone that is phosphorylated on the S10 in the G2/M phase transition, suggesting that both methylated H3 K9 and phosphorylated H3 S10 could coexist (Figure **1-4** D) (Mateescu et al., 2004). While HP1 binds to both methylated H3 K9 in the presence of phosphorylated H3 S10, it is the acetylation of H3 K14 in the M phase in combination with S3 S10 phosphorylation that dissociates HP1 from methylated H3 K9 (Mateescu et al., 2004).

1.1.3.5 Histone ubiquitylation

Protein ubiquitylation is known to be associated with degradation (Russell et al., 1999). However, monoubiquitylation of histone proteins is not related to a degradation pathway. Just like other covalent modifications, histone ubiquitylation seems to adhere to a histone code hypothesis in which it confers effects on other histone modifications and dictates a specified transcriptional outcome. To date, histone H2A and H2B are known to be ubiquitylated.

Dynamic changes in levels of histone H2B ubiquitylation at the promoter play an intriguing role in transcription control and the regulation of histone methylation. In *Saccharomyces cerevisiae,* histone H2B K123 ubiquitylation is controlled by the Rad6-Bre1 complex (Kao et al., 2004). At the Gal1 promoter, the Rad6-Bre1 complex is recruited to monoubiquitylate histone H2B K123, promoting histone H3 K4 tri-methylation by Set1 but suppressing histone H3 K36 di-methylation by Set2 (Henry et

al., 2003; Kao et al., 2004). However, ubiquitylation levels at histone H2B K123 drop upon the recruitment of the SAGA complex. The Ubp8 SAGA subunit deubiquitylates the monoubiquitin on histone H2B, catalyzed by the Rad6-Bre1 complex (Daniel et al., 2004). Deubiquitylation of histone H2B K123 results in an increase of di-methylated histone H3 K36 and transcription of GAL1 (Henry et al., 2003). However, Upb8 of the SAGA complex is not required for full transcriptional activation of GAL1 gene because deletion of this subunit causes a slight decrease in the transcription of GAL1. A diagram illustrating the relationship between histone ubiquitylation and methylation is shown in Figure **1-5**. In addition to Ubp8, Ubp10 is another enzyme that removes ubiquitin from histone H2B. In contrast to Upb8, Ubp10 localizes to the telomere to maintain a low level of methylated histone H3 K4 and K79 by Set1 and Dot1, respectively (Gardner et al., 2005). Together, these studies illustrate the interplay between ubiquitylation and histone methylation in transcriptional regulation.

Unlike histone H2B ubiquitylation that regulates histone methylations, histone H2A ubiquitylation is facilitated by a specific histone methylation. In flies and vertebrates, histone H2A K119 is ubiquitylated by the PRC1 complex which is involved in the silencing of a subset of homeobox genes such as HoxC13 (Cao et al., 2005). Loss of SUZ12, a component of the EZH2 complex which methylates histone H3 K27, derepresses expression of Hoxc13, and is accompanied by a significant decrease in histone H2A K119 ubiquitylation. In addition, deletion of the Bmi-1 subunit of the PRC1 complex results in a loss of histone H2A K119 ubiquitylation but does not affect methylation of histone H3 K27. These results suggest that ubiquitylation of histone H2A K119 is downstream of histone H3 K27 methylation. Ubiquitylation of histone H2A K119 also associates with inactivation of an X chromosome in mammals (Baarends et al., 2005; Fang et al., 2004; Smith et al., 1998). However, the relationship between histone H2A ubiquitylation and histone methylation and their connection with the X inactivation process is yet to be determined.

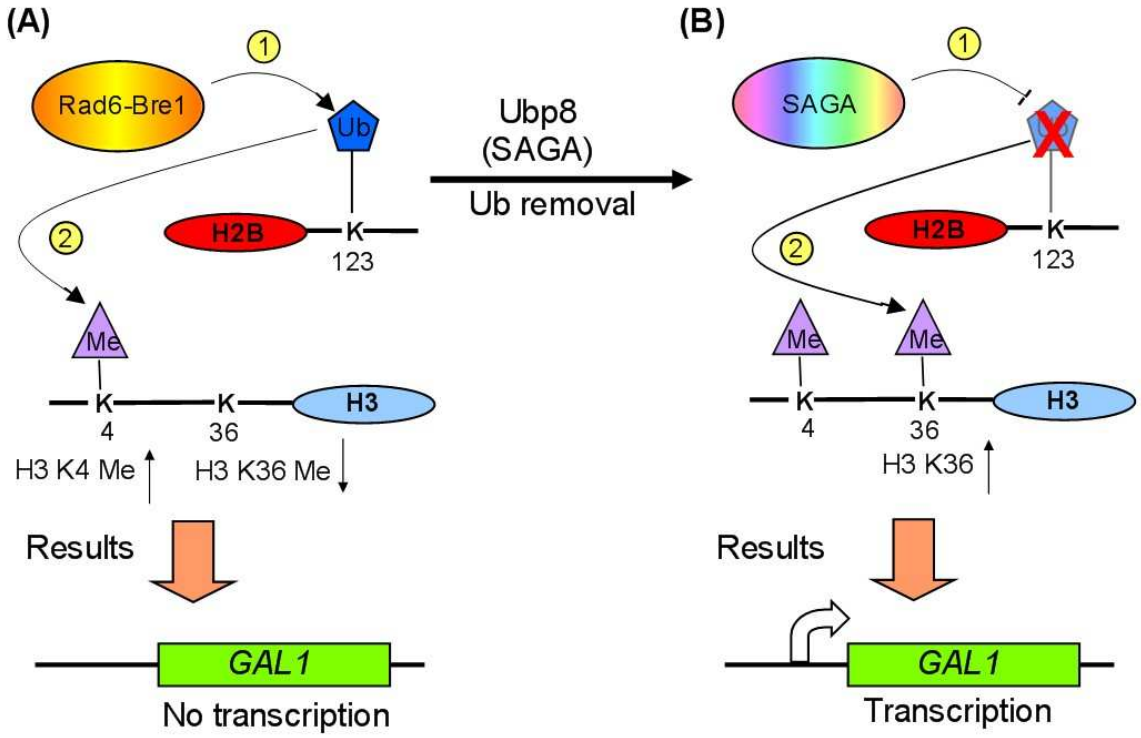

Figure **1-5**: Dynamic histone ubiquitylation controls transcription of the *GAL1* gene.

(A) Monoubiquitylation of histone H2B K123 by the Rad6-Bre1 complex is required for tri-methylation of histone H3 K4 at the GAL1 promoter and coding region, while di-methylation of histone H3 K36 is repressed (Henry et al., 2003; Kao et al., 2004; Shukla et al., 2006b). (B) Following ubiquitylation of histone H2B, the SAGA complex is recruited to GAL1 promoter to remove the ubiquitin on histone H2B (Daniel et al., 2004; Henry et al., 2003; Shukla et al., 2006a). Upon the loss of ubiquitin, di-methylation of histone H3 K36 by Set2 is promoted. Deubiquitylation of histone H2B and di-methylation of histone H3 K36 are associated with transcription of the GAL1 gene (Henry et al., 2003).

1.1.3.6 Histone sumoylation

Besides acetylation, phosphorylation, methylation, and ubiquitylation, histones can also be sumolyated. The small ubiquitin-related modifier (SUMO) is structurally related to ubiquitin and is well conserved from yeast to human (Melchior, 2000). Like ubiquitylation, sumoylation of histones is not linked to the degradation process. To date,

only one histone SUMO modifying enzyme has been identified: Ubc9, which catalyzes the SUMO transfer to histone H4 (Shiio and Eisenman, 2003). A consensus protein sequence for sumoylation in other proteins has been known (Gill, 2005) but a specific site for histone H4 sumoylation has yet to be determined. The resulting modification has an implication for gene repression as sumolyated nucleosomes recruit histone deacetylase 1 (HDAC1) and HP1 repressor chromatin to initiate and maintain chromatin silencing, respectively (Shiio and Eisenman, 2003). However, the interaction between histone sumolyase and HDAC1 or HP1 is not known, and the interplay between sumoylation of histones and other histone modifications has yet to be discovered.

In summary, different histone modifications can be achieved by different transcriptional coactivators or corepressors. Modifying histone tails in nucleosomes impacts many cellular activities including gene transcription. A structure of a nucleosome core particle is well established, and our knowledge of how nucleosome modifications affect gene transcription and vise versa is being expanded. Perhaps, understanding how those histone modification complexes bind to nucleosomes is an important key of gene regulation.

1.2 TATA-binding protein (TBP)

Transcription initiation of class I, II, and III RNA polymerases of eukaryotes requires TATA-binding protein (TBP) (Cormack and Struhl, 1992). In the case of RNA polymerase II, transcription initiation is dependent on assembly of the preinitiation complex (PIC), which consists of TFIIA, -B, -D, -E, -F, and RNA polymerase II, at the core promoter (Ghosh and Van Duyne, 1996). Among these factors, TFIID is the first factor to initiate the assembly and show preferential binding specificity towards the TATA element at the promoter (Buratowski et al., 1988). Isolation of the yeast TFIID reveals a single 240-amino acid polypeptide, leading to the idea that TFIID was identical to TBP (Hahn et al., 1989a). However, TBP functions similarly but not identically to TFIID: TBP by itself is capable of initiating basal transcription and yet it cannot be substituted for the activated transcription initiation by TFIID (Dynlacht et al., 1991). The

explanation for this observation emerged when Dynlacht et al. discovered that the *Drosophila's* TFIID is comprised of the TATA-binding protein and TBP-associated factors (TAFs) (Albright and Tjian, 2000; Dynlacht et al., 1991).

1.2.1 TAF

The finding that recombinantly purified TBP is not sufficient to substitute for the function of TFIID in transcriptional activation led to the discovery of TAF and the proposal of the coactivator model. It has been shown that the TFIID complex contains TBP and 14 different TBP-associated factors (TAFs), which enable TBP to respond to an activation by activator proteins (Dynlacht et al., 1991; Pugh and Tjian, 1990; Tanese et al., 1991). Components of the TFIID complex are depicted in Figure **1-6**. The TAFs can be considered to be a coactivator complex since it interacts with TBP. A subset of TAF proteins (Taf10, Taf12, Taf5, Taf6, and Taf9) is also found in the SAGA complex (Grant et al., 1998).

Some of the TAF proteins contain a histone fold domain, leading to a hypothesis of the TAF octamer complex (Gangloff et al., 2000; Nikolov et al., 1992). Results from our laboratory have shown that the histone fold domains from TAF proteins form an octamer structure (Selleck et al., 2001). A list of TAF components that contain a histone fold domain and their homologues is presented in the Table **1-1**. It is possible that the presence of a TAF octamer might interact with DNA. However, not all residues in the histone proteins are conserved in TAF subunits (Birck et al., 1998; Luger et al., 1997; Selleck et al., 2001), suggesting that the way TAF octamer interacts with DNA might be different than that of the histone octamer if it interacts with DNA at all.

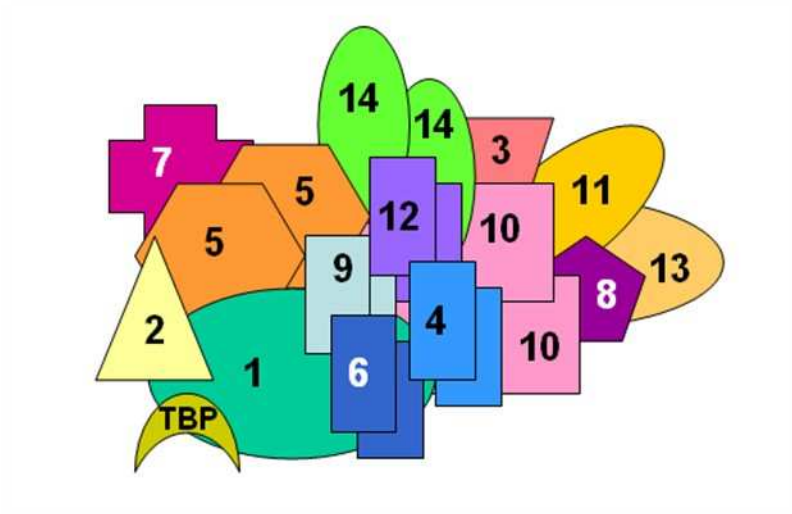

Figure **1-6**: Cartoon shows subunits of the TFIID complex.

TFIID complex consists of TBP and 14 TBP-associated factors (TAFs). Each number indicates the name of each TAF subunit. It has been shown that the N-terminal of TAF1 makes a direct contact with TBP (Kokubo et al., 1998; Kotani et al., 1998; Reese et al., 1994). There are more than one copy for each TAF5, TAF6, TAF9, TAF12, TAF4, TAF10 and TAF14 per TFIID (Sanders et al., 2002). Some of the TAFs, such as TAF9, TAF6, TAF12, TAF4, TAF10, TAF3, TAF8, TAF11, and TAF13, contain the histone fold domain (See Table Table **1-1**).

Table **1-1**: Histone fold domains in TAFs and SAGA subunits

Yeast TAFs	Histones	Complex	References
yTAF9-yTAF6	H3-H4	TFIID	(Michel et al., 1998; Selleck et al., 2001)
yTAF12-yTAF4	H2B-H2A	TFIID	(Nikolov et al., 1992; Selleck et al., 2001)
yTAF3[a]-yTAF10[b]	H2A-H2B?	TFIID	(Gangloff et al., 2000; Kirchner et al., 2001; Klebanow et al., 1996)
yTAF8-yTAF10	H3-H4?	TFIID	(Gangloff et al., 2000; Kirchner et al., 2001; Klebanow et al., 1996)
ySpt7[d]-yTAF10	H2A-H2B?	SAGA	(Gangloff et al., 2000; Sullivan et al., 2000)
yTAF12-yAda1	H2B-H2A	SAGA	(Michel et al., 1998; Selleck et al., 2001)
yTAF11-yTAF13	H3-H4	TFIID	(Moqtaderi et al., 1996b; Xie et al., 2000)
Spt3[c]-Spt3[c]	H3-H4	SAGA	(Birck et al., 1998)

[a]yTAF3 is a homologue of hTAF135, which aligns with H2A
[b]yTAF10 has a-1, L1, and a-2 similar to hTAF28*
[c]N-terminus histone fold domain (HFD) of Spt3 is hTAF18 homologue (H4) and the C-terminus HFD of Spt3 is hTAF28 homologue (H3)
[d]HFD of Spt7 is similar to HFD of yTAF3
*hTAF28 is difficult to be classified because it has the alpha-1 which is a homologue of H4 but its alpha-2 and alpha-3 are comparable to both H3 and H4 (Birck et al., 1998).

Almost all TAF proteins are essential for cell viability, and some are involved in cell cycle progression (Albright and Tjian, 2000; Green, 2000). Because TAF proteins are required for transcriptional activation, one could assume that TFIID, which is comprised of TBP and TAF proteins, is present at all RNA polymerase II promoters. However, Moqtaderi et al tested the requirement of TAFs in transcription by RNA polymerase II and found that TAF depletion reduces transcription of a subset of genes, especially those that lack the consensus TATA element (Moqtaderi et al., 1996b). This study suggests that TFIID is not generally required for the transcription of all RNA polymerase II dependent genes. Consistent with this idea, TAF-dependent and TAF-independent genes have been classified (Kuras et al., 2000; Li et al., 2000; Li et al., 2002). Interestingly, TAF-dependent genes do not have consensus TATA (Basehoar et al., 2004; Martinez et al., 1994; Moqtaderi et al., 1996a; Tanese et al., 1991). On the other hand, TAF-independent genes have a well-defined TATA element at their promoters, and do not require TAFs to recruit and stabilize TBP to their promoters (Basehoar et al., 2004; Li et

al., 2000). Recruitment of TBP to TAF-independent genes is accomplished by a different coactivator complex such as the SAGA complex.

1.2.2 Characterizations of TBP

TBP is well conserved among eukaryotes. Yeast TBP shares greater than 80% identity with the human homologue. The region of conservation that lies at the C-terminal 180 amino acids was thought to bind strongly to the consensus 6-basepair TATA element (TATAAA) (Hahn et al., 1989b; Singer et al., 1990). However, crystal structures of the TBP/TATA DNA complexes reveal that TBP occupies up to 8-basepair sequence (Kim et al., 1993). A computational analysis reveals that only about 20% of the yeast genome contain the consensus TATA(A/T)A(A/T)(A/G) TATA element (Basehoar et al., 2004). TBP is among the transcription factors that recognize the minor groove of DNA (Bewley et al., 1998). The group of Hahn has shown that expression of the core conserved domain of the yeast TBP by itself is sufficient for cell viability and transcriptional activation by TAFs (Reddy and Hahn, 1991). Furthermore, the conserved domain of yeast TBP is able to interact with all human TAFs and supports transcriptional activation *in vitro* (Zhou et al., 1993). Despite the high conservation, neither the yeast-human (N-terminus from yeast and conserved core from human) TBP hybrid nor the *Drosophila* TBP can restore the full functionality of yeast TBP *in vivo*, suggesting some defect in interaction with other factors (Cormack et al., 1991; Gill and Tjian, 1991). The cell growth defect of the mutant might be due to the inability of human TBP to support transcription by RNA polymerase III and the inability to support transcription of all three classes of RNA polymerases at TATA-less promoters (Cormack et al., 1994). Thus, evolutionary differences in the conserved domain of TBP reflect specific interactions necessary for the recruitment of TBP to TATA-less promoters.

In contrast to the DNA binding domain of the TBP, the N-terminal region of TBP is highly diverged among species. This non-conserved sequence has both negative and

positive regulatory roles in gene transcription. First, the N-terminus region of TBP negatively regulates gene transcription. For example, removal of the N-terminus in the TBP mutants that have defects in DNA binding rescues the phenotype (Lee and Struhl, 2001). In addition, the repressor NC2 has the ability to bind to TBP-DNA complex to prevent of the formation of the pre-initiation complex (PIC) (Denko et al., 2003; Kamada et al., 2001). Only human NC2, not the yeast homologue, requires the presence of the N-terminus of TBP for full repression effect (Goppelt and Meisterernst, 1996). In contrast to the negative role, the N-terminus of TBP also has a positive regulatory role. Deletion of the N-terminus of yeast TBP in combination with some TFIIA and Brf-1 interaction deficient mutants shows a severe growth defect and lethality (Lee and Struhl, 2001). In addition, the N-terminus of human and *Drosophila* TBP is required for the interaction with glutamine rich activators such as Sp1 (Peterson et al., 1990; Pugh and Tjian, 1990). Therefore, the non-conserved N-terminus residues of TBP play both positive and negative roles by regulating the interaction of TBP and other factors.

1.2.3 A crystal structure of TBP and structure of a TBP/DNA complex

The crystal structure of the *Arabidopsis thaliana*'s TBP was first solved by the group of Burley (Nikolov et al., 1992). The structure of yeast TBP was solved in the following year by the group of Kornberg (Chasman et al., 1993). The structure of yeast TBP is identical to that of *Arabidopsis thaliana*, and it is illustrated in Figure **1-7** A. Sequence analysis reveals two repeats: α and β (89 and 90 amino acids, respectively). Although these two repeats share only 30% identity, their structures are nearly identical, creating a pseudosymmetrical saddle-like structure of TBP. Half of the TBP saddle is composed of five anti-parallel β-sheets with two α-helixes: one long and one short: S1-H1-S2-S3-S4-S5-H2. The short H1 positions on the edge of the structure near S2 while the long H2 lies above S3-S5 β strands. Ten β strands create a concave surface of the saddle while the two long helixes and the two shorts near the S2 strands form convex surface of the structure. Overall TBP is highly positively charged with the exception of the concave

surface that is quite hydrophobic. In addition, two molecules of TBP homodimerize through the concave surface (Figure **1-7** B). The role of TBP dimerization on gene transcription will be discussed in **1.2.4.1**.

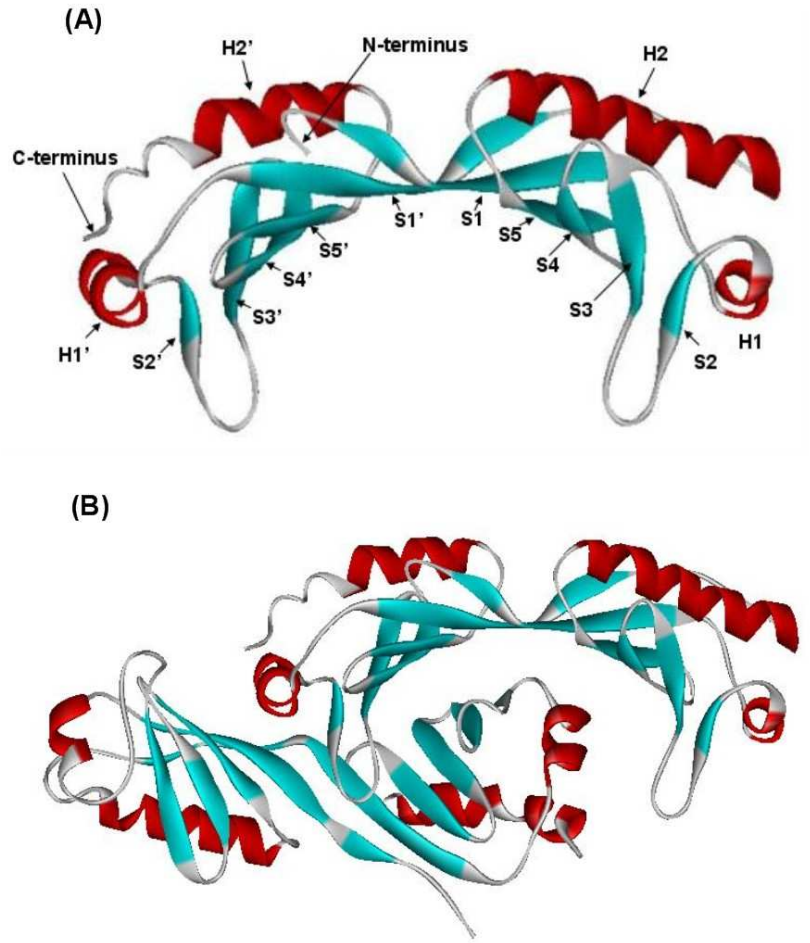

Figure **1-7**: Structure of the yeast TBP.

(A) Structure of monomeric yeast TBP posts a pseudo-two fold symmetry (Chasman et al., 1993). S and H strand for beta-sheet and alpha-helix, respectively. (B) TBP can dimerize through the concave surface of the molecule (Chasman et al., 1993). The program WebLab ViewerLite was used to render the structure (1TBP).

The structures of TBP binding to the TATA box DNA were solved by the groups of Burley and Sigler (Kim et al., 1993). Sigler and his colleagues solved the structure of

yeast TBP bound to a 29-nucleotides DNA fragment that has a 12-bp DNA hairpin, which includes 5'-TATATAAA-3' as part of the yeast CYC1 promoter (Kim et al., 1993). Burley and his colleagues solved a similar structure using the TBP from *Arabiodpsis thaliana* binding to the TATA element (5'-TATAAAAG-3') of the adenovirus major late promoter (Kim et al., 1993). Although the two proteins came from different organisms, their structures are identical. The structure of the yeast TBP that binds to the DNA is illustrated in Figure **1-8**. TBP binds to the TATA box via the minor groove. While the structural conformation of the TBP does not change, the DNA is severely distorted and bent by approximately 100˚. This suggests that DNA is highly flexible and can accommodate the binding of protein factors. 70% of the overall interaction between the two components is hydrophobic or van der Waals interactions. Despite of the large hydrophobic contribution, the binding affinity of the yeast TBP to DNA decreases as the salt concentration increases (Petri et al., 1998). This suggests that the electrostatic interaction is important for the complex stability.

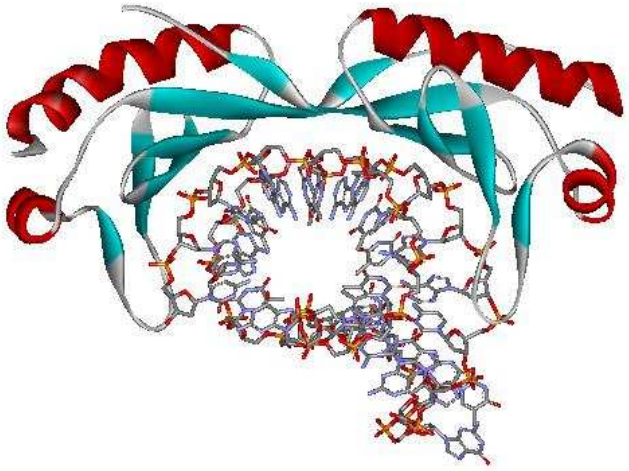

Figure **1-8**: Crystal structure of yeast TBP bound to the yeast CYC1 promoter

Structure of the yeast TBP remains identical to the structure of the TBP by itself (Kim et al., 1993). However, upon the binding to the minor groove of the TATA box, DNA is severely bent by approximately 100˚.

The binding orientation of the TBP is important for the successful transcription of a gene. *In vitro,* there is a 60% chance for TBP to bind to the TATA box in a correct orientation (Cox et al., 1997); however, this binding preference to a correct orientation is increased to 95% upon the addition of TFIIA and TFIIB (Kays and Schepartz, 2000). Some of the directional binding preferences might be contributed by the DNA sequence as well as the properties of the TBP. Computational analysis has suggested a consensus 5'-TATA(A/T)A(A/T)(A/G)-3' (Basehoar et al., 2004). The 5' half of the TATA element is invariant whereas the 3' half is more diverged. This 5' half of the TATA is also more flexible than the 3' half. It has also been reported that two residues within the concave surface of the TBP (A100 and P191) contribute to the directional binding of TBP to a TATA box (Spencer and Arndt, 2002). In addition, an asymmetric distribution of positive charge is observed with more positive charge located on the TBP domain that interacts with the 3' half of the TATA box. While other factors such as TFIIA and TFIIB help TBP to DNA in a correct orientation (Nikolov et al., 1995; Tan et al., 1996), the asymmetric distribution of the positive charge could also contribute to the binding directionality of TBP.

1.2.4 Regulation of the binding of TBP to promoters

Binding of TBP to a promoter is a nucleation step for the formation of PIC. Thus, regulation of the binding of TBP to promoters is a key for transcription control. Both basal and activated transcriptions require TBP at a promoter. Thus, there are many ways to regulate the binding of TBP to the DNA, including TBP dimerization, the positive and negative factors that impact the consequence of TBP binding to a promoter element.

1.2.4.1 TBP dimerization

TBP dimerization seen in the crystal structure was initially thought to be an artifact influenced by crystal packing (Figure **1-7** B) (Nikolov et al., 1992). However, it has been experimentally shown that TBP has an intrinsic ability to dimerize (Coleman et al., 1995; Taggart and Pugh, 1996), and dimerization of TBP has a biological implication. It has been shown that mutations in the TBP residues that lie along the concave surface destabilize TBP dimerization (Jackson-Fisher et al., 1999). As a result, the rate of basal transcription *in vivo*, but not activated transcription of a reporter gene, increases, suggesting that TBP dimerization negatively regulates its function (Jackson-Fisher et al., 1999). In addition, it has been shown that TBP dimer dissociation is a rate-limiting step for the DNA binding (Jackson-Fisher et al., 1999; Weideman et al., 1997). However, an increase in basal transcription cannot be explained by an increase in TBP/DNA stability since those mutations that dissociate a TBP dimer also decrease its binding affinity to the DNA (Kou et al., 2003). Perhaps the binding of TBP to the TATA sequence is promoted and stabilized by other transcription factors. Thus, the TBP dimerization acts on itself to prevent unregulated transcription in cells. My investigations show that TBP dimerization also regulates its binding with a SAGA coactivator complex (Chapter 3).

1.2.4.2 Negative regulatory factors

Because TBP is important for transcriptional initiation, its activities in cells must be controlled to prevent unregulated transcription which could lead to deleterious effects to the cells. A number of negative regulatory factors for TBP binding to DNA have been identified. For example, the classic corepressor complex NC2, which is comprised of α and β subunits, stabilizes the TBP/DNA complex and prevents association with TFIIA and/or TFIIB (Kamada et al., 2001; Xie et al., 2000). A similar mechanism of repression is observed in the NZFP, a zinc finger protein from *Xenopus laevis*, which binds and occludes a TBP/DNA complex from association with both TFIIA and TFIIB (Kim et al.,

1993). A different mechanism of repression is introduced by Mot1, which promotes TBP-DNA dissociation in an ATP-dependent manner (Kang et al., 1995). In addition, Mot1 has the ability to prevent the association of NC2 with a TBP/DNA complex but this does not necessarily promote an active transcription (Geisberg and Struhl, 2004). In contrast to Mot1, the Tk-TIP26 repressor from the hyperthermophilic archaeon *Thermococcus kodakaraensis* is proposed to form a complex with a TBP dimer and prevents it from binding to TATA box DNA (Yamamoto et al., 2006). Lastly, Not proteins, components of the CCR4-Not complex, negatively regulate the binding of TBP to the TATA box, probably by sequestering TBP from Spt3, a SAGA subunit that promotes TBP recruitment to the core promoter (Badarinarayana et al., 2000; Collart, 1996).

1.2.4.3 Positive regulatory factors

While negative regulatory factors prevent or inhibit TBP binding to the TATA box DNA, positive regulatory factors promote or stabilize TBP binding to the core promoter element. Like negative regulatory factors, a number of positive regulatory factors for TBP binding to DNA have been described. For example, the general transcription factor IIA (TFIIA) has been shown to destabilize TBP dimers and accelerate binding of TBP and TFIID to the TATA box (Coleman et al., 1999). Moreover, TFIIA can antagonize the effect of repressor proteins including NC2 (Kim et al., 1993; Marcus et al., 1996). In addition to TFIIA, several factors in cells act to promote the binding of TBP to promoters. These factors include coactivator complexes such as SAGA, Swi/Snf, and mediator complexes. Besides those positive regulatory factors, some negative regulatory factors can also play a positive role. For example, the NC2 alpha subunit is found in actively transcribed genes (Creton et al., 2002; Geisberg and Struhl, 2004).

Overall, TBP is an important general transcription factor that binds to the DNA and initiates the PIC formation. The binding of TBP to DNA is tightly regulated by many

positive and negative regulatory factors. In addition, TBP has an intrinsic ability to dimerize and this property has a significant implication on gene regulation. The relationship between TBP and the SAGA coactivator complex is also affected by TBP dimerization, which will be discussed in Chapters 2 and 3.

1.3 The yeast SAGA coactivator complex

A coactivator usually exists as a multisubunit complex, is recruited by a specific activator protein to function at a promoter to facilitate transcriptional activation. Yeast SAGA complex is among coactivator complexes that is recruited by specific activator proteins. This 1.8 MDa complex is comprised of at least 15 different subunits (Figure **1-9**), which include Tra1, Spt3, Spt8, Spt7, Spt20, Ada1, Ada2, Ada3, Gcn5, Taf5, Taf6, Taf12, Taf9, Taf10, and Ubp8 (Daniel et al., 2004; Grant et al., 1997; Grant et al., 1998). Additional studies have also suggested Sgf11, Sgf73, Chd1 and Sus1 as components of the complex (Lee et al., 2004; Pray-Grant et al., 2005; Sanders et al., 2002). None of the SAGA subunits except the TAFs, which are also present in TFIID complex, is essential for yeast viability. Of these 19 subunits, only Spt7, Spt20, and Ada1 are required for the complex's structural integrity (Sterner et al., 1999). Several human homologues of the yeast SAGA complex, such as human PCAF (Ogryzko, 2001; Ogryzko et al., 1998; Vassilev et al., 1998), human TFTC (TATA-free TAF_{II}-containing) complex (Cavusoglu et al., 2003; Wieczorek et al., 1998), and human STAGA (Spt3-TAF_{II}31-Gcn5L acetyltransferase) complex (Martinez et al., 1998), have been discovered. In yeast, the SAGA complex regulates approximately 10% of the entire yeast genome and functions mainly at stress-response genes (Huisinga and Pugh, 2004; Lee et al., 2000).

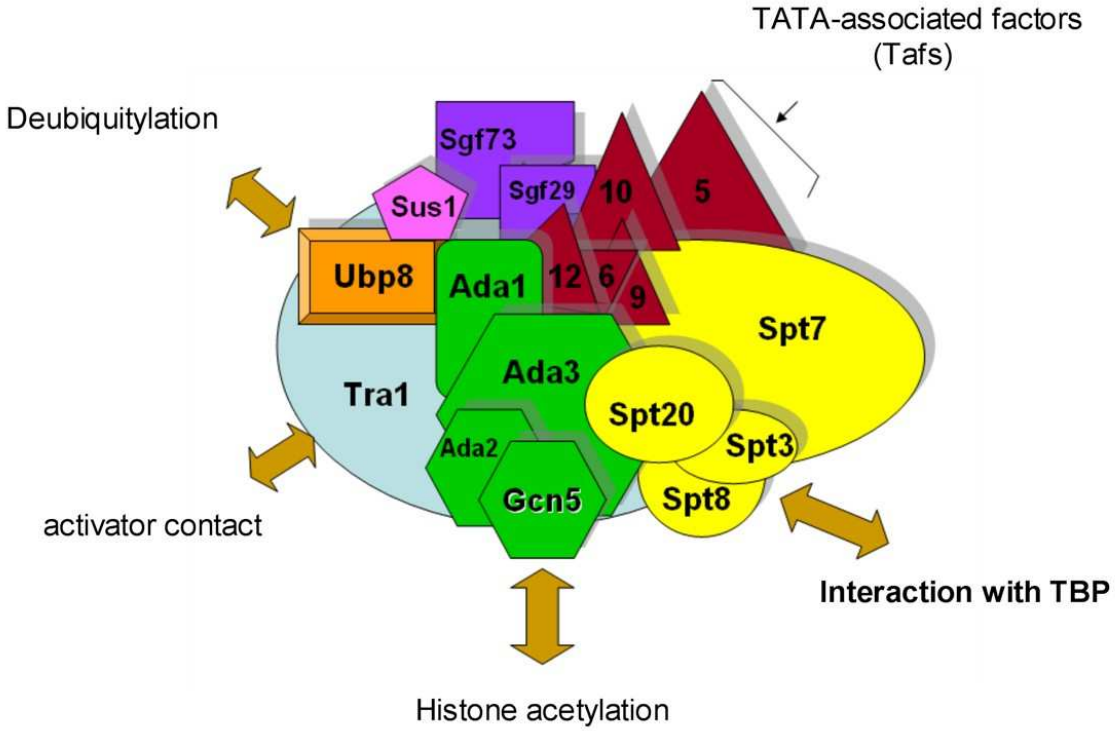

Figure **1-9**: Yeast SAGA complex

This cartoon illustrates all the SAGA subunits known up to date. However, it does not depict the accurate size of each subunit nor the correct arrangement of all subunits in the complex.

Because the SAGA complex contains several different subunits, it is capable of performing four major functions, such as 1) recruitment of the TBP; 2) nucleosome acetylation; 3) interaction with an activator protein; and 4) ubiquitin removal.

1.3.1 The SAGA complex functions to interact and recruit TBP to promoters

Recruitment of TBP to a promoter is a nucleating step for the formation of the pre-initiation complex (PIC) and the rate limiting step of the process (Blair and Cullen, 1997; Chatterjee and Struhl, 1995; Jackson-Fisher et al., 1999; Klein and Struhl, 1994). Several coactivators are involved in TBP recruitment, including the SAGA complex. The ability

of the SAGA complex to recruit TBP to a promoter was initially thought to be mediated by the TAF components in the complex. However, more recent experimental evidence argues against this hypothesis. For example, temperature-sensitive mutations in TAFs do not prevent TBP interaction *in vitro* but only cause TBP recruitment defects at some SAGA-dependent promoters (Bhaumik and Green, 2002; Grant et al., 1998). In contrast to TAFs, several studies have suggested the role of Spt components in the SAGA complex in mediating this function. For instance, phenotypes associated with mutations in SPT15, which encodes for the yeast TBP, can be suppressed by mutations in other SPT genes (Eisenmann et al., 1992; Eisenmann et al., 1994). In addition, deletion of Spt subunits, including Spt3, Spt20, and Spt7, universally affects the TBP recruitment to all SAGA-dependent promoters (Bhaumik and Green, 2001; Bhaumik and Green, 2002; Dudley et al., 1999; Larschan and Winston, 2001). Therefore, some Spt proteins appear to mediate the interaction of the SAGA complex with TBP. How SAGA interacts with TBP will be discussed in details in Chapters 2 and 3.

1.3.2 The SAGA complex functions to acetylate nucleosomes

Histone acetylation is generally associated with active gene transcription. The ability of the SAGA complex to modify histone tails of nucleosomes is mediated by the Gcn5 subunit, a member of the GNAT superfamily (Grant et al., 1997). Deletion of Gcn5 affects the global histone H3 but not histone H4 acetylation (Howe et al., 2001; Teng et al., 2002). By itself, Gcn5 can acetylate core histones but not nucleosomes (Balasubramanian et al., 2002; Grant et al., 1997). However, the Ada3/Ada2/Gcn5 SAGA subcomplex is sufficient for nucleosome acetylation function (Balasubramanian et al., 2002). It is important to note that the nucleosome acetylation ability of Gcn5 in the Ada3/Ada2/Gcn5 or the SAGA complex is not only dependent on Ada3 and Ada2 subunits, but is also dependent on the presence of the bromodomain of the Gcn5. The role of the bromodomain on nucleosome acetylation of the SAGA and Ada3/Ada2/Gcn5 complexes is discussed in chapter 5. The significance of histone acetylation on gene transcription is discussed in **1.1.3.1**.

1.3.3 The SAGA complex interacts with an activator protein

As a transcriptional coactivator complex, the SAGA complex can be recruited by an activator protein to mediate transcriptional activation. It was originally thought that Ada proteins, especially the Ada2 subunit of the SAGA complex, interacted with an activator protein (Berger et al., 1992; Pina et al., 1993). However, *in vitro* cross-linking assays, mutation analysis, as well as the *in vivo* fluorescence resonance energy transfer (FRET) demonstrate that the Tra1 subunit, but not the Ada components, functions to interact with activator proteins (Bhaumik et al., 2004; Brown et al., 2001; Reeves and Hahn, 2005). Tra1 is the largest component of the SAGA complex and is also present in the NuA4 coactivator complex. Tra1 from both SAGA and NuA4 complexes can cross-link with several acidic activators *in vitro* (Brown et al., 2001). However, experiment in the *in vivo* context, using the fluorescence resonance energy transfer (FRET) shows that only Tra1 in the SAGA but not the NuA4 complex interacts with the Gal4 activator protein (Bhaumik et al., 2004), suggesting that the NuA4 complex is recruited by activator proteins other than the Gal4. To date, Pho2 is the only activator protein known to recruit the NuA4 complex to the PHO5 promoter. The histone acetylation function of the NuA4 complex promotes transcription of the PHO5 gene by regulating the recruitments of the Pho4 activator and the SAGA complex (Nourani et al., 2004).

1.3.4 The SAGA complex deubiquitylates nucleosomes for transcriptional activation

Dynamic histone modifications affect transcriptional activity of genes. Besides Gcn5, the SAGA complex also contains Ubp8, an ubiquitin protease enzyme that also regulates gene transcription. Ubp8 plays a role in regulating gene transcription at certain promoters such as GAL1 and ARG1 (Daniel et al., 2004; Henry et al., 2003; Lee et al., 2005b). The ability of Ubp8 to deubiquitylate histone H2B is dependent on the Sgf11 subunit and the integrity of the SAGA complex (Ingvarsdottir et al., 2005; Lee et al., 2005b).

Other components of the SAGA complex serve additional functions. For example, the presence of the Chd1 subunit links the SAGA complex to nucleosome remodeling activity and transcriptional elongation (Pray-Grant et al., 2005; Tran et al., 2000). Chd1 contains a chromodomain, which recognizes a methylated histone tail and required for full acetylation of GAL1, a SAGA dependent promoter (Pray-Grant et al., 2005). The SAGA complex also contains a subset of TAF proteins, but the precise role of TAF components in the complex is not known.

1.4 Bibliography

Adams, C. R., and Kamakaka, R. T. (1999). Chromatin assembly: biochemical identities and genetic redundancy. Curr Opin Genet Dev *9*, 185-190.

Albright, S. R., and Tjian, R. (2000). TAFs revisited: more data reveal new twists and confirm old ideas. Gene *242*, 1-13.

Allard, S., Utley, R. T., Savard, J., Clarke, A., Grant, P., Brandl, C. J., Pillus, L., Workman, J. L., and Cote, J. (1999). NuA4, an essential transcription adaptor/histone H4 acetyltransferase complex containing Esa1p and the ATM-related cofactor Tra1p. Embo J *18*, 5108-5119.

Arents, G., and Moudrianakis, E. N. (1995). The histone fold: a ubiquitous architectural motif utilized in DNA compaction and protein dimerization. Proc Natl Acad Sci U S A *92*, 11170-11174.

Auble, D. T., Hansen, K. E., Mueller, C. G., Lane, W. S., Thorner, J., and Hahn, S. (1994). Mot1, a global repressor of RNA polymerase II transcription, inhibits TBP binding to DNA by an ATP-dependent mechanism. Genes Dev *8*, 1920-1934.

Baarends, W. M., Wassenaar, E., van der Laan, R., Hoogerbrugge, J., Sleddens-Linkels, E., Hoeijmakers, J. H., de Boer, P., and Grootegoed, J. A. (2005). Silencing of unpaired chromatin and histone H2A ubiquitination in mammalian meiosis. Mol Cell Biol *25*, 1041-1053.

Badarinarayana, V., Chiang, Y. C., and Denis, C. L. (2000). Functional interaction of CCR4-NOT proteins with TATAA-binding protein (TBP) and its associated factors in yeast. Genetics *155*, 1045-1054.

Balasubramanian, R., Pray-Grant, M. G., Selleck, W., Grant, P. A., and Tan, S. (2002). Role of the Ada2 and Ada3 transcriptional coactivators in histone acetylation. J Biol Chem *277*, 7989-7995.

Banks, D. D., and Gloss, L. M. (2004). Folding mechanism of the (H3-H4)2 histone tetramer of the core nucleosome. Protein Sci *13*, 1304-1316.

Basehoar, A. D., Zanton, S. J., and Pugh, B. F. (2004). Identification and distinct regulation of yeast TATA box-containing genes. Cell *116*, 699-709.

Berger, S. L., Pina, B., Silverman, N., Marcus, G. A., Agapite, J., Regier, J. L., Triezenberg, S. J., and Guarente, L. (1992). Genetic isolation of ADA2: a potential transcriptional adaptor required for function of certain acidic activation domains. Cell *70*, 251-265.

Berndsen, C. E., and Denu, J. M. (2005). Assays for mechanistic investigations of protein/histone acetyltransferases. Methods *36*, 321-331.

Bewley, C. A., Gronenborn, A. M., and Clore, G. M. (1998). Minor groove-binding architectural proteins: structure, function, and DNA recognition. Annu Rev Biophys Biomol Struct *27*, 105-131.

Bhaumik, S. R., and Green, M. R. (2001). SAGA is an essential in vivo target of the yeast acidic activator Gal4p. Genes Dev *15*, 1935-1945.

Bhaumik, S. R., and Green, M. R. (2002). Differential requirement of SAGA components for recruitment of TATA-box-binding protein to promoters in vivo. Mol Cell Biol *22*, 7365-7371.

Bhaumik, S. R., Raha, T., Aiello, D. P., and Green, M. R. (2004). In vivo target of a transcriptional activator revealed by fluorescence resonance energy transfer. Genes Dev *18*, 333-343.

Birck, C., Poch, O., Romier, C., Ruff, M., Mengus, G., Lavigne, A. C., Davidson, I., and Moras, D. (1998). Human TAF(II)28 and TAF(II)18 interact through a histone fold encoded by atypical evolutionary conserved motifs also found in the SPT3 family. Cell *94*, 239-249.

Blair, W. S., and Cullen, B. R. (1997). A yeast TATA-binding protein mutant that selectively enhances gene expression from weak RNA polymerase II promoters. Mol Cell Biol *17*, 2888-2896.

Brown, C. E., Howe, L., Sousa, K., Alley, S. C., Carrozza, M. J., Tan, S., and Workman, J. L. (2001). Recruitment of HAT complexes by direct activator interactions with the ATM-related Tra1 subunit. Science *292*, 2333-2337.

Brownell, J. E., and Allis, C. D. (1995). An activity gel assay detects a single, catalytically active histone acetyltransferase subunit in Tetrahymena macronuclei. Proc Natl Acad Sci U S A *92*, 6364-6368.

Brownell, J. E., Zhou, J., Ranalli, T., Kobayashi, R., Edmondson, D. G., Roth, S. Y., and Allis, C. D. (1996). Tetrahymena histone acetyltransferase A: a homolog to yeast Gcn5p linking histone acetylation to gene activation. Cell *84*, 843-851.

Brukner, I., Sanchez, R., Suck, D., and Pongor, S. (1995). Trinucleotide models for DNA bending propensity: comparison of models based on DNaseI digestion and nucleosome packaging data. J Biomol Struct Dyn *13*, 309-317.

Buratowski, S., Hahn, S., Sharp, P. A., and Guarente, L. (1988). Function of a yeast TATA element-binding protein in a mammalian transcription system. Nature *334*, 37-42.

Candau, R., and Berger, S. L. (1996). Structural and functional analysis of yeast putative adaptors. Evidence for an adaptor complex in vivo. J Biol Chem *271*, 5237-5245.

Cao, R., Tsukada, Y., and Zhang, Y. (2005). Role of Bmi-1 and Ring1A in H2A ubiquitylation and Hox gene silencing. Mol Cell *20*, 845-854.

Carrozza, M. J., Li, B., Florens, L., Suganuma, T., Swanson, S. K., Lee, K. K., Shia, W. J., Anderson, S., Yates, J., Washburn, M. P., and Workman, J. L. (2005). Histone H3 methylation by Set2 directs deacetylation of coding regions by Rpd3S to suppress spurious intragenic transcription. Cell *123*, 581-592.

Carruthers, L. M., and Hansen, J. C. (2000). The core histone N termini function independently of linker histones during chromatin condensation. J Biol Chem *275*, 37285-37290.

Cavusoglu, N., Brand, M., Tora, L., and Van Dorsselaer, A. (2003). Novel subunits of the TATA binding protein free TAFII-containing transcription complex identified by matrix-assisted laser desorption/ionization-time of flight mass spectrometry following one-dimensional gel electrophoresis. Proteomics *3*, 217-223.

Chadwick, B. P., Valley, C. M., and Willard, H. F. (2001). Histone variant macroH2A contains two distinct macrochromatin domains capable of directing macroH2A to the inactive X chromosome. Nucleic Acids Res *29*, 2699-2705.

Chadwick, B. P., and Willard, H. F. (2001). Histone H2A variants and the inactive X chromosome: identification of a second macroH2A variant. Hum Mol Genet *10*, 1101-1113.

Chasman, D. I., Flaherty, K. M., Sharp, P. A., and Kornberg, R. D. (1993). Crystal structure of yeast TATA-binding protein and model for interaction with DNA. Proc Natl Acad Sci U S A *90*, 8174-8178.

Chatterjee, S., and Struhl, K. (1995). Connecting a promoter-bound protein to TBP bypasses the need for a transcriptional activation domain. Nature *374*, 820-822.

Cheung, P., Tanner, K. G., Cheung, W. L., Sassone-Corsi, P., Denu, J. M., and Allis, C. D. (2000). Synergistic coupling of histone H3 phosphorylation and acetylation in response to epidermal growth factor stimulation. Mol Cell *5*, 905-915.

Clark, D. J., and Kimura, T. (1990). Electrostatic mechanism of chromatin folding. J Mol Biol *211*, 883-896.

Cockell, M. M., Perrod, S., and Gasser, S. M. (2000). Analysis of sir2p domains required for rDNA and telomeric silencing in saccharomyces cerevisiae. Genetics *155*, 2021.

Coleman, R. A., and Pugh, B. F. (1997). Slow dimer dissociation of the TATA binding protein dictates the kinetics of DNA binding. Proc Natl Acad Sci U S A *94*, 7221-7226.

Coleman, R. A., Taggart, A. K., Benjamin, L. R., and Pugh, B. F. (1995). Dimerization of the TATA binding protein. J Biol Chem *270*, 13842-13849.

Coleman, R. A., Taggart, A. K., Burma, S., Chicca, J. J., 2nd, and Pugh, B. F. (1999). TFIIA regulates TBP and TFIID dimers. Mol Cell *4*, 451-457.

Collart, M. A. (1996). The NOT, SPT3, and MOT1 genes functionally interact to regulate transcription at core promoters. Mol Cell Biol *16*, 6668-6676.

Cormack, B. P., Strubin, M., Ponticelli, A. S., and Struhl, K. (1991). Functional differences between yeast and human TFIID are localized to the highly conserved region. Cell *65*, 341-348.

Cormack, B. P., Strubin, M., Stargell, L. A., and Struhl, K. (1994). Conserved and nonconserved functions of the yeast and human TATA-binding proteins. Genes Dev *8*, 1335-1343.

Cormack, B. P., and Struhl, K. (1992). The TATA-binding protein is required for transcription by all three nuclear RNA polymerases in yeast cells. Cell *69*, 685-696.

Cosgrove, M. S., and Wolberger, C. (2005). How does the histone code work? Biochem Cell Biol *83*, 468-476.

Cox, J. M., Hayward, M. M., Sanchez, J. F., Gegnas, L. D., van der Zee, S., Dennis, J. H., Sigler, P. B., and Schepartz, A. (1997). Bidirectional binding of the TATA box binding protein to the TATA box. Proc Natl Acad Sci U S A *94*, 13475-13480.

Creton, S., Svejstrup, J. Q., and Collart, M. A. (2002). The NC2 alpha and beta subunits play different roles in vivo. Genes Dev *16*, 3265-3276.

Daniel, J. A., Torok, M. S., Sun, Z. W., Schieltz, D., Allis, C. D., Yates, J. R., 3rd, and Grant, P. A. (2004). Deubiquitination of histone H2B by a yeast acetyltransferase complex regulates transcription. J Biol Chem *279*, 1867-1871.

Davey, C. A., and Richmond, T. J. (2002). DNA-dependent divalent cation binding in the nucleosome core particle. Proc Natl Acad Sci U S A *99*, 11169-11174.

Davey, C. A., Sargent, D. F., Luger, K., Maeder, A. W., and Richmond, T. J. (2002). Solvent mediated interactions in the structure of the nucleosome core particle at 1.9 a resolution. J Mol Biol *319*, 1097-1113.

Denko, N., Wernke-Dollries, K., Johnson, A. B., Hammond, E., Chiang, C. M., and Barton, M. C. (2003). Hypoxia actively represses transcription by inducing negative cofactor 2 (Dr1/DrAP1) and blocking preinitiation complex assembly. J Biol Chem *278*, 5744-5749.

Dhillon, N., Oki, M., Szyjka, S. J., Aparicio, O. M., and Kamakaka, R. T. (2006). H2A.Z functions to regulate progression through the cell cycle. Mol Cell Biol *26*, 489-501.

Dorigo, B., Schalch, T., Bystricky, K., and Richmond, T. J. (2003). Chromatin fiber folding: requirement for the histone H4 N-terminal tail. J Mol Biol *327*, 85-96.

Dudley, A. M., Rougeulle, C., and Winston, F. (1999). The Spt components of SAGA facilitate TBP binding to a promoter at a post-activator-binding step in vivo. Genes Dev *13*, 2940-2945.

Dynlacht, B. D., Hoey, T., and Tjian, R. (1991). Isolation of coactivators associated with the TATA-binding protein that mediate transcriptional activation. Cell *66*, 563-576.

Eisenmann, D. M., Arndt, K. M., Ricupero, S. L., Rooney, J. W., and Winston, F. (1992). SPT3 interacts with TFIID to allow normal transcription in Saccharomyces cerevisiae. Genes Dev *6*, 1319-1331.

Eisenmann, D. M., Chapon, C., Roberts, S. M., Dollard, C., and Winston, F. (1994). The Saccharomyces cerevisiae SPT8 gene encodes a very acidic protein that is functionally related to SPT3 and TATA-binding protein. Genetics *137*, 647-657.

Fang, J., Chen, T., Chadwick, B., Li, E., and Zhang, Y. (2004). Ring1b-mediated H2A ubiquitination associates with inactive X chromosomes and is involved in initiation of X inactivation. J Biol Chem *279*, 52812-52815.

Finch, J. T., and Klug, A. (1976). Solenoidal model for superstructure in chromatin. Proc Natl Acad Sci U S A *73*, 1897-1901.

Gangloff, Y. G., Sanders, S. L., Romier, C., Kirschner, D., Weil, P. A., Tora, L., and Davidson, I. (2001). Histone folds mediate selective heterodimerization of yeast

TAF(II)25 with TFIID components yTAF(II)47 and yTAF(II)65 and with SAGA component ySPT7. Mol Cell Biol *21*, 1841-1853.

Gardner, R. G., Nelson, Z. W., and Gottschling, D. E. (2005). Ubp10/Dot4p regulates the persistence of ubiquitinated histone H2B: distinct roles in telomeric silencing and general chromatin. Mol Cell Biol *25*, 6123-6139.

Geisberg, J. V., Holstege, F. C., Young, R. A., and Struhl, K. (2001). Yeast NC2 associates with the RNA polymerase II preinitiation complex and selectively affects transcription in vivo. Mol Cell Biol *21*, 2736-2742.

Geisberg, J. V., Moqtaderi, Z., Kuras, L., and Struhl, K. (2002). Mot1 associates with transcriptionally active promoters and inhibits association of NC2 in Saccharomyces cerevisiae. Mol Cell Biol *22*, 8122-8134.

Georgakopoulos, T., Gounalaki, N., and Thireos, G. (1995). Genetic evidence for the interaction of the yeast transcriptional co-activator proteins GCN5 and ADA2. Mol Gen Genet *246*, 723-728.

Georgakopoulos, T., and Thireos, G. (1992). Two distinct yeast transcriptional activators require the function of the GCN5 protein to promote normal levels of transcription. Embo J *11*, 4145-4152.

Ghosh, G., and Van Duyne, G. D. (1996). Pieces of the puzzle: assembling the preinitiation complex of Pol II. Structure *4*, 891-895.

Gill, G. (2005). Something about SUMO inhibits transcription. Curr Opin Genet Dev *15*, 536-541.

Gill, G., and Tjian, R. (1991). A highly conserved domain of TFIID displays species specificity in vivo. Cell *65*, 333-340.

Goppelt, A., and Meisterernst, M. (1996). Characterization of the basal inhibitor of class II transcription NC2 from Saccharomyces cerevisiae. Nucleic Acids Res *24*, 4450-4455.

Goto, H., Yasui, Y., Nigg, E. A., and Inagaki, M. (2002). Aurora-B phosphorylates Histone H3 at serine28 with regard to the mitotic chromosome condensation. Genes Cells *7*, 11-17.

Grant, P. A., Duggan, L., Cote, J., Roberts, S. M., Brownell, J. E., Candau, R., Ohba, R., Owen-Hughes, T., Allis, C. D., Winston, F., *et al.* (1997). Yeast Gcn5 functions in two multisubunit complexes to acetylate nucleosomal histones: characterization of an Ada complex and the SAGA (Spt/Ada) complex. Genes Dev *11*, 1640-1650.

Grant, P. A., Schieltz, D., Pray-Grant, M. G., Steger, D. J., Reese, J. C., Yates, J. R., 3rd, and Workman, J. L. (1998). A subset of TAF(II)s are integral components of the SAGA

complex required for nucleosome acetylation and transcriptional stimulation. Cell *94*, 45-53.

Gray, S. G., and Teh, B. T. (2001). Histone acetylation/deacetylation and cancer: an "open" and "shut" case? Curr Mol Med *1*, 401-429.

Green, M. R. (2000). TBP-associated factors (TAFIIs): multiple, selective transcriptional mediators in common complexes. Trends Biochem Sci *25*, 59-63.

Hahn, S., Buratowski, S., Sharp, P. A., and Guarente, L. (1989a). Isolation of the gene encoding the yeast TATA binding protein TFIID: a gene identical to the SPT15 suppressor of Ty element insertions. Cell *58*, 1173-1181.

Hahn, S., Buratowski, S., Sharp, P. A., and Guarente, L. (1989b). Yeast TATA-binding protein TFIID binds to TATA elements with both consensus and nonconsensus DNA sequences. Proc Natl Acad Sci U S A *86*, 5718-5722.

Harvey, A. C., and Downs, J. A. (2004). What functions do linker histones provide? Mol Microbiol *53*, 771-775.

Hassan, A. H., Prochasson, P., Neely, K. E., Galasinski, S. C., Chandy, M., Carrozza, M. J., and Workman, J. L. (2002). Function and selectivity of bromodomains in anchoring chromatin-modifying complexes to promoter nucleosomes. Cell *111*, 369-379.

Henry, K. W., Wyce, A., Lo, W. S., Duggan, L. J., Emre, N. C., Kao, C. F., Pillus, L., Shilatifard, A., Osley, M. A., and Berger, S. L. (2003). Transcriptional activation via sequential histone H2B ubiquitylation and deubiquitylation, mediated by SAGA-associated Ubp8. Genes Dev *17*, 2648-2663.

Hoey, T., Dynlacht, B. D., Peterson, M. G., Pugh, B. F., and Tjian, R. (1990). Isolation and characterization of the Drosophila gene encoding the TATA box binding protein, TFIID. Cell *61*, 1179-1186.

Hoffmann, A., Chiang, C. M., Oelgeschlager, T., Xie, X., Burley, S. K., Nakatani, Y., and Roeder, R. G. (1996). A histone octamer-like structure within TFIID. Nature *380*, 356-359.

Hong, L., Schroth, G. P., Matthews, H. R., Yau, P., and Bradbury, E. M. (1993). Studies of the DNA binding properties of histone H4 amino terminus. Thermal denaturation studies reveal that acetylation markedly reduces the binding constant of the H4 "tail" to DNA. J Biol Chem *268*, 305-314.

Horiuchi, J., Silverman, N., Marcus, G. A., and Guarente, L. (1995). ADA3, a putative transcriptional adaptor, consists of two separable domains and interacts with ADA2 and GCN5 in a trimeric complex. Mol Cell Biol *15*, 1203-1209.

Howe, L., Auston, D., Grant, P., John, S., Cook, R. G., Workman, J. L., and Pillus, L. (2001). Histone H3 specific acetyltransferases are essential for cell cycle progression. Genes Dev *15*, 3144-3154.

Huisinga, K. L., and Pugh, B. F. (2004). A genome-wide housekeeping role for TFIID and a highly regulated stress-related role for SAGA in Saccharomyces cerevisiae. Mol Cell *13*, 573-585.

Hyland, E. M., Cosgrove, M. S., Molina, H., Wang, D., Pandey, A., Cottee, R. J., and Boeke, J. D. (2005). Insights into the role of histone H3 and histone H4 core modifiable residues in Saccharomyces cerevisiae. Mol Cell Biol *25*, 10060-10070.

Igo-Kemenes, T., Horz, W., and Zachau, H. G. (1982). Chromatin. Annu Rev Biochem *51*, 89-121.

Ingvarsdottir, K., Krogan, N. J., Emre, N. C., Wyce, A., Thompson, N. J., Emili, A., Hughes, T. R., Greenblatt, J. F., and Berger, S. L. (2005). H2B ubiquitin protease Ubp8 and Sgf11 constitute a discrete functional module within the Saccharomyces cerevisiae SAGA complex. Mol Cell Biol *25*, 1162-1172.

Jackson-Fisher, A. J., Chitikila, C., Mitra, M., and Pugh, B. F. (1999). A role for TBP dimerization in preventing unregulated gene expression. Mol Cell *3*, 717-727.

Jacobs, S. A., Taverna, S. D., Zhang, Y., Briggs, S. D., Li, J., Eissenberg, J. C., Allis, C. D., and Khorasanizadeh, S. (2001). Specificity of the HP1 chromo domain for the methylated N-terminus of histone H3. Embo J *20*, 5232-5241.

Jenuwein, T., and Allis, C. D. (2001). Translating the histone code. Science *293*, 1074-1080.

Kaeberlein, M., Kirkland, K. T., Fields, S., and Kennedy, B. K. (2005a). Genes determining yeast replicative life span in a long-lived genetic background. Mech Ageing Dev *126*, 491-504.

Kaeberlein, M., Powers, R. W., 3rd, Steffen, K. K., Westman, E. A., Hu, D., Dang, N., Kerr, E. O., Kirkland, K. T., Fields, S., and Kennedy, B. K. (2005b). Regulation of yeast replicative life span by TOR and Sch9 in response to nutrients. Science *310*, 1193-1196.

Kamada, K., Shu, F., Chen, H., Malik, S., Stelzer, G., Roeder, R. G., Meisterernst, M., and Burley, S. K. (2001). Crystal structure of negative cofactor 2 recognizing the TBP-DNA transcription complex. Cell *106*, 71-81.

Kamakaka, R. T., and Biggins, S. (2005). Histone variants: deviants? Genes Dev *19*, 295-310.

Kao, C. F., Hillyer, C., Tsukuda, T., Henry, K., Berger, S., and Osley, M. A. (2004). Rad6 plays a role in transcriptional activation through ubiquitylation of histone H2B. Genes Dev *18*, 184-195.

Kasten, M., Szerlong, H., Erdjument-Bromage, H., Tempst, P., Werner, M., and Cairns, B. R. (2004). Tandem bromodomains in the chromatin remodeler RSC recognize acetylated histone H3 Lys14. Embo J *23*, 1348-1359.

Kays, A. R., and Schepartz, A. (2000). Virtually unidirectional binding of TBP to the AdMLP TATA box within the quaternary complex with TFIIA and TFIIB. Chem Biol *7*, 601-610.

Keogh, M. C., Mennella, T. A., Sawa, C., Berthelet, S., Krogan, N. J., Wolek, A., Podolny, V., Carpenter, L. R., Greenblatt, J. F., Baetz, K., and Buratowski, S. (2006). The Saccharomyces cerevisiae histone H2A variant Htz1 is acetylated by NuA4. Genes Dev *20*, 660-665.

Kim, J. L., Nikolov, D. B., and Burley, S. K. (1993a). Co-crystal structure of TBP recognizing the minor groove of a TATA element. Nature *365*, 520-527.

Kim, M., Park, C. H., Lee, M. S., Carlson, B. A., Hatfield, D. L., and Lee, B. J. (2003). A novel TBP-interacting zinc finger protein represses transcription by inhibiting the recruitment of TFIIA and TFIIB. Biochem Biophys Res Commun *306*, 231-238.

Kim, T. K., Zhao, Y., Ge, H., Bernstein, R., and Roeder, R. G. (1995). TATA-binding protein residues implicated in a functional interplay between negative cofactor NC2 (Dr1) and general factors TFIIA and TFIIB. J Biol Chem *270*, 10976-10981.

Kim, Y., Geiger, J. H., Hahn, S., and Sigler, P. B. (1993b). Crystal structure of a yeast TBP/TATA-box complex. Nature *365*, 512-520.

Kirchner, J., Sanders, S. L., Klebanow, E., and Weil, P. A. (2001). Molecular genetic dissection of TAF25, an essential yeast gene encoding a subunit shared by TFIID and SAGA multiprotein transcription factors. Mol Cell Biol *21*, 6668-6680.

Klebanow, E. R., Poon, D., Zhou, S., and Weil, P. A. (1996). Isolation and characterization of TAF25, an essential yeast gene that encodes an RNA polymerase II-specific TATA-binding protein-associated factor. J Biol Chem *271*, 13706-13715.

Klein, C., and Struhl, K. (1994). Increased recruitment of TATA-binding protein to the promoter by transcriptional activation domains in vivo. Science *266*, 280-282.

Kokubo, T., Swanson, M. J., Nishikawa, J. I., Hinnebusch, A. G., and Nakatani, Y. (1998). The yeast TAF145 inhibitory domain and TFIIA competitively bind to TATA-binding protein. Mol Cell Biol *18*, 1003-1012.

Kotani, T., Miyake, T., Tsukihashi, Y., Hinnebusch, A. G., Nakatani, Y., Kawaichi, M., and Kokubo, T. (1998). Identification of highly conserved amino-terminal segments of dTAFII230 and yTAFII145 that are functionally interchangeable for inhibiting TBP-DNA interactions in vitro and in promoting yeast cell growth in vivo. J Biol Chem *273*, 32254-32264.

Kou, H., Irvin, J. D., Huisinga, K. L., Mitra, M., and Pugh, B. F. (2003). Structural and functional analysis of mutations along the crystallographic dimer interface of the yeast TATA binding protein. Mol Cell Biol *23*, 3186-3201.

Kouzarides, T. (2002). Histone methylation in transcriptional control. Curr Opin Genet Dev *12*, 198-209.

Kristjuhan, A., Walker, J., Suka, N., Grunstein, M., Roberts, D., Cairns, B. R., and Svejstrup, J. Q. (2002). Transcriptional inhibition of genes with severe histone h3 hypoacetylation in the coding region. Mol Cell *10*, 925-933.

Kuras, L., Kosa, P., Mencia, M., and Struhl, K. (2000). TAF-Containing and TAF-independent forms of transcriptionally active TBP in vivo. Science *288*, 1244-1248.

Kurdistani, S. K., and Grunstein, M. (2003). Histone acetylation and deacetylation in yeast. Nat Rev Mol Cell Biol *4*, 276-284.

Lamming, D. W., Latorre-Esteves, M., Medvedik, O., Wong, S. N., Tsang, F. A., Wang, C., Lin, S. J., and Sinclair, D. A. (2005). HST2 mediates SIR2-independent life-span extension by calorie restriction. Science *309*, 1861-1864.

Larschan, E., and Winston, F. (2001). The S. cerevisiae SAGA complex functions in vivo as a coactivator for transcriptional activation by Gal4. Genes Dev *15*, 1946-1956.

Lee, K. K., Florens, L., Swanson, S. K., Washburn, M. P., and Workman, J. L. (2005). The deubiquitylation activity of Ubp8 is dependent upon Sgf11 and its association with the SAGA complex. Mol Cell Biol *25*, 1173-1182.

Lee, K. K., Prochasson, P., Florens, L., Swanson, S. K., Washburn, M. P., and Workman, J. L. (2004). Proteomic analysis of chromatin-modifying complexes in Saccharomyces cerevisiae identifies novel subunits. Biochem Soc Trans *32*, 899-903.

Lee, M., and Struhl, K. (2001). Multiple functions of the nonconserved N-terminal domain of yeast TATA-binding protein. Genetics *158*, 87-93.

Lee, T. I., Causton, H. C., Holstege, F. C., Shen, W. C., Hannett, N., Jennings, E. G., Winston, F., Green, M. R., and Young, R. A. (2000). Redundant roles for the TFIID and SAGA complexes in global transcription. Nature *405*, 701-704.

Lemaire, M., and Collart, M. A. (2000). The TATA-binding protein-associated factor yTafII19p functionally interacts with components of the global transcriptional regulator Ccr4-Not complex and physically interacts with the Not5 subunit. J Biol Chem *275*, 26925-26934.

Li, B., Pattenden, S. G., Lee, D., Gutierrez, J., Chen, J., Seidel, C., Gerton, J., and Workman, J. L. (2005). Preferential occupancy of histone variant H2AZ at inactive promoters influences local histone modifications and chromatin remodeling. Proc Natl Acad Sci U S A *102*, 18385-18390.

Li, X. Y., Bhaumik, S. R., and Green, M. R. (2000). Distinct classes of yeast promoters revealed by differential TAF recruitment. Science *288*, 1242-1244.

Li, X. Y., Bhaumik, S. R., Zhu, X., Li, L., Shen, W. C., Dixit, B. L., and Green, M. R. (2002). Selective recruitment of TAFs by yeast upstream activating sequences. Implications for eukaryotic promoter structure. Curr Biol *12*, 1240-1244.

Lo, W. S., Duggan, L., Emre, N. C., Belotserkovskya, R., Lane, W. S., Shiekhattar, R., and Berger, S. L. (2001). Snf1--a histone kinase that works in concert with the histone acetyltransferase Gcn5 to regulate transcription. Science *293*, 1142-1146.

Lo, W. S., Trievel, R. C., Rojas, J. R., Duggan, L., Hsu, J. Y., Allis, C. D., Marmorstein, R., and Berger, S. L. (2000). Phosphorylation of serine 10 in histone H3 is functionally linked in vitro and in vivo to Gcn5-mediated acetylation at lysine 14. Mol Cell *5*, 917-926.

Lowary, P. T., and Widom, J. (1998). New DNA sequence rules for high affinity binding to histone octamer and sequence-directed nucleosome positioning. J Mol Biol *276*, 19-42.

Luger, K., and Hansen, J. C. (2005). Nucleosome and chromatin fiber dynamics. Curr Opin Struct Biol *15*, 188-196.

Luger, K., Mader, A. W., Richmond, R. K., Sargent, D. F., and Richmond, T. J. (1997). Crystal structure of the nucleosome core particle at 2.8 A resolution. Nature *389*, 251-260.

Ma, D., Olave, I., Merino, A., and Reinberg, D. (1996). Separation of the transcriptional coactivator and antirepression functions of transcription factor IIA. Proc Natl Acad Sci U S A *93*, 6583-6588.

Ma, X. J., Wu, J., Altheim, B. A., Schultz, M. C., and Grunstein, M. (1998). Deposition-related sites K5/K12 in histone H4 are not required for nucleosome deposition in yeast. Proc Natl Acad Sci U S A *95*, 6693-6698.

Marcus, G. A., Silverman, N., Berger, S. L., Horiuchi, J., and Guarente, L. (1994). Functional similarity and physical association between GCN5 and ADA2: putative transcriptional adaptors. Embo J *13*, 4807-4815.

Maresca, T. J., Freedman, B. S., and Heald, R. (2005). Histone H1 is essential for mitotic chromosome architecture and segregation in Xenopus laevis egg extracts. J Cell Biol *169*, 859-869.

Margueron, R., Trojer, P., and Reinberg, D. (2005). The key to development: interpreting the histone code? Curr Opin Genet Dev *15*, 163-176.

Martinez, E., Chiang, C. M., Ge, H., and Roeder, R. G. (1994). TATA-binding protein-associated factor(s) in TFIID function through the initiator to direct basal transcription from a TATA-less class II promoter. Embo J *13*, 3115-3126.

Martinez, E., Kundu, T. K., Fu, J., and Roeder, R. G. (1998). A human SPT3-TAFII31-GCN5-L acetylase complex distinct from transcription factor IID. J Biol Chem *273*, 23781-23785.

Mateescu, B., England, P., Halgand, F., Yaniv, M., and Muchardt, C. (2004). Tethering of HP1 proteins to chromatin is relieved by phosphoacetylation of histone H3. EMBO Rep *5*, 490-496.

Melchior, F. (2000). SUMO--nonclassical ubiquitin. Annu Rev Cell Dev Biol *16*, 591-626.

Michel, B., Komarnitsky, P., and Buratowski, S. (1998). Histone-like TAFs are essential for transcription in vivo. Mol Cell *2*, 663-673.

Millar, C. B., Xu, F., Zhang, K., and Grunstein, M. (2006). Acetylation of H2AZ Lys 14 is associated with genome-wide gene activity in yeast. Genes Dev *20*, 711-722.

Min, J., Feng, Q., Li, Z., Zhang, Y., and Xu, R. M. (2003). Structure of the catalytic domain of human DOT1L, a non-SET domain nucleosomal histone methyltransferase. Cell *112*, 711-723.

Moqtaderi, Z., Bai, Y., Poon, D., Weil, P. A., and Struhl, K. (1996a). TBP-associated factors are not generally required for transcriptional activation in yeast. Nature *383*, 188-191.

Moqtaderi, Z., Yale, J. D., Struhl, K., and Buratowski, S. (1996b). Yeast homologues of higher eukaryotic TFIID subunits. Proc Natl Acad Sci U S A *93*, 14654-14658.

Nikolov, D. B., Chen, H., Halay, E. D., Usheva, A. A., Hisatake, K., Lee, D. K., Roeder, R. G., and Burley, S. K. (1995). Crystal structure of a TFIIB-TBP-TATA-element ternary complex. Nature *377*, 119-128.

Nikolov, D. B., Hu, S. H., Lin, J., Gasch, A., Hoffmann, A., Horikoshi, M., Chua, N. H., Roeder, R. G., and Burley, S. K. (1992). Crystal structure of TFIID TATA-box binding protein. Nature *360*, 40-46.

Nourani, A., Utley, R. T., Allard, S., and Cote, J. (2004). Recruitment of the NuA4 complex poises the PHO5 promoter for chromatin remodeling and activation. Embo J *23*, 2597-2607.

Ogryzko, V. V. (2001). Mammalian histone acetyltransferases and their complexes. Cell Mol Life Sci *58*, 683-692.

Ogryzko, V. V., Kotani, T., Zhang, X., Schiltz, R. L., Howard, T., Yang, X. J., Howard, B. H., Qin, J., and Nakatani, Y. (1998). Histone-like TAFs within the PCAF histone acetylase complex. Cell *94*, 35-44.

Ornaghi, P., Ballario, P., Lena, A. M., Gonzalez, A., and Filetici, P. (1999). The bromodomain of Gcn5p interacts in vitro with specific residues in the N terminus of histone H4. J Mol Biol *287*, 1-7.

Oudet, P., Gross-Bellard, M., and Chambon, P. (1975). Electron microscopic and biochemical evidence that chromatin structure is a repeating unit. Cell *4*, 281-300.

Peterson, C. L. (2002). HDAC's at work: everyone doing their part. Mol Cell *9*, 921-922.

Peterson, C. L., and Laniel, M. A. (2004). Histones and histone modifications. Curr Biol *14*, R546-551.

Peterson, M. G., Tanese, N., Pugh, B. F., and Tjian, R. (1990). Functional domains and upstream activation properties of cloned human TATA binding protein. Science *248*, 1625-1630.

Petri, V., Hsieh, M., Jamison, E., and Brenowitz, M. (1998). DNA sequence-specific recognition by the Saccharomyces cerevisiae "TATA" binding protein: promoter-dependent differences in the thermodynamics and kinetics of binding. Biochemistry *37*, 15842-15849.

Pina, B., Berger, S., Marcus, G. A., Silverman, N., Agapite, J., and Guarente, L. (1993). ADA3: a gene, identified by resistance to GAL4-VP16, with properties similar to and different from those of ADA2. Mol Cell Biol *13*, 5981-5989.

Porter, I. M., Khoudoli, G. A., and Swedlow, J. R. (2004). Chromosome condensation: DNA compaction in real time. Curr Biol *14*, R554-556.

Pray-Grant, M. G., Daniel, J. A., Schieltz, D., Yates, J. R., 3rd, and Grant, P. A. (2005). Chd1 chromodomain links histone H3 methylation with SAGA- and SLIK-dependent acetylation. Nature *433*, 434-438.

Pugh, B. F., and Tjian, R. (1990). Mechanism of transcriptional activation by Sp1: evidence for coactivators. Cell *61*, 1187-1197.

Pugh, B. F., and Tjian, R. (1991). Transcription from a TATA-less promoter requires a multisubunit TFIID complex. Genes Dev *5*, 1935-1945.

Rea, S., Eisenhaber, F., O'Carroll, D., Strahl, B. D., Sun, Z. W., Schmid, M., Opravil, S., Mechtler, K., Ponting, C. P., Allis, C. D., and Jenuwein, T. (2000). Regulation of chromatin structure by site-specific histone H3 methyltransferases. Nature *406*, 593-599.

Reddy, P., and Hahn, S. (1991). Dominant negative mutations in yeast TFIID define a bipartite DNA-binding region. Cell *65*, 349-357.

Reese, J. C., Apone, L., Walker, S. S., Griffin, L. A., and Green, M. R. (1994). Yeast TAFIIS in a multisubunit complex required for activated transcription. Nature *371*, 523-527.

Reeves, W. M., and Hahn, S. (2005). Targets of the Gal4 transcription activator in functional transcription complexes. Mol Cell Biol *25*, 9092-9102.

Rine, J., and Herskowitz, I. (1987). Four genes responsible for a position effect on expression from HML and HMR in Saccharomyces cerevisiae. Genetics *116*, 9-22.

Robyr, D., Suka, Y., Xenarios, I., Kurdistani, S. K., Wang, A., Suka, N., and Grunstein, M. (2002). Microarray deacetylation maps determine genome-wide functions for yeast histone deacetylases. Cell *109*, 437-446.

Rosaleny, L. E., Antunez, O., Ruiz-Garcia, A. B., Perez-Ortin, J. E., and Tordera, V. (2005). Yeast HAT1 and HAT2 deletions have different life-span and transcriptome phenotypes. FEBS Lett *579*, 4063-4068.

Russell, S. J., Steger, K. A., and Johnston, S. A. (1999). Subcellular localization, stoichiometry, and protein levels of 26 S proteasome subunits in yeast. J Biol Chem *274*, 21943-21952.

Sanders, S. L., Garbett, K. A., and Weil, P. A. (2002a). Molecular characterization of Saccharomyces cerevisiae TFIID. Mol Cell Biol *22*, 6000-6013.

Sanders, S. L., Jennings, J., Canutescu, A., Link, A. J., and Weil, P. A. (2002b). Proteomics of the eukaryotic transcription machinery: identification of proteins associated with components of yeast TFIID by multidimensional mass spectrometry. Mol Cell Biol *22*, 4723-4738.

Sandman, K., and Reeve, J. N. (2005). Archaeal chromatin proteins: different structures but common function? Curr Opin Microbiol *8*, 656-661.

Santisteban, M. S., Kalashnikova, T., and Smith, M. M. (2000). Histone H2A.Z regulats transcription and is partially redundant with nucleosome remodeling complexes. Cell *103*, 411-422.

Santos-Rosa, H., Schneider, R., Bannister, A. J., Sherriff, J., Bernstein, B. E., Emre, N. C., Schreiber, S. L., Mellor, J., and Kouzarides, T. (2002). Active genes are tri-methylated at K4 of histone H3. Nature *419*, 407-411.

Schalch, T., Duda, S., Sargent, D. F., and Richmond, T. J. (2005). X-ray structure of a tetranucleosome and its implications for the chromatin fibre. Nature *436*, 138-141.

Schneider, R., Bannister, A. J., Myers, F. A., Thorne, A. W., Crane-Robinson, C., and Kouzarides, T. (2004). Histone H3 lysine 4 methylation patterns in higher eukaryotic genes. Nat Cell Biol *6*, 73-77.

Selleck, W., Howley, R., Fang, Q., Podolny, V., Fried, M. G., Buratowski, S., and Tan, S. (2001). A histone fold TAF octamer within the yeast TFIID transcriptional coactivator. Nat Struct Biol *8*, 695-700.

Shiio, Y., and Eisenman, R. N. (2003). Histone sumoylation is associated with transcriptional repression. Proc Natl Acad Sci U S A *100*, 13225-13230.

Shrader, T. E., and Crothers, D. M. (1989). Artificial nucleosome positioning sequences. Proc Natl Acad Sci U S A *86*, 7418-7422.

Shukla, A., Stanojevic, N., Duan, Z., Sen, P., and Bhaumik, S. R. (2006a). Ubp8p, a histone deubiquitinase whose association with SAGA is mediated by Sgf11p, differentially regulates lysine 4 methylation of histone H3 in vivo. Mol Cell Biol *26*, 3339-3352.

Shukla, A., Stanojevic, N., Duan, Z., Shadle, T., and Bhaumik, S. R. (2006b). Functional analysis of H2B-K123 ubiquitination in regulation of H3-K4 methylation and recruitment of RNA polymerase II at the coding sequences of several active genes in vivo. J Biol Chem.

Singer, V. L., Wobbe, C. R., and Struhl, K. (1990). A wide variety of DNA sequences can functionally replace a yeast TATA element for transcriptional activation. Genes Dev *4*, 636-645.

Smith, E. R., Eisen, A., Gu, W., Sattah, M., Pannuti, A., Zhou, J., Cook, R. G., Lucchesi, J. C., and Allis, C. D. (1998). ESA1 is a histone acetyltransferase that is essential for growth in yeast. Proc Natl Acad Sci U S A *95*, 3561-3565.

Smith, K. P., Byron, M., Clemson, C. M., and Lawrence, J. B. (2004). Ubiquitinated proteins including uH2A on the human and mouse inactive X chromosome: enrichment in gene rich bands. Chromosoma *113*, 324-335.

Spencer, J. V., and Arndt, K. M. (2002). A TATA binding protein mutant with increased affinity for DNA directs transcription from a reversed TATA sequence in vivo. Mol Cell Biol *22*, 8744-8755.

Sterner, D. E., Grant, P. A., Roberts, S. M., Duggan, L. J., Belotserkovskaya, R., Pacella, L. A., Winston, F., Workman, J. L., and Berger, S. L. (1999). Functional organization of the yeast SAGA complex: distinct components involved in structural integrity, nucleosome acetylation, and TATA-binding protein interaction. Mol Cell Biol *19*, 86-98.

Strahl, B. D., and Allis, C. D. (2000). The language of covalent histone modifications. Nature *403*, 41-45.

Suka, N., Suka, Y., Carmen, A. A., Wu, J., and Grunstein, M. (2001). Highly specific antibodies determine histone acetylation site usage in yeast heterochromatin and euchromatin. Mol Cell *8*, 473-479.

Sullivan, S. A., Aravind, L., Makalowska, I., Baxevanis, A. D., and Landsman, D. (2000). The histone database: a comprehensive WWW resource for histones and histone fold-containing proteins. Nucleic Acids Res *28*, 320-322.

Swedlow, J. R., and Hirano, T. (2003). The making of the mitotic chromosome: modern insights into classical questions. Mol Cell *11*, 557-569.

Taggart, A. K., and Pugh, B. F. (1996). Dimerization of TFIID when not bound to DNA. Science *272*, 1331-1333.

Tan, S., Hunziker, Y., Sargent, D. F., and Richmond, T. J. (1996). Crystal structure of a yeast TFIIA/TBP/DNA complex. Nature *381*, 127-151.

Tanese, N., Pugh, B. F., and Tjian, R. (1991). Coactivators for a proline-rich activator purified from the multisubunit human TFIID complex. Genes Dev *5*, 2212-2224.

Tanner, K. G., Trievel, R. C., Kuo, M. H., Howard, R. M., Berger, S. L., Allis, C. D., Marmorstein, R., and Denu, J. M. (1999). Catalytic mechanism and function of invariant glutamic acid 173 from the histone acetyltransferase GCN5 transcriptional coactivator. J Biol Chem *274*, 18157-18160.

Teng, Y., Yu, Y., and Waters, R. (2002). The Saccharomyces cerevisiae histone acetyltransferase Gcn5 has a role in the photoreactivation and nucleotide excision repair of UV-induced cyclobutane pyrimidine dimers in the MFA2 gene. J Mol Biol *316*, 489-499.

Thomas, J. O., and Kornberg, R. D. (1975). An octamer of histones in chromatin and free in solution. Proc Natl Acad Sci U S A *72*, 2626-2630.

Tran, H. G., Steger, D. J., Iyer, V. R., and Johnson, A. D. (2000). The chromo domain protein chd1p from budding yeast is an ATP-dependent chromatin-modifying factor. Embo J *19*, 2323-2331.

Tse, C., Sera, T., Wolffe, A. P., and Hansen, J. C. (1998). Disruption of higher-order folding by core histone acetylation dramatically enhances transcription of nucleosomal arrays by RNA polymerase III. Mol Cell Biol *18*, 4629-4638.

Vassilev, A., Yamauchi, J., Kotani, T., Prives, C., Avantaggiati, M. L., Qin, J., and Nakatani, Y. (1998). The 400 kDa subunit of the PCAF histone acetylase complex belongs to the ATM superfamily. Mol Cell *2*, 869-875.

Vogelauer, M., Wu, J., Suka, N., and Grunstein, M. (2000). Global histone acetylation and deacetylation in yeast. Nature *408*, 495-498.

Wang, L., Liu, L., and Berger, S. L. (1998). Critical residues for histone acetylation by Gcn5, functioning in Ada and SAGA complexes, are also required for transcriptional function in vivo. Genes Dev *12*, 640-653.

Widom, J. (1986). Physicochemical studies of the folding of the 100 A nucleosome filament into the 300 A filament. Cation dependence. J Mol Biol *190*, 411-424.

Wieczorek, E., Brand, M., Jacq, X., and Tora, L. (1998). Function of TAF(II)-containing complex without TBP in transcription by RNA polymerase II. Nature *393*, 187-191.

Woodcock, C. L., Frado, L. L., and Rattner, J. B. (1984). The higher-order structure of chromatin: evidence for a helical ribbon arrangement. J Cell Biol *99*, 42-52.

Workman, J. L., and Kingston, R. E. (1998). Alteration of nucleosome structure as a mechanism of transcriptional regulation. Annu Rev Biochem *67*, 545-579.

Xie, J., Collart, M., Lemaire, M., Stelzer, G., and Meisterernst, M. (2000). A single point mutation in TFIIA suppresses NC2 requirement in vivo. Embo J *19*, 672-682.

Yamamoto, T., Matsuda, T., Inoue, T., Matsumura, H., Morikawa, M., Kanaya, S., and Kai, Y. (2006). Crystal structure of TBP-interacting protein (Tk-TIP26) and implications for its inhibition mechanism of the interaction between TBP and TATA-DNA. Protein Sci *15*, 152-161.

Yan, Y., Harper, S., Speicher, D. W., and Marmorstein, R. (2002). The catalytic mechanism of the ESA1 histone acetyltransferase involves a self-acetylated intermediate. Nat Struct Biol *9*, 862-869.

Zhang, H., Roberts, D. N., and Cairns, B. R. (2005). Genome-wide dynamics of Htz1, a histone H2A variant that poises repressed/basal promoters for activation through histone loss. Cell *123*, 219-231.

Zhang, W., Bone, J. R., Edmondson, D. G., Turner, B. M., and Roth, S. Y. (1998). Essential and redundant functions of histone acetylation revealed by mutation of target lysines and loss of the Gcn5p acetyltransferase. Embo J *17*, 3155-3167.

Zhong, C. X., Marshall, J. B., Topp, C., Mroczek, R., Kato, A., Nagaki, K., Birchler, J. A., Jiang, J., and Dawe, R. K. (2002). Centromeric retroelements and satellites interact with maize kinetochore protein CENH3. Plant Cell *14*, 2825-2836.

Zhou, Q., Boyer, T. G., and Berk, A. J. (1993). Factors (TAFs) required for activated transcription interact with TATA box-binding protein conserved core domain. Genes Dev *7*, 180-187.

Chapter 2

Identification of TBP interacting subunits in the yeast SAGA coactivator complex

2.1 Abstract

Recruitment of the TATA-binding protein (TBP) by a coactivator complex to a promoter is an important step for initiation of transcription. Here I examined the interaction between TBP and the SAGA coactivator complex. I analyzed TBP mutants and found that the R171E TBP mutant is defective in the interaction with the SAGA complex. I utilized photo-cross-linking label transfer and pull down assays to identify and confirm the interaction between Spt8 and TBP. SAGA may utilize other subunits to bind to TBP since SAGA complex lacking Spt8 can still interact with TBP, albeit at a lower level. Ada1, which directly photo-cross-links with the TBP, is an additional potential target of TBP. Although Spt3 has been suggested to bind directly to TBP, these results indicate that Spt3 by itself is not sufficient for the interaction with TBP. However, in the context of the SAGA complex, Spt3 contributes to the overall interaction with TBP.

2.2 Introduction

Coactivators play a role in assisting an activator to stimulate transcriptional activation. The SAGA complex is a coactivator complex that can interact with both activator and TBP proteins. Despite the physical interaction, it has not been clearly determined which components of SAGA make contact with TBP. TBP is encoded by the SPT15 gene whose specific mutations can be reversed or suppressed by specific mutations in other related SPT genes, including SPT3 and SPT8 (Eisenmann et al., 1992; Eisenmann et al.,

1994). Out of these two genes, SPT3 has received more initial attention for interaction with TBP. Through the chromatin immunoprecipitation technique (ChIP), several studies have shown that deletion of the SPT3 gene affects the recruitment of yeast TBP to the Gal1 promoter and other SAGA dependent promoters (Bhaumik and Green, 2001; Bhaumik and Green, 2002; Dudley et al., 1999; Larschan and Winston, 2001). Therefore, one could naturally assume a direct interaction between Spt3 in SAGA and TBP protein. However, some *in vitro* binding experiments contradict the conclusion from genetic and ChIP studies. First, Grant et al. have shown that the SAGA complex that loses Spt3, as a result of the temperature sensitive mutation in TAF12, is still able to interact with the yeast TBP (Grant et al., 1998). Second, purified SAGA complex from the *spt8*Δ strain exhibits less binding with TBP compared with the wild type SAGA (Sterner et al., 1999). Third, Warfield et al. have shown that TBP binds to Spt8 directly in a pull down assay, and Spt8 competes with the binding of the transcription factor IIA with TBP (Warfield et al., 2004). Together, those results suggest an interaction between Spt8 in the SAGA complex and the yeast TBP protein.

In this work, I examined the interaction between TBP and the SAGA complex. R171E and T153I TBP mutants were included in this study because the amino acid substitutions at the R171 suppressed the phenotype of spt3 mutants (Eisenmann et al., 1992), while the T153I TBP was shown to be an activation defective mutant (Stargell and Struhl, 1996). I found that the R171E but not the T153I TBP mutant is defective in the interaction with the complex. Using a photo-cross-linking label-transfer technique, I found that Spt8 and Ada1 subunits in the SAGA complex photo-cross-linked with TBP. Pull down experiment confirmed the interaction between Spt8 and TBP. I also show that purified Spt3 is not sufficient for the interaction with TBP. However, the SAGA complex lacking Spt3 negatively affects the interaction with TBP, suggesting that Spt3 may indirectly facilitate the interaction between TBP and the SAGA complex. Additionally, my data show that Ada1 in SAGA complex lacking Spt8 photo-cross-links with TBP. Together, my results suggest a role of Spt and Ada subunits in the regulation of TBP recruitment to a promoter.

2.3 Results

2.3.1 Purification of the yeast SAGA complex

The SAGA complex could be purified in a conventional way or with the TAP tag. I utilized the Flag-tagged Tra1 yeast strain in the conventional technique, which uses nickel-nitrilotriacetic acid agarose (Ni-NTA), a metal affinity resin as the first step of purification, followed by MonoQ fractionations and the Flag Immunoprecipitation (Flag IP) (See **2.5.4**) The Flag-tagged Tra1 yeast strain was created by Dr. Christine Brown a former Postdoctoral scientist in the Workman Lab) (Figure **2-1** A). Purification of the SAGA complex after the MonoQ column and the Flag IP is shown in Figure **2-1** B-E. I also utilized the Tandem Affinity tag (TAP)-tagged Ada1 yeast strain for SAGA purification. As illustrated in Figure **2-2** A, the TAP tag at the C-terminus of Ada1 subunit is comprised of the Calmodulin tag (CBP), the TEV cleavage site (N), and the Protein A tag. Our TAP tag purification for the SAGA complex involves three main steps: the IgG Sepharose and the TEV cleavage, MonoQ fractionations, and the Calmodulin affinity matrix (CAM) (Figure **2-3** A). The wild type Ada1-TAP yeast strain was a gift from Dr. Patrick Grant, the University of Virginia.

Both purification techniques have advantages and disadvantages. For example, without any affinity tag, the native HAT complexes can be purified with the conventional technique at a low purity, which is sufficient for a simple biochemical assay such as the HAT assay (Figure **2-1** D). Because the Flag tag is fused to the Tra1, a shared subunit among the NuA4, SLIK, and SAGA complexes, an additional purification for those complexes after the MonoQ column is necessary. One of the drawbacks of the conventional purification of the SAGA complex is that the resin-bound anti-Flag antibody is expensive. Although I have not performed the simultaneous experiments to compare the SAGA complex purified from the conventional technique and from the TAP tag procedures side by side, I estimate that the conventional purification technique yields approximately 5-10 times less material than the TAP tag purification. Comparing the

amount and the quality of the SAGA complex purified from both techniques, the silver stained gel of the SAGA complex after the second step of the TAP tag procedure shows discrete protein bands and better purity than that purified after the Flag IP in the conventional technique (compare Figure **2-1** E and Figure **2-2** C). It is possible that some material has been lost during the first step of purification using the Ni-NTA resin. Because the SAGA and other coactivator complexes bind to the resin in the absence of a hexahistidine (6x His) tag, the binding affinity of the complex to the Ni-NTA resin is low and inefficient. In contrast, the TAP tag, which contains the Protein A portion of the tag, has a high specificity and efficiently binds to the IgG antibodies linked to the Sepharose resin. Thus, yield is one advantage of using the TAP tag purification technique. One disadvantage of the TAP tag purification is that it requires the use of the tobacco etch virus (TEV) protease, which has to be eliminated from the purified complex. I remove the TEV protease by further purifying the SAGA complex with the MonoQ column and the CAM. Thus, because the TAP tag purification technique yields a higher quality complex, it is a preferred method for the SAGA purification (Figure **2-3**).

The SLIK complex is characterized by the SAGA complex missing Spt8 subunit and the C-terminal truncated Spt7 (Belotserkovskaya et al., 2000; Sterner et al., 2002a; Wu and Winston, 2002). In addition, it has been suggested that the SLIK complex contains Rtg2 as an additional subunit, which is not present in the SAGA complex (Balasubramanian et al., 2002). The presence of the C-terminal truncated Spt7 in *spt8*Δ and *spt8*Δ*spt3*Δ SAGA complexes might suggest a possibility that those complexes were slightly contaminated by the SLIK and the SLIK with *spt3*Δ complexes, respectively. In the MonoQ fractionations, the SLIK complex (purified from the wild type yeast) and the *spt8*Δ SAGA complex (purified from the *spt8*Δ yeast) fractionated at a similar salt concentration (data not shown). Because the TAP-tag is on the Ada1, a shared subunit between the SAGA and SLIK complex, it would not be possible to separate the SLIK from the *spt8*Δ SAGA complex. However, the SLIK complex purified from the wild type yeast contains both full length and C-terminal truncated Spt7 (data not shown). Therefore, the presence of the C-terminal truncated Spt7 in the *spt8*Δ SAGA complex

may not be the best indicator for SLIK contamination. Because the Rtg2 subunit might be a unique characteristic of the SLIK complex (Balasubramanian et al., 2002), deletion of the Rtg2 gene might be a necessary task to remove the SLIK contamination. However, I do not observe a unique, stoichiometric band, which might indicate the Rtg2 subunit within the SLIK complex. In addition, I do not have Western blot results that indicate the presence of this protein within the SLIK complex. Therefore, it may be difficult to judge if there the *spt8*Δ SAGA complex has been contaminated by the SLIK complex, and purifying the *spt8*Δ SAGA from the SLIK complex might not be a trivial task.

2.3.2 The histone acetyl transferase (HAT) assay

The HAT complexes fractionated by the MonoQ column can also be analyzed by the HAT assay, besides the silver staining and the Western blotting techniques. One advantage of the HAT assay is that it measures the enzyme activity of the complex rather than the overall amount of the proteins, some of which might be inactive. For the TAP tag purification, the HAT assay can be a quick method to help select fractions that contain the SAGA complex after the MonoQ fractionations since the SAGA peak is well resolved from the SLIK peak (Figure **2-2** B and C). My protocol for the HAT assay is described in **2.5.5.**

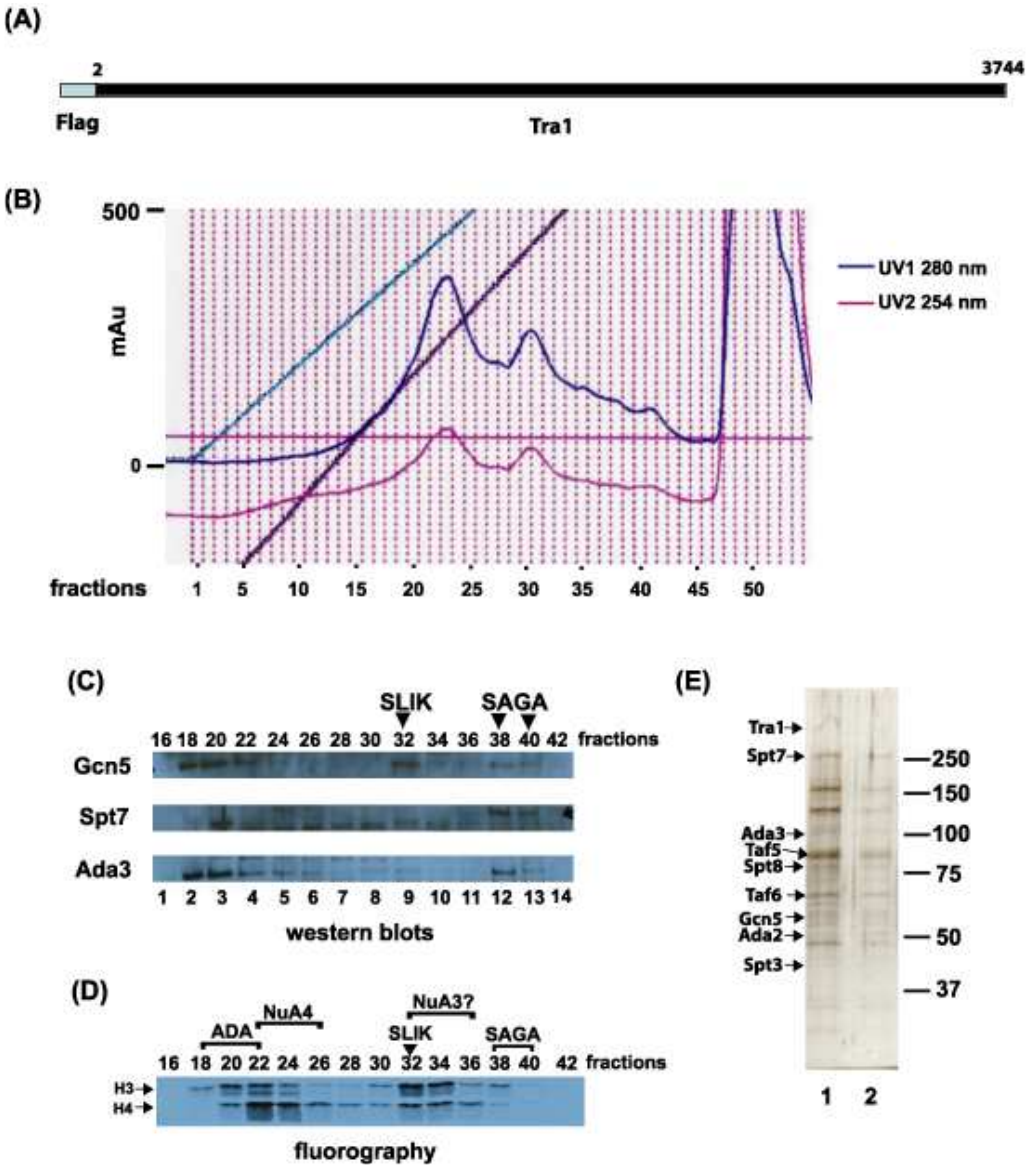

Figure **2-1**: Purification of the SAGA complex with the conventional method from a 6-liter cluture.

(A) Tra1, which is a subunit of the SAGA, SLIK, and NuA4 complexes, is fused with an N-terminal Flag tag. (B) A chromatogram of the MonoQ fractionations of the Ni-NTA eluates, using the AKTA purification system (Pharmarcia). (C) Western blots show some components of the SAGA and SLIK complexes present in those MonoQ fractions. (D) Fluorography of the same MonoQ fractions used in (C). The HeLa cell core histones were used as the HAT assay substrates. (E) A silver stained gel shows some components of the SAGA complex purified after the Flag IP in fraction 1 and 2 (lanes 1 and 2, respectively) from the MonoQ fractions 38-40 in (D).

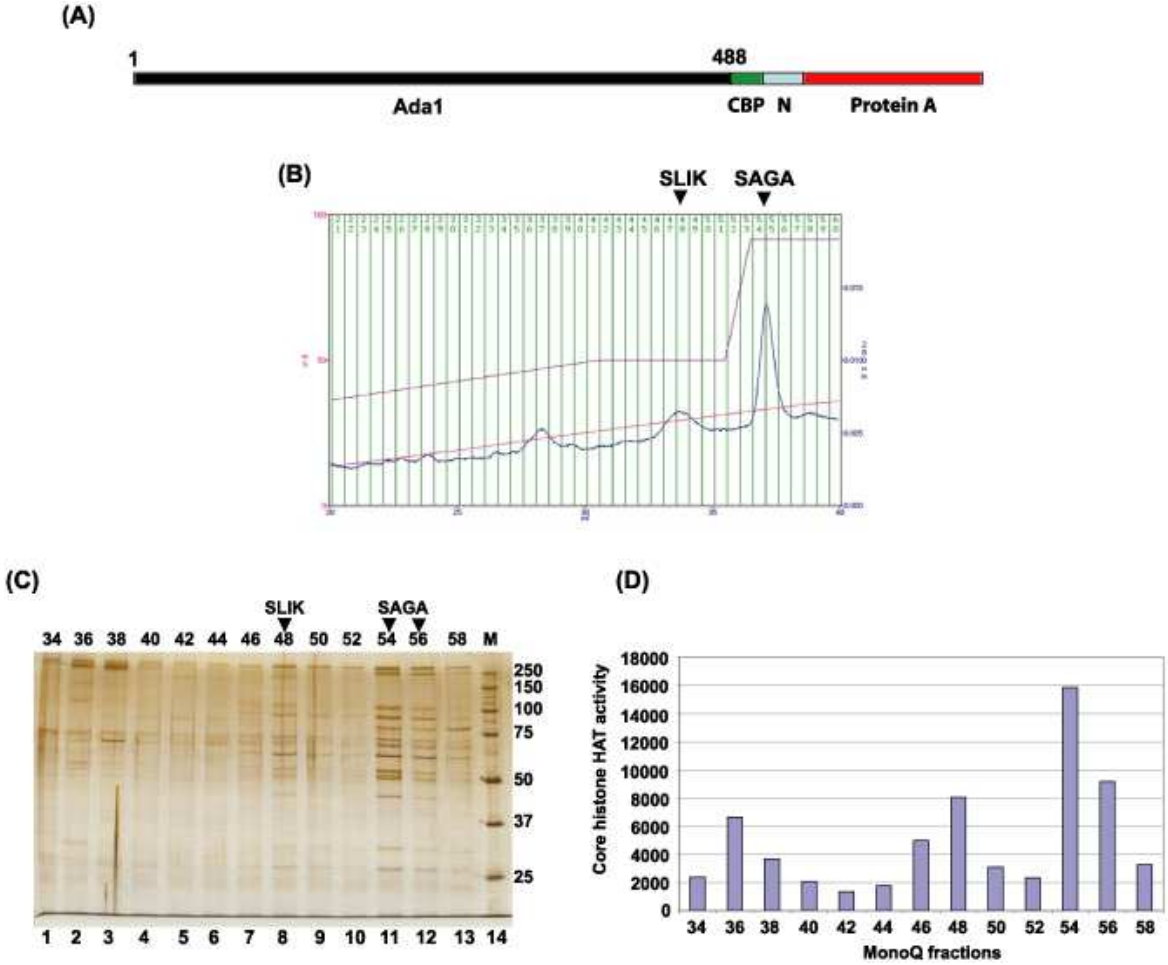

Figure **2-2**: TAP tag purification of the SAGA complex from a 6-liter culture.

Panel (A) shows a schematic representation of the C-terminal TAP-tagged Ada1, which is found in both SAGA and SLIK complex. The TAP tag consists of the CBP affinity tag, TEV cleavage site (N), and the Protein A tag from the N to C terminus, respectively. Panel (B) is a chromatogram of the MonoQ fractionation of the complexes released from the IgG binding to the protein A tag by using the TEV protease which digests at the TEV cleavage site (N). The MonoQ fractionation was performed with the BioCAD Sprint HPLC system. The last two peaks from the right contain the SAGA and SLIK complexes, respectively. (C) A silver stained gel shows purify of the MonoQ fractions from (B). (D) The bar chart shows core histone HAT activity of those MonoQ fractions from (C).

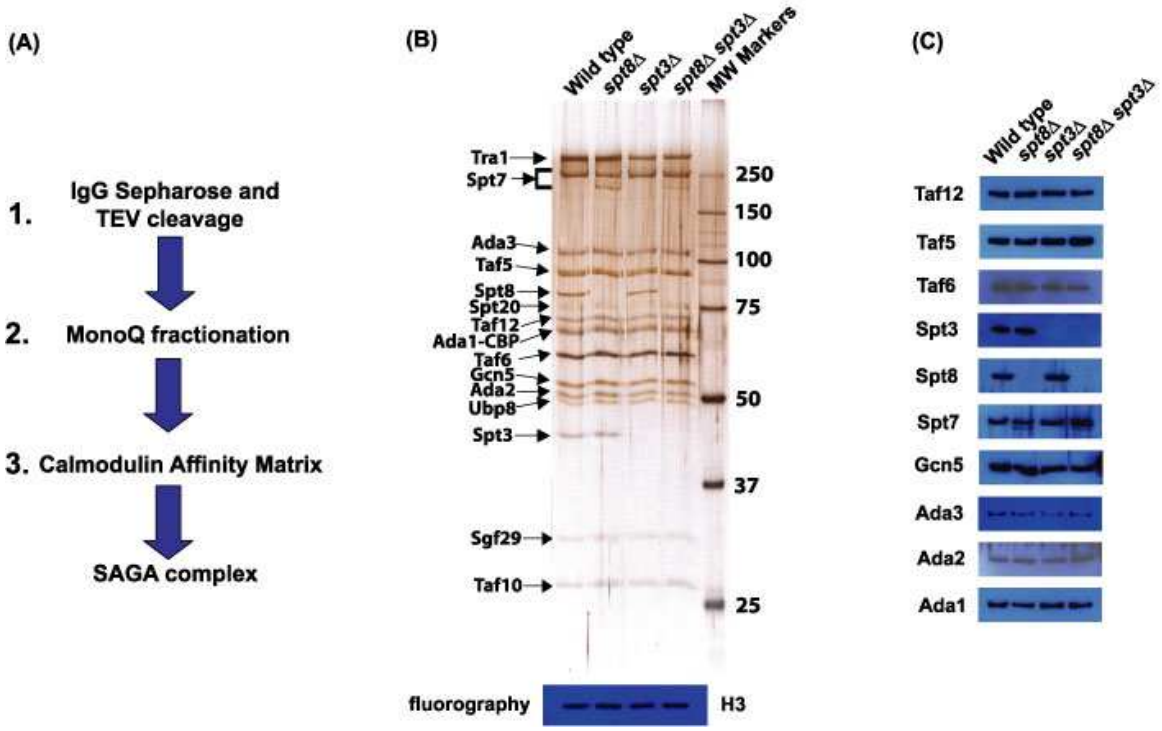

Figure **2-3**: Purification of the SAGA complexes with the TAP tag.

(A) TAP tag purification of the SAGA complexes involves 3 steps: 1) binding to IgG Sepharose and cleavaging with the TEV protease; 2) MonoQ anion-exchange fractionations; and 3) Calmodulin Affinity Matrix. (B) Silver stained gel and fluorography from the HAT assay with the core histones from HeLa cells show a normalized amount and the HAT activity among the SAGA complexes: wild type, *spt8*Δ, *spt3*Δ, and double *spt8*Δ*spt3*Δ SAGA. Panel (C) shows Western blot results of most SAGA subunits after normalization.

It is important to use the right substrate to analyze the specific HAT complex; otherwise the HAT activity obtained will not accurately reflect the overall active amount of the complex. Initially, I analyzed the HAT activity of the complex during purification procedures (i.e. after MonoQ column) by using chicken core histones. However, I discovered that the same SAGA MonoQ fractions possessed a higher HAT activity with core histones extracted from HeLa cells than the core histones from chick blood. Therefore, I analyzed both core histones and long oligo nucleosomes (LON) substrates extracted from chicken blood and HeLa cells in HAT assays using either the NuA4 or the

SAGA complex. With a similar amount of each HAT assay substrates, core histones or LON from different organisms conferred a different level of the HAT activity (Figure **2-4**). As shown in Figure **2-4** A, the purified NuA4 complex (E1-E3) had the highest HAT activity with the chicken LON, but not the HeLa LON. In addition, figure **2-4** C shows that the NuA4 complex acetylated the chicken histone H4 and H2A in LON better than core histones. Because the NuA4 complex fractionated with the MonoQ column was not well resolved from the ADA complex (Figure **2-1** D), the HAT activity of these fraction was not the best representation of the NuA4 complex (Figure **2-4** A and C). Together, I conclude that the purified NuA4 complex prefers acetylating LON to core histones, consistent with previous reports (Allard et al., 1999; Eberharter et al., 1998; Ohba et al., 1999).

In contrast to the NuA4 complex, the SAGA complex preferred core histone to nucleosome acetylation, especially at the histone H3 (Figure **2-4** B and D), consistent with previous published results (Eberharter et al., 1996; Grant et al., 1997). The SAGA complex also acetylated histone H4 in a very low level compared with histone H3 (Figure **2-4** D). Furthermore, the SAGA complex seemed to acetylate HeLa cell core histones better than chicken core histones (Figure **2-4** B and D and Figure **B-1**). Because the core histones isolated from the HeLa cells conferred the best SAGA HAT activity, I isolated core histones and LON from HeLa cells for the HAT assays with the SAGA complex. The protocol for isolating the core histones and LON from the HeLa cells, and more discussion about the HAT activity, are provided in Appendix B.

2.3.3 The SAGA but not NuA4 complex interacts with TBP

One of the functions of the SAGA complex is to recruit TBP to a core promoter; therefore, the complex must have a physical interaction with TBP. The ability of partially purified SAGA complex to interact with TBP *in vitro* has been demonstrated previously (Grant et al., 1998; Sterner et al., 1999). As a simple control experiment, I need to show that my purified SAGA complex can interact with TBP. Thus, I performed

pull down experiments using a tagged TBP to test its interaction with the SAGA complex. The initial pull down experiments were conducted using the CBP-tagged TBP to pull down the Flag-tagged NuA4 and the Flag-tagged SAGA complexes.

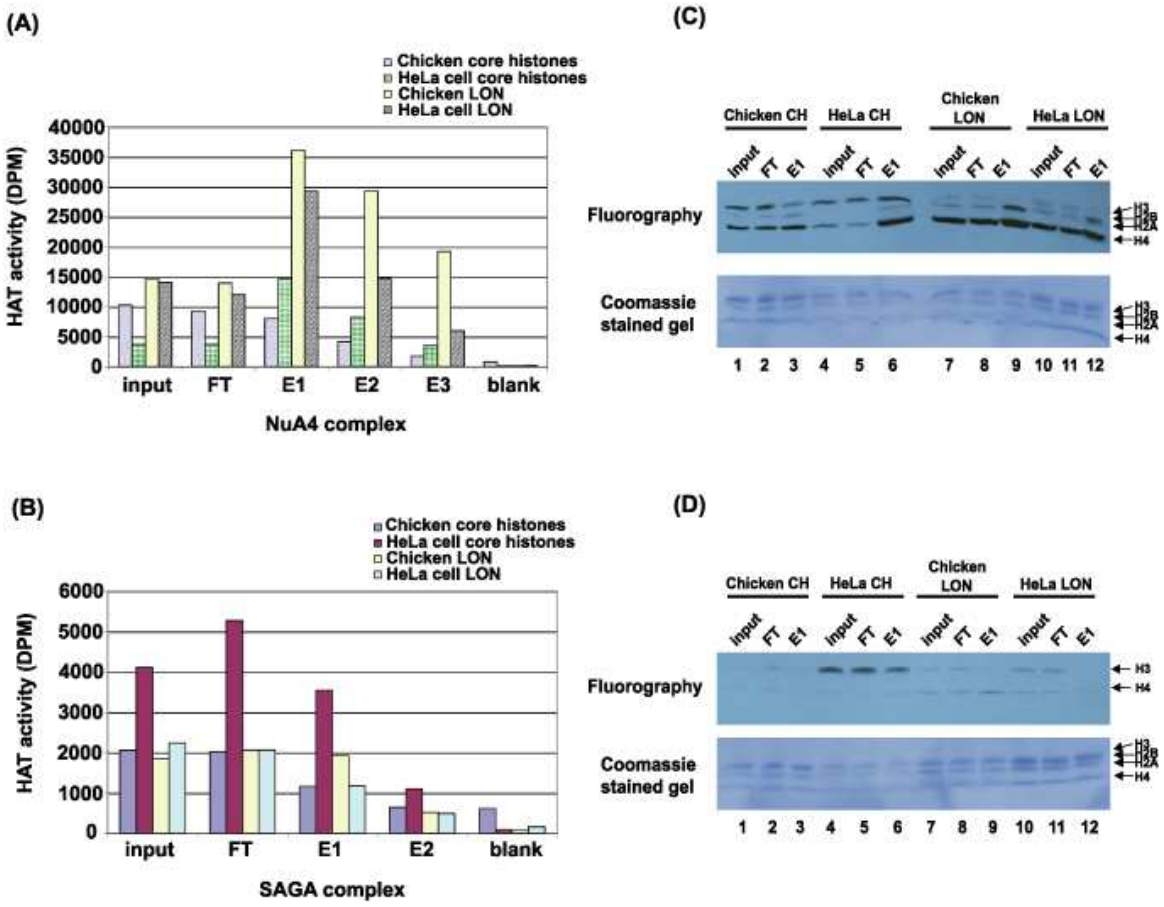

Figure **2-4**: HAT assays of the HAT complexes purified with the Flag IP using different core histones and LON as substrates.

(A) The bar chart shows the HAT assay results of the Flag-tagged Tra1 NuA4 complex: input (the MonoQ pooled fractions), FT (flow through), and E1-E3 (eluates). The purified NuA4 complex (E1-E3) shows the highest HAT activity with chicken LON. (B) The bar chart shows the HAT assay results of the Flag-tagged Tra1 SAGA complex: input (the MonoQ pooled fractions), FT (flow through), and E1-E2 (eluates). The purified SAGA complex (E1-E2) shows the highest HAT activity with HeLa cell core histones. (C) Fluorography of some of the HAT assay samples in (A) and a Coomassie stained gel showing relative amounts of histones and LON substrates. (D) Fluorography of some of the HAT assay samples in (B) and a Coomassie stained gel showing relative amounts of histones and LON substrates.

The CBP pull down experiments were performed by incubating the HAT complex with either Calmodulin affinity matrix (CAM) by itself (a negative control), or the CBP-tagged TBP bound to the resin in the presence of Calcium ions (Ca^{2+}). Then, the CBP-tagged TBP was eluted from the resin by adding ethylenebis(oxyethylenenitrilo) tetraacetic acid (EGTA), which chelates calcium ions (Ca^{2+}). Consequently, the complex, which bound to TBP on the resin, was liberated into the supernatant. Levels of interaction were measured by performing the HAT assay of the input, supernatant, and the eluates. If the interaction occurred, the HAT activity of the supernatant would be reduced compared with the input while the eluates gained the HAT activity due to the presence of the HAT complex. The complex by itself should not fortuitously bind to the resin since there was no CBP tag present within the HAT complex. Thus, the HAT activity in the supernatant of the blank was expected to be comparable with that of the input. This experiment performed with the NuA4 complex purified after the Flag IP in the conventional purification yielded a surprising result in which the complex could bind to CAM without the CBP tag (Figure **2-5** A). Moreover, this interaction was specific since the NuA4 complex binds to CAM even in the presence of 1 mg/ml BSA, and could be eluted when EGTA was added (Figure **2-5** A). A Blast search did not find any protein in the NuA4 components that share sequence homology with the CBP tag. Based on the results of the pull down, I conclude that the CBP tag might not be appropriate for the pull down experiment since the CAM resin that binds to CBP tag recognized the NuA4, and possibly the SAGA complex. In fact, I have tested whether I could utilize this technique for SAGA and NuA4 purification. I found that both SAGA and NuA4 complex from the Flag-Tra1 yeast strain could be purified with CAM and subsequently fractionated with the MonoQ column (data not shown). The reason for this observation is not known. It is very unlikely that the Flag tag would be responsible for this interaction since there is no sequence homology between the Flag tag and the CBP tag. More experiments should be performed to understand the basic mechanism of how this interaction takes place. I do not have evidence whether or not the untagged SAGA complex could interact with CAM. In addition, I did not pursue further use of the CBP tag but instead, I considered using a different affinity tag for the pull down experiments. The second tag of choice was the

Strep-tag II (STR tag), which consists of only 8 amino acids (NH_2-WSHPQFEK-COOH) and binds to the *Strep*-Tactin resin.

I tested whether the *Strep*-Tactin Sepharose could interact with the NuA4 complex as in the case of the CAM. The data showed that the majority of the NuA4 complex remained unbound to the *Strep*-Tactin resin and did not elute upon the addition of the biotin derivative, d-Desthiobiotin (Sigma) (Figure **2-5** B). Thus, these results suggest that the *Strep*-Tactin and the *Strep* tag are suitable for the pull down experiments. Therefore, the STR-tagged TBP, which has the TEV cleavage site (N) between the STR tag and the protein, was created (See **2.5.1**). The STR pull down experiment was performed by immobilizing the STR-tagged TBP to the *Strep*-Tactin resin before incubating with either the NuA4 or the SAGA complex purified after the Flag IP in the conventional purification technique. The experiment was conducted as described for the CBP pull down except, that a biotin derivative (d-Desthiobiotin) was used to elute the STR-tagged TBP. Samples from the input, supernatant, and beads were subjected to the HAT assay to determine the level of interaction.

The STR pull down experiment with the NuA4 complex in Figure **2-6** A showed that the activity of the supernatant in both blank (resin only) and STR-tagged TBP samples were comparable with the input signal. In addition, the HAT activity between the eluates from the blank (resin only) and the STR-tagged TBP was similar. Thus, I conclude that the NuA4 complex does not interact or interacts very weakly with TBP. I also decided not to pursue further experiments for TBP-NuA4 interaction. The interaction of TBP with the SAGA complex was also analyzed. As shown in Figure **2-6** B, the SAGA complex did not non-specifically interact with the resin. As expected, I observed a decrease in the HAT activity in the supernatant and a significant HAT activity in the eluates (E1 and E2) of the pull down experiment with SAGA. Therefore, I conclude that my purified SAGA complex can interact with TBP.

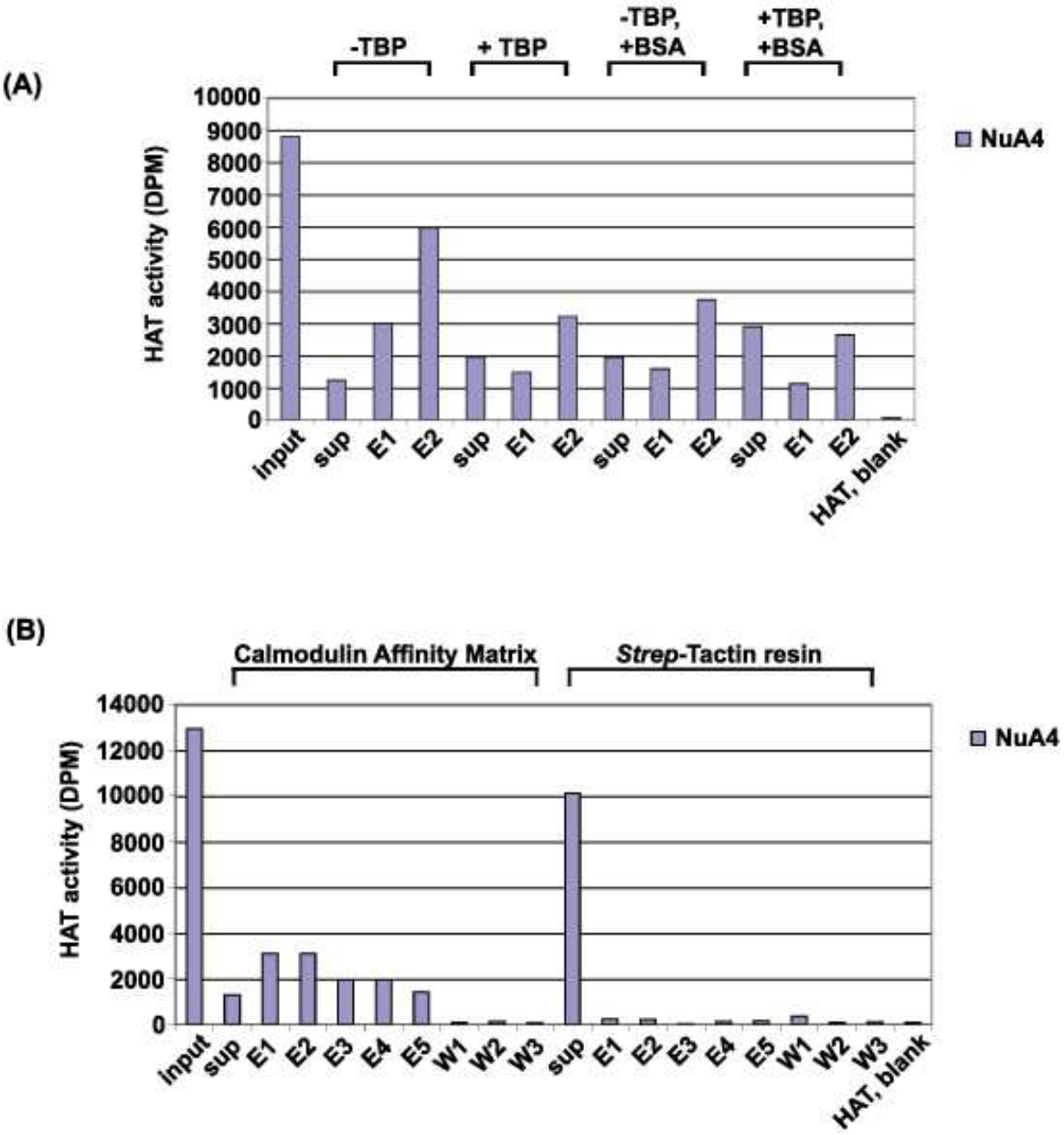

Figure **2-5**: The NuA4 complex specifically interacts with CAM but not the *Strep*-Tactin resin.

(A) The CBP pull down experiment indicates that the NuA4 complex interacts with CAM even in the present of 1 mg/ml BSA. Supernatant is abbreviated as Sup. Blank contains the resin without TBP. E1 and E2 are the eluates from the resin. (B) Testing the interaction between the NuA4 complex and either Calmodulin affinity matrix (CAM) or the *Strep*-Tactin resin. The NuA4 complex does not interact with the *Strep*-Tactin resin. W indicates the washes.

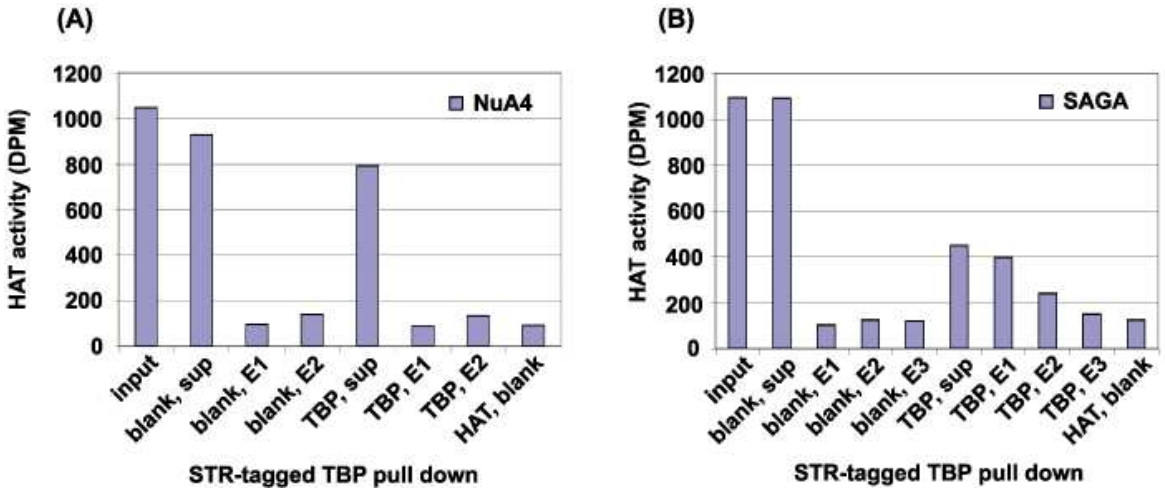

Figure **2-6**: STR pull down experiments with either NuA4 or SAGA complex purified after the Flag IP. .

(A) The STR pull down experiment with the NuA4 complex suggests that the NuA4 complex does not interact with TBP. (B) The same pull down experiment but performed with the SAGA complex shows that the complex binds to TBP on the resin

2.3.4 The R171E TBP mutant does not interact with the SAGA complex

I utilized the highly purified TAP-tagged SAGA complex to test the interaction with the STR-tagged TBP proteins. Because all the STR-tagged TBP could not be eluted from the resin within the first elution, the comparison with the input and supernatant became more difficult. I increased the concentration of the biotin derivative or used biotin, which has a higher affinity toward the *Strep*-Tactin resin, and was not able to elute all the STR-tagged TBP from the resin within the first eluate. Therefore, I changed the strategy of the pull down experiment: instead of eluting TBP from the resin, I cleaved the STRN tag on TBP to liberate the SAGA complex from the resin. As a result, the TEV-cleaved product could be used directly for HAT assays. My data showed that all the STR-tagged TBP could be cleaved by this specific protease, which does not inhibit the ability of the SAGA

complex to acetylate the core histones (data not shown). Therefore, the comparison among the activity of the input, supernatant and the TEV-cleaved product could easily be made. Alternatively, the level of interaction could be assessed by comparing the Western blot signal among the input, supernatant, and the beads. However, I had inconsistently experienced high background signals, which made it difficult to quantify the signal and compare levels of interaction among different samples. Therefore, I used the HAT assay to analyze the interaction between the SAGA complex and TBP.

In addition to the wild type TBP, I analyzed the interaction between the SAGA complex and two TBP mutants. I included two TBP mutants: the R171E and the T153I for specific reasons. The amino acid substitutions at R171 residue have been shown to suppress the phenotype of the *spt3*-401 mutation (Eisenmann et al., 1992). Because amino acid substitution mutations at R171 have genetic interactions with SPT3, the R171E TBP mutant might be a good candidate for a mutant that does not interact with the SAGA complex. In contrast, T153I mutant is unable to respond to acidic activators but is able to activate transcription and bypass the requirement of activators when it is artificially bound to a promoter (Stargell and Struhl, 1996). Because TBP has to be recruited to a promoter by a coactivator, this T153I mutant might be defective in the interaction with coactivators such as the SAGA complex.

Based on three independent pull down assay data sets, the bar chart in Figure **2-7** B represents the average activity of the bound complex after subtracting the blank of the pull down assay. As expected, the wild type TBP was able to interact with the SAGA complex (Figure **2-4** A lanes 4-5). It was unlikely that some SAGA complex remains in the resin since the blank had a small background (Figure **2-4** A lane 3). In addition, almost, if not all of the resin bound TBP were cleaved by the TEV protease (data not shown). I found that the R171E TBP mutant was severely defective for this interaction (Figure **2-7** A lanes 6 and 7). Compared to wild type TBP, only 36% of the SAGA complex was pulled down by the R171E TBP mutant (Figure **2-7** B). On the other hand, the T153I TBP mutant was able to interact with SAGA complex as well as the wild type

TBP with no significant difference (Figure **2-7** A lanes 8 and 9 compared with lanes 4 and 5).

2.3.5 Spt8 and Ada1 subunits of the SAGA complex photo-cross-link with TBP

Evidence in the literature suggests that Spt8 and Spt3 SAGA subunits are possible candidates for interaction with TBP (Eberharter et al., 1999; Eisenmann et al., 1992; Eisenmann et al., 1994; Grant et al., 1998; Warfield et al., 2004). To determine which components in the complex interact with TBP, I utilized the photo-cross-linking label transfer technique. This is the same technique used to identify Tra1, a shared component of the SAGA and NuA4 complexes, and Swi1, Snf5 and Swi2/Snf2 subunits in the Swi/Snf complex as targets of activator proteins (Brown et al., 2001; Neely et al., 1999). One advantage of this technique is that it allows us to investigate the interaction in the context of a native complex.

I used a lysine-specific cross-linking reagent: Sulfosuccinimidyl 2-(6-(biotinamido)-2-(*p*-azidobenzamido)-hexanoamido) ethyl-1,3'-dithiopropionate, which is also referred to as the Sulfo-SBED (Pierce). A schematic representation of the Sulfo-SBED is shown in Figure **2-8** A. For this experiment, the untagged TBP was conjugated with the Sulfo-SBED, purified, and incubated with purified SAGA complex before being irradiated with UV light. The mechanism by which this photo-cross-linking works is illustrated in Figure **2-8** B. Upon UV exposure, the aryl azide on Sulfo-SBED was activated and non-specifically cross-links to any protein that comes within a proximity of 23 Å. After the reaction, dithiothreitol (DTT) was added to reduce the disulfide bond so that a biotin label was transferred from the bait protein to the target protein.

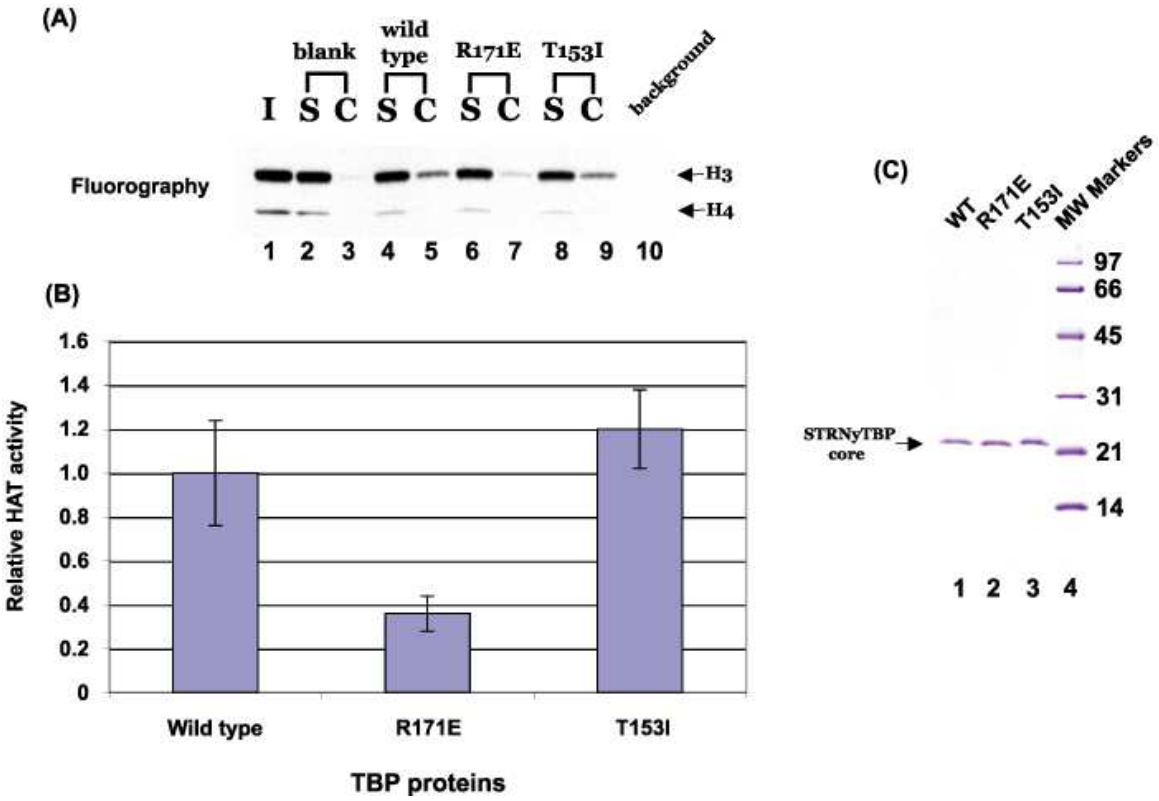

Figure **2-7**: Interactions between TBP mutants and wild type SAGA complex.

(A) Pull down results show the interactions between the SAGA complex and the wild type TBP or the T153I TBP mutant. The R171E TBP mutant is defective for this interaction. I, S, and C are abbreviated for the input, supernatant, and TEV cleaved product, respectively. (B) Average core histone HAT activity of SAGA complex bound to the wild type or mutant TBP proteins. The error bars represent standard deviations from three independent experiments. (C) A Coomassie stained gel shows the purity of the STR-tagged TBP proteins used for the pull down experiment.

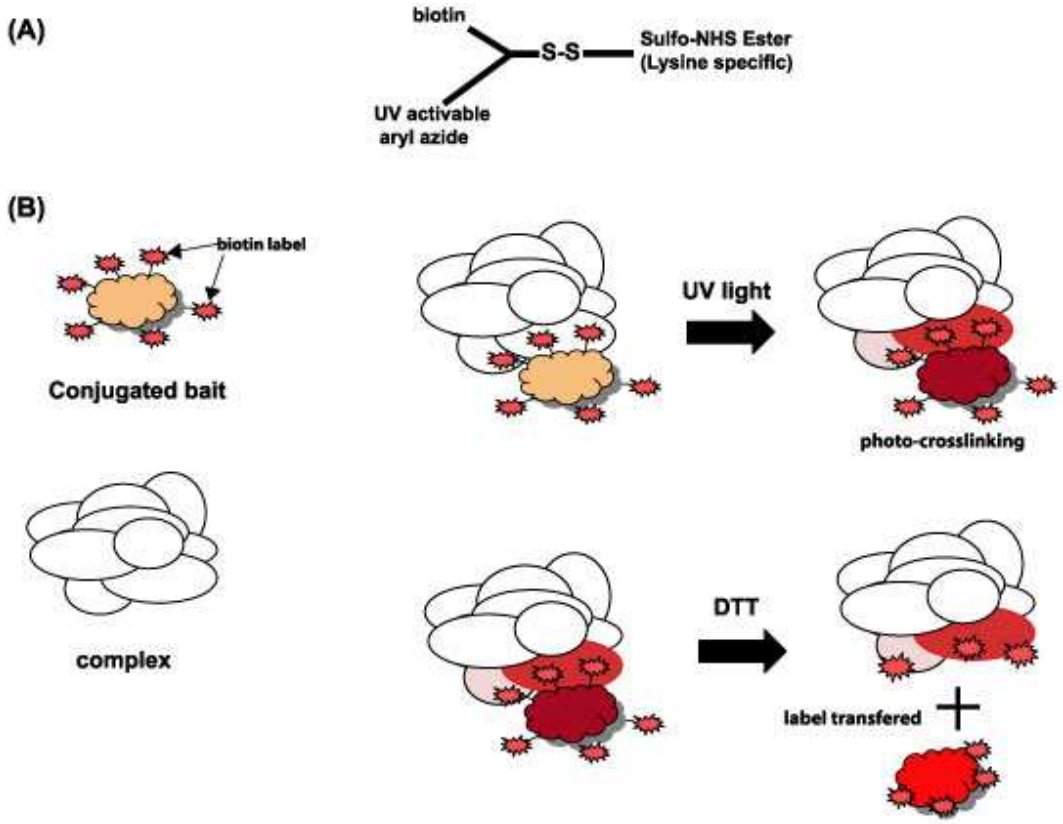

Figure **2-8**: Photo-cross-linking label transfer.

(A) Schematic representation of the chemical cross-linker: Sulfo-SBED. (B) The cartoon illustrates how the photo-cross-linking assay works.

This assay could be technically challenging and could produce a high background which further complicates the interpretation. Based on my experience, I found that the quality of the cross-linking reaction greatly depends on the quality of both the complex and the bait protein. Contaminations of the bait protein produced a high background, and the partially purified complex might result in cross-linked bands of other proteins which are not components of the SAGA. Therefore, I performed the photo-cross-linking assay using highly purified untagged TBP and the highly purified SAGA complex (Figure **2-3** B). As a positive control, I reproduced the cross-linking data between the activator and the NuA4 complex (Brown et al., 2001). The activation domain of the Gcn4 protein was used to conjugate with the Sulfo-SBED for cross-linking with the Flag

immunoprecipitated NuA4 complex. Aside from a high background, which due to the property of Strepavidin-HRP used for the Western blot, I found that Tra1 subunit of the NuA4 complex cross-linked with the activation domain of the Gcn4 (Figure **2-9** lanes 1 and 2), consistent with published results (Brown et al., 2001). Thus, I was confident that the technique could work and might be able to obtain some meaningful data from the TBP-SAGA cross-linking assay.

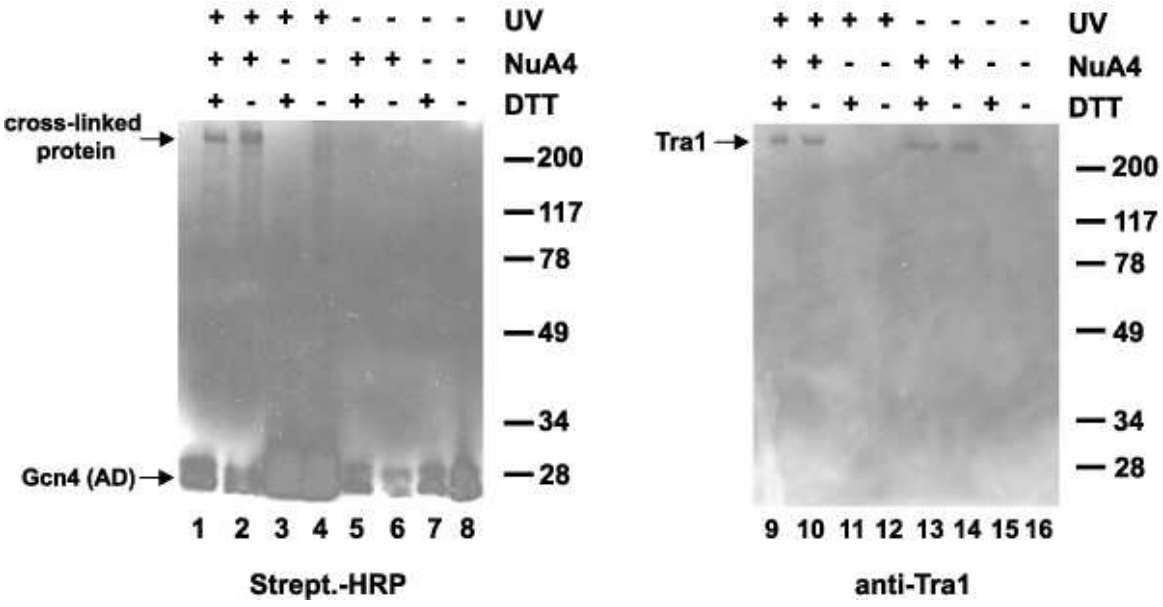

Figure **2-9**: A positive control experiment for the photo-cross-linking assay.

The photo-cross-linking assay was performed by cross-linking the activation domain (AD) of Gcn4 to the NuA4 complex. The left panel is the Western blot analysis with Streptavidin-HRP conjugated (Strept.-HRP), which detects biotinylated proteins. The right panel is the Western blot with a separate membrane and probed with anti-Tra1 antibodies.

I proceeded with the cross-linking assay using TBP as a bait to cross-link the SAGA complex. The Streptavidin-HRP conjugated used in Figure **2-10** was purchased from Pierce, whereas the one that was used in Figure **2-9** was purchased from the IBA (IBA

US Distribution Center, St. Louis, MO). The Pierce's Streptavidin-HRP conjugated gives a much lower background level than the one used in Figure **2-9**. I consistently found a strong cross-linked band migrating at approximately 80 kDa and another weaker cross-linked band at about 70 kDa (Figure **2-10** A lane 1). Using specific antibodies against protein candidates at these positions on the same membrane, I identified the strong cross-linked band as the Spt8 subunit and the lower band as the Ada1 subunit (Figure **2-10** A lanes 5, 6, 9, and 10). In addition to the Spt8 and Ada1 cross-linked band, there were some additional cross-linked bands at about 37 and 28 kDa (Figure **2-10** C lane 1). However, these protein bands were not consistently observed. Those cross-linked proteins represents background of the cross-linking reaction and were less significant than Spt8 and Ada1 subunits.

I considered the possibility that the Ada1 subunit might not be directly cross-linked with TBP because of the presence of the C-terminal CBP tag portion of the TAP tag. To test whether the Ada1 subunit could cross-link with TBP, the photo-cross-linking experiment using the Spt7-TAP SAGA complex was performed. The yeast Spt7-TAP strain was a gift from the Pugh lab. As shown in Figure **2-10** B, the mobility of the cross-linked band in the Spt7-TAP SAGA complex was faster than that in the Ada1-TAP SAGA complex, corresponding to the absence of the CBP tag on the Ada1 in the Spt7-TAP yeast. Therefore, this result demonstrates that the Ada1 can be cross-linked to TBP independently of the C-terminal CBP tag. It also suggests that this subunit is located in close proximity to TBP.

Surprisingly, Spt3, a strong candidate for the interaction with TBP, did not appear to be cross-linked with TBP. I considered the possibility that the Spt3 might not be able to transfer to the nitrocellulose membrane; thereby, it remained invisible under the Western blot with Strep.-HRP. To eliminate this possibility, anti-Spt3 antibodies were used to detect the Spt3 on the same membrane after probing with the Strep.-HRP. I was able to detect the Spt3 protein after the cross-linking reaction (Figure **2-10** C lane 5). Therefore, I conclude that Spt3 does not cross-link with TBP.

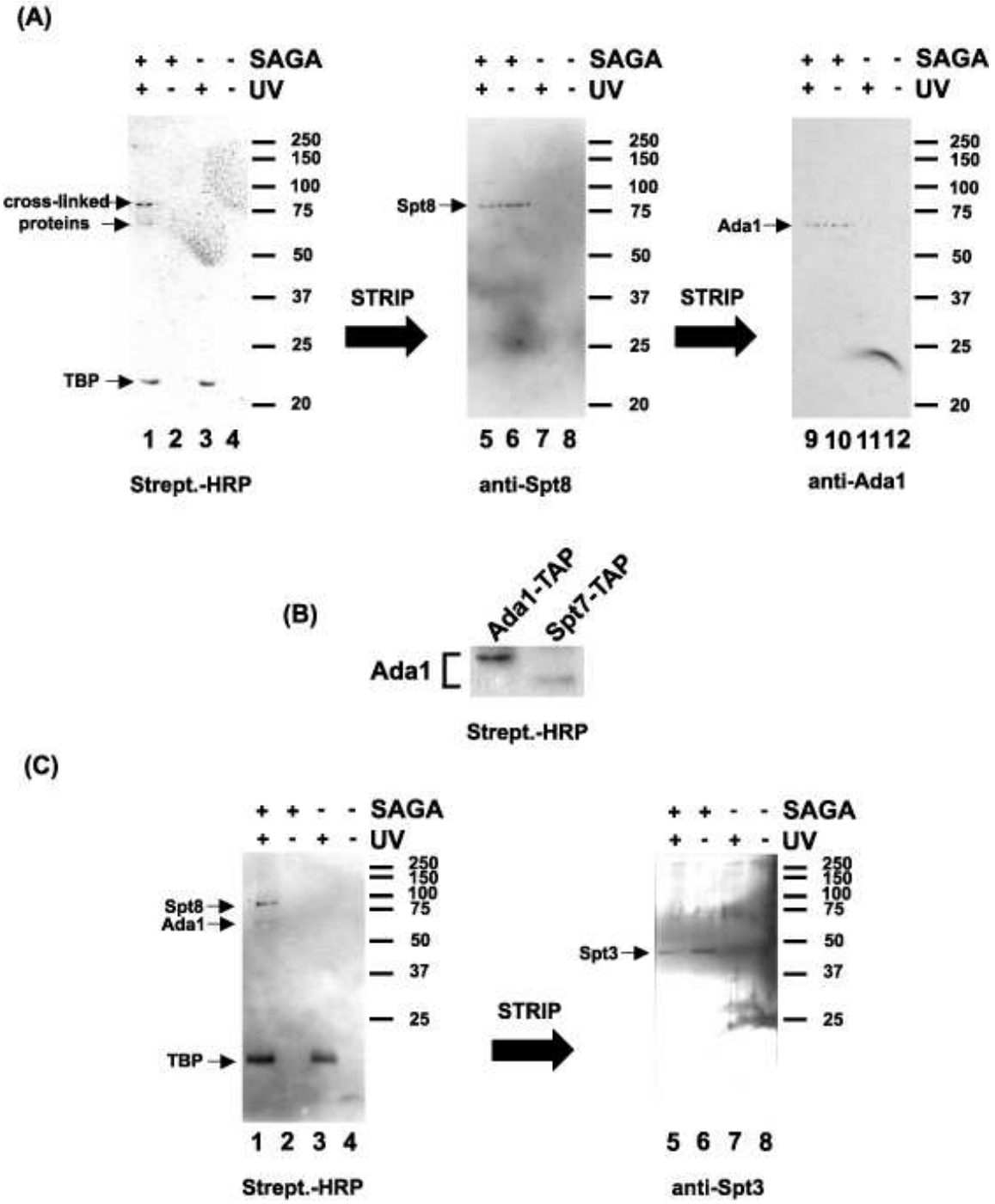

Figure **2-10**: Photo-cross-linking reveals Spt8 and Ada1 subunits of SAGA complex as the main targets of TBP.

(A) After cross-linking, protein samples were electrophoresed on a polyacrylamide gel and transferred to a nitrocellulose membrane for a Western blot analysis with Streptavidin-HRP conjugated (Strept.-HRP), which detects biotin. The same membrane was stripped before probing with different antibodies. The result indicates that the two cross-linked bands migrate at the positions corresponding to the Spt8 and Ada1 subunits. (B) Photo-cross-linking of the conjugated TBP with the Spt7-TAP SAGA shows that Ada1 is cross-linked with TBP, suggesting that Ada1 might directly interact with the TBP. (C) Photo-cross-linking of the conjugated TBP with the Spt7-TAP SAGA shows that the Spt3 is still present on the membrane after the cross-linking reaction.

2.3.6 Purified Spt8 directly interacts with TBP

Based on the photo-cross-linking result, I hypothesized that Spt8, but not Spt3, has an ability to interact with TBP. To test this hypothesis, a pull down strategy was utilized to test the interaction between TBP and either recombinantly purified C-terminal His-tagged Spt8 or Spt3 protein. As shown in Figure **2-11** A, the wild type TBP was able to interact with Spt8, consistent with the photo-cross-linking result. The T153I TBP mutant was also able to interact with Spt8 at the same level as the wild type TBP (Figure **2-11** lanes 8 and 9). However, the R171E TBP mutant was partially defective in the interaction with Spt8 (Figure **2-11** A lanes 6 and 7). Interestingly, Spt3 did not seem to interact with TBP protein in the experiment (Figure **2-11** B lanes 1-9). However, it was possible that the presence of the 6xHis tag on the C-terminus of Spt3 prevented the interaction with TBP. I have also overexpressed and purified the untagged Spt3 protein. The Spt3 fractionated at approximately 44 kDa from a Superdex 200 gel filtration column, suggesting that it existed as a monomer and was not aggregated (data not shown). Consistently, I observed no interaction between the untagged Spt3 and TBP under a pull down experiment (data not shown). Therefore, I conclude that the purified Spt8, but not Spt3, directly interacts with TBP.

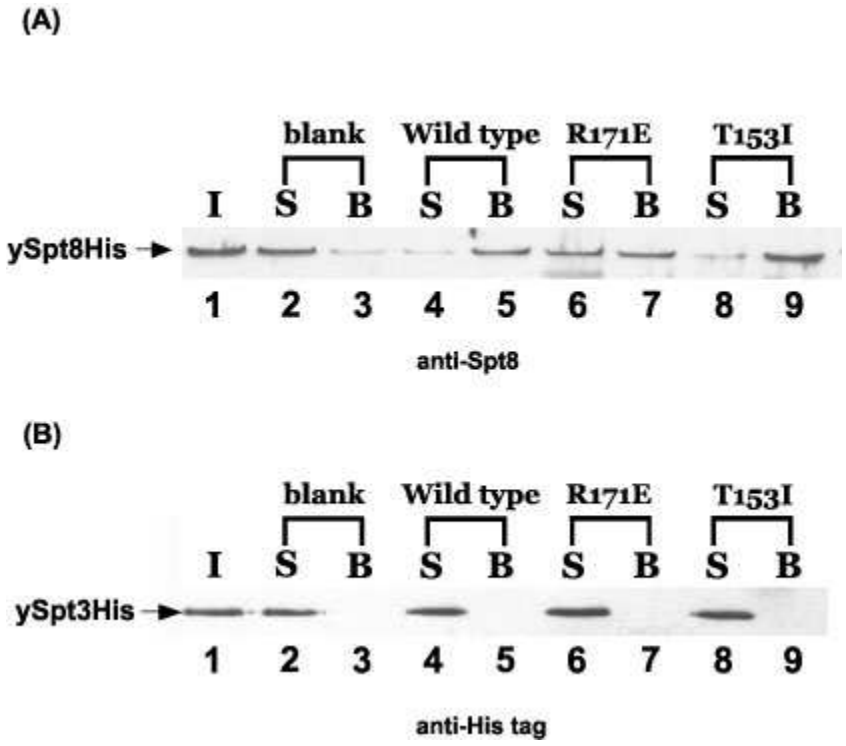

Figure **2-11**: Purified Spt8 but not Spt3 physically interacts with TBP.

Pull down experiment was performed using STR-tagged TBP proteins to test interaction with either Spt8 or Spt3. (A) A Western blot analysis using the anti-Spt8 antibodies shows the interaction between TBP and Spt8 from a pull down experiment. The result also shows that Spt8 (ySpt8His) does not interact well with the R171E mutant TBP. I, S, and B are abbreviated for the input, supernatant, and beads, respectively. (B) A Western blot analysis using the anti-His tag antibodies to detect the His-tagged Spt3. These results indicate that Spt3 does not interact with TBP.

2.3.7 Interaction between the wild type TBP and the SAGA mutants

I have shown that TBP primarily photo-cross-linked with the Spt8 subunit of the SAGA complex and I confirmed the interaction by a pull down experiment. Therefore, most of the interaction between the SAGA complex and TBP is conferred by Spt8. If only Spt8 in the SAGA complex is required for the interaction with TBP, the SAGA complex without Spt8 should lose this interaction. But if Spt8 and other subunits of SAGA cooperatively interact with TBP, the complex without Spt8 would show defectiveness in

this interaction. To test these hypotheses, yeast mutant strains with deletions of the SPT8 gene (*spt8*Δ) and both SPT8 and SPT3 genes (*spt8*Δ*spt3*Δ) were created (See **2.5.3**). The *spt3*Δ Ada1-TAP SAGA yeast strain was a gift from Dr. Patrick Grant of the University of Virginia. Those SAGA complexes were purified using TAP tag as described in **2.5.6** and normalized by histone acetyl transferase (HAT) activity with HeLa cell core histones (Figure **2-2** B fluorography). With an equal HAT activity among the complexes, each SAGA subunit appeared equivalent on both silver stained gel and Western blots (Figure **2-2** B and C). Therefore, for pull down experiments, a portion of bound and unbound complex can be shown simply by the amount of their HAT activity and fluorography.

Using the same strategy and analysis of TBP proteins-SAGA complex pull down assays described in **2.5.8.** I found that the SAGA complex without Spt8 significantly diminished the interaction with TBP (Figure **2-12** A) when compared with the wild type SAGA complex. This result suggests that Spt8 in SAGA largely contributes to the interaction with TBP; however, one or more SAGA subunits probably functions to interact with TBP. Surprisingly, deletion of Spt3 (*spt3*Δ SAGA) also caused a negative effect on the SAGA-TBP interaction (Figure **2-12** A). Based on the purification and detection methods in Figure **2-3** B and C, it did not appear that the deletion of Spt3 affected Spt8 incorporation in the complex. Finally, a defect in the interaction when both Spt8 and Spt3 were absent from the complex was also observed (Figure **2-12** A). Therefore, these results suggest that both Spt8 and Spt3 contribute to the interaction with TBP, but Spt8 is more important for the interaction with TBP than Spt3. The Spt3 subunit in SAGA somehow contributes to the interaction with TBP, possibly by the interaction with Spt8. Furthermore, I hypothesize that there is at least one more subunit other than Spt8 and Spt3 that contribute to this interaction.

To determine what subunits in the SAGA complex lacking Spt8 interact with TBP, the same photo-cross-linking assay was performed. The result from Figure **2-10** shows that Ada1 is the second strongest protein that cross-links with TBP. Therefore, it is possible

that the Ada1 subunit in SAGA makes some contribution to the interaction with TBP. Photo-cross-linking experiments between the wild type TBP and four different SAGA complexes were conducted as described in **2.5.7**. I found that both Spt8 and Ada1 subunits could still photo-cross-link with TBP when Spt3 was absent from the complex (Figure **2-12** B lane 3). Interestingly, Ada1 was cross-linked with TBP even in the absence of Spt8 in the complex, indicating a potential role of Ada1 in the interaction (Figure **2-12** B lane 2). In addition, the complex lacking both Spt8 and Spt3 showed very little or no cross-linking with TBP (Figure **2-12** B lane 4). These results were consistent with the observations from the pull down experiment (Figure **2-12** A). Therefore, Ada1 is most likely to be another SAGA subunit that interacts with TBP.

2.4 Discussion

2.4.1 Purification of the SAGA complex

I have discussed the purification of the SAGA complex from both the conventional technique, which involves the binding of the whole cell extract to the metal affinity resin (Ni-NTA) as the first step of purification, and the TAP tag procedure, which utilizes the two affinity tags: the protein A tag, which binds to the IgG molecule, and the CBP tag. I have also pointed out some advantages and disadvantages of purification in each technique. I prefer the TAP tag purification to the conventional purification for several reasons, including the high purity of the SAGA complex. The amount of the SAGA complex purified with the TAP tag purification procedures varied from approximately 10 to 40 µg from a 12-liter culture. In my best TAP tag purification, I obtained approximately 54 µg pure SAGA complex from a 9-liter culture.

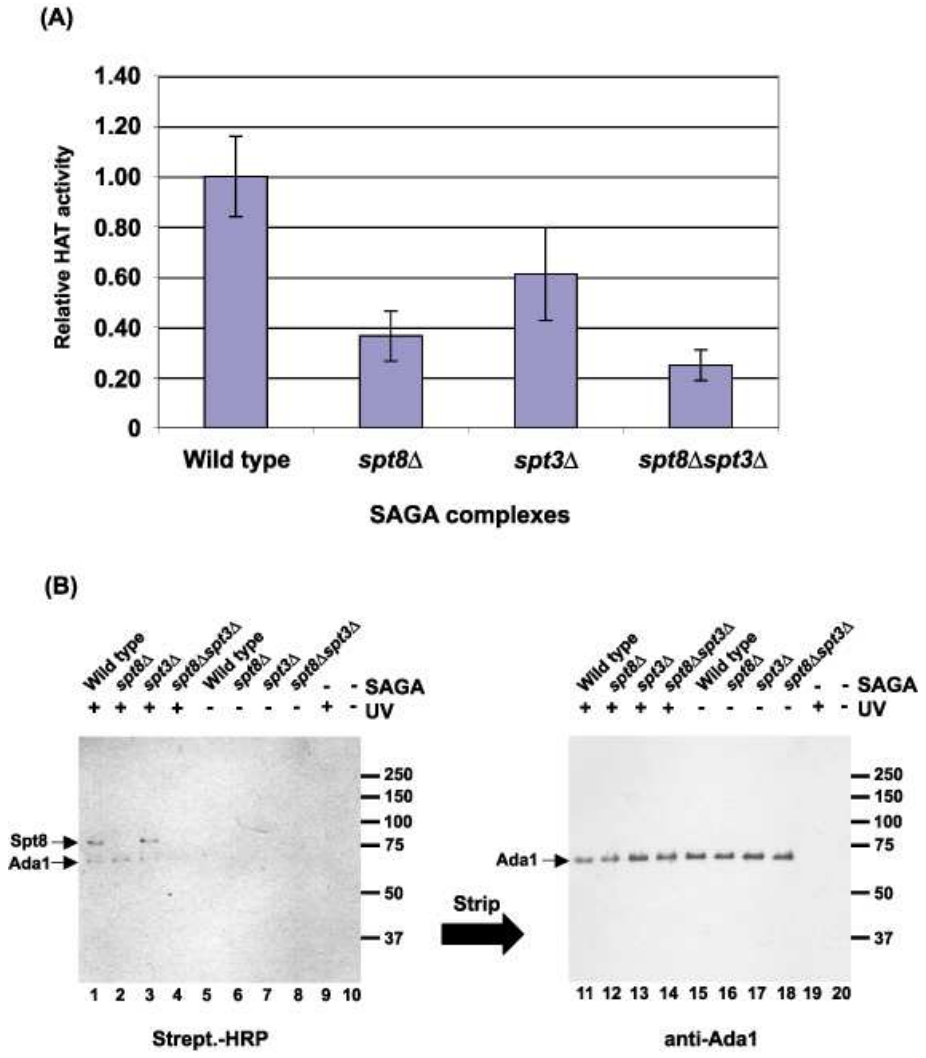

Figure **2-12**: SAGA complex lacking spt8, spt3 or both spt8 and spt3 is defective in the interaction with TBP.

(A) STR pull down experiment was performed with wild type STR-tagged TBP (WT) and the wild type, *spt8*Δ, *spt3*Δ, or *spt8*Δ*spt3*Δ SAGA complexes. The pull down assay was conducted with the same procedures for TBP-SAGA pull down. The results are represented as a bar chart of the average core histone HAT activity of SAGA complexes bound to TBP. The error bars represent standard deviation from 3 independent experiments. (B) Photo-cross-linking between the wild type TBP and 4 different SAGA complexes. Ada1 is cross-linked with the SAGA complex lacking Spt8 or Spt3.

Several purification procedures could contribute to the overall amount of the complex obtained after the last step of purification. Based on my experience, I usually obtained more SAGA complex as I let the cells grow to an OD_{600} of approximately 2-2.5, the cell density at 6.2 x 10^7 cells/ml, or approximately 4-5 grams of cells per liter of culture than the culture grown to an OD_{600} of 0.8-1.0. During the incubation of the soluble extract with the IgG Sepharose resin, I would recover more SAGA complex if the incubation volume was divided into several smaller aliquots than when the purification was performed in one large pool. For example, with approximately 80-100 ml soluble extract from a 12-liter culture, I did not perform one set of incubation with 1200-1600 µl of the IgG Sepharose resin. Instead, the extract was divided equally into six to eight tubes for incubation with 200 µl of the IgG Sepharose resin in each tube. In addition, the last step of the purification procedures with Calmodulin affinity matrix (CAM) could result in a substantial loss of the material in the flow through. I observed a significant amount of the complex remaining unbound in the flow through of the Calmodulin affinity matrix when the MonoQ fractions were used directly as the input. However, the binding of the SAGA complex was greatly improved if the MonoQ fractions were subjected to dialysis against the $CaCl_2$ binding buffer prior to the incubation with Calmodulin affinity matrix. Possibly, the high salt content in the MonoQ fractions reduces the binding affinity of the CBP tag to the Calmodulin affinity matrix. I also noticed that the complex recovered from the Calmodulin affinity matrix was eluted in a broad range of fractions rather than a sharp peak within a few elutions. Thus, concentration of the Calmodulin affinity matrix eluates might be necessary to obtain a concentrated form of the complex.

2.4.2 Substrate specificity of the SAGA and NuA4 complexes

Just as the SAGA complex has an Ada3/Ada2/Gcn5 subcomplex that is capable of nucleosome acetylation (See Chapter 4), the NuA4 has the Piccolo complex, Yng2/Epl1/Esa1, that can acetylate nucleosomes (See Appendix C). As discussed in **1.1.3.1**, the mechanism of histone acetylation of the Esa1 is distinct from the mechanism of the Gcn5 protein. Our data that suggest a preference of the NuA4 complex toward the

acetylation of a nucleosomal substrate are consistent with previous results suggested in literature (Boudreault et al., 2003; Eberharter et al., 1998). In contrast, the SAGA complex can acetylate core histones about 2 times better than the nucleosomes, even though it is thought that nucleosomes would be a more physiologically relevant substrate in cells. Perhaps the difference in preferential acetylation between the acetylation of the NuA4 and SAGA complex is independent of the difference in the catalytic mechanism of the Esa1 and the Gcn5, but rather reflects the functions of other subunits such as Ada3 and Ada2 in SAGA (Balasubramanian et al., 2002), and the Epl1 and Yng2 in the NuA4 complex (Selleck et al., 2005) in nucleosome recognition. Does this mean that the SAGA complex does not recognize nucleosomes as well as the NuA4 complex? Unfortunately, no study has ever compared the binding affinity of those two coactivator complexes to nucleosomes *in vitro*. The dissociation constant between the nucleosome core particle and the Piccolo NuA4 complex is approximately 10 nanomolar (Will Selleck's unpublished data). In contrast, the dissociation constant between the nucleosome core particle and the Ada3/Ada2/Gcn5 complex is unknown. The Piccolo NuA4 complex produces a well defined peak on a size-exclusion chromatography (Selleck et al., 2005) and a clear gel shifted band on a native gel when the Piccolo complex is added in 10 fold excess to the nucleosome core particle (See Appendix C). On the other hand, the yeast Ada3/Ada2/Gcn5 complex produces a less defined—broader peak on a size-exclusion chromatography, and a smear on a native gel, even when the complex was added in a large excess to the nucleosome core particle (Adam Barrios's results; data not shown). The smear and broader peak on the size-exclusion chromatography could result from the dissociation between the Ada3/Ada2/Gcn5 and the nucleosome core particle complexes. Based on these data, I speculate that in the *in vitro* context, at least under gel shift and size-exclusion chromatography conditions, the Piccolo NuA4 complex might bind to nucleosomes better than the Ada3/Ada2/Gcn5 complex. Because the Ada3/Ada2/Gcn5 and the Piccolo NuA4 complexes are sub-complexes of the SAGA and NuA4, respectively, the NuA4 complex may bind to nucleosomes better than the SAGA complex does. Future experiments to address the binding affinity between the Ada3/Ada2/Gcn5 complex will be necessary to test this hypothesis. It is important to note

that the binding affinity of those HAT complexes to chromatin in the *in vivo* context is further complicated by the presence of histone modifications, which impact the behavior of coactivators including the SAGA and NuA4 complexes (See Chapter 1).

2.4.3 Could the NuA4 coactivator complex promote transcription by recruiting TBP to a promoter?

Both SAGA and NuA4 HAT complexes have been shown to interact with several activator proteins through the shared Tra1 subunit *in vitro* (Bhaumik and Green, 2001; Brown et al., 2001; Larschan and Winston, 2001; Lee et al., 2005a; Nourani et al., 2004). The SAGA complex can be recruited by many activator proteins such as Gal4, Gcn4, and Pho4 proteins (Barbaric et al., 2003; Bhaumik and Green, 2001; Bhaumik and Green, 2002; Larschan and Winston, 2001). Once recruited to a promoter, the SAGA complex can promote gene transcription by its histone acetylation function and/or by recruiting TBP to the core promoter. The histone acetylation function of the complex is catalyzed by the Gcn5 subunit whose nucleosomal acetylation function is dependent on the Ada3 and Ada2 components of the complex (See chapter 4 for more discussion). In addition, this chapter discusses the role of Spt8 and possibly Ada1 of the SAGA complex in the interaction with TBP.

Unlike SAGA, the HAT function seems to be the best characterized mechanism used by the NuA4 complex to regulate gene transcription. Here I show that the NuA4 complex does not interact with TBP. To my knowledge, none of the literature has described the direct connection between the NuA4 complex and the recruitment of TBP to the core promoter. Although it was shown *in vitro* that the same set of activator proteins interact with both NuA4 and SAGA complexes, both coactivators are not recruited by the same set of activators *in vivo*. To date, only the Pho2 activator protein has been shown to recruit the NuA4 to regulate the transcription of the *PHO5* gene (Nourani et al., 2004). Pho2 recruits the NuA4 complex to the *PHO5* prior to the binding of Pho4, which recruits SAGA complex. It was also shown that the HAT function of the Esa1 in the

NuA4 context is required for the *PHO5* activation. Mutation in the HAT domain of Esa1 causes global histone H4/H2A acetylation and transcription defects (Boudreault et al., 2003; Durant and Pugh, 2006). It is possible that the direct connection between the NuA4 complex and TBP recruitment is yet to be discovered.

The function of the NuA4 complex is indirectly linked to the recruitment of TFIID rather than TBP itself. Durant and Pugh have shown that histone H4 acetylation by Esa1 is important for the recruitment of Bdf1, which binds to the acetylated histone H4 (Durant and Pugh, 2006). The acetylation by Esa1 (possibly from the NuA4 complex) has a better correlation to Bdf1 recruitment than to TAF1 (TFIID) recruitment. In other words, the recruitment of Bdf1 does not necessary result in the recruitment of TFIID since Bdf1 can also recruit SWR-C complex, which plays a role in a deposition of Htz1 to nucleosomes (Li et al., 2005; Zhang et al., 2005). Given the connection between the NuA4 complex and the TFIID recruitment through Bdf1 protein, the NuA4 complex indirectly recruits TFIID, which contains TBP, through the HAT function of the Esa1 subunit. Therefore, the transcriptional activation by the NuA4 complex is more highly linked to its acetylation function rather than a physical interaction with TBP.

2.4.4 Spt8 and possibly Ada1 subunits of SAGA interact with TBP

Since the SAGA, but not the NuA4 complex, has been known to interact with TBP, I would like to understand how the interaction between the SAGA and TBP takes place, and which SAGA subunits mediate such interaction with TBP. With the photo-cross-linking label transfer assay, I identify Spt8 and Ada1 as specific subunits in the SAGA complex that interact with TBP. Like other *SPT* genes, *SPT8* has been identified as a suppressor of Ty transposon element insertion (Eisenmann et al., 1994). SPT8 displays an allele specific genetic interaction with SPT3. In other words, only certain mutations on the SPT3 gene can reverse a phenotype of SPT8 deletion (Eisenmann et al., 1994). Interestingly, Spt8 was only found to support a functional interaction between Spt3 and TBP (Eisenmann et al., 1994). In contrast to genetic evidence, this study has

revealed that one role of Spt8 in SAGA is to contact TBP directly. First, the Spt8 subunit of the SAGA complex is primarily cross-linked with TBP. Second, the ability of Spt8 to cross-link with TBP is independent of the presence of Spt3 in the SAGA complex. Lastly, the isolated Spt8 protein interacts with TBP under a pull down assay, showing that Spt8 is sufficient to bind to TBP. The role of Spt8 in the TBP interaction from this study is consistent with previous reports (Bhaumik and Green, 2002; Eberharter et al., 1999; Grant et al., 1998; Warfield et al., 2004). Thus, Spt8 in the SAGA complex has functional and physical interactions with TBP.

Our study also suggests a role of Ada1 as another potential TBP interacting subunit. First, I consistently observe another TBP cross-linked band migrating faster than the position of the Spt8. This protein band was identified as the Ada1 subunit. Second, the mobility of this fast migrating band is changed when I use the Spt7-TAP SAGA complex, confirming the identity of this band as the Ada1. And lastly, the Ada1 subunit in the *spt8*Δ SAGA complex cross-links with TBP, indicating that the cross-linked band is not a degradation product of Spt8 during the cross-linking reaction. Thus, the Ada1 cross-linking is independent of the presence of the Spt8 subunit. However, the level of TBP cross-linking to Ada1 is relatively weak compared to the Spt8. Because the SAGA complex lacking Spt8 can weakly bind to TBP, perhaps a low level of Ada1 cross-linking reflects a low binding affinity between the Ada1 and TBP. Another possibility is that the interface for the Ada1-TBP contact is significantly less than that of the Spt8-TBP.

The finding that Ada1 interacts with TBP has never been discussed in the literature. Perhaps one of the reasons is that Ada1 is required for the SAGA complex's integrity (Eberharter et al., 1999; Wu and Winston, 2002). Our attempt to isolate Ada1 to directly test the interaction with TBP was compromised by the fact that Ada1, by itself, is insoluble even when coexpressed with TAF12, the Ada1's histone-fold partner (Gangloff et al., 2000). Other SAGA subunits would probably be required to stabilize Ada1. While my study has suggested a new role for Ada1 in the binding of TBP by the SAGA complex, future experiments will be required to demonstrate direct binding and how Ada1 in the SAGA complex may interact with TBP.

2.4.5 A possible role of Spt3 in the SAGA complex

The question of whether Spt3 in the SAGA complex interacts with TBP is an intriguing one which requires further investigation. The genetic evidence, as well as experiments in the *in vivo* context, has suggested a direct interaction between the Spt3 and TBP. For example, mutations in several residues in yeast TBP such as the R171, G174, and F177 reversed the phenotype associated with the specific mutation in SPT3 (Eisenmann et al., 1992). Furthermore, deletion of the SPT3 reduces the TBP recruitment to the core promoters of SAGA dependent genes (Bhaumik and Green, 2001; Bhaumik and Green, 2002; Larschan and Winston, 2001). Thus, Spt3 might be important for the SAGA complex to interact with TBP. In contrast, the experiments done in the context of the isolated SAGA complex do not agree with the conclusion from those *in vivo* studies. For instance, the SAGA complex lacking the Spt3 subunit is capable of interacting with TBP (Grant et al., 1998; Sterner et al., 1999). For the first time, my study shows that the purified Spt3 protein does not interact with TBP. Moreover, the Spt3 in SAGA does not appear to cross-link with TBP in the photo-cross-linking assay. Therefore, it appears that the Spt3 does not have a physical interaction with TBP.

The negative results should be interpreted with caution. The failure of Spt3 to interact with TBP in the pull down assay does not rule out the possibility that the two proteins do interact. The interaction between the two proteins might be much weaker than the interaction observed between the Spt8 and TBP. It is also possible that the purified Spt3 is not sufficient for the interaction with TBP. Although my photo-cross-linking assay using TBP as bait for SAGA subunits does not reveal Spt3 as a cross-linked subunit, it remains possible that Spt3 might be cross-linked with TBP but at a level lower than the detection limit. Another possibility is that the area in which the Spt3 in SAGA makes contact with TBP does not have an available lysine for cross-linking. This would result in no biotin label transfer from TBP to the Spt3. Therefore, I consider it a possibility that the Spt3 in the SAGA complex interacts with TBP. In fact, deletion of the Spt3 decreases the binding of the SAGA complex to TBP, suggesting that the Spt3 in SAGA somehow

interacts with TBP. Precisely how Spt3 in the SAGA complex contributes to the interaction with TBP (whether directly or indirectly) still remains a subject for future investigation. Additional protein-protein interaction assays, such as using a different cross-linking reagent, might reveal a hidden clue of the Spt3-TBP interaction.

2.4.6 A possible mechanism for the interaction and the relationship between TBP and the SAGA complex

The results of the pull down experiment with the R171E TBP mutant, which is defective in the interaction with the SAGA complex, suggest an interesting mechanism of how TBP may interact with Spt8 or the SAGA complex. The crystal structure of yeast TBP in which TBP dimerizes with another molecule reveals that R171 faces R98, which is located at the TBP dimer interface (Chasman et al., 1993). Either R171E or R98E point mutation results in a stronger TBP-TBP dimer (Kou et al., 2003; Kou and Pugh, 2004), suggesting a reverse correlation between TBP dimerization and the binding to Spt8 or SAGA complex. Thus, I propose that Spt8 binds to a TBP monomer and prevents TBP dimerization. The fact that the SAGA complex that lacks Spt8 does not bind to TBP with a high affinity suggests that Spt8 plays an important role in the SAGA's ability to bind to TBP. Therefore, it may be expected that the SAGA complex will bind to TBP and prevent TBP dimerization as well. Interestingly, it has been shown *in vitro* that the SAGA complex inhibits TBP from binding to the TATA box DNA (Belotserkovskaya et al., 2000). Thus, it will be interesting to investigate the interplay between the SAGA complex and the TATA box DNA toward the binding with TBP and how Spt8 binds to TBP. I discuss my results about how Spt8 or the SAGA complex binds to TBP and a mechanism whereby the SAGA complex recruits TBP to the core promoter in Chapter 3.

2.5 Materials and Methods

2.5.1 Overexpression and purification of TBP

Throughout the work described in this chapter, I used the 180 amino acids core conserved domain of TBP, which is also referred to as TBP. In this section, the conserved core domain of yeast TBP will be referred to as yTBPcore. The tagged TBP, STRNyTBPcore describes the 180 amino acids, core conserved C-terminus domain of the yeast TBP, which is N-terminally fused with a tandem *Strep*-tag II (NH_2-WSHPQFEK-COOH) (IBA) and a seven-residue recognition site of TEV NIa protease (ENLYFQ | G, represented as N). The recombinant STRNyTBPcore gene was constructed on the polycistronic expression plasmid pST39 (Tan, 2001). The plasmid containing the STRNyTBPcore gene was transformed into the *Escherichia coli* BL21(DE3)pLysS cells and plated on a TYE plate (1.0% bacto tryptone, 0.5% yeast extract, 0.8% NaCl, 1.5% agar, 100 µg/ml ampicillin, and 25 µg/ml chloramphenicol). After 8-12 hours of incubation at 37°C, 3 or 4 colonies from the plate were incubated in a 100 ml pre-culture 2xTY medium (1.6% bacto tryptone, 1.0% yeast extract, and 0.5% NaCl) with ampicillin and chloramphenicol added to 50 µg/ml and 25 µg/ml, respectively. The pre-culture was incubated at a 37°C shaking incubator. Once the optical density (OD_{600}) reached 0.1-0.5, this pre-culture was used directly to inoculate in 6x 500 ml (3-liter culture) of Soluble Protein Media or SPM (1.6% bacto tryptone, 1.0% yeast extract, 0.5% NaCl, 1M sorbitol, and 2.5mM betaine) with ampicillin and chloramphenicol added to 50 µg/ml and 25 µg/ml, respectively. Cells in the SPM were grown at 37°C. Once the OD_{600} reached between 0.5-1.0, expression was induced by the addition of isopropyl-β-D-thiogalactopyranoside (IPTG) to a final concentration of 0.1 mM. Cells were allowed to grow for 2-3 hours before harvesting. Harvested cells were resuspended with approximately 150 ml of T300 buffer (20 mM Tris-Cl pH 8.0, 300 mM NaCl, 0.5 mM Ethylenediaminetetraacetic acid (EDTA), 1 mM benzamidine, and 10 mM 2-mercaptoethanol), and stored at -80°C until the purification.

The purification strategy of the STRNyTBPcore involved two main steps: the Heparin Sepharose and the *Strep*-Tactin Sepharose columns. All the steps of the purifications were performed at 4°C. In brief, cells were thawed, divided equally among 4x 100 ml beakers, and glycerol added to a final concentration of 10%. Cell lysate was prepared by sonication. Each aliquot of cells was sonicated with Branson Digital Sonifier (450D) at 70% power for 3 repeats of 14 pulses (0.5 second on and 0.5 second off). There was at least a 30-second incubation on ice between the sonication. Soluble extract was prepared by centrifugation and was passed through a 30 ml Heparin-Sepharose CL-6B (Pharmacia Biotech) column chromatography. Unbound proteins were washed off the column with TG300 buffer (T300 with 10% glycerol). Non-specifically bound proteins were washed off the column with TGU300 buffer (TG300 with 3 M Urea). Subsequently, the bound STRNyTBPcore was eluted off the column with a 4 CV linear salt gradient from 300 mM to 1500 mM NaCl, using TG300 and TG1500 buffers. Peak fractions were pooled and dialyzed for 12 hours against TG150 buffer (20 mM Tris-Cl pH 8.0, 150 mM NaCl, 0.1 mM EDTA, 10% glycerol, 1 mM benzamidine, and 10 mM 2-mercaptoethanol). The dialyzed sample was passed over a column containing 10 ml of the *Strep*-Tactin Sepahrose resin (IBA). After washes, STRNyTBPcore protein was eluted off the column with the TG150 buffer with 2.5 mM D-desthiobiotin (Sigma). Peak fractions were pooled and dialyzed against H200 buffer (10 mM HEPES pH 7.5, 200 mM NaCl, and 0.1 mM EDTA). An aliquot of the protein was stored in 20% glycerol, and kept frozen at -80°C.

An aliquot of the STRNyTBPcore fusion protein was subjected to the Tobacco Etch Virus (TEV) NIa protease treatment to cleave the STRN fusion tag from the yTBPcore. The molar ratios between the TEV protease and TBP were from 1:50 to 1:100. After cleavage, the sample was purified over a 10 ml cationic exchange Source S10 HPLC column (Pharmacia Biotech) on BioCAD Sprint HPLC System (PerSeptive Biosystems, Inc). The bound yTBPcore was eluted off the column with a 20 CV linear salt gradient from 200 mM to 1000 mM NaCl HPLC buffers (10 mM HEPES pH 7.5, 200 mM or 1000 mM NaCl, and 0.1 mM EDTA). Peak fractions were pooled and glycerol

added to 20%. Then, the sample was aliquot in 1.7 ml eppendorf tubes, and kept frozen at -80°C.

2.5.2 Overexpression and purification of Spt8 and Spt3

For the purification procedures, the yeast Spt8 and Spt3 will be referred to as ySpt8 and ySpt3, respectively. I fused an N-terminal STRN tag and C-terminal His tags (-NH_2-HHHHHH-COOH) to ySpt8 and ySpt3 to create STRNySpt8His or STRNySpt3His constructs, respectively. A plasmid containing either Spt8 or Spt3 construct was transformed into the *Escherichia coli* BL21(DE3)pLysS cells and plated on a TYE plate (1.0% bacto tryptone, 0.5% yeast extract, 0.8% NaCl, 1.5% agar, 100 µg/ml ampicillin, and 25 µg/ml chloramphenicol). After 8-12 hours of incubation at 37°C, 3 or 4 colonies from the plate were incubated in a 100 ml pre-culture 2xTY medium (1.6% bacto tryptone, 1.0% yeast extract, and 0.5% NaCl) with ampicillin and chloramphenicol added to 50 µg/ml and 25 µg/ml, respectively. The pre-culture was incubated in a 37°C shaking incubator. Once the optical density (OD_{600}) reached 0.1-0.5, this pre-culture was used directly to inoculate in 12x 500 ml (6-liter culture) of the same 2x TY medium, containing ampicillin and chloramphenicol at 50 µg/ml and 25 µg/ml, respectively. The culture was grown initially at 37°C and was transferred to a 28°C shaking incubator when the OD_{600} reached 0.1-0.2. Cells were allowed to grow and induced with 0.2 mM IPTG at an OD_{600} about 0.5-0.7. After 3-4 hrs of induction, cells were harvested and resuspended with approximately 150 ml of P100-EDTA buffer, which contains 50 mM sodium phosphate pH 7.0, 100 mM NaCl, 1 mM benzamidine, and 5 mM 2-mercaptoethanol, and stored at -80°C until the purification.

The purification strategy of ySpt8His and ySpt3His involved four main steps: a metal affinity column, the *Strep*-Tactin Sepharose column, cleaving the STRN tag, and ion-exchange HPLC. All steps except the ion-exchange HPLC were performed at 4°C. Both proteins were purified the same way except that they required a different ion-exchange HPLC column. First, soluble extract was prepared with the same procedures as described

for the STRNyTBPcore protein, except no glycerol was added. Then, the extract was subjected to purification with a 20 ml Talon Metal Affinity Resin (Clontech). After several washes with the same buffer that contains 10 mM imidazole, the bound protein was eluted off the column with P100-EDTA, also containing 150 mM imidazole. Peak fractions were pooled and dialyzed for 12 hours against T150 buffer (20 mM Tris-Cl pH 8.0, 150 mM NaCl, 0.1 mM EDTA, 1 mM benzamidine, and 10 mM 2-mercaptoethanol). The dialyzed sample was subsequently purified with the *Strep*-Tactin Sepharose resin (IBA), the same way as described above. Peak fractions were pooled and dialyzed against a H100 buffer (10 mM HEPES pH 7.5, 100 mM NaCl, 0.1 mM EDTA, and 10 mM 2-mercaptoethanol), and against a T150 buffer (20 mM Tris-Cl pH 8.0, 150 mM NaCl, 0.1 mM EDTA, and 10 mM 2-mercaptoethanol), for STRNySpt3His and STRNySpt8His, respectively. The STRN tag was cleaved off the proteins with the TEV NIa protease treatment. The TEV-cleaved product was further purified with an ion-exchange HPLC column. Source S10 HPLC cation exchange was used for the ySpt3His protein, but Source Q10 HPLC anion exchange was used for the ySpt8His protein purification. The ySpt3His protein was purified with a linear salt concentration from 100 to 1000 mM NaCl HPLC buffers (10 mM HEPES pH 7.5, 100 mM or 1000 mM NaCl, 0.1 mM EDTA, and 10 mM 2-mercaptoethanol), whereas the ySpt8His protein requires a linear gradient of 150 to 600 mM NaCl HPLC buffers (20 mM Tris-Cl pH 8.0, 150 mM or 600 mM NaCl, 0.1 mM EDTA, and 10 mM 2-mercaptoethanol). The purified proteins were stored in 10% glycerol, aliquoted, and kept at -80°C.

2.5.3 Yeast strains and gene deletion

The yeast wild type SAGA complex in this study was isolated from wild type BY4742 *MATα*, which contains a TAP tag at the C-terminus of ADA1 in the genome. All the yeast mutants included in this study share the same background with the wild type strain. The *spt3*Δ (*spt3*Δ::kanMX4) yeast mutant was a gift from Dr. Patrick Grant of the University of Virginia. The other two yeast mutants, *spt8*Δ (*spt8*Δ::kanMX4) and *spt8*Δ;

*spt3*Δ (*spt8*Δ::LEU2; *spt3*Δ::kanMX4), were created by the PCR mediated deletion method (Brachmann et al., 1998).

The deletion method requires two 60 nucleotide (nt) PCR primers in which the first 40 nt sequence from the 5' end of each primer is identical to the sequences upstream and downstream flanking the coding region of the gene of interest (*SPT8*), and the other 20 nt sequence for each primer is specific for the amplification of any auxotrophic marker gene from the pRS set of plasmids (Brachmann et al., 1998). For deletion of the SPT8, the forward oligo STO1601 (5'-TACTAAAGGCTCAGTTTTTTTTTTTTCTTCTTTTACGTAAGATTGTACTGAGAGTGCAC-3') and the reverse oligo STO1602 (5'-TTATGATTATGATTATGGTTATGATTATTATTACAACTCACTGTGCGGTATTTCACACCG-3') were used to amplify the pRS400, which contain the kanMX4, the gene that confers resistance to the G418 drug. The resulting PCR product, which has an expected size of approximately 1,500 base pairs (bp), was analyzed with a 1% agarose gel. Once the amplification was confirmed, the remaining PCR product was purified with 2 extractions of a phenol/CIA mix (1:1 mixture of TE (10 mM Tris pH 8.0 and 0.1 mM EDTA)-equilibrated phenol and CIA), followed by one extraction of CIA (a mixture of 24 volumes chloroform with 1 volume of isoamyl alcohol). The cleaned PCR product can be concentrated by ethanol precipitation, and the pellet was resuspended in a 20-30 µl sterile TE. The concentration of the DNA could be estimated by electrophoresis or by UV absorption.

The competent yeast cells were prepared as follows. All steps were performed at room temperature. Briefly, the Ada1-TAP wild type yeast in the BY4742 background was cultured in a 20 ml rich media until the OD_{600} reached 0.8-1.2. Cells were harvested by centrifugation and resuspended in 1 ml sterile distilled water and transferred into a 1.7 ml screw capped tube. The supernatant was removed from the cells after centrifugation, and the resulting pellet was resuspended in 1 ml sterile LioAc-TE (100 mM LioAc pH 7.5, 10 mM Tris-Cl pH 7.5, and 1 mM EDTA). The centrifugation was repeated and the cell

pellet was resuspended in 250 µl sterile LioAc-TE. The resuspended cells can be stored at 4°C for up to one week.

With a sterile 1.7 ml tube, these followings were added in order: about 2 µg of the PCR product, 10 µl of 5 mg/ml carrier DNA, and 50 µl of cell suspension. Immediately, 300 µl of sterile PLATE solution (100 mM LioAc pH 7.5, 10 mM Tris-Cl pH 7.5, 1 mM EDTA, and 40% PEG 3500) was added to the tube. The tube was vortexed at a maximum speed for 10 seconds and incubated at 30°C for 30 minutes with constant rotation. Subsequently, the cells were heat-shocked at 42°C for15 minutes, and precipitated by centrifugation. The supernatant was removed, and the cell pellet was resuspended in 1 ml YPD medium (10 g/l yeast extract (Difco), 20 g/l Peptone (Difco), 40 mg/l Adenine (Sigma), and 2% Dextrose) and transferred to a sterile glass tube. The tube was incubated at 30°C for 4-5 hours before plating on the YPD plates that contained 300 µg/ml G418 (Gibco). Colonies will appear after two or three days of incubation at 30°C. A few selected colonies were streaked onto a new YPD + G418 plate to further purify a single colony. The genotype of the mutant was verified with a PCR method to confirm the presence of the kanMX4 marker at the correct location.

As for the double deletion of the SPT8 and SPT3 (*spt8*Δ;*spt3*Δ mutant), the deletion strategy was similar to that described previously for deleting the SPT8 with kanMX4, except that the PCR amplification was performed using the pRS405 (LEU2) plasmid as a template, and the Ada1-TAP BY4742 yeast strain with *spt3*Δ::kanMX4 was used to create the competent cells. I chose LEU2 as a selection marker since the kanMX4 was already used to delete the SPT3. In addition, the transformants after the heat-shock at 42°C were resuspended in 500 µl sterile water and plated directly to the minimum –Leu plates without incubation for 4-5 hours as in the case of the G418 selection.

2.5.4 Purification of the SAGA complex with the conventional technique

The yeast containing Flag-tagged Tra1 was created by transforming the YCB650 yeast strain (TRA1::LEU2) with the pCB163 (containing the TRP3 selection marker and the N-terminal Flag-tagged Tra1). Because Tra1 is essential, the yeast strain can be cultured with a rich media. Yeast was grown in a total of 6 liters Yeast extract-Peptone-Dextrose (YPD) medium (10 g/l Yeast extract (Difco), 20 g/l Peptone (Difco), 40 mg/l Adenine (Sigma), and 2% Dextrose), and harvested at an approximate density of 6.2 x 10^7 cells/ml, and stored at -80°C. The conventional method for the HAT complex purification involved the metal affinity: nickel-nitrilotriacetic acid (Ni-NTA) and MonoQ fractionation. Since the Tra1 was fused with a Flag tag on its N-terminus, the MonoQ fractions that contain the SAGA complex were further purified using the Flag Immunoprecipitation (Flag IP) method. For purifications, cells were thawed and resuspended with an approximately 40-50 ml extraction buffer (40 mM HEPES pH 7.5, 350 mM NaCl, 10% glycerol, 0.1% Tween20, 1 mM benzamidine, 1 mM phenylmethylsulfonyl fluoride (PMSF), 2 µg/ml pepstatin, and 2 µg/ml leupeptin). Cells were disrupted by using 0.5 mm Glass beads (BioSpec Products, Inc.) in a 40-ml bead beater chamber (BioSpec Inc.) for 8 repeats of 30 seconds, with a 1 minute break in between the beating. It is important to keep the sample cold at all times during the cell disruption steps to prevent proteins from being degraded. Then, the sample was centrifuged at 15,000 rpm in a SS34 rotor for 30 minutes at 4°C. The soluble portion of the extract was collected and ultracentrifuged at 100,000xg for 1 hour at 4°C, using a 45Ti rotor (Beckman) at 43,000 rpm. Alternatively, the sample can also be centrifuged with a 50.2Ti rotor (Beckman) at 35,000 rpm for 2 hours. After ultracentrifugation, the supernatant was combined and the overall protein content was estimated by the Bradford assay using the Bovine serum albumin (BSA) as a standard. The SAGA and other transcriptional coactivator complexes can naturally bind to a metal affinity (Ni-NTA) resin: 1 ml of the resin was used for incubation with every 50 milligram of proteins in the extract. After at least 3 hours of incubation at 4°C, the resin was washed with 3CV of the extraction buffer and 3CV of the 20 mM imidazole buffer (20 mM imidazole pH 7.2, 100

mM NaCl, 10% glycerol, 0.1% Tween 20, 2 µg/ml leupeptin, 2 µg/ml pepstatin, and 1 mM PMSF). Bound proteins were eluted with 3CV of the 300 mM Imidazole buffer (300 mM Imidazole pH 7.2, 100 mM NaCl, 10% glycerol, 0.1% Tween 20, 2 µg/ml leupeptin, 2 µg/ml pepstatin, and 1 mM PMSF). This Ni-NTA eluate contained many transcriptional coactivators, including the SAGA complex, which was further purified with MonoQ HR 5/5 (Pharmacia Biotech) on the Pharmarcia AKTA Purifier. Briefly, the SAGA complex was eluted from the MonoQ column at ~350 mM NaCl concentration within a 22.5 CV linear salt gradient of 100 to 500 mM NaCl in buffer B (50 mM Tris-Cl pH 8.0, 10% glycerol, 0.1% Tween 20, 2 µg/ml leupeptin, 2 µg/ml pepstatin, and 1 mM PMSF). The MonoQ fractionation was done at a flow rate of 0.5 ml/min. and the 0.5 ml fractions were collected. Fractions that contained the SAGA complex were identified with Western blot analysis and HAT assay (Eberharter et al., 1998), and combined for the final step of purification with the resin-bound anti-Flag antibody, which recognizes the Flag tag on the Tra1 SAGA subunit.

2.5.5 Histone acetyl transferase (HAT) assay and fluorography

The HAT assay was performed as described previously (Eberharter et al., 1998). Briefly, 2 µl of the HAT complex were mixed into a 30 µl reaction that contains 6 µl 5x HAT buffer (250 mM Tris-Cl pH 8.0, 25% glycerol, 0.5 mM EDTA, 250 mM KCl, and 62.5 µl/ml PSC-protector solution (Roche)), 1 mM DTT, 10 mM sodium butyrate, 1 mM Pefabloc SC (Roche), 1 µg of HeLa cell core histones, and 0.125 µCi tritiated acetyl-CoA. The HAT assay with the HeLa cell long oligo nucleosomes (LON) reaction was prepared the same way but 1µg HeLa cell core hisotones were substituted for 1 µg LON per reaction. The reaction mixture was incubated at 30°C for 30 minutes. After incubation, the reaction mix was placed on ice to stop the reaction. Then, 15 µl reaction samples were spotted onto P81 phosphocellulose filters (Whatman), cut in half, and allowed to completely air-dry. Dried filters were washed with a 4x 50 ml 1x wash buffer (50 mM $NaHCO_3$-$NaCO_3$, pH ~9.2), rinsed in 50 ml acetone, and dried. The filters were

placed in scintillation vials which contained 4 ml scintillation fluid (ScintiSafe Econo F, FisherChemcial). Each vial was counted in a scintillation counter for 1 minute.

The other 15 µl HAT reaction was mixed with 5 µl 4xPGLB (2.5 M Bis-Tris pH 6.8, 40% glycerol, 8% SDS, 4.32 M 2-mercaptoethanol, and 0.8 mg/ml bromophenol blue), and boiled for 5 minutes. 10 µl of each sample was electrophoresed with an 18% SDS PAGE gel. The gel was fixed with a fix solution (45% ethanol and 10% acetic acid) and subsequently stained with a coomassie blue dye (fix solution with a coomassie dye at 5 mg/l concentration). After destaining until histone bands became visible, the gel was incubated with EN^{3}HANCE autoradiography enhancer (PerkinElmer Life Sciences, Inc.) for 30 minutes at room temperature. After washing, the gel was incubated with water for at least 30 minutes at room temperature. The gel was dried under vacuum at 65°C for 90 minutes before exposing to an X-ray film at -80°C. Depending on the strength of the signal, the exposure time could take several hours or weeks.

2.5.6 Purification of the SAGA complex using the TAP tag

Yeast was grown in a total of 12 liters YPD medium, harvested at an approximate density of 6.2 x 10^7 cells/ml, and kept in -80°C. Purification procedures were modified from the literature (Puig et al., 2001), and all steps except Mono Q fractionations were performed at 4°C. The cells were resuspended with about 80-100 ml extraction buffer and disrupted with glassbeads in a bead-beater as described in **2.5.4**. Soluble cell extract, which was prepared by centrifugation at 16,000*g* for 30 minutes at 4C, was equally divided into 8 aliquots, and directly incubated for 3-12 hours with 8x 200 µl aliquots of IgG Sepharose 6 Fast Flow resin (Amersham Biosciences). Next, the resin was subsequently washed with 2 x 10 ml IPP150 buffer (10 mM Tris-Cl pH 8.0, 150 mM NaCl, and 0.1% NP-40), and 2 x 10 ml TEV buffer (10 mM Tris-Cl pH 8.0, 100 mM NaCl, 10% glycerol, 0.1% NP-40, 0.5 mM EDTA, and 1 mM dithiothreitol, DTT). For cleavage of the TAP tag, 0.1-0.3 µM of the TEV NIa protease in 1 ml TEV buffer was added to the washed resin. Incubation was performed for 24 hours at 4ºC with constant rotation. The TEV-

cleaved product was further purified with Mono Q HR 5/5 (Pharmacia Biotech) on the BioCAD Sprint HPLC System. As shown in Figure **2-2** B and C, peak fractions containing the SLIK and SAGA complexes can easily be identified. A small aliquot from each fraction was analyzed by the HAT assay, Western blots and silver stained gel. Fractions containing the SAGA complex were dialyzed against the $CaCl_2$ binding buffer (50 mM Tris-Cl pH 8.0, 150 mM NaCl, 1.0 mM Magnesium Acetate, 1.0 mM imidazole, 2.0 mM $CaCl_2$, 10% glycerol, 0.1% Tween 20, 1.0 mM benzamidine, 2.0 µg/ml leupeptin, 2.0 µg/ml pepstatin, and 1.0 mM PMSF) for the incubation with the Calmodulin Affinity Matrix (CAM) from Stratagene. 200 µl of CAM were used for every 1 ml of the pooled sample, and the incubation took at least 2 hours at 4°C. The resins were washed with 3 x 10 ml $CaCl_2$ binding buffer, and eluted with a CAM elution buffer (20 mM HEPES pH 7.5, 2.0 mM Ethylenebis(Oxyethylenenitrilo) Tetraacetic Acid, EGTA, 150 mM NaCl, 10% glycerol, 0.1% Tween 20, 1.0 mM benzamidine, 2.0 µg/ml leupeptin, 2.0 µg/ml pepstatin, and 1.0 mM PMSF). Fractions were pooled and concentrated with a 20 ml Vivaspin 30,000 MWCO PES (Vivascience). The purified SAGA complex was aliquoted and kept at -80ºC.

2.5.7 Photo-cross-linking label transfer assay

Photo-cross-linking label transfer assay was performed as described previously (Neely et al., 1999) with some modifications. Conjugation of TBP was conducted by mixing 500 µl of 12.4 µM yeast TBP with 4-5 times concentration of the Sulfosuccinimidyl (2-6-(biotinamido)-2-(*p*-azidobenzamido)-hexanoamido) ethyl-1,3'-dithiopropionate, which is also known as the Sulfo-SBED (Pierce), dissolved in the dimethyl fluoride. The incubation was conducted in the dark at room temperature for 30 minutes. The conjugated TBP was purified away from free cross-linking reagents with a Source S1 HPLC cation exchange column (Pharmacia Biotech). The bound TBP was eluted off the column with the same linear salt gradient used for purification of TBP (see above). The presence of the Sulfo-SBED conjugated to TBP was tested by a dot-blot analysis using the Streptavidin, Horseradish Peroxidase Conjugated (Pierce), which detects the presence

of biotin on the cross-linking reagent. The concentration of the conjugated TBP was estimated based on the known concentration of TBP electrophoresed on the same Sodium Dodecyl Sulfate-Polyacrylamide Gel Electrophoresis (SDS-PAGE) gel, stained with a coomassie dye. Approximately 2.48 µM conjugated TBP was diluted to lower concentration with HG0 (10 mM HEPES pH 7.5, 0.1 mM EDTA, 10% glycerol, 0.1% Tween 20). Initial photo-cross-linking experiments were performed to select the optimal concentrations of conjugated TBP and SAGA complex. In the optimized condition, 10 µl of ~10-20 nM SAGA complex was mixed with 10 µl of ~177 nM conjugated TBP. The mixture was incubated in the dark at 4ºC for 30 minutes before exposing to UV light (XX-15B lamp, Spectroline) at a distance of 6 cm for 8 min at room temperature. After photo-cross-linking, 2.2 µl of 1 M DTT was added to reaction tubes, and 7.4 µl of 4x protein gel loading buffer (PGLB), which contains 0.5 M Bis-Tris pH 6.8, 30% glycerol, and 8% SDS was added. The mixtures were boiled for 5 minutes before loaded on an 18% polyacrylamide gel. Label transfer from TBP to SAGA subunit was analyzed by a Western blot. Briefly, the proteins were transferred to nitrocellulose membrane (Hybond-ECL, Amersham Biosciences), which were subsequently blocked by 3% BSA in 1x TBST (0.025 M Tris-Cl pH 8.0, 150 mM NaCl, and 0.05% Tween 20) for 1 hour at room temperature. The membrane was washed 3x 5 min with 1x TBST and incubated with 10 ml of 1:5000 dilution of Streptavidin, Horseradish Peroxidase (HRP) conjugated (Pierce) in 1x TBST for 1 hour at room temperature. Because Streptavidin has HRP conjugated, there is no need to use the secondary antibodies for detection. The membrane was subsequently washed 3x 5 minutes with 1x TBST before developing with the SuperSignal West Pico Chemiluminescent Substrate (Pierce). The membrane was stripped of bound streptavidin or antibodies and reprobed with appropriate antibodies.

2.5.8 Pull down assays

The STR tag pull down in this study was divided into two categories: TBP-SAGA complex pull down and TBP-Spt protein pull down. Both pull down experiments were performed in a similar condition with some slight differences. For TBP-SAGA complex

pull down, 3 µg of STRNyTBPcore wild type or STRNyTBPcore mutants (R171E and T153I) were incubated with 25 µl equilibrated *Strep*-Tactin Superflow (IBA) in HGN150 buffer (20 mM HEPES pH 7.5, 150 mM NaCl, 10% glycerol, 0.1% NP-40, and 10 mM 2-mercaptoethanol) for 1 hour at 4ºC with constant rotations. The resin was washed 3x 500 µl with HGN150 buffer before incubating with 25 µl of approximately 0.05-0.1 nM SAGA complex for 2 hours at 4ºC with constant rotations. The supernatant was saved and the resin was washed 4x 500 µl with HGN150 buffer. Gel loading samples from the input, supernatant, or beads from the pull down experiment were prepared, and equal amount of each were loaded on an 18% polyacrylamide gel for Western blots. To quantify the levels of SAGA complex that were pulled down by TBP proteins, the experiment was conducted as follows. The STRN tag on yTBPcore that interacts with the SAGA complex was cleaved with 25 µl of TEV NIa protease at a final concentration of 12.5 µM. Consequently, the SAGA complex was no longer immobilized by TBP on the resin, thus allowing HAT assays to be performed directly with the supernatant. HAT assays with HeLa cell core histones were performed as described in **2.5.5**. Pull down assays between the wild type STRNyTBPcore and the SAGA mutants were also performed in the same way.

A pull down experiment between TBP and Spt proteins (Spt8His or Spt3His) was performed using the same procedures described above, except that only 0.1% Tween 20 was used and the HAT assays were no longer applicable. An equivalent amount of input, supernatant, or beads was loaded on an 18% polyacrylamide gel. Proteins on the gel were transferred to a nitrocellulose membrane. A Western blot experiment with anti-His antibodies was carried out using the same procedures described above (see **2.5.7**) except that an extra incubation step with the anti-rabbit IgG, Horseradish Peroxidase linked antibodies (Amersham Biosciences) was included after incubation with the primary antibodies.

2.6 Acknowledgements

I would like to thank Dr. Patrick Grant of the University of Virginia, for giving us the wild type and the *spt3*Δ Ada1-TAP yeast strain. I am grateful to Joe Reese and the members of the Reese lab for useful advice and discussion, for sharing protocols, reagents and equipment for creating the *spt8*Δ and *spt8*Δ;*spt3*Δ Ada1-TAP yeast mutant strains, and for sharing the anti-Taf6 antibodies. Also, many thanks to Jerry L. Workman for lending us the UV lamp, and his lab members for help and suggestions, for sharing reagents and equipments, and for providing the anti-Spt8, anti-Taf5, anti-Taf12, anti-Spt7, and anti-Ada1 antibodies. I would also like to thank all Tan lab members for their help and support throughout this project. Lastly, I would like to thank the Penn State gene regulation community for useful suggestion and discussion.

2.7 Bibliography

Allard, S., Utley, R. T., Savard, J., Clarke, A., Grant, P., Brandl, C. J., Pillus, L., Workman, J. L., and Cote, J. (1999). NuA4, an essential transcription adaptor/histone H4 acetyltransferase complex containing Esa1p and the ATM-related cofactor Tra1p. Embo J *18*, 5108-5119.

Balasubramanian, R., Pray-Grant, M. G., Selleck, W., Grant, P. A., and Tan, S. (2002). Role of the Ada2 and Ada3 transcriptional coactivators in histone acetylation. J Biol Chem *277*, 7989-7995.

Barbaric, S., Reinke, H., and Horz, W. (2003). Multiple mechanistically distinct functions of SAGA at the PHO5 promoter. Mol Cell Biol *23*, 3468-3476.

Belotserkovskaya, R., Sterner, D. E., Deng, M., Sayre, M. H., Lieberman, P. M., and Berger, S. L. (2000). Inhibition of TATA-binding protein function by SAGA subunits Spt3 and Spt8 at Gcn4-activated promoters. Mol Cell Biol *20*, 634-647.

Bhaumik, S. R., and Green, M. R. (2001). SAGA is an essential in vivo target of the yeast acidic activator Gal4p. Genes Dev *15*, 1935-1945.

Bhaumik, S. R., and Green, M. R. (2002). Differential requirement of SAGA components for recruitment of TATA-box-binding protein to promoters in vivo. Mol Cell Biol *22*, 7365-7371.

Boudreault, A. A., Cronier, D., Selleck, W., Lacoste, N., Utley, R. T., Allard, S., Savard, J., Lane, W. S., Tan, S., and Cote, J. (2003). Yeast enhancer of polycomb defines global Esa1-dependent acetylation of chromatin. Genes Dev *17*, 1415-1428.

Brachmann, C. B., Davies, A., Cost, G. J., Caputo, E., Li, J., Hieter, P., and Boeke, J. D. (1998). Designer deletion strains derived from Saccharomyces cerevisiae S288C: a useful set of strains and plasmids for PCR-mediated gene disruption and other applications. Yeast *14*, 115-132.

Brown, C. E., Howe, L., Sousa, K., Alley, S. C., Carrozza, M. J., Tan, S., and Workman, J. L. (2001). Recruitment of HAT complexes by direct activator interactions with the ATM-related Tra1 subunit. Science *292*, 2333-2337.

Chasman, D. I., Flaherty, K. M., Sharp, P. A., and Kornberg, R. D. (1993). Crystal structure of yeast TATA-binding protein and model for interaction with DNA. Proc Natl Acad Sci U S A *90*, 8174-8178.

Cormack, B. P., Strubin, M., Stargell, L. A., and Struhl, K. (1994). Conserved and nonconserved functions of the yeast and human TATA-binding proteins. Genes Dev *8*, 1335-1343.

Dudley, A. M., Rougeulle, C., and Winston, F. (1999). The Spt components of SAGA facilitate TBP binding to a promoter at a post-activator-binding step in vivo. Genes Dev *13*, 2940-2945.

Durant, M., and Pugh, B. F. (2006). Genome-Wide Relationships between TAF1 and Histone Acetyltransferases in Saccharomyces cerevisiae. Mol Cell Biol *26*, 2791-2802.

Eberharter, A., Lechner, T., Goralik-Schramel, M., and Loidl, P. (1996). Purification and characterization of the cytoplasmic histone acetyltransferase B of maize embryos. FEBS Lett *386*, 75-81.

Eberharter, A., Sterner, D. E., Schieltz, D., Hassan, A., Yates, J. R., 3rd, Berger, S. L., and Workman, J. L. (1999). The ADA complex is a distinct histone acetyltransferase complex in Saccharomyces cerevisiae. Mol Cell Biol *19*, 6621-6631.

Eisenmann, D. M., Arndt, K. M., Ricupero, S. L., Rooney, J. W., and Winston, F. (1992). SPT3 interacts with TFIID to allow normal transcription in Saccharomyces cerevisiae. Genes Dev *6*, 1319-1331.

Eisenmann, D. M., Chapon, C., Roberts, S. M., Dollard, C., and Winston, F. (1994). The Saccharomyces cerevisiae SPT8 gene encodes a very acidic protein that is functionally related to SPT3 and TATA-binding protein. Genetics *137*, 647-657.

Gangloff, Y. G., Sanders, S. L., Romier, C., Kirschner, D., Weil, P. A., Tora, L., and Davidson, I. (2001). Histone folds mediate selective heterodimerization of yeast

TAF(II)25 with TFIID components yTAF(II)47 and yTAF(II)65 and with SAGA component ySPT7. Mol Cell Biol *21*, 1841-1853.

Grant, P. A., Duggan, L., Cote, J., Roberts, S. M., Brownell, J. E., Candau, R., Ohba, R., Owen-Hughes, T., Allis, C. D., Winston, F., *et al.* (1997). Yeast Gcn5 functions in two multisubunit complexes to acetylate nucleosomal histones: characterization of an Ada complex and the SAGA (Spt/Ada) complex. Genes Dev *11*, 1640-1650.

Grant, P. A., Schieltz, D., Pray-Grant, M. G., Steger, D. J., Reese, J. C., Yates, J. R., 3rd, and Workman, J. L. (1998). A subset of TAF(II)s are integral components of the SAGA complex required for nucleosome acetylation and transcriptional stimulation. Cell *94*, 45-53.

Kou, H., Irvin, J. D., Huisinga, K. L., Mitra, M., and Pugh, B. F. (2003). Structural and functional analysis of mutations along the crystallographic dimer interface of the yeast TATA binding protein. Mol Cell Biol *23*, 3186-3201.

Kou, H., and Pugh, B. F. (2004). Engineering dimer-stabilizing mutations in the TATA-binding protein. J Biol Chem *279*, 20966-20973.

Larschan, E., and Winston, F. (2001). The S. cerevisiae SAGA complex functions in vivo as a coactivator for transcriptional activation by Gal4. Genes Dev *15*, 1946-1956.

Lee, D., Ezhkova, E., Li, B., Pattenden, S. G., Tansey, W. P., and Workman, J. L. (2005). The proteasome regulatory particle alters the SAGA coactivator to enhance its interactions with transcriptional activators. Cell *123*, 423-436.

Li, B., Pattenden, S. G., Lee, D., Gutierrez, J., Chen, J., Seidel, C., Gerton, J., and Workman, J. L. (2005). Preferential occupancy of histone variant H2AZ at inactive promoters influences local histone modifications and chromatin remodeling. Proc Natl Acad Sci U S A *102*, 18385-18390.

Neely, K. E., Hassan, A. H., Wallberg, A. E., Steger, D. J., Cairns, B. R., Wright, A. P., and Workman, J. L. (1999). Activation domain-mediated targeting of the SWI/SNF complex to promoters stimulates transcription from nucleosome arrays. Mol Cell *4*, 649-655.

Nourani, A., Utley, R. T., Allard, S., and Cote, J. (2004). Recruitment of the NuA4 complex poises the PHO5 promoter for chromatin remodeling and activation. Embo J *23*, 2597-2607.

Puig, O., Caspary, F., Rigaut, G., Rutz, B., Bouveret, E., Bragado-Nilsson, E., Wilm, M., and Seraphin, B. (2001). The tandem affinity purification (TAP) method: a general procedure of protein complex purification. Methods *24*, 218-229.

Selleck, W., Fortin, I., Sermwittayawong, D., Cote, J., and Tan, S. (2005). The Saccharomyces cerevisiae Piccolo NuA4 histone acetyltransferase complex requires the Enhancer of Polycomb A domain and chromodomain to acetylate nucleosomes. Mol Cell Biol *25*, 5535-5542.

Stargell, L. A., and Struhl, K. (1996). A new class of activation-defective TATA-binding protein mutants: evidence for two steps of transcriptional activation in vivo. Mol Cell Biol *16*, 4456-4464.

Sterner, D. E., Belotserkovskaya, R., and Berger, S. L. (2002). SALSA, a variant of yeast SAGA, contains truncated Spt7, which correlates with activated transcription. Proc Natl Acad Sci U S A *99*, 11622-11627.

Sterner, D. E., Grant, P. A., Roberts, S. M., Duggan, L. J., Belotserkovskaya, R., Pacella, L. A., Winston, F., Workman, J. L., and Berger, S. L. (1999). Functional organization of the yeast SAGA complex: distinct components involved in structural integrity, nucleosome acetylation, and TATA-binding protein interaction. Mol Cell Biol *19*, 86-98.

Tan, S. (2001). A modular polycistronic expression system for overexpressing protein complexes in Escherichia coli. Protein Expr Purif *21*, 224-234.

Utley, R. T., Ikeda, K., Grant, P. A., Cote, J., Steger, D. J., Eberharter, A., John, S., and Workman, J. L. (1998). Transcriptional activators direct histone acetyltransferase complexes to nucleosomes. Nature *394*, 498-502.

Warfield, L., Ranish, J. A., and Hahn, S. (2004). Positive and negative functions of the SAGA complex mediated through interaction of Spt8 with TBP and the N-terminal domain of TFIIA. Genes Dev *18*, 1022-1034.

Wu, P. Y., and Winston, F. (2002). Analysis of Spt7 function in the Saccharomyces cerevisiae SAGA coactivator complex. Mol Cell Biol *22*, 5367-5379.

Zhang, H., Roberts, D. N., and Cairns, B. R. (2005). Genome-wide dynamics of Htz1, a histone H2A variant that poises repressed/basal promoters for activation through histone loss. Cell *123*, 219-231.

Chapter 3

DNA competes with Spt8 in SAGA to bind to TBP: a model for gene transcriptional activation

3.1 Abstract

TBP recruitment to a promoter is a critical step for transcriptional initiation. My previous work showed that the Spt8 and Ada1 interact with TBP protein but the mechanism of TBP binding remained not well understood. In this study, I propose that Spt8 contains a WD40 repeat domain, which might contain only six WD40 repeats. I found that truncated Spt8 that contains the putative WD40 domain can only be purified in the presence of 3 M urea. By means of pull down experiments, this putative WD40 domain of Spt8 is found to be sufficient for TBP binding. In addition, the Spt8-TBP interaction is salt dependent, suggesting the role of electrostatic interaction in the complex stabilization. Spt8 or the SAGA complex competes with TBP dimerization and binds to TBP monomer. In addition, the TATA box DNA has to compete with Spt8 or the SAGA complex for binding with TBP. Thus, I propose a simple hand off model, in which the SAGA complex drops TBP off to the core promoter through competition from the TATA box element without forming a complex with TBP/TATA box DNA.

3.2 Introduction

My previous results have identified Spt8 and possibly Ada1 in the SAGA complex as subunits that interact with TBP. The R171E TBP mutant is defective for the interaction with both Spt8 and the SAGA complex. However, this mutation stabilizes TBP dimerization (Kou et al., 2003; Kou and Pugh, 2004), suggesting that the Spt8 or the

SAGA complex may compete with TBP dimerization for the association with TBP. One important question to ask is whether the binding of Spt8 or the SAGA complex would prevent the formation of TBP/DNA complex. If so, how could a complex that inhibits the binding of TBP/DNA still be able to promote gene activation?

As a coactivator complex, SAGA can interact with an activator to help activate the binding of TBP to a promoter. It is unknown whether the complex simultaneously interacts with an activator and TBP. A coactivator model suggests that a coactivator serves as a physical bridge between an activator and TBP (Belotserkovskaya et al., 2000; Bhaumik and Green, 2001; Larschan and Winston, 2001) (Figure **3-1** A). However, all studies reported in the literature, using the chromatin immunoprecipitation (ChIP) assay, find the association of the SAGA complex at the upstream activating sequence (UAS), but not at the core promoter which contains the TATA box element (Bhaumik and Green, 2001; Larschan and Winston, 2001). Conversely TAFs, the coactivator complex in TFIID that regulates transcription at TAF-dependent gene such as the RPS5 (Belotserkovskaya et al., 2000; Kuras et al., 2000), is only localized to the core promoter but not the UAS (Bhaumik and Green, 2001). Thus, a coactivator might not physically 'bridge' the activator and the DNA bound TBP (Figure **3-1** B and C). Another interesting observation is that SAGA seems to inhibit the binding of TBP to a promoter under uninducing conditions, as in the case of HIS3, TRP, and ARG1 promoters, but to promote the binding of TBP under activation conditions (Belotserkovskaya et al., 2000; Ricci et al., 2002; Takahata et al., 2003).

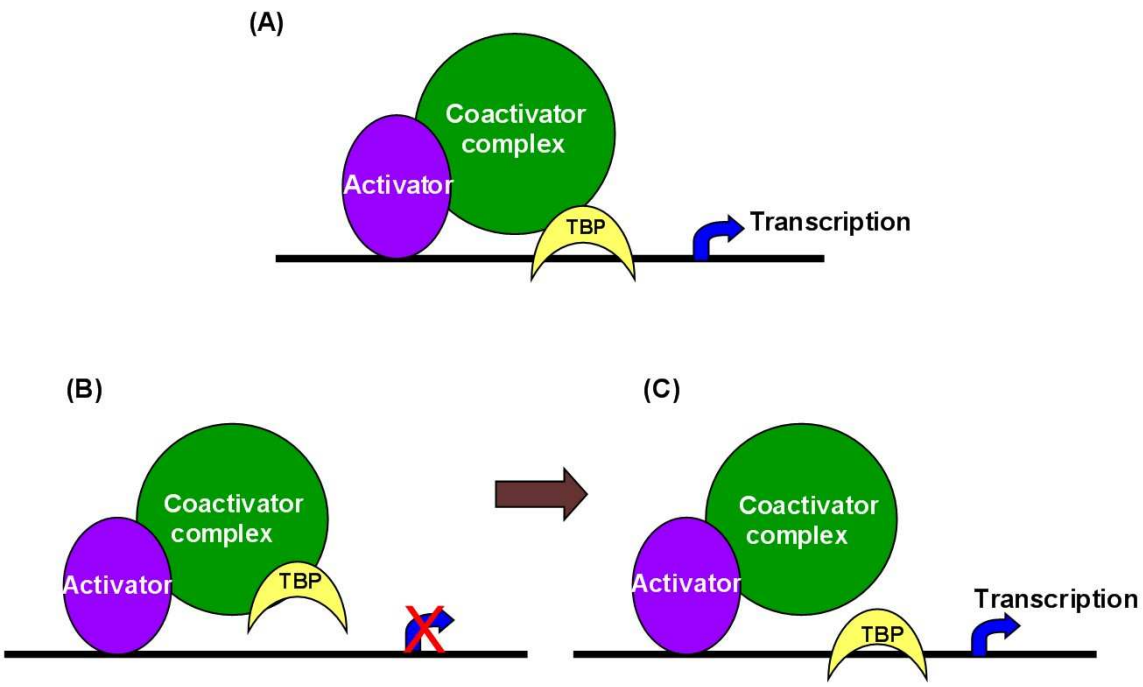

Figure **3-1**: Coactivator models

(A) The bridging model describes that a coactivator physically contact an activator and TBP while they bind to their promoter. (B) and (C) The hand off model describes that the coactivator complex does not interact TBP that binds to the promoter. However, the DNA breaks the coactivator-TBP contact by competition.

Results in this chapter show that Spt8 contains a putative WD40 domain, which is sufficient for the interaction with TBP. The binding of Spt8 to TBP is salt dependent, indicating that electrostatic interaction mainly stabilizes the complex. In addition, the binding Spt8 or the SAGA complex to TBP dissociates TBP dimers. Interestingly, SAGA complex without the Spt8 subunit also dissociates TBP dimers. Furthermore, the TATA box DNA dissociates Spt8 or the SAGA complex upon binding to TBP. These results indicate that Spt8 may bind to TBP through the concave surface of the saddle-like structure of TBP, and the SAGA complex functions to regulate TBP binding to the core promoter. Thus, I propose a hand off model in which the SAGA complex brings TBP to the promoter and hands it off to the promoter without physically "bridging" an activator

to the TBP/DNA complex. This simple mechanism can explain many behaviors of the SAGA complex *in vivo*.

3.3 Results

3.3.1 Purification of the full length Spt8

The experimental procedures for the purification of the full length Spt8 are described in **2.5.2**. Expression and purification of the full length Spt8 are summarized in Figure **3-2**. Full length Spt8 is expressed at low levels but could be detected by Western blotting. Expression at 37°C yielded the insoluble protein; however, the solubility improves when the expression was performed at 28°C (data not shown). I also found that the expression and yield of full length Spt8 could be improved by about two-fold when the protein was expressed in the Rosetta(DE3)pLysS cells (Novagen) at 18°C.

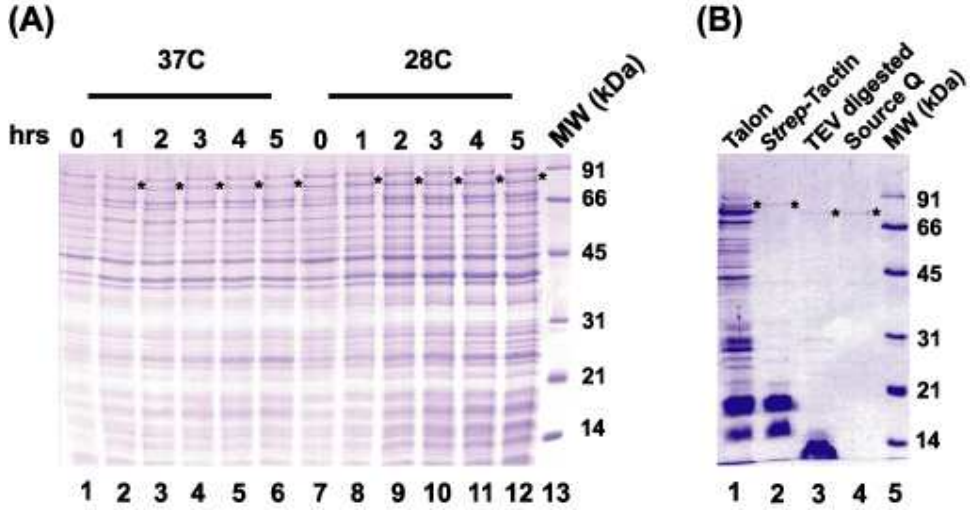

Figure **3-2**: Expression and purification of the full length Spt8

(A) Expression of the full length Spt8 with the N-terminal STRN tag and the C-terminal His tag in the BL21(DE3)pLysS cells. The asterisk indicates the position of the protein. Time points for the expression were taken every hour from 1 to 5 hours after induction with IPTG. (B) A summary of the purification of the full length Spt8

3.3.2 Purification of the putative WD40 domain of Spt8

Based on a sequence alignment and a secondary structure prediction, yeast Spt8 protein contains a highly acidic cluster toward the N-terminus and a putative WD40 domain with six repeats toward the C-terminus (Figure **3-3** A). The WD40 domain is found in several eukaryotic proteins involved in various functions, including signal transduction pathways, cytoskeleton assembly and transcriptional regulation (Hartman et al., 1998; Lodowski et al., 2003; Sprague et al., 2000). The WD40 repeat motif is characterized by β-sheets and loops that connect each β-sheet. One repeat is usually comprised of 40 amino acids which begin with GH and end with WD dipeptides. The amino acid sequences of β-strands and the dipeptides GH and WD may varies among different WD40 repeats of the same protein. For example, the dipeptides WD found in Spt8 could become FD, EN, or YN. Seven WD40 repeat motifs constitute a stable propeller-like structure in which each of the propeller blades consists of four antiparallel β-stranded sheets. The four β-sheets of one WD40 motif are part of two blades: the first β-sheet is part of the 1^{st} blade while the other 3 β-sheets continue on the next blade. The final three β-sheets of the last motif complete the first propeller blade to create a closed ring propeller-like structure Figure **3-3** C. The existent of the putative WD40 domain of Spt8 suggests that the function of the protein might lie within this conserved domain. Because the full length Spt8 directly interacts with TBP, the putative WD40 domain of Spt8 is sufficient for this interaction.

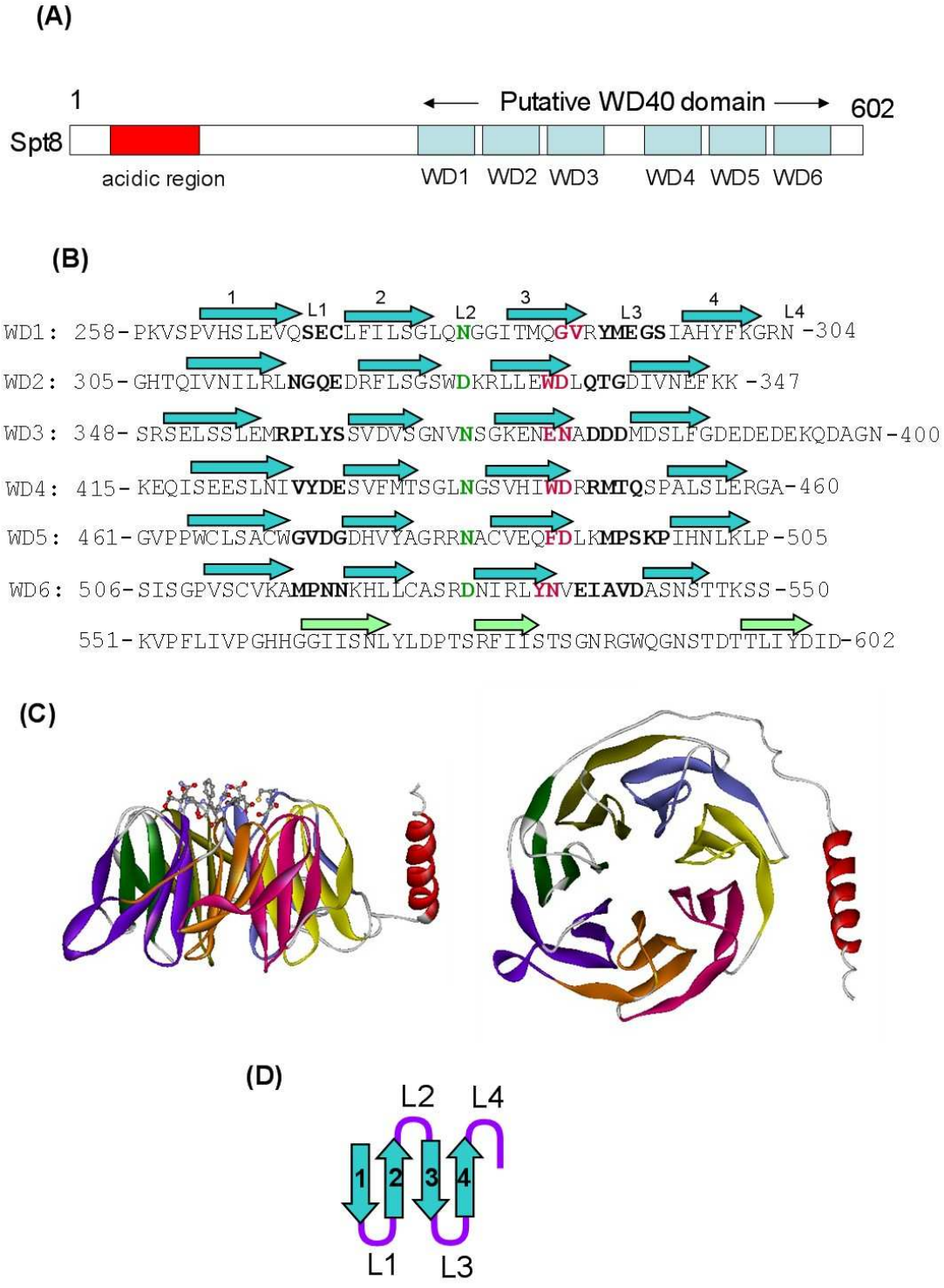

Figure **3-3**: Spt8 contains a putative WD40 domain near the C-terminus.

(A) A representation of the full length Spt8 which contains an acidic cluster near the N-terminus and six putative WD40 repeats located on its C-terminus part. (B) A secondary structure prediction of the WD40 motifs found in Spt8. The arrows represent the β-sheets. The letter L indicates the loop position. Residues in L1 and L3 loops are in bold. The three almost invariant residues are shown in green and red. Based on the secondary structure prediction, the C-terminal part of the Spt8 (551-602) consists of only 3 β-sheets, which probably do not constitute a WD40 repeat. (C) The WD40 domain of the G protein β subunit with loop residues shown in a ball and stick model (left picture) (Lodowski et al., 2003). These loop residues make a contact with other proteins. The right picture is the picture of the same structure but rotated 90°, and show a closed ring propeller-like structure. The WebLab ViewerLite program was used to manipulate the structure (1OMW). (D) A relationship between the loop and the beta strands. Notice that L1 and L3 loops are always facing the same side, while L2 and L4 loops are facing the opposite side. Therefore, mutations of residues within L1 and L3 or L2 and L4 loops would share the same interaction defect.

To test whether this putative domain of Spt8 is sufficient for the interaction with TBP, the domain has to be isolated for a pull down assay. I initially created the Spt8 truncation 2 (210-602) that fused with an N-terminal tandem STRHisN tag, which consists of the *Strep*-tag II (STR), 6x His tags (His), and the TEV cleavage recognition site (N), respectively. This truncated Spt8Δ2 can be highly expressed at 37°C, 28°C, and 18°C Figure **3-4** A and B). However, a protein solubility test indicates that a majority, if not all, of the expressed STRHisNySpt8Δ2 is insoluble and cannot be purified with a metal affinity resin. To purify the truncated Spt8 in a native state, I have tried the following methods: using a different affinity tag to improve the solubility of the protein, coexpression with other proteins, using urea to improve the solubility of the protein, and making different truncations.

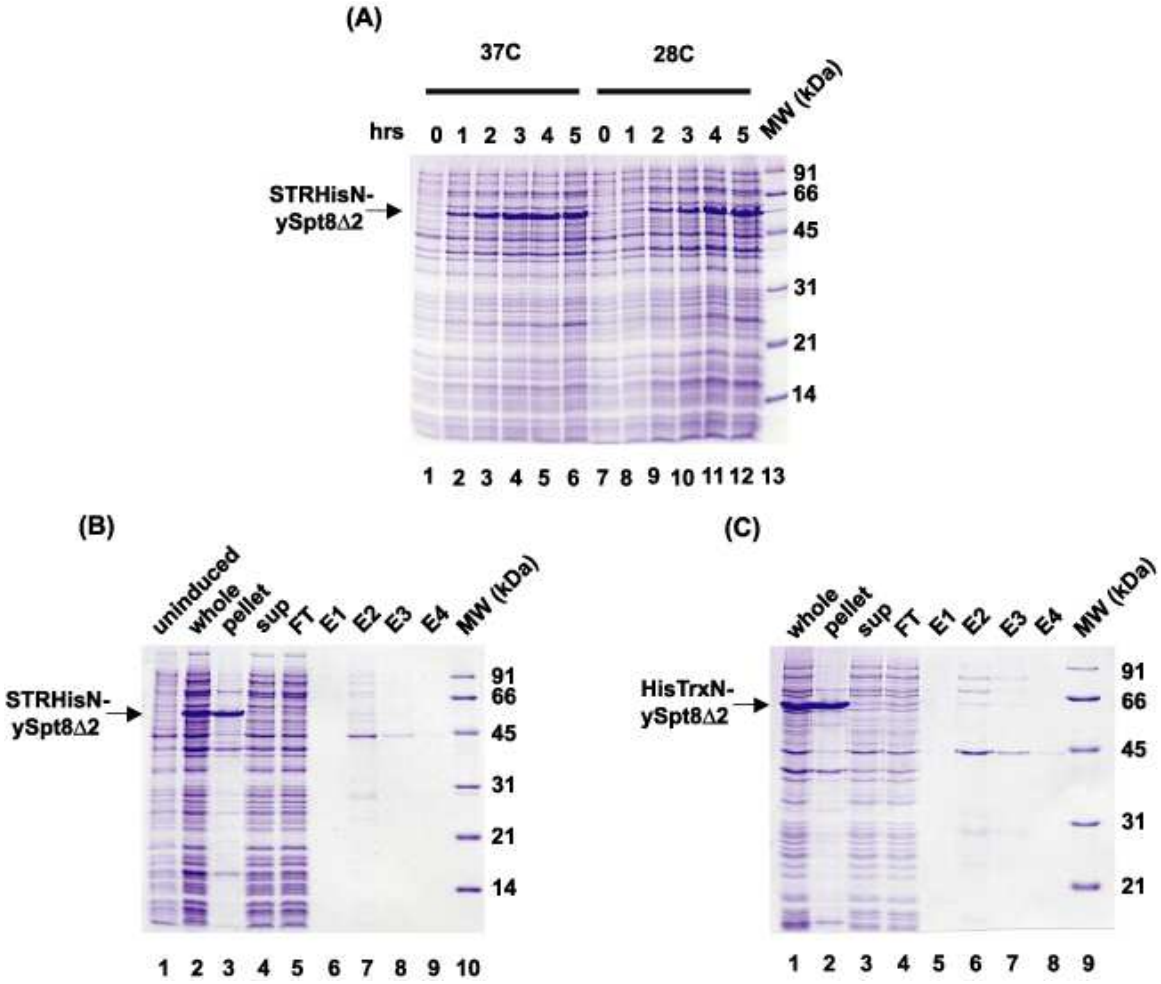

Figure **3-4**: Expression and a metal affinity purification of STRHisN-tagged Spt8Δ2.

(A) Expression of STRHisNySpt8Δ2 at 37°C and 28°C. Expression time points from 1 to 5 hours were monitored. (B) A metal affinity purification of STRHisNySpt8Δ2 expressed at 28°C. The protein was purified with P100 buffer (50 mM sodium phosphate pH 7.0, 100 mM NaCl, 1 mM benzamidine, and 5 mM 2-mercaptoethanol). Since a majority of STRHisNySpt8Δ2 is insoluble, none is purified. (C) A metal affinity purification of HisTrxN-tagged Spt8Δ2, which was expressed at 18°C. The protein was purified with PG200 buffer (50 mM sodium phosphate pH 7.0, 200 mM NaCl, 10% glycerol, 0.1% NP40, 1 mM benzamidine, and 5 mM 2-mercaptoethanol). Again, the protein cannot be purified because it remains insoluble.

3.3.2.1 Using a different affinity tag to improve the solubility of the Spt8Δ2

A fusion tag could influence the behavior of a protein such as its solubility and folding properties. The goal was to use an affinity tag that could promote the solubility of Spt8Δ2. The tandem STRHisN tag, which consists of the STR and His tags located at the N-terminus of the TEV NIa recognition sequence (N), is comprised of about 30 amino acids in total and did not increase protein solubility because majority of the STRHisNySpt8Δ2 remained insoluble (Figure **3-4** B). Among the affinity tags we use in the lab, the HisTrxN fusion tag could be very useful since it contains Thioredoxin, which is a thermostable protein and has been shown to promote protein solubility and purification (Leone et al., 2004; Strahilevitz et al., 2005). Thus, the HisTrxN tag, which contains the 6x His tag, Thioredoxin, and TEV NIa cleavage recognition site (N), was fused to the N-terminus of Spt8Δ2.

Temperature is another factor that affects protein solubility. Temperature affects the timing of the cell cycle of bacteria so that the cell cycle of bacteria is extended when they are grown at 18°C (data observation). We have observed in many cases that the protein of interest that is expressed at 18°C is more soluble than that expressed at a higher temperature. A longer cell cycle probably allows sufficient time for the protein to fold and solubilize.

I performed the expression of HisTrxNySpt8Δ2 at 18°C and purified it using a metal affinity resin with PG200 buffer (50 mM sodium phosphate pH 7.0, 200 mM NaCl, 10% glycerol, 0.1% NP40, 1 mM benzamidine and 5 mM 2-mercaptoethanol). I found that a large amount of this protein remains insoluble and could not be purified with a metal affinity resin (Figure **3-4** C). Thus, these results suggest that the HisTrxN tag cannot effectively improve the solubility of the protein. Expression at 18°C might still be useful, but not sufficient, to promote solubility and purification of Spt8Δ2.

3.3.2.2 Coexpression with other proteins

Spt8 might be stabilized when coexpressed with other SAGA components. It is known that the SAGA-like (SLIK) complex is almost identical to the SAGA complex except that it lacks Spt8 and contains the C-terminally truncated Spt7 (Sterner et al., 2002a). A previous study has suggested that the amino acids 1150-1332 in the Spt7 protein are required for association with Spt8 (Wu and Winston, 2002). For example, purification of the SAGA complex from the yeast strain that has the truncated version of Spt7 (1-1150) yields a complete loss of Spt8 from the SAGA, while the deletion of Spt8 itself has minimal effect on the integrity of the Spt7 subunit (Wu and Winston, 2002). Thus, it might be possible that the C-terminal end of Spt7 interacts with Spt8 in the SAGA complex, and the coexpression of the C-terminal portion of Spt7 together with Spt8Δ2 might stabilize each other. Therefore, I decided to coexpress the C-terminal part of Spt7 (1150-1332, designated as truncation 3 or Spt7Δ3) with Spt8Δ2 and tested whether this coexpression would improve the solubility and purification of Spt8Δ2. I also attempted to coexpress Spt3, STRN-tagged TBP and Flag-tagged Spt7Δ3 with Spt8Δ2. In addition, I tried to coexpress Spt8Δ2 with TBP since the presence of TBP may promote solubility of Spt8Δ2.

However, the effort to coexpress Spt8Δ2 with other proteins was compromised by the fact that there was no clear coexpression of other proteins except for Spt3 (Figure **3-5**), even though the Spt7Δ3 and TBP could be expressed independently (data not shown). Thus, I was not able to test whether Spt7Δ3 could co-fold and solubilize Spt8Δ2. Although Spt3 was coexpressed with Spt8Δ2 and was partially soluble, it did not promote solubility of Spt8Δ2 (data not shown). Thus, I could not coexpress Spt8Δ2 with Spt7Δ3, Spt3 and TBP proteins in order to improve its solubility.

3.3.2.3 Using urea to improve solubility of the truncated Spt8

Urea is a chaotropic agent and is used to purify protein under denaturing condition (Roark et al., 1976). However, urea at low concentration such as 2 or 3 M does not necessarily denature proteins, but can dissociate proteins that bind non-specifically through a hydrophobic interaction. Urea at this concentration was used to assist purification of some proteins such as MCM1 (1-100) (Cheung et al., 2000) including the WD40 domain of Tup1 (Sprague et al., 2000).

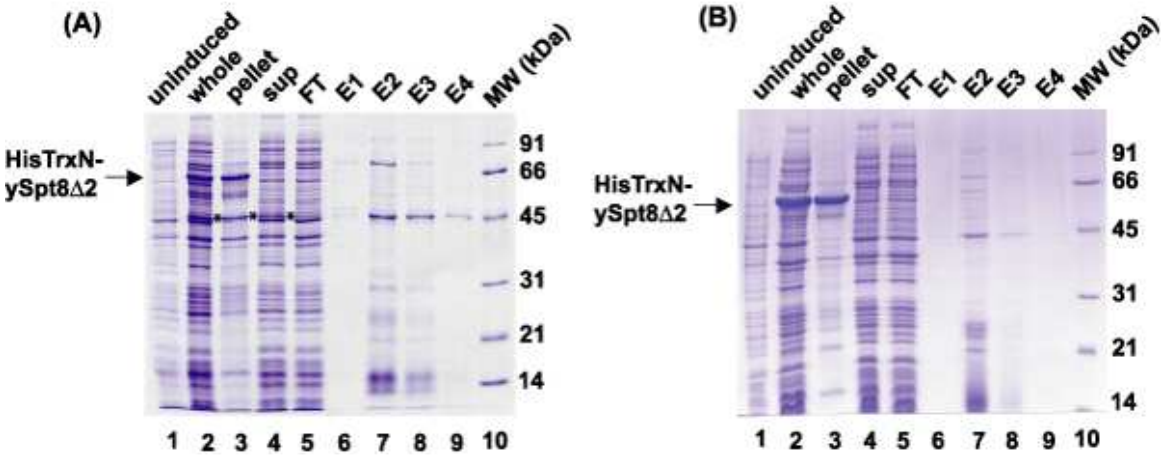

Figure **3-5**: Coexpression and metal affinity purifications of HisTrxNySpt8Δ2.

(A) A metal affinity purification of HisTrxNySpt8Δ2 coexpressed with STRNyTBPcore, FlagySpt7Δ3, and ySpt3 proteins at 18°C. The proteins were purified with PG200 buffer (50 mM sodium phosphate pH 7.0, 200 mM NaCl, 10% glycerol, 0.1% NP40, 1 mM benzamidine, and 5 mM 2-mercaptoethanol). No expression of FlagySpt7Δ3 nor STRNyTBPcore was observed. The position of HisTrxNySpt8Δ2 is marked by the arrow. Spt3 (*) is present in the sup but not in the fractions. (B) A metal affinity purification of HisTrxNySpt8Δ2 coexpressed with STRNyTBPcore at 18°C. The proteins were purified with PG200 buffer buffer (50 mM sodium phosphate pH 7.0, 200 mM NaCl, 10% glycerol, 0.1% NP40, 1 mM benzamidine, and 5 mM 2-mercaptoethanol). No expression of STRNyTBPcore was observed and the test batch purification was unsuccessful.

I found that 3 M urea promotes Spt8Δ2 solubility and purification. As shown in Figure **3-6** , HisTrxNySpt8Δ2 expressed at 18°C could be purified only when 3 M urea is included (compare A and B). HisTrxNySpt8Δ2 expressed at 28°C could also be purified in the presence of 3 M urea (data not shown).

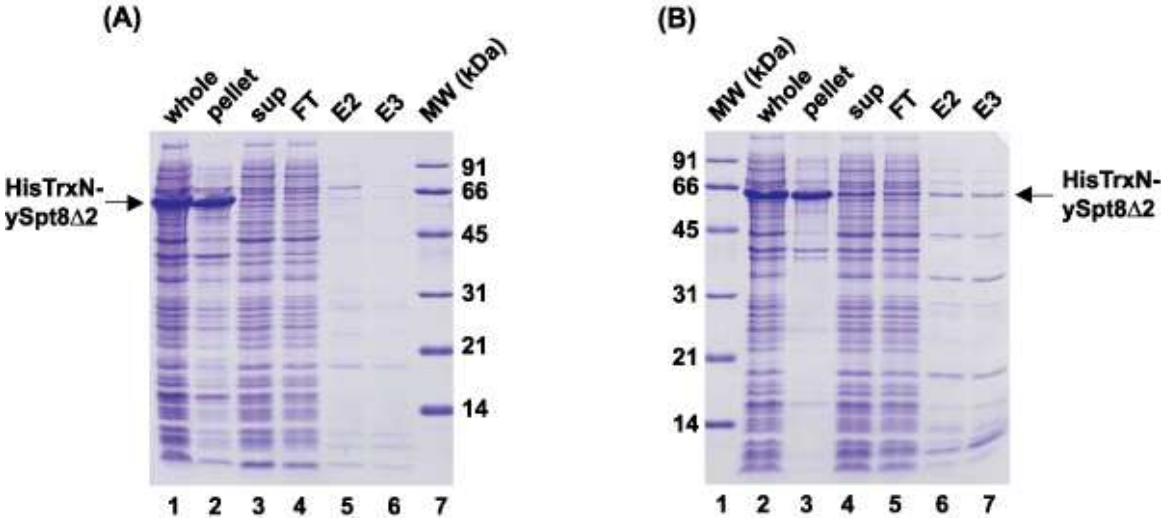

Figure **3-6**: Urea improves solubility and purification of Spt8Δ2.

(A) A metal affinity purification of HisTrxNySpt8Δ2 expressed at 18°C. The protein was purified with PG300 buffer (50 mM sodium phosphate pH 7.0, 300 mM NaCl, 10% glycerol, 0.1% NP40, 1 mM benzamidine, and 5 mM 2-mercaptoethanol). Under this condition, a majority of tagged Spt8Δ2 is insoluble and is could not be purified. (B) A metal affinity purification of the same HisTrxNySpt8Δ2 but purified with PGU300 buffer (50 mM sodium phosphate pH 7.0, 300 mM NaCl, 3 M urea, 10% glycerol, 0.1% NP40, 1 mM benzamidine, and 5 mM 2-mercaptoethanol). The purification of HisTrxNySpt8Δ2 was successful, as the HisTrxNySpt8Δ2 is present in the fractions.

3.3.2.4 Spt8 truncations

It is possible that the Spt8Δ2 (210-602) truncation is not the optimal piece for purification. I cannot exclude the possibility that the Spt8Δ2 lacks parts of the sequence necessary for a proper folding. If a more optimized truncation of Spt8 is found, urea might not be necessary for purification. In addition, most WD40 domains reported to date contain at least seven WD40 motifs, while the results shown here only suggests six WD40 motifs in the Spt8. Thus, I reexamined the sequence alignment and used a secondary structure prediction (Prof; http://cubic.bioc.columbia.edu/predictprotein/) to predict the location of possible WD40 motifs. The sequence alignment of the yeast Spt8 with hypothetical Spt8 from other fungi shows sequence conservation within the putative WD40 domain, and some similarities within the acidic region (Figure **3-7**). It is possible that expressing the highly conserved regions of the yeast Spt8 would confer some stability and solubility to the truncated protein. Therefore, two new constructs with a C-terminal His tag; Spt8Δ3His (76-602) and Spt8Δ4His (146-602) were created. These two truncations of Spt8 could be highly expressed; however, they were insoluble and yield very little material after purification with a metal affinity resin (data not shown). Thus, I conclude that those two Spt8 truncations are not appropriate constructs for purification.

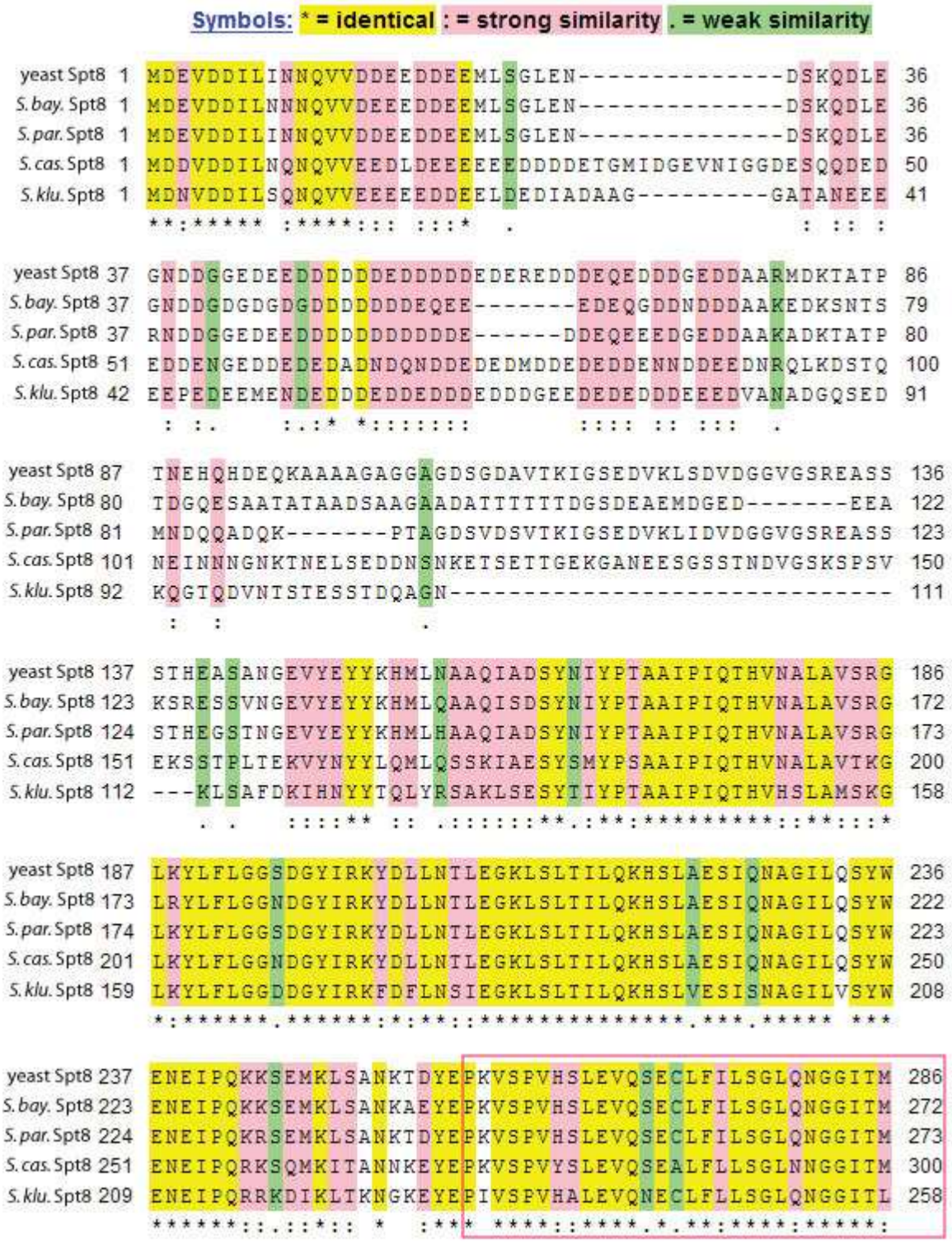
Symbols: * = identical : = strong similarity . = weak similarity
yeast Spt8 1 MDEVDDILINNQVVDDEEDDEEMLSGLEN--------------DSKQDLE 36
S. bay. Spt8 1 MDEVDDILNNNQVVDEEEDDEEMLSGLEN--------------DSKQDLE 36
S. par. Spt8 1 MDEVDDILINNQVVDDEEDDEEMLSGLEN--------------DSKQDLE 36
S. cas. Spt8 1 MDDVDDILNQNQVVEEDLDEEEEEEDDDDETGMIDGEVNIGGDESQQDED 50
S. klu. Spt8 1 MDNVDDILSQNQVVEEEEEDDEELDEDIADAAG---------GATANEEE 41
yeast Spt8 37 GNDDGGEDEEDDDDDEDDDDDEDEREDDDEQEDDDGEDDAARMDKTATP 86
S. bay. Spt8 37 GNDDGDGDGDGDDDDDDDEQEE-------EDEQGDDNDDDAAKEDKSNTS 79
S. par. Spt8 37 RNDDGGEDEEDDDDDDDDDDDE------DDEQEEEDGEDDAAKADKTATP 80
S. cas. Spt8 51 EDDENGEDDEDEDADNDQNDDEDEDMDDEDEDDENNDDEEDNRQLKDSTQ 100
S. klu. Spt8 42 EEPEDEEMENDEDDDEDDEDDDEDDDGEEDEDEDDDEEEDVANADGQSED 91
yeast Spt8 87 TNEHQHDEQKAAAAGAGGAGDSGDAVTKIGSEDVKLSDVDGGVGSREASS 136
S. bay. Spt8 80 TDGQESAATATAADSAAGAADATTTTTTDGSDEAEMDGED-------EEA 122
S. par. Spt8 81 MNDQQADQK-------PTAGDSVDSVTKIGSEDVKLIDVDGGVGSREASS 123
S. cas. Spt8 101 NEINNNGNKTNELSEDDNSNKETSETTGEKGANEESGSSTNDVGSKSPSV 150
S. klu. Spt8 92 KQGTQDVNTSTESSTDQAGN------------------------------ 111
yeast Spt8 137 STHEASANGEVYEYYKHMLNAAQIADSYNIYPTAAIPIQTHVNALAVSRG 186
S. bay. Spt8 123 KSRESSVNGEVYEYYKHMLQAAQISDSYNIYPTAAIPIQTHVNALAVSRG 172
S. par. Spt8 124 STHEGSTNGEVYEYYKHMLHAAQIADSYNIYPTAAIPIQTHVNALAVSRG 173
S. cas. Spt8 151 EKSSTPLTEKVYNYYLQMLQSSKIAESYSMYPSAAIPIQTHVNALAVTKG 200
S. klu. Spt8 112 ---KLSAFDKIHNYYTQLYRSAKLSESYTIYPTAAIPIQTHVHSLAMSKG 158
yeast Spt8 187 LKYLFLGGSDGYIRKYDLLNTLEGKLSLTILQKHSLAESIQNAGILQSYW 236
S. bay. Spt8 173 LRYLFLGGNDGYIRKYDLLNTLEGKLSLTILQKHSLAESIQNAGILQSYW 222
S. par. Spt8 174 LKYLFLGGSDGYIRKYDLLNTLEGKLSLTILQKHSLAESIQNAGILQSYW 223
S. cas. Spt8 201 LKYLFLGGNDGYIRKYDLLNTLEGKLSLTILQKHSLAESIQNAGILQSYW 250
S. klu. Spt8 159 LKYLFLGGDDGYIRKFDFLNSIEGKLSLTILQKHSLVESISNAGILVSYW 208
yeast Spt8 237 ENEIPQKKSEMKLSANKTDYEPKVSPVHSLEVQSECLFILSGLQNGGITM 286
S. bay. Spt8 223 ENEIPQKKSEMKLSANKAEYEPKVSPVHSLEVQSECLFILSGLQNGGITM 272
S. par. Spt8 224 ENEIPQKRSEMKLSANKTDYEPKVSPVHSLEVQSECLFILSGLQNGGITM 273
S. cas. Spt8 251 ENEIPQRKSQMKITANNKEYEPKVSPVYSLEVQSEALFLLSGLNNGGITM 300
S. klu. Spt8 209 ENEIPQRRKDIKLTKNGKEYEPIVSPVHALEVQNECLFLLSGLQNGGITL 258

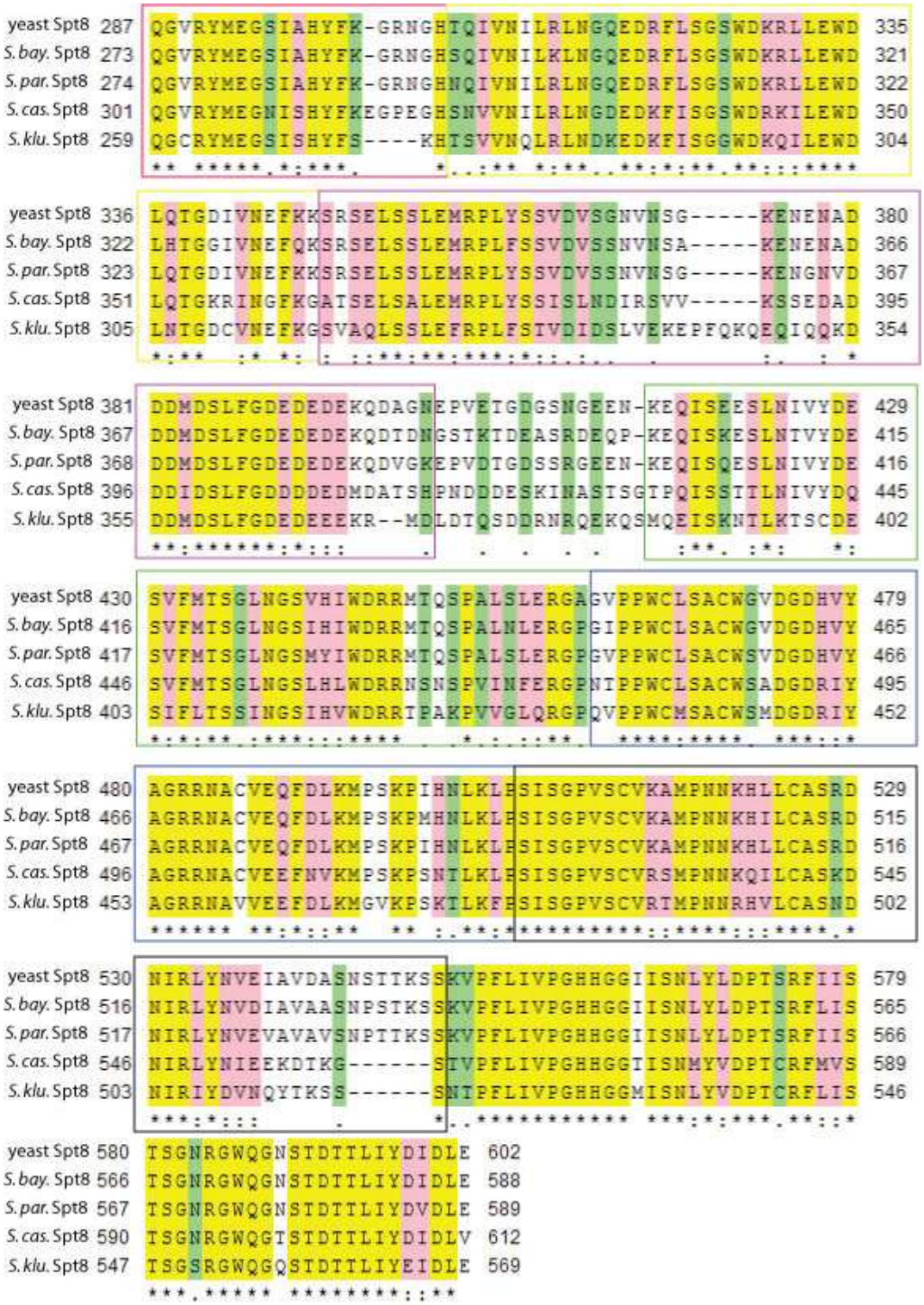

Figure **3-7**: *Saccharomyces cerevisiae*'s Spt8 sequence alignment with Spt8 orthologues in other fungal species.

The ClustalW sequence alignment from the yeast genome database shows a conservation within the putative WD40 domain of the proteins and a high similarity within the acidic domain of the Spt8 (Cliften et al., 2003; Kellis et al., 2003). From top to bottom: S. *cerevisiae*, *S. bayanus*, *S. paradoxus*, *S. castellii*, and *S. kluyveri*, respectively. Each box in the same color indicates a predicted WD40 repeat motif based on the yeast Spt8 sequence shown in Figure **3-3** B.

The secondary structure prediction (Prof; http://cubic.bioc.columbia.edu/predictprotein/) indicated that the Spt8 might contain an additional WD40 motif at the amino acid residues 173 to 220 (Figure **3-8**). Therefore, three additional truncations; Spt8Δ5 (165-602), Spt8Δ6 (165-550) and Spt8Δ7 (210-550), were created. All of which had the HisTrxN fusion tag fused to their N-termini. Again, these three constructs could be highly expressed but appear to be insoluble even when expressed at 18°C (data not shown). Interestingly, only Spt8Δ7 (210-550) could be purified in the presence of 3 M urea (data not shown and Figure **3-9**).

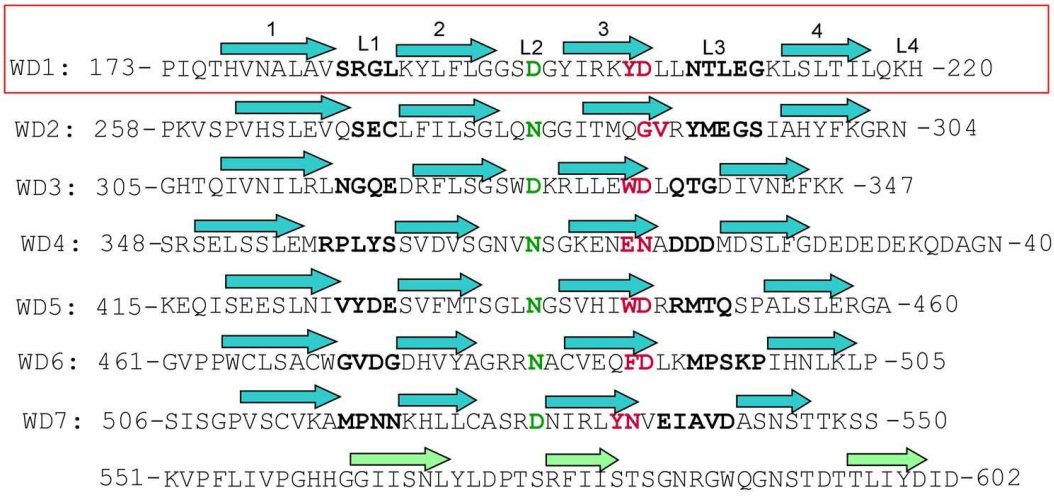

Figure **3-8**: An additional WD40 motif in Spt8, based on the secondary structure prediction, is shown in the red box.

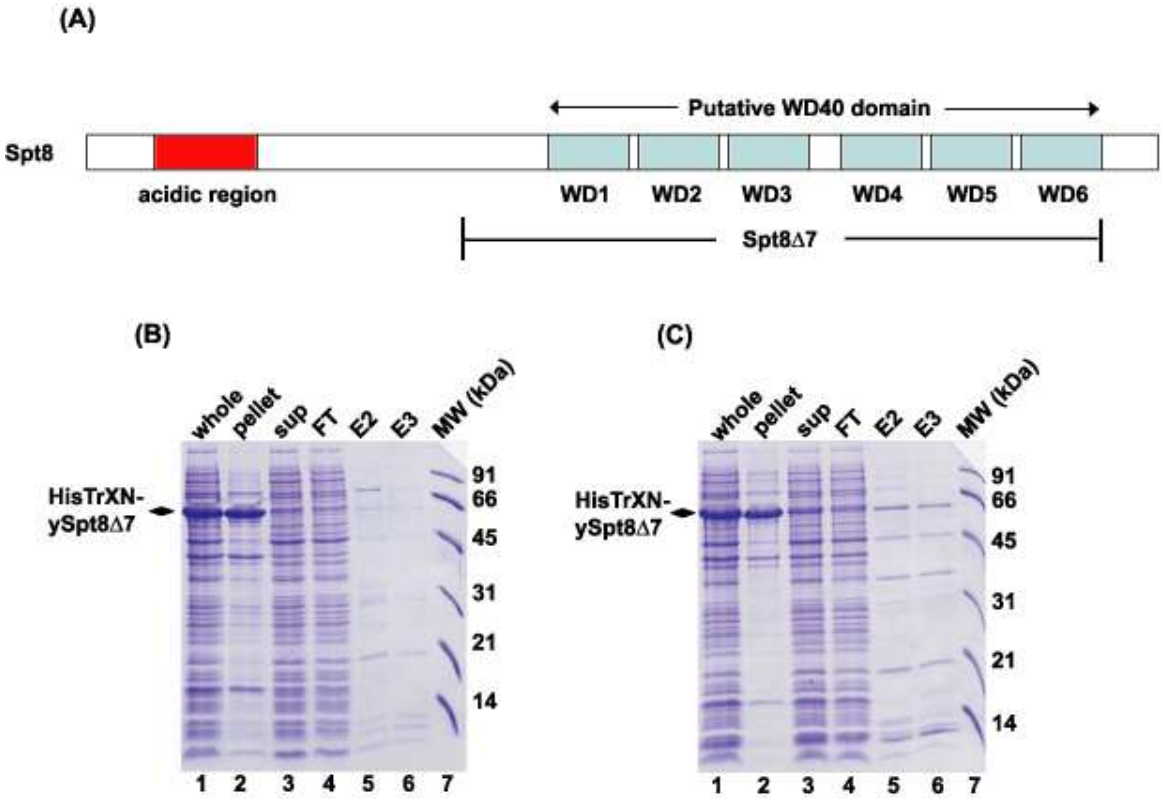

Figure **3-9**: Urea improves solubility and purification of Spt8Δ7.

(A) A schematic representation of the Spt8Δ7. (B) A metal affinity purification of HisTrxNySpt8Δ7 expressed at 18°C. The protein was purified with PG300 buffer (50 mM sodium phosphate pH 7.0, 300 mM NaCl, 10% glycerol, 0.1% NP40, 1 mM benzamidine, and 5 mM 2-mercaptoethanol). Under this condition, the majority of tagged Spt8Δ7 is insoluble and is could not be purified. (C) A metal affinity purification of the same HisTrxNySpt8Δ7 but purified with PGU300 buffer (50 mM sodium phosphate pH 7.0, 300 mM NaCl, 3 M urea, 10% glycerol, 0.1% NP40, 1 mM benzamidine, and 5 mM 2-mercaptoethanol). The purification of HisTrxNySpt8Δ7 was successful, as the HisTrxNySpt8Δ7 is present in the elution fractions.

3.3.3 The putative WD40 domain of Spt8 is sufficient for the interaction with TBP

I performed a pull down assay to evaluate whether the N-terminally truncated Spt8 would interact with TBP. For this experiment, a GST fusion construct with the C-terminal part of Spt8 (210-602) was created to use in a GST pull down assay with the wild type STR-tagged TBP, the R171E, and the T153I TBP mutants. I found that the R171E TBP mutant had very little or no interaction with the C-terminal part of Spt8 (Figure **3-10** lanes 6-10), while a better interaction was observed when the full length Spt8 was used (Figure **2-5** A lanes 6 and 7). In addition, the C-terminal part of Spt8 interacted with the wild type TBP as well as the T153I TBP mutant (Figure **3-10** lanes 4 and 5 for the wild type TBP, and lanes 14 and 15 for the T153I mutant, respectively). Therefore, I conclude that the putative WD40 domain of Spt8 (210-602) is sufficient for the interaction with TBP.

Because the putative WD40 domain of Spt8 is highly acidic (pI = 4.82), the interaction observed between the Spt8Δ2 and the conserved domain of TBP (pI = 10.66) may be non-specifically mediated by a charge-charge interaction. In other words, the Spt8Δ2 might possibly interact with other highly positively charged protein. To examine the possibility, I performed the pull down experiment between the C-terminal part of Spt8 and the human Dot1Δ1 (2-416), which is a highly positively charged protein (pI = ~10). I did not observe the interaction between the two polypeptides (data not shown). Therefore, I conclude that the interaction between Spt8Δ2 and TBP is specific, and not due to a non-specific charge-charge interaction.

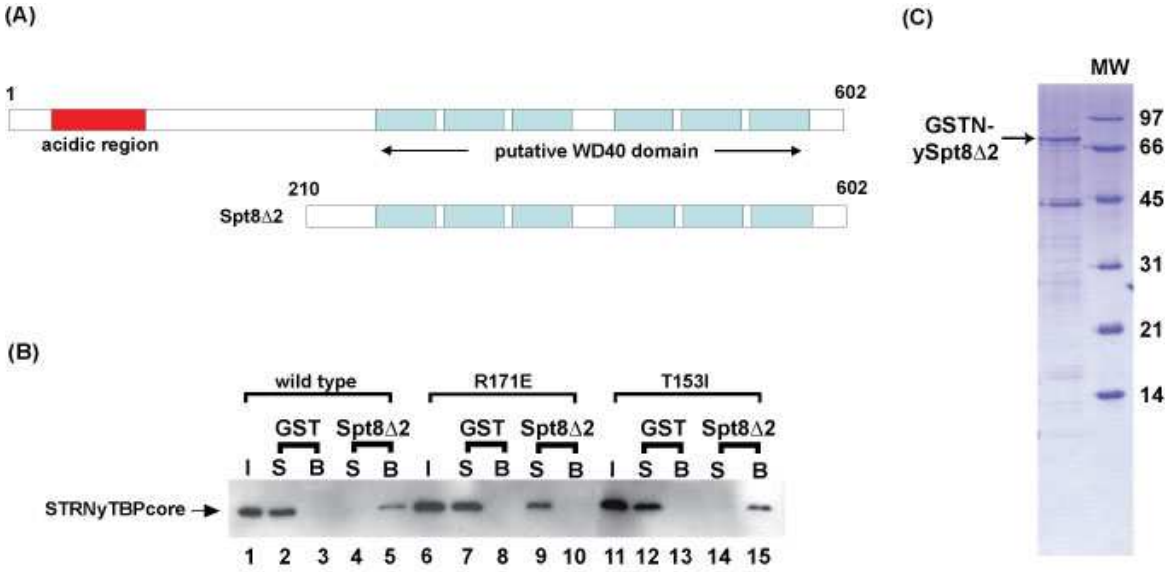

Figure **3-10**: The putative WD40 domain of Spt8 is sufficient for the interaction with TBP.

(A) A representation of the full length Spt8, which contains an acidic cluster near the N-terminus and seven putative WD40 repeats located on its C-terminus part. (B) GST pull down of the GST-tagged Spt8Δ2 with TBP proteins. Western blot analysis using the anti-*Strep* tag monoclonal antibody that recognizes the *Strep* tag located at the N-terminus of TBP. The putative WD40 of Spt8 can interact with the wild type TBP and the T153I TBP mutant, but not the R171E TBP mutant. I, S, and B are abbreviated for the input, supernatant, and beads, respectively. GST indicates the GST tag used as a negative control for each pull down experiment. (C) A Coomassie stained gel of the GSTN-tagged Spt8Δ2 used for the pull down in (B).

Since a smaller piece of Spt8 than the previous truncation (Spt8Δ2) could be purified, I performed a pull down experiment to test whether this truncation can interact with TBP. As shown in Figure **3-11**, the HisTrxN-tagged Spt8Δ7 was able to interact with the wild type as well as the T153I TBP mutant STRN-tagged TBP proteins (lane 9 and 13). However, this protein did not interact well with the R171E TBP mutant (Figure **3-11** lane 11), consistent with finding that the R171E point mutation stabilizes TBP dimerization (Kou et al., 2003; Kou and Pugh, 2004). HisTrxNyEsa1 and HisTrxNySpt8Δ2 were used as a negative and a positive control for the experiment (lane 1-4, respectively). Thus, I

conclude that the putative WD40 domain of Spt8 is sufficient for the interaction with TBP.

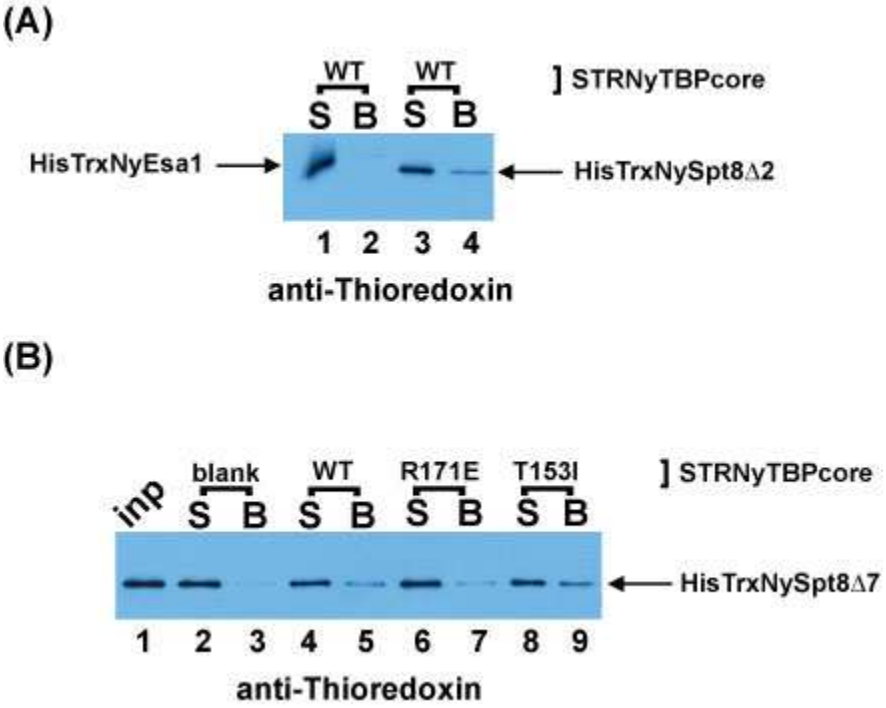

Figure **3-11**: Interaction between TBP and Spt8Δ7.

(A) A negative control (lanes 1 and 2) and a positive control (lanes 3 and 4) experiment for the STR-tagged TBP pull down in (B). TBP does not interact with HisTrxN-tagged Esa1 but could interact with HisTrxN-tagged Spt8Δ2. (B) Pull down experiment shows the interaction between HisTrxN-tagged Spt8Δ7 and the STRN-tagged wild type TBP or the T153I TBP mutant immobilized to the *Strep*-Tactin resin (lanes 9 and 13, respectively). Spt8Δ7 interacts weakly with the STRN-tagged R171E TBP mutant (lane 11). Blank does not contain TBP on the resin.

3.3.4 Binding of Spt8 to TBP is salt dependent

I would like to understand how Spt8 and TBP interact with each other. My data have shown that the putative WD40 domain of Spt8 was sufficient for the interaction with TBP. A well characterized WD40 domain containing protein is the G protein β subunit, which is involved in a signal transduction pathway (Hamm, 1998; Vaughan, 1998). The

interface of the G protein β subunit (G_β) that interacts with the G protein-coupled receptor kinase (GRK) is highly acidic, suggesting the role of the electrostatic interaction between the G_β and the GRK (Lodowski et al., 2003). Based on the secondary structure prediction shown in Figure **3-3** B, a number of residues within the loops of the putative WD40 domain of Spt8 are acidic, suggesting that electrostatic interaction might be important for the Spt8-TBP interaction. To analyze whether this type of interaction plays a role in the TBP/Spt8 complex stabilization, pull down experiments with different salt concentrations in the binding conditions were performed. As shown in Figure **3-12** A and C, binding of Spt8 to the wild type TBP became weaker when the NaCl concentration was close to 300 mM. I also analyzed the binding of the R171E mutant at different salt concentrations in relation to the wild type TBP. At 150 mM NaCl, the interaction between Spt8 and TBP was weak, consistent with my previous result Figure **2-11** A. However, at 300 mM NaCl or greater, the binding of Spt8 to the R171E TBP mutant was completely abolished (Figure **3-12** D lane 4-7). These results suggest that electrostatic interaction plays a critical role in the interaction between TBP and Spt8.

3.3.5 TBP binds to Spt8 and the SAGA complex as a monomer

My previous results indicate that the R171E TBP mutant is defective for the interaction with both Spt8 and the SAGA complex. The crystal structure of the yeast TBP dimer indicates that this R171 residue contacts the R98 of another molecule and perhaps contributing to dimer stabilization (Figure **3-13**). When either R171 or R98 is mutated to E171 (R171E or R98E), the TBP-TBP interaction (dimerization) is stronger (Kou and Pugh, 2004). Therefore, Spt8 might interact with TBP in such a way that it interferes with the TBP dimerization.

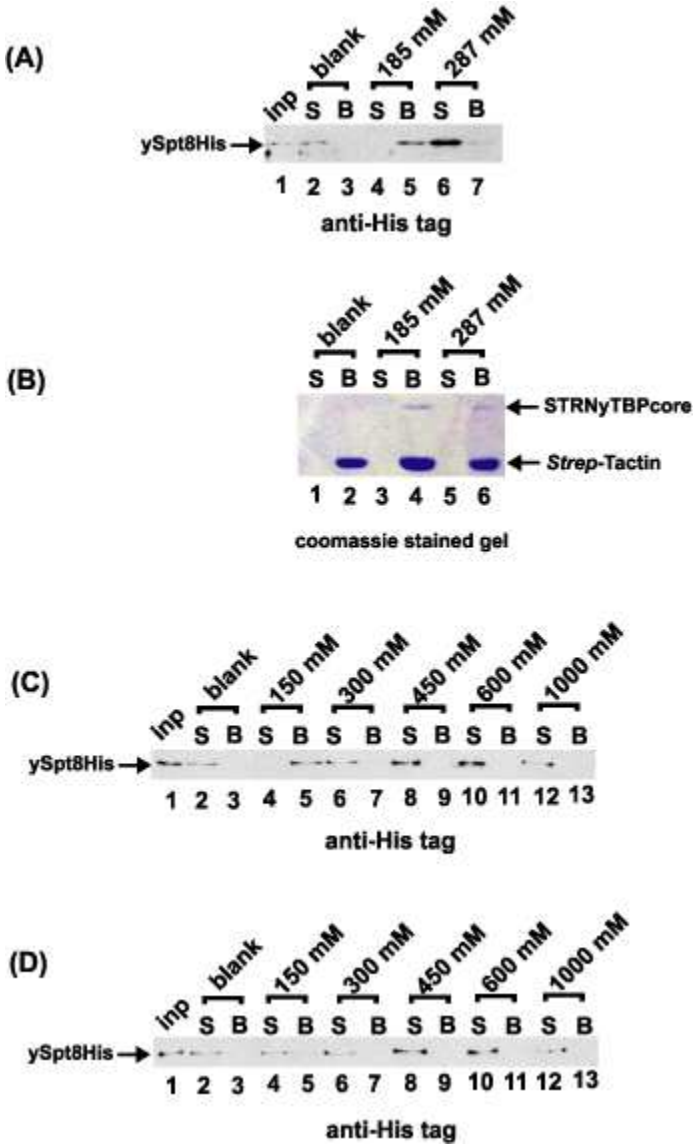

Figure **3-12**: Binding of Spt8 to TBP is salt dependent.

(A) Pull down experiment between Spt8 and TBP was performed at two different salt concentrations. At higher salt, the binding of Spt8 to the STR-tagged TBP decreased. S is for supernatant and B is for beads. (B) The coomassie stained gel from the same pull down experiment shows the presence of the STR-tagged TBP on the beads at the higher salt concentration. (C) Western blot of the similar pull down experiment between the wild type STRNyTBPcore and the His-tagged Spt8 with a titration of NaCl concentration. At 300 mM NaCl, Spt8 could no longer interact with TBP (lanes 6 and 7). (D) The same analysis but the STR-tagged R171E TBP mutant was used instead. (C) and (D) were performed once.

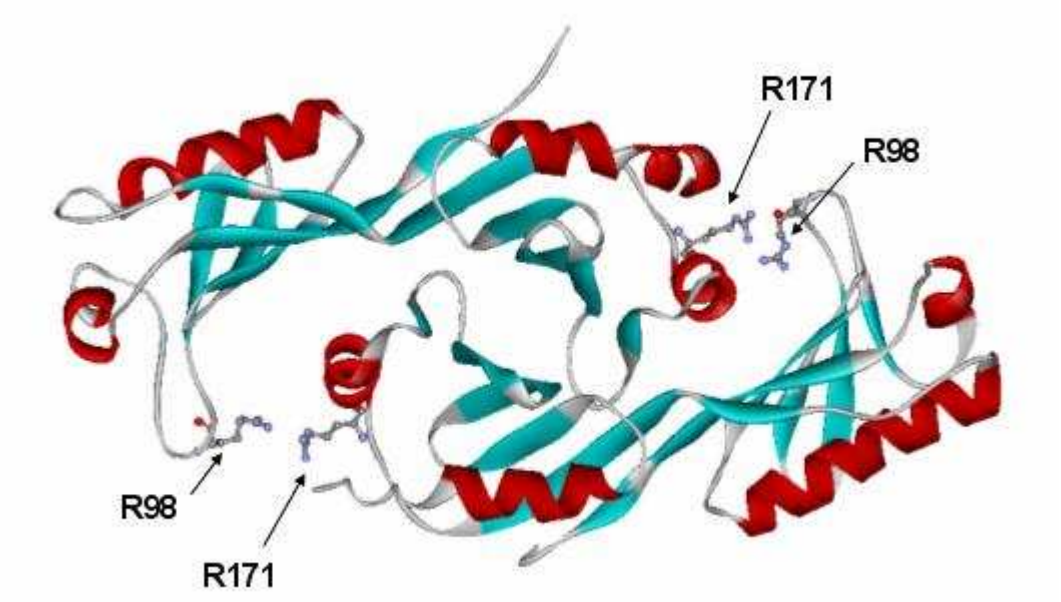

Figure **3-13**: Crystal structure of TBP dimer.

Yeast TBP homodimerizes through the concave surface of the saddle-like structure (Chasman et al., 1993). Shown in ball and stick is the R171 and R98 residues of the two molecules that affect the dimerization when mutated. The structure (1TBP) was manipulated with the WebLab ViewerLite program.

To test this possibility, I performed a competition assay by creating TBP dimers with two different tags: the STR-tagged TBP that binds to the *Strep*-Tactin resin and the CBP-tagged TBP that dimerizes with the resin bound TBP (Figure **3-14** A). Then, I increasingly added either Spt8 or the SAGA complex. I reason that if the binding of Spt8 or the SAGA complex interferes with dimer formation, an increasing amount of the CBP-tagged TBP present in the supernatant would be observed as an increasing amount of Spt8 or the SAGA complex binds to TBP on the resin. However, if Spt8 or the SAGA complex binds to other surface area of TBP that is not involved with TBP dimerization, no increasing amount of free CBP-tagged TBP should be observed in the supernatant, even though Spt8 or SAGA binds to the TBP on the resin. As shown in Figure **3-14** B, the CBP-tagged TBP was being liberated from the beads (lanes 3-6) as Spt8 binds to the

TBP on the resin (lanes 8-11). However, when Spt3 was used, I could not detect free CBPyTBPcore in the supernatant (Figure **3-14** C, lanes 3-6). It was because Spt3 did not interact with TBP (lanes 8-11), consistent with my previous results that Spt3 does not interact with TBP. Like the Spt8, the SAGA complex binds to the STR-tagged TBP on the resin and displaced the CBP-tagged TBP from the STR-tagged TBP (Figure **3-14** D). Together, I conclude that either Spt8 or the SAGA complex binds to TBP and competes with TBP dimer formation. Interestingly, *spt8*Δ SAGA complex also bound and competed with TBP dimer (Figure **3-14** E). This result raised the possibility that Ada1, which is another potential TBP interacting subunit, may interact and interfere with TBP dimerization.

I also utilized photo-cross-linking experiment to test if a TBP monomer binds to the SAGA complex. The R171E and T153I TBP mutants that were used for my previous pull down experiment were used for photo-cross-linking with the SAGA complex. The photo-cross-linking experiments were conducted with the untagged TBP mutant. If the SAGA complex binds to a TBP dimer, then both TBP mutants should photo-cross-link to the SAGA complex. However, if TBP dimerization inhibits the interaction with SAGA complex, the T153I TBP mutant should still cross-link with the SAGA complex, whereas the R171E mutant, which produces a more stable TBP dimer, should yield a less or no cross-linking to the SAGA complex when compared to the T153I mutant. As shown in Figure **3-15**, the R171E TBP mutant did not photo-cross-link with the SAGA complex while the T153I TBP mutant could still cross-link with Spt8 in the complex (Figure **3-15** A and B, lanes 1-4). However, one could argue that perhaps the R171E TBP mutant was aggregated. To rule out this possibility, I performed a gel-shift experiment to test the formation of TFIIA/TBP/DNA complex using those TBP mutants and the wild type TBP as a positive control (Appendix, Figure **A-1).** These results indicated that both TBP mutants were capable of the interaction with TFIIA, suggesting that the negative result seen in the photo-cross-linking experiment is not due to protein aggregation but rather reflects the inverse relationship between the stronger TBP dimer formation and the binding to the SAGA complex.

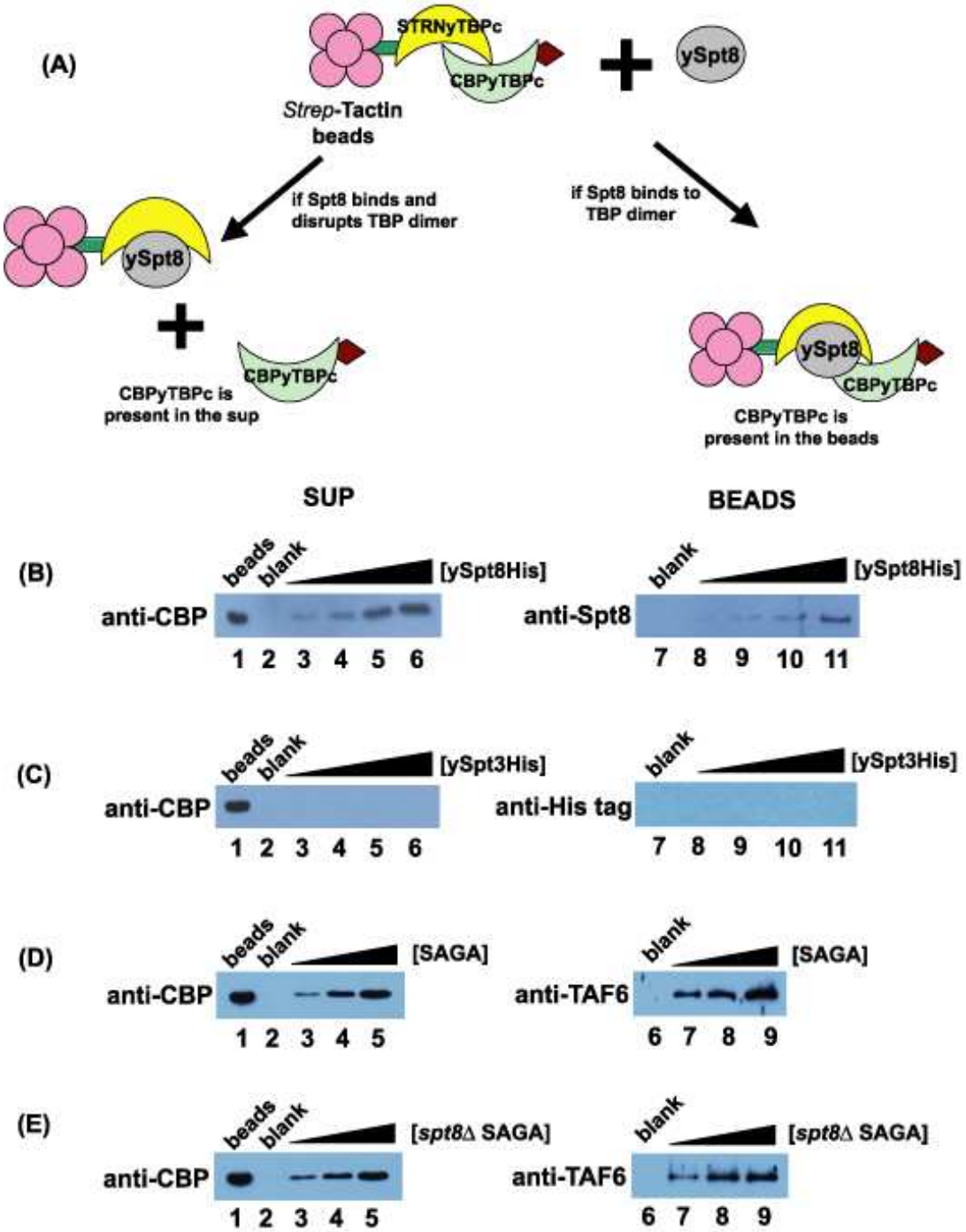

Figure **3-14**: Competition assay shows that the binding of Spt8 or the SAGA complex to TBP competes with TBP dimerization.

(A) A cartoon illustrates the competition assay. CBPyTBPcore was allowed to heterodimerize with the resin bound STRNyTBPcore. Upon the addition of Spt8, 1) if Spt8 binds and disrupt TBP dimers, then CBPyTBPcore should be dissociated from the resin and present in the supernatant; or 2) if Spt8 binding to TBP does not interfere with TBP dimerization, then the CBPyTBPcore should be detected in the beads. (B) Spt8 competed with TBP dimer for binding to TBP monomer. Western blots using anti-CBP tag detected the presence of CBP-tagged TBP in the supernatant, as the evidence for competition. Spt8 that bound to the TBP on resin was also detected by Western blot analysis with anti-Spt8 antibodies. Blank did not contain protein sample (C) Spt3 did not bind to TBP. Same procedures as for (B), except that Spt3 was used instead of Spt8, and anti-HIS antibodies were used to detect Spt3. (D) SAGA competed with TBP dimer for binding to TBP monomer. Same procedures as for (B), except that the SAGA complex was used for analysis, and anti-TAF6 was used to detect SAGA complex that bound to the beads. (E) The *spt8*Δ SAGA complex also competed with TBP dimer for binding to TBP monomer. Same procedures as for (D), except that the *spt8*Δ SAGA complex was used in the experiment.

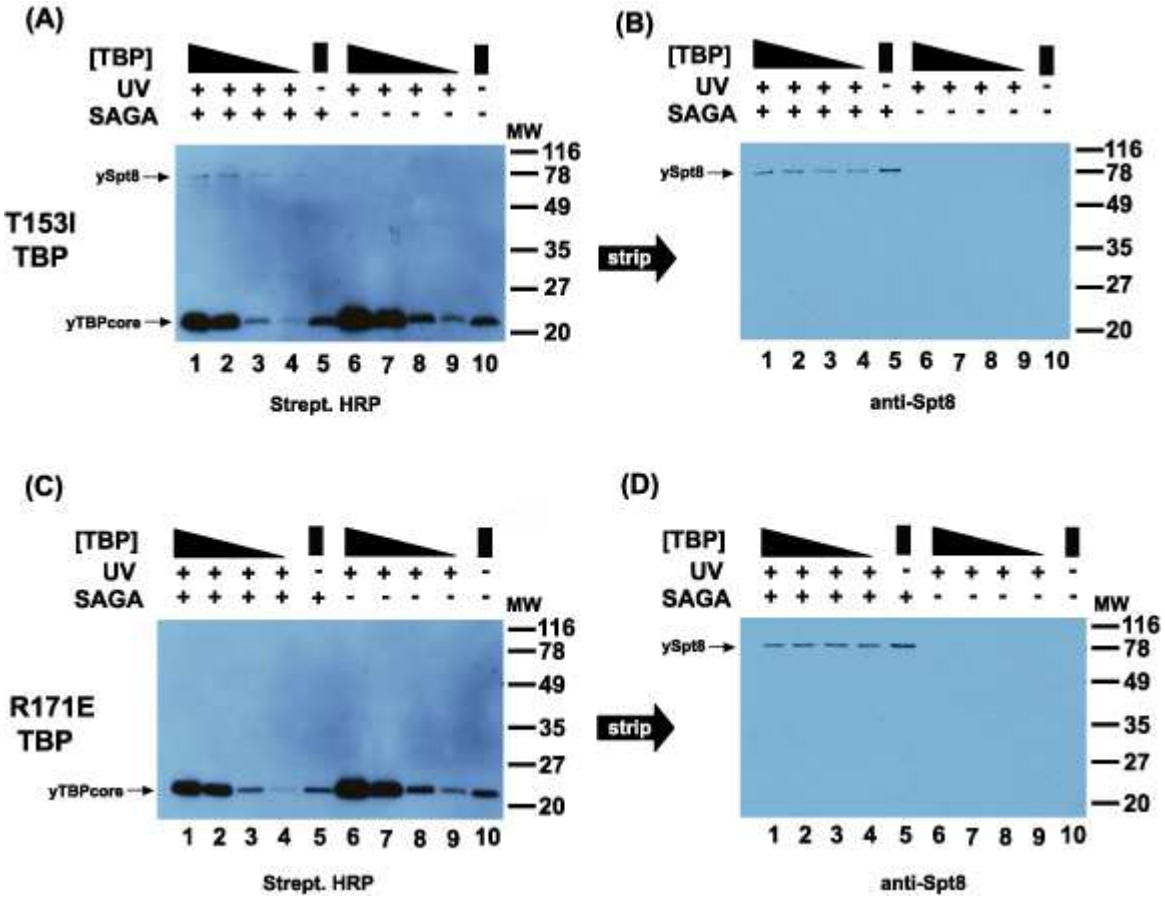

Figure **3-15**: The R171E TBP mutant does not photo-cross-link with the sAGA complex.

(A) Photo-cross-link of the T153I TBP mutant with the Spt8 in the SAGA complex. Cross-linking products were detected with Strep.-HRP that recognizes biotinylated proteins. (B) The signal from the same membrane was stripped before re-probing with the anti-Spt8 antibodies. (C) Same as (A) except that R171E TBP mutant was used in the experiment. (D) Same as (B) except that the membrane from (C) was used.

3.3.6 DNA competes with either Spt8 or SAGA to bind to TBP

TBP dimerizes through the concave surface of the saddle-like structure (Chasman et al., 1993), and this prevents the binding of DNA unless the TBP dimer dissociates first (Coleman et al., 1999). Because Spt8 or SAGA binds to TBP and prevents TBP dimerization, it is possible that the association of the SAGA complex or Spt8 with TBP

might occlude the binding of DNA. To test this hypothesis, I designed a similar competition experiment to test the binding of DNA to the Spt8/TBP or the SAGA/TBP complex (Figure **3-16** A). In this experiment, the STR-tagged TBP that binds to *Strep*-Tactin resin was incubated with either Spt8 protein or the SAGA complex. Then, an increasing amount of either TATA box or non-TATA box DNA was added, and the presence of Spt8 or the SAGA complex in the supernatant was monitored. The TATA box DNA should bind to TBP on the resin as expected. However, if the presence of Spt8 does not interfere with the binding of TATA box DNA, Spt8 should not be found in the supernatant. On the other hand, if TATA box DNA binding to TBP competes with the binding of Spt8, more Spt8 protein should be found in the supernatant as more DNA is added to the resin. The experiment with the SAGA complex follows the same logic. As shown in Figure **3-16** B, the more TATA box DNA added to TBP on the resin (lane 7-9), the more Spt8 found present in the supernatant (lane 2-5). Similarly, the TATA box DNA confers the same effect to the binding of SAGA to TBP (Figure **3-16** D). In contrast, non-TATA box DNA had no effect on the binding of Spt8 to TBP because the non-TATA box DNA did not bind to TBP (Figure **3-16** C). However, for the experiment with the SAGA complex, a small, but not increasing amount of Taf6 was detected in the supernatant when non-TATA box DNA was used (Figure **3-16** E). Perhaps, this reflects the non-specific biding of the SAGA complex to DNA (Lee et al., 2005a). I also analyzed the amount of bound STR-tagged TBP on the resin and found that the amount of TBP in all samples was similar, suggesting that the DNA directly competes with the binding of the SAGA complex but not the TBP binding to the resin (Figure **3-16** F). Together, these results suggest that binding of Spt8 or SAGA to a TBP monomer mutually excludes a formation of TBP/TBP dimer or TBP/DNA complex.

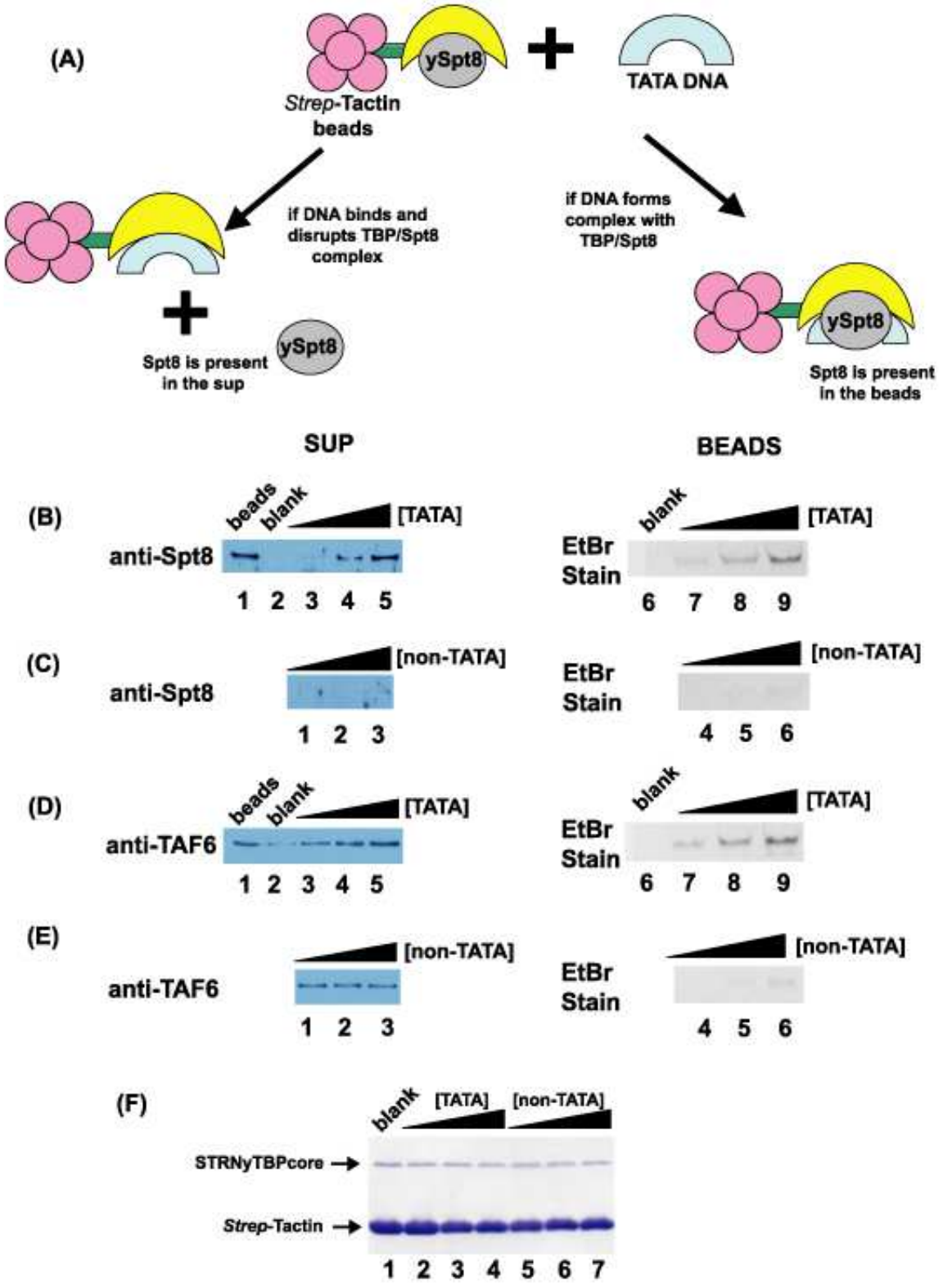

Figure **3-16**: The TATA box DNA competes with the binding of Spt8 or SAGA to TBP.

(A) A cartoon illustrates a competition assay. Spt8 was incubated with STR-tagged TBP bound to the resin. Upon adding TATA box DNA, 1) if the binding of DNA to TBP was mutually exclusive with the Spt8, then the bound Spt8 would be replaced by the DNA and present in the supernatant; or 2) if the binding of DNA to TBP was not mutually exclusive with the Spt8, then the bound Spt8 would not be replaced by the DNA and still remain bound with TBP/DNA complex in the beads. (B) The TATA box DNA competed with the Spt8 that bound to TBP. Western blots using anti-Spt8 antibodies detected the presence of Spt8 in the supernatant, as the evidence for competition. The TATA box DNA that bound to the TBP on resin was visualized by ethidium bromide staining. Blank did not contain DNA in the competition reaction. (C) Similar to (B), except that non-TATA DNA was used in the experiment. (D) Similar to (B), except that the SAGA complex was used instead of Spt8, and the Western blot was performed with anti-TAF6 to detect SAGA in the supernatant. (E) Similar to (D), except that non-TATA DNA was used for the experiment. (F) A Coomassie stained gel shows the equal amount of STR-tagged TBP remains on the beads after competition experiment in (D) and (E). This result suggests that the DNA does not compete with the binding of STR-tagged TBP to the resin.

3.4 Discussion

3.4.1 The putative WD40 domain of Spt8

I have identified that Spt8 contains a putative WD40 domain at the C-teriminus, which is highly conserved among other fungi. Despite the high conservation, N-terminal truncations of Spt8 are highly insoluble, and only the presence of 3 M urea confers some solubility. However, only certain truncations of Spt8: Spt8Δ2 and Spt8Δ7, which contain six WD40 motifs, but not Spt8Δ5 (165-602) and Spt8Δ6 (165-550), which have seven WD40 motif, could be purified with 3 M urea. These results have led to the interesting possibility that perhaps only six WD40 motifs of the Spt8 are sufficient to form a WD40 domain. Many proteins that contain the WD40 domain have seven WD40 motifs that make up a stable propeller-like structure. One exception is the structure of the WD40 domain of Cdc4, which has eight motifs (Orlicky et al., 2003). Although it seems unusual that the putative WD40 domain of Spt8 may be comprised of six motifs, one small, 247-amino acid protein from *Saccharomyces mikatae* (c673_14566), which shares

almost 90% identity with the C-terminal domain of the Spt8, may only contain 4 WD40 motifs (Cliften et al., 2003; Kellis et al., 2003). Thus, it might be possible that the WD40 domain could be built with less than seven WD40 repeats, or that those repeats form a structure that is distinct from a propeller structure.

3.4.2 Spt8 in the context of the SAGA complex

I have previously shown that Spt8, and perhaps Ada1, in the SAGA complex interact with the yeast TATA-binding protein. In higher eukaryotic cells, complexes which are similar to the yeast SAGA complex, such as human PCAF, human TFTC (TATA-free TAF_{II}-containing), and human STAGA (Spt3-TAF_{II}31-Gcn5L acetyltransferase) complexes have been described (Cavusoglu et al., 2003; Helmlinger et al., 2004; Martinez et al., 1998; Vassilev et al., 1998). It is interesting to note that no yeast Spt8 homologue has been discovered in human or flies, while the yeast homologue of Spt3 in other eukaryotes has been discovered (Martinez et al., 1998). Despite the existence of the yeast Spt3 counterparts in human, human Spt3 could not interact with TBP or TFIID (Martinez et al., 1998). While the SAGA complex from yeast is among the best characterized coactivator complex, the mechanism of how the human STAGA, TFTC or PCAF interacts or recruits TBP is less well understood. It is possible that if those human complexes interact with TBP, they may utilize a different subunit other than Spt8, or a WD40 containing protein to recruit TBP. My results in Chapter 2 suggest that the yeast SAGA without Spt8 may utilize Ada1 to interact with TBP. Because the yeast Ada1 is identified as the human STAF42, which is a component of the human STAGA complex (Martinez et al., 2001), STAF42 in the human STAGA might interact with TBP.

3.4.3 Interaction between Spt8 and TBP

My work in this chapter has contributed to our understanding of how SAGA regulates TBP binding to DNA. Since Spt8 in SAGA mainly interacts with TBP, I have tried to understand how the two proteins interact with each other. Here I show that 1) the putative WD40 domain of Spt8 is sufficient for the interaction with TBP; 2) the electrostatic interaction plays a critical role in the complex stabilization; and 3) Spt8 may interact through the concave side surface of the TBP structure and prevent TBP dimerization as well as TBP/TATA box DNA complex formation.

The main question is how the WD40 domain of Spt8 interacts and prevents the TBP/TBP and TBP/DNA complex formation. Three models of how a WD40 domain interacts with other proteins have been illustrated. The first model is that the edge around the propeller shaped WD40 domain interacts with its protein partner, as in the case of the clathrin (ter Haar et al., 2000). The second model emphasizes the role of the loops as being required for the interaction with other proteins, as in the case of Tup1, G protein β subunit, and Cdc4 (Lodowski et al., 2003; Orlicky et al., 2003; Sprague et al., 2000; Wall et al., 1995). The third model combines the first two interaction modes, as in the case of the interaction between the G protein β subunit and the G protein α subunit (Wall et al., 1995). Based on 1) the overall negative charge of the WD40 domain of Spt8; 2) the electrostatic interaction between the Spt8 and TBP; and 3) and several acidic residues located at the loops (Figure **3-3** B), the loops of the WD40 domain of Spt8 might play an important role in this interaction. Consistent with this idea, I present four different models of how a WD40 domain uses the loops to interact and occlude a TBP dimer formation (Figure **3-17**). Additional analysis such as cross-linking studies, artificial protease cleavage, and mutation analysis will provide better insight into the interactions of the two proteins.

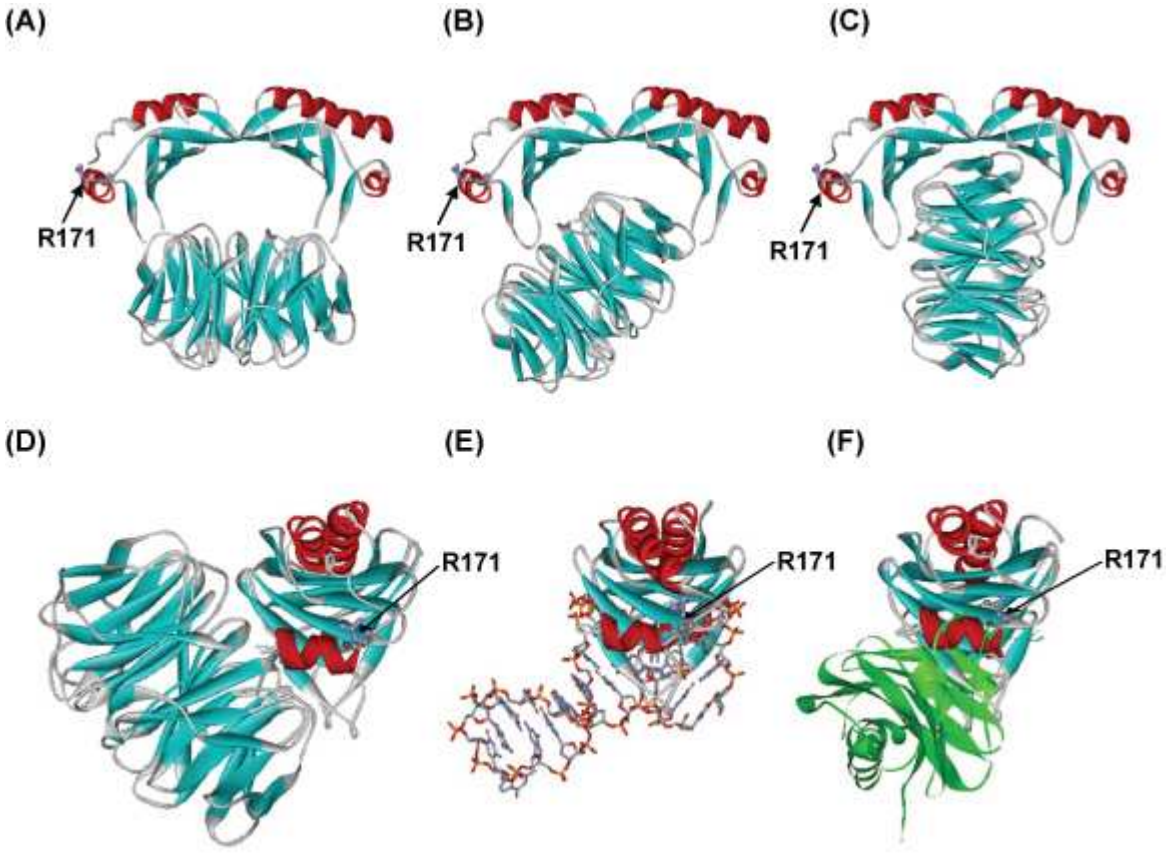

Figure **3-17**: Models for a WD40 domain interacts with TBP.

(A)-(D) are predicted models for how a WD40 domain can interact with TBP. The TBP structure (1TBP), (Chasman et al., 1993) was placed together with the WD40 domain of the G-protein β subunit (1OMW) (Lodowski et al., 2003) in the same scale. The WebLab ViewerLite program was used to manipulate the structures. (E) and (F) are the structure of TBP/TATA box DNA (1YTB) (Kim et al., 1993) and the TBP dimer (1TBP) (Chasman et al., 1993), respectively, and shown here for comparison with the model in (D).

The role of electrostatic interaction between TBP and other proteins has also been suggested. For example, the complex between the yeast TAF N-terminal domain (TAND) of TAF1 protein and the TBP is disrupted in a high salt concentration (Kotani et al., 1998). Interestingly, TAND, which consists of subdomain 1 and 2, occupies both concave and convex surfaces of TBP and prevents TBP dimerization (Kotani et al., 1998;

Mal et al., 2004). Even though the structures of the TAND and the WD40 domain are different, they bind to TBP and compete with TBP dimerization. Thus, regulation of TBP dimerization is one important step for transcriptional control, consistent with the previous study that showed a correlation between TBP dimer destabilization and transcriptional derepression (Jackson-Fisher et al., 1999).

3.4.4 Hand off model as a model for gene activation through the SAGA coactivator complex

Not only does Spt8 or the SAGA complex bind to the concave surface of TBP and prevent TBP dimerization, but it also prevents the binding of the TATA box DNA to TBP. This is an interesting and surprising observation but not inconsistent with the role of SAGA that promotes the recruitment of TBP *in vivo* (Bhaumik and Green, 2001; Larschan and Winston, 2001). Those studies have not been able to detect the SAGA complex at the core promoter region upon the activation of SAGA complex, suggesting that SAGA might not interact with a TBP/DNA complex. This is consistent with the competition assay results (Figure **3-16**). Therefore, I propose a hand off model that can reconcile *in vitro* and *in vivo* observations reported in literature (Figure **3-18**).

In this model, the SAGA complex binds to a TBP monomer and prevents the non-regulated binding of TBP to the core promoter. Upon transcription activation, a specific activator protein recruits the SAGA complex, which has TBP associated through the Spt8 and possibly Ada1, to the UAS. Then, TATA box DNA competes with the SAGA complex to bind to the TBP, creating a drop off or hand off mechanism in which the complex does not physically bridge an activator and the DNA bound TBP.

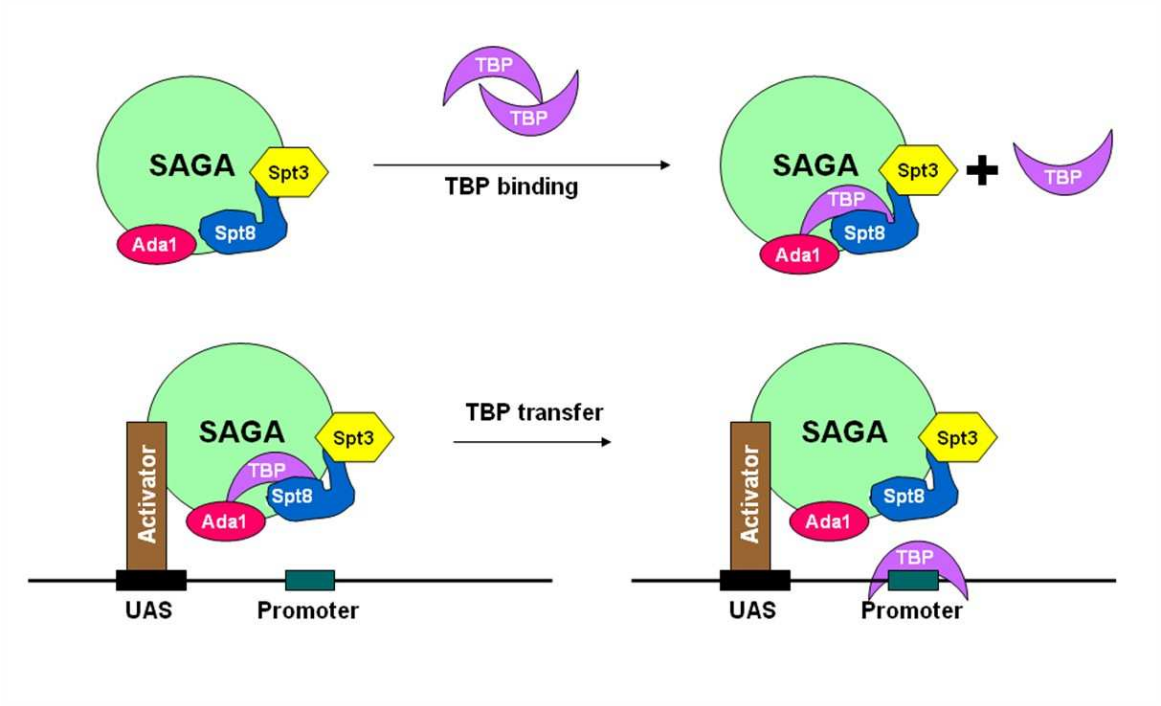

Figure **3-18**: Model for gene activation facilitated by the SAGA complex.

(A) Under non-inducing condition, TBP binds to Spt8, and presumably Ada1 in the SAGA complex, as a monomer through the concave surface of the saddle-like structure. As a result, SAGA prevents a constitutive binding of TBP to promoters. (B) Upon gene activation, the SAGA/TBP complex is recruited to the upstream activating sequence (UAS) by an activator protein. Then, the SAGA complex delivers TBP to the promoter by the competition from the TATA box DNA, creating a drop off or hand off mechanism by the SAGA complex.

How can this hand off model explain SAGA's behavior *in vivo*? Deletion of either SPT3 or SPT8 derepresses transcription of HIS3, TRP3, and HO under non-inducing conditions, suggesting that either Spt8 or Spt3 prevents the unregulated binding of TBP (Belotserkovskaya et al., 2000; Takahata et al., 2003). The HO promoter is different than those of HIS3 and TRP3 in which, while Spt3 seems to inhibit the TBP binding to the promoter, the HAT activity of Gcn5 functions to antagonize the repressive role of the Spt3 (Takahata et al., 2003). Together, the role of Spt3 and Spt8 on those genes is consistent with the model in which SAGA binds to a TBP monomer under a non-inducing condition (Figure **3-18** A). However, in the *spt7*Δ or *spt20*Δ strains where the

SAGA's integrity is disrupted, HIS3 and TRP3 transcription is being affected even in the inducing condition, suggesting a positive role for the SAGA complex in transcriptional regulation of those genes.

The role of Spt3 in regulation of TBP binding is also interesting. Deletion of Spt3 universally affects the TBP recruitment to all SAGA dependent promoters tested, while Spt8 also appear to be generally important for TBP recruitment, except for the GAL1 promoter (Barbaric et al., 2003; Bhaumik and Green, 2002; Takahata et al., 2003). At Gcn5-independent promoters such as *GAL1* and *PHO5*, Spt3 controls expression of those genes by regulating TBP recruitment during activation (Barbaric et al., 2003; Bhaumik and Green, 2001; Dudley et al., 1999; Larschan and Winston, 2001). These results suggest that Spt3 might interact with TBP either directly or indirectly. However, interpretations from those *in vivo* experiments could be complicated by the existence of an alternative form of SAGA: SAGA-like (SLIK) or SAGA altered, Spt8 absent (SALSA) complex (Sterner et al., 2002a; Wu and Winston, 2002). The SLIK complex has almost all SAGA subunits except the Spt8 but contains the C-terminal truncated Spt7. A study has proposed the role of SLIK as an active form of SAGA complex (Belotserkovskaya et al., 2000). In addition, it has been suggested that the complex contains a unique Rtg2 component, which is not present in the SAGA complex (Balasubramanian et al., 2002). Whether SLIK is a functionally distinct complex from SAGA or only representing an artifact of the MonoQ fractionation, additional investigations are required. My previous results do not reveal a direct physical interaction between the Spt3 in SAGA and the yeast TBP. Yet, the results show that the SAGA complex without Spt8 could still interact with TBP, and bind to a TBP monomer. It remains possible that Spt3 in the SAGA complex may interact with Spt8 and somehow affect SAGA-TBP interaction. Another possibility is Spt3 may be responsible for the process of TBP handed off to core promoter. Future experiments to test the hand off model in the *in vitro* context and the role of Spt3 in the hand off process are proposed in **5.2.2**.

While the SAGA complex interacts and recruits TBP to promoters, other coactivator complexes also mediate a proper TBP recruitment. For example, it was found that mutations in other coactivators such as the Swi/Snf, RSC and mediator complexes affect the kinetic recruitment of TBP to ARG1 promoters (Govind et al., 2005). How could those coactivator complexes involve in the TBP recruitment to a promoter? One of the explanations is that the RSC, as well as the Swi/Snf complexes, promote TBP recruitment by repositioning nucleosomes. Another explanation is that a coactivator complex functions to promote recruitment of other coactivators to the same UAS. For example, at the ARG1 UAS, the recruitment of SAGA is affected by the *rox3*Δ mutation in mediator complex; this could explain why the recruitment of TBP is impaired when the mediator complex is mutated (Govind et al., 2005). However, different activators utilize different mechanisms for their activation. The GAL1 promoter is activated by the Gal4 activator, which recruits the SAGA complex. Unlike the ARG1 system which depends on the Gcn4 activator, the recruitment of SAGA to the GAL1 UAS is not affected by mutations in Gal11 or Srb4, components of the mediator complex (Bhaumik et al., 2004; Bryant and Ptashne, 2003). In fact, it has been shown that the association of Srb8-Srb11 mediator complex at the Gal1 promoter is dependent on Spt3 in the SAGA complex (Larschan and Winston, 2005). Thus, even though TBP recruitment is mainly promoted by the SAGA complex, mechanisms of how TBP is recruited could be different from one promoter to another. Nonetheless, the SAGA complex has never been shown to associate at the core promoter (Bhaumik and Green, 2001; Larschan and Winston, 2001), consistent with the hand off model in which DNA binds to TBP only through competition with the SAGA complex.

DNA competition with coactivator complexes that bind to TBP might also be a general principle of other promoter systems. Some RNA polymerase II dependent genes recruit TBP through their association with TFIID, not the SAGA complex (Huisinga and Pugh, 2004). TAF1 subunit of TFIID utilizes its N-terminal domains (TAND) to interact with both concave and convex surfaces of TBP (Kotani et al., 1998; Takahata et al., 2003). TAND inhibits TBP binding and TBP dimerization, implying that TAND has a role in

repression (Kotani et al., 1998). However, when the TAND, especially TAND-1 (10-37 amino acids), is fused with the DNA binding domain of an activator protein, it can activate transcription, much like an activation domain (Kotani et al., 2000). Conversely, an activation domain can behave just like TAND-1, when it is placed within the context of TFIID, suggesting that an activation domain also binds to the concave underside surface of TBP (Kotani et al., 2000). This property of TAND-1 has led to the proposal of the two-step hand off model for transcriptional initiation by TFIID (Figure **3-19**) (Kotani et al., 2000). In the first step, TFIID is recruited by an activator protein, whose activation domain competes with the TAND-1 that occupies the concave underside surface of TBP. As a result, the activator domain binds to a concave surface of TBP. Because the activation domain binds to the concave surface of TBP, it is unlikely that the activator, TBP in TFIID, and the DNA at the core promoter form a ternary complex. This leads to the second step of the model in which the activator hands off TFIID to the core promoter. The process of handing off TFIID from the activator may also be assisted by TFIIA, which has been shown to dissociate TBP dimerization and assist TFIID binding to the core promoter (Coleman et al., 1999; Emami et al., 1997; Ozer et al., 1998). TFIIA might direct the binding of TFIID to the core promoter by weakening interaction between TAND-1 and TBP or TAND-1 and activation domain (Kotani et al., 2000). Thus, Kokubo's hand off model, which is summarized in Figure **3-19**, is similar to the hand off model proposed in this Chapter of the thesis, and yet there are some differences. The SAGA complex only transfers TBP to core promoters, while both TAFs and TBP in TFIID are transferred. In addition, the SAGA complex is preferentially localized at the upstream activating sequence (UAS), while the TAFs in TFIID are preferentially localized at the core promoter (Bhaumik and Green, 2001).

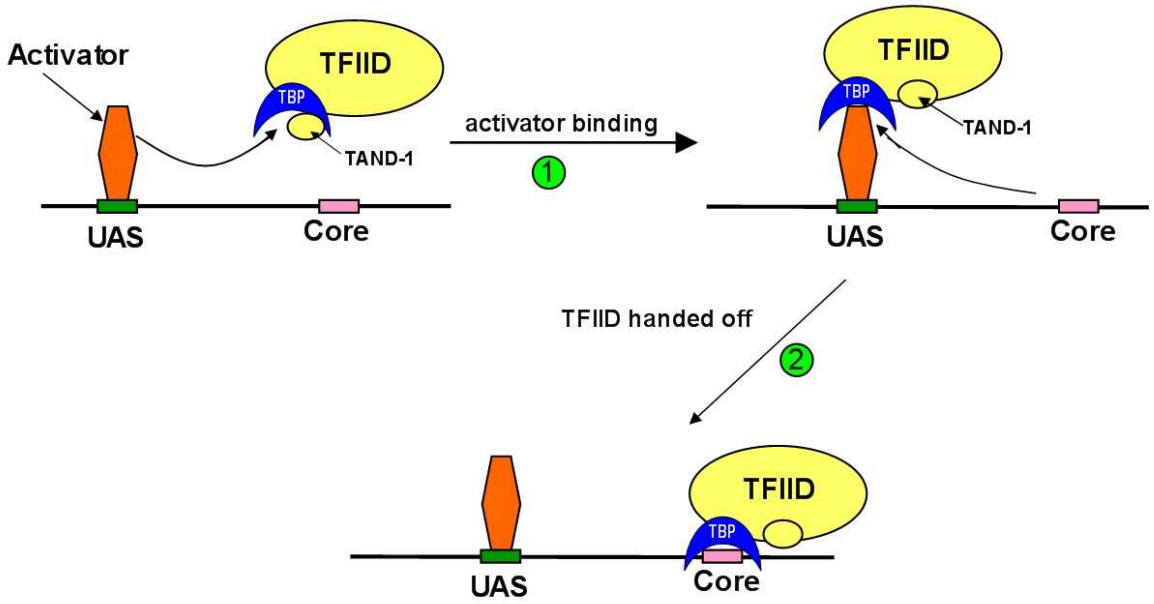

Figure **3-19**: Kokubo's TFIID hand off model

A simplified diagram illustrates Kokubo's TFIID hand off model (Kotani et al., 2000). The hand off model has two steps. First step, the activation domain from an activator-bound UAS competes with TAND-1 from TAF1 subunit. As a result, TFIID binds to an activator protein. Second step, the activator hands TFIID off to a core promoter. As a result, both TAFs and TBP in TFIID bind to the core promoter

Overall, results from this study indicate that the SAGA complex binds to a TBP monomer, mainly through the Spt8 and perhaps the Ada1 subunits. Once recruited by activators, DNA completes with the SAGA complex to bind to the TBP, causing the SAGA complex to hand off TBP to the core promoters. A simple model can be used to explain many *in vivo* results and reconcile many observations from both *in vivo* and *in vitro* experiments.

3.5 Materials and Methods

3.5.1 Expression plasmids for truncated Spt8

pST50Tr-STRHisNySpt8Δ1 was created by ligating a BamHI-NgoMIV ySpt8Δ1 insert into a BamHI-NgoMIV pST50Tr-STRHisN vector. The insert was a PCR product using a forward STO1399 (5'-CGGGATCCGACGAGGTTGACGATATTC-3') oligo and a reverse STO1567 (5'-GCCCGCCGGCCTCAAGCGTGTTCAGC-3') oligo to amplify the Spt8 gene on a pWM528-ySpt8x3 plasmid from codon 2 to 209, and to attach 5' BamHI and 3' NgoMIV restriction sites, respectively.

pST50Tr-STRHisNySpt8Δ2x3 was created by ligating a BamHI-NgoMIV ySpt8Δ2x3 insert into a BamHI-NgoMIV pST50Tr-STRHisN vector. The insert was a PCR product using a forward STO1568 (5'-CGGGATCCGGGAAACTTTCTCTAACTATCC-3') oligo and a reverse STO1400 (5'-GCCCGCCGGCTTCTAAGTCTATATCGTAAATAAGG-3') oligo to amplify a pWM528-ySpt8x3 plasmid from codon 210 to 602, and to attach 5' BamHI and 3' NgoMIV restriction sites, respectively.

pST50Tr-HisTrxNySpt8Δ2x3 was created by ligating a BamHI-NgoMIV ySpt8Δ2x3 insert into a BamHI-NgoMIV pST50Tr-HisTrxN vector. The BamHI-NgoMIV ySpt8Δ2x3 insert was created by digesting pST50Tr-STRHisNySpt8Δ2x3 with BamHI and NgoMIV restriction enzymes.

pST50Tr-ySpt8Δ3Hisx3 was created by ligating a BamHI-NgoMIV ySpt8Δ3x3 insert into a BamHI-NgoMIV pST50Tr-His vector. The insert was a PCR product using a forward STO1714 (5'-GCGGATCCGACGCCGCAAGAATGG3') oligo and a reverse STO1400 (5'-GCCCGCCGGCTTCTAAGTCTATATCGTAAATAAGG-3') oligo to

amplify the Spt8 gene on a pWM528-ySpt8x3 plasmid from codon 76 to 602, and to attach 5'BamHI and 3' NgoMIV restriction sites, respectively.

pST50Tr-ySpt8Δ4Hisx3 was created by ligating a BamHI-NgoMIV ySpt8Δ4x3 insert into a BamHI-NgoMIV pST50Tr-His vector. The insert was a PCR product using a forward STO1715 (5'-GCGGATCCGAGGTTTATGAGTACTATAAGCACATG-3') oligo and a reverse STO1400 (5'-GCCCGCCGGCTTCTAAGTCTATATCGTAAATAAGG-3') oligo to amplify the Spt8 gene on a pWM528-ySpt8x3 plasmid from codon 146 to 602, and to attach 5'BamHI and 3' NgoMIV restriction sites, respectively.

pST50Tr-HisTrxNySpt8Δ5x3, pST50Tr-HisTrxNySpt8Δ6x3, and pST50T3-HisTrxNySpt8Δ7x3 constructs were created by Dr. Song Tan with the same cloning strategy described above. Spt8Δ5 insert was a PCR product using a forward STO1902 (5'-CGGGATCCAATATCTACCCCACGGCA-3') oligo and a reverse STO1400 (5'-GCCCGCCGGCTTCTAAGTCTATATCGTAAATAAGG-3') oligo to amplify a pWM528-ySpt8x3. Spt8Δ6 insert was a PCR product using a forward STO1902 (5'-CGGGATCCAATATCTACCCCACGGCA-3') oligo and a reverse STO1903 (5'-GCCCGCCGGCAGAACTCTTTGTAGTCGAGTTCG-3') oligo to amplify a pWM528-ySpt8x3. Lastly, Spt8Δ7 insert was a PCR product using a forward STO1568 (5'-CGGGATCCGGGAAACTTTCTCTAACTATCC-3') oligo and a reverse STO1903 (5'-GCCCGCCGGCAGAACTCTTTGTAGTCGAGTTCG-3') oligo to amplify pWM528-ySpt8x3.

3.5.2 Expression of truncated Spt8 proteins

BL21(DE3)pLysS was transformed with a pST50Tr plasmid containing a desired truncation of Spt8, and plated on a TYE plate (1.0% bacto tryptone, 0.5% yeast extract, 0.8% NaCl, 1.5% agar, 100 µg/ml ampicillin, and 25 µg/ml chloramphenicol). After 8-

12 hours of incubation at 37°C, 3 or 4 colonies from the plate were incubated in a 100 ml 2xTY medium (1.6% bacto tryptone, 1.0% yeast extract, and 0.5% NaCl) with ampicillin and chloramphenicol added to 50 µg/ml and 25 µg/ml, respectively. Cells were incubated at a 37°C shaker and transferred to a lower temperature incubator when the OD_{600} reached between 0.1 and 0.2. For 37°C expression, the culture remained in the same incubator. The culture was induced when the OD_{600} reached between 0.4 and 0.7 by addition of isopropyl-β-D-thiogalactopyranoside (IPTG) to a final concentration of 0.2 mM. For each expression at 37°C and 28°C, cell samples from uninduced, to 1, 2, 3, and 4 or 5 hours after induction, were collected for a SDS PAGE gel. To get the uninduced sample, 500 µl of cells, which were used for OD_{600} measurement, were transferred to an eppendorf tube, spun for 1 minute at 13,000 rpm, aspirated off supernatant, and resuspended in 100 µl 2x PGLB (0.125 M Bis-Tris pH 6.8, 20% glycerol, 4% SDS, 2.16 M 2-mercaptoethanol, and 0.04% bromophenol blue). Samples from each hour time point after induction were prepared with 250 µl cell cultures from the flask, spun, aspirated off supernatant, and resuspended in 100 µl 2x PGLB. Samples were analyzed with an 18% SDS PAGE gel. At 3 hours after induction, a 50-ml cell culture for solubility test and metal affinity purification was collected in a 50 ml Falcon tube. A cell pellet was obtained by centrifugation and resuspended with a 10 ml phosphate buffer pH 7.0 (see **3.5.3**).

For 18°C expression, cells were grown and transferred to an 18°C incubator at the same OD_{600}. They were induced for 12-16 hours with the same amount of IPTG. Only uninduced and 12-16 induced samples for the SDS PAGE gel were also prepared. Samples for solubility test and metal affinity purification was prepared after 12-16 hours of induction, in the same way as described for the 37°C and 28°C expressions.

3.5.3 Solubility test

I analyzed the solubility of the expressed protein by determining how much of it was present in the supernatant and cell pellet. Frozen cells in a buffer were thawed on ice and sonicated for 3x 10 seconds at 45 % power output (Branson, Digital Sonifier). The "whole," (as an abbreviation for whole cell extract) sample was prepared by mixing 25 µl of the sonicated sample with 25 µl 2xPGLB. Then, 500 µl of sonicated material was centrifuged in a microfuge at 13,000 rpm for 3 minutes. The supernatant was removed to a new tube for the soluble portion of the cells. This soluble portion of the protein was used to create the "supernatant" by mixing 1:1 with 2xPGLB. The tube containing cell debris and insoluble proteins was centrifuged again for 1 minute at the maximum speed, and the left over supernatant was removed from the cell pellet by aspiration. The pellet was resuspended with 150 µl of the same buffer used for cell resuspension, using a P-200 Pipet. Once the pellet was completely and thoroughly resuspended, another 350 µl buffer was added to bring the final volume back to 500 µl. The resulting resuspended pellet was used to prepare the "pellet" sample by mixing 1:1 with 2xPGLB. This way, the whole cell extract (sonicated cells), pellet and supernatant were in equivalent volumes, making the comparison among the three easy. If the experiment were conducted properly, the intensity of a protein band appearing in the supernatant lane, combined with the same protein in the pellet, should result in an equal intensity of that protein in the whole cell extract.

3.5.4 Metal affinity purification

Cells expressing the truncated Spt8 were resuspended with 10 ml P100 buffer (50 mM Sodium Phosphate buffer pH 7.0, 100 mM NaCl, 5 mM 2-mercaptoethanol, and 1 mM benzamidine). Cells were allowed to thaw on ice and sonicated for 3x 10 seconds at 45% power output (Branson, Digital Sonifier). An aliquot of the sonicated material was used for the solubility test (See **3.5.3**). The remainder of sonicated sample was centrifuged to

isolate the soluble material from cell debris. Roughly 5 ml of the soluble extract was incubated with 0.5 ml Talon resin (Clontech, CA), equilibrated with P100 buffer, for 15 minutes at 4°C with constant rotation. After incubation, the sample was centrifuged to collect the flow through (FT). The resin with Spt8 peptide bound was washed 2x 10 ml with P100 buffer. Then, the washed resin was transferred with a total of 3 ml P100 buffer to a Bio-RAD, Bio-Spin column and the protein was eluted with 250 µl (E1), 500 µl (E2, E3 and E4) of P100 + 100 mM imidazole. Equal volume samples from the whole cell extract (sonicated sample), pellet, supernatant, and FT, together with E2 and E3 fractions were analyzed with an 18% SDS PAGE gel

The purification with urea was similar: cells expressing the desired Spt8 peptide were previously resuspended in 10 ml PGU300 buffer (50 mM sodium phosphate buffer pH 7.0, 300 mM NaCl, 10% glycerol, 0.1% NP40, 5 mM 2-mercaptoethanol, 1 mM benzamidine, and 3 M urea). For some experiments, the salt concentration was 200 mM NaCl. The salt concentration can be added to 500 mM, as in the case for purification of GSTNySpt8Δ2His (see **3.5.5**). Cell disruption and purification procedures were conducted the same way as described above, except that the buffer for this purification was PGU300 and the resin was washed once with PGU300 while the next wash omitted urea (PG300 buffer). The PG300 (without urea) containing 100 mM imidazole was used to elute the protein off the resin.

3.5.5 Overexpression and purification of the recombinant GSTNySpt8Δ2His protein

The truncated version of yeast Spt8, designated as ySpt8Δ2 (210-602), was purified differently from the full length protein. The protein was fused with a GSTN tag on the N-terminus and 6xHis (His) tag on the C-terminus, respectively. Media, bacteria strain, and overexpression procedures for this protein were the same as the method described in **3.5.2**. BL21(DE3)pLysS cells from a 6-liter culture expressing GSTNySpt8Δ2His

protein were resuspended with approximately 150 ml PGU500 buffer (50 mM Sodium Phosphate pH 7.0, 500 mM NaCl, 1 mM benzamidine, 5 mM 2-mercaptoethanol, 10% glycerol, 0.1% NP-40, and 3 M urea) and kept at -80ºC. Purification of this protein involved two steps: Talon Affinity matrix and Glutathione Sepharose 4B. All purification steps were performed at 4°C. Soluble extract was prepared using the same procedures as described above and passed through a Talon affinity column (Clontech), which was equilibrated with PGU500 buffer. Non-specific bound protein was washed with PG500 (50 mM sodium phosphate pH 7.0, 500 mM NaCl, 1 mM benzamidine, 5 mM 2-mercaptoethanol, 10% glycerol, 0.1% NP-40) and with 15 mM imidazole. GSTNySpt8Δ2His was eluted from the column with PG500 containing 150 mM imidazole. Peak fractions were pooled and used directly as an input for the next step of purification. 300 µl Glutathione Sepharose 4B resin was equilibrated with PG500 and used for binding of GSTNySpt8Δ2His. After washing, the bound GSTNySpt8Δ2His was directly used for a GST pull down assay.

3.5.6 Pull down experiments

A STR pull down experiment was performed similarly to that described in **2.5.6**. Briefly, 3 µg of the STR-tagged wild type TBP, the R171 and the T153I TBP mutants were immobilized in the *Strep*-Tactin resin, previously equilibrated with HG200 buffer (20 mM HEPES pH 7.5, 200 mM NaCl, 10% glycerol, 0.1% Tween 20, and 10 mM 2-mercaptoethanol). HisTrxNyEsa1, HisTrxNySpt8Δ2, and HisTrxNySpt8Δ7 proteins were dialyzed against HG200 buffer, and the amount was normalized with an 18% SDS PAGE gel. Each protein was incubated with the tagged-TBP on the resin for 1 hour at 4°C with rotations. The blank contained only the *Strep*-Tactin without the bound TBP. After 1 hour of incubation, the sample tubes were centrifuged and the supernatant was collected. The resin was washed 3x 500 µl with HG200. Equivalent amounts of input, supernatant and beads were loaded and electrophoresed on an 18% SDS PAGE gel.

Proteins were transferred to a nitrocellulose membrane for western blot analysis with the anti-Thioredoxin antibodies.

GST tag pull down was performed in a similar manner. 25 µl Glutathione Sepharose 4B resin which contains either GST tag or GSTNySpt8Δ2His was equilibrated with HG200 (20 mM HEPES pH 7.5, 200 mM NaCl, 10% glycerol, 0.1% Tween 20, and 10 mM 2-mercaptoethanol). Wild type, R171E, or T153I STRNyTBPcore protein was diluted with H200G to 0.01 µg/µl, and 25 µl used for incubation with 25 µl of both resins containing either GST or GSTNySpt8Δ2His. After 1 hour of incubation, the resin was washed 4x 500 µl with HG200. An equivalent volume amount of input, supernatant, and beads were used for the SDS PAGE and subjected to Western blot analysis with an anti-*Strep*-tag monoclonal antibody.

3.5.7 Competition assay

A competition experiment to test the binding of Spt8 or SAGA complex to TBP was performed as follows. 6 µg of STRNyTBPcore was immobilized on a 25 µl *Strep*-Tactin resin, which was pre-equilibrated by a T150G buffer (50 mM Tris-Cl, pH 8.0, 150 mM NaCl, 10% glycerol, 0.1% Tween 20, and 10 mM 2-mercaptoethanol). Then, 3 µg of CBPyTBPcore was mixed with the bound STRNyTBPcore for 2 hours at 4°C to heterodimerize the STRNyTBPcore/CBPyTBPcore. After 3 washes with T150G buffer, 25 µl of Spt8 or the SAGA complex was added to the final concentration of 0.8 to 20 nM, and 10 to 40 nM, respectively. The mixture was incubated for 90 minutes. The supernatant was collected, while the beads were washed 4 x 500 µl with T150G buffer. 25 µl T150G buffer was added to the resin to make an equivalent volume between the beads and the supernatant. Samples were analyzed by western blotting with anti-Spt8 antibodies (a gift from Workman lab) for Spt8 protein, anti-His antibodies (Santa Cruz) for Spt3 protein, anti-Taf6 (a gift from the Workman lab), and anti-CBP (Upstate) for CBPyTBPcore protein.

A competition experiment to test the binding of DNA to either Spt8/TBP or SAGA/TBP bound was done in a similar procedure. 3 µg instead of 6 µg of STRNyTBPcore was immobilized on a 25 µl *Strep*-Tactin resin, and equilibrated with T150G buffer. After washes, the resin was incubated with 25 µl of either 2 µM Spt8 or 25 µM SAGA complex for 1 hour at 4°C. Unbound proteins were washed away with the same buffer before adding 25 µl of TATA box DNA from the yeast CYC1 promoter (26 bp double-stranded oligonucleotide CYC1 promoter DNA: 5'-TGCTCTGTATGTATATAAAACTCTTG-3') or the non-TATA box DNA (29 bp double-stranded oligonucleotide DNA 5'-GTAGATGCTTCGAACTCGACTACAAAGCG-3'). The amount of the DNA added in both the Spt8 and SAGA containing reaction was from 0.31 to 5.0 µM. After 90 minutes incubation at 4°C, the supernatant was collected, and the beads were washed 4 x 500 µl T150G. Supernatant portions were analyzed by western blots analysis using anti-Spt8 and anti-Taf6 antibodies to detect the presence of the Spt8 protein or the SAGA complex, respectively. 25 µl of T150G buffer was added to the beads to make an equal volume to the supernatant. DNA that was bound to TBP in the beads was extracted once with phenol/CIA (1:1 mixture), and again with CIA (24:1, chloroform : isoamyl alcohol). Extracted DNA was analyzed on a 10% native polyacrylamide gel and visualized by UV transillumination.

3.6 Acknowledgements

I would like to thank the Pugh lab for the Spt7-TAP yeast strain. I am grateful to Jerry L. Workman, Frank Pugh, and Joe Reese for suggestions on this project. I would also like to thank to all Tan lab members for their valuable discussion and support.

3.7 Bibliography

Barbaric, S., Reinke, H., and Horz, W. (2003). Multiple mechanistically distinct functions of SAGA at the PHO5 promoter. Mol Cell Biol *23*, 3468-3476.

Belotserkovskaya, R., Sterner, D. E., Deng, M., Sayre, M. H., Lieberman, P. M., and Berger, S. L. (2000). Inhibition of TATA-binding protein function by SAGA subunits Spt3 and Spt8 at Gcn4-activated promoters. Mol Cell Biol *20*, 634-647.

Bhaumik, S. R., and Green, M. R. (2001). SAGA is an essential in vivo target of the yeast acidic activator Gal4p. Genes Dev *15*, 1935-1945.

Bhaumik, S. R., and Green, M. R. (2002). Differential requirement of SAGA components for recruitment of TATA-box-binding protein to promoters in vivo. Mol Cell Biol *22*, 7365-7371.

Bhaumik, S. R., Raha, T., Aiello, D. P., and Green, M. R. (2004). In vivo target of a transcriptional activator revealed by fluorescence resonance energy transfer. Genes Dev *18*, 333-343.

Bryant, G. O., and Ptashne, M. (2003). Independent recruitment in vivo by Gal4 of two complexes required for transcription. Mol Cell *11*, 1301-1309.

Cavusoglu, N., Brand, M., Tora, L., and Van Dorsselaer, A. (2003). Novel subunits of the TATA binding protein free TAFII-containing transcription complex identified by matrix-assisted laser desorption/ionization-time of flight mass spectrometry following one-dimensional gel electrophoresis. Proteomics *3*, 217-223.

Chasman, D. I., Flaherty, K. M., Sharp, P. A., and Kornberg, R. D. (1993). Crystal structure of yeast TATA-binding protein and model for interaction with DNA. Proc Natl Acad Sci U S A *90*, 8174-8178.

Cliften, P., Sudarsanam, P., Desikan, A., Fulton, L., Fulton, B., Majors, J., Waterston, R., Cohen, B. A., and Johnston, M. (2003). Finding functional features in Saccharomyces genomes by phylogenetic footprinting. Science *301*, 71-76.

Coleman, R. A., Taggart, A. K., Burma, S., Chicca, J. J., 2nd, and Pugh, B. F. (1999). TFIIA regulates TBP and TFIID dimers. Mol Cell *4*, 451-457.

Dudley, A. M., Rougeulle, C., and Winston, F. (1999). The Spt components of SAGA facilitate TBP binding to a promoter at a post-activator-binding step in vivo. Genes Dev *13*, 2940-2945.

Emami, K. H., Jain, A., and Smale, S. T. (1997). Mechanism of synergy between TATA and initiator: synergistic binding of TFIID following a putative TFIIA-induced isomerization. Genes Dev *11*, 3007-3019.

Govind, C. K., Yoon, S., Qiu, H., Govind, S., and Hinnebusch, A. G. (2005). Simultaneous recruitment of coactivators by Gcn4p stimulates multiple steps of transcription in vivo. Mol Cell Biol *25*, 5626-5638.

Hamm, H. E. (1998). The many faces of G protein signaling. J Biol Chem *273*, 669-672.

Hartman, J. J., Mahr, J., McNally, K., Okawa, K., Iwamatsu, A., Thomas, S., Cheesman, S., Heuser, J., Vale, R. D., and McNally, F. J. (1998). Katanin, a microtubule-severing protein, is a novel AAA ATPase that targets to the centrosome using a WD40-containing subunit. Cell *93*, 277-287.

Helmlinger, D., Hardy, S., Sasorith, S., Klein, F., Robert, F., Weber, C., Miguet, L., Potier, N., Van-Dorsselaer, A., Wurtz, J. M., *et al.* (2004). Ataxin-7 is a subunit of GCN5 histone acetyltransferase-containing complexes. Hum Mol Genet *13*, 1257-1265.

Huisinga, K. L., and Pugh, B. F. (2004). A genome-wide housekeeping role for TFIID and a highly regulated stress-related role for SAGA in Saccharomyces cerevisiae. Mol Cell *13*, 573-585.

Jackson-Fisher, A. J., Chitikila, C., Mitra, M., and Pugh, B. F. (1999). A role for TBP dimerization in preventing unregulated gene expression. Mol Cell *3*, 717-727.

Kellis, M., Patterson, N., Endrizzi, M., Birren, B., and Lander, E. S. (2003). Sequencing and comparison of yeast species to identify genes and regulatory elements. Nature *423*, 241-254.

Kim, Y., Geiger, J. H., Hahn, S., and Sigler, P. B. (1993). Crystal structure of a yeast TBP/TATA-box complex. Nature *365*, 512-520.

Kotani, T., Banno, K., Ikura, M., Hinnebusch, A. G., Nakatani, Y., Kawaichi, M., and Kokubo, T. (2000). A role of transcriptional activators as antirepressors for the autoinhibitory activity of TATA box binding of transcription factor IID. Proc Natl Acad Sci U S A *97*, 7178-7183.

Kotani, T., Miyake, T., Tsukihashi, Y., Hinnebusch, A. G., Nakatani, Y., Kawaichi, M., and Kokubo, T. (1998). Identification of highly conserved amino-terminal segments of dTAFII230 and yTAFII145 that are functionally interchangeable for inhibiting TBP-DNA interactions in vitro and in promoting yeast cell growth in vivo. J Biol Chem *273*, 32254-32264.

Kou, H., Irvin, J. D., Huisinga, K. L., Mitra, M., and Pugh, B. F. (2003). Structural and functional analysis of mutations along the crystallographic dimer interface of the yeast TATA binding protein. Mol Cell Biol *23*, 3186-3201.

Kou, H., and Pugh, B. F. (2004). Engineering dimer-stabilizing mutations in the TATA-binding protein. J Biol Chem *279*, 20966-20973.

Kuras, L., Kosa, P., Mencia, M., and Struhl, K. (2000). TAF-Containing and TAF-independent forms of transcriptionally active TBP in vivo. Science *288*, 1244-1248.

Larschan, E., and Winston, F. (2001). The S. cerevisiae SAGA complex functions in vivo as a coactivator for transcriptional activation by Gal4. Genes Dev *15*, 1946-1956.

Larschan, E., and Winston, F. (2005). The Saccharomyces cerevisiae Srb8-Srb11 complex functions with the SAGA complex during Gal4-activated transcription. Mol Cell Biol *25*, 114-123.

Lee, D., Ezhkova, E., Li, B., Pattenden, S. G., Tansey, W. P., and Workman, J. L. (2005). The proteasome regulatory particle alters the SAGA coactivator to enhance its interactions with transcriptional activators. Cell *123*, 423-436.

Leone, M., Di Lello, P., Ohlenschlager, O., Pedone, E. M., Bartolucci, S., Rossi, M., Di Blasio, B., Pedone, C., Saviano, M., Isernia, C., and Fattorusso, R. (2004). Solution structure and backbone dynamics of the K18G/R82E Alicyclobacillus acidocaldarius thioredoxin mutant: a molecular analysis of its reduced thermal stability. Biochemistry *43*, 6043-6058.

Lodowski, D. T., Pitcher, J. A., Capel, W. D., Lefkowitz, R. J., and Tesmer, J. J. (2003). Keeping G proteins at bay: a complex between G protein-coupled receptor kinase 2 and Gbetagamma. Science *300*, 1256-1262.

Martinez, E., Kundu, T. K., Fu, J., and Roeder, R. G. (1998). A human SPT3-TAFII31-GCN5-L acetylase complex distinct from transcription factor IID. J Biol Chem *273*, 23781-23785.

Martinez, E., Palhan, V. B., Tjernberg, A., Lymar, E. S., Gamper, A. M., Kundu, T. K., Chait, B. T., and Roeder, R. G. (2001). Human STAGA complex is a chromatin-acetylating transcription coactivator that interacts with pre-mRNA splicing and DNA damage-binding factors in vivo. Mol Cell Biol *21*, 6782-6795.

Orlicky, S., Tang, X., Willems, A., Tyers, M., and Sicheri, F. (2003). Structural basis for phosphodependent substrate selection and orientation by the SCFCdc4 ubiquitin ligase. Cell *112*, 243-256.

Ozer, J., Mitsouras, K., Zerby, D., Carey, M., and Lieberman, P. M. (1998). Transcription factor IIA derepresses TATA-binding protein (TBP)-associated factor inhibition of TBP-DNA binding. J Biol Chem *273*, 14293-14300.

Pray-Grant, M. G., Schieltz, D., McMahon, S. J., Wood, J. M., Kennedy, E. L., Cook, R. G., Workman, J. L., Yates, J. R., 3rd, and Grant, P. A. (2002). The novel SLIK histone acetyltransferase complex functions in the yeast retrograde response pathway. Mol Cell Biol *22*, 8774-8786.

Qiu, H., Hu, C., Zhang, F., Hwang, G. J., Swanson, M. J., Boonchird, C., and Hinnebusch, A. G. (2005). Interdependent recruitment of SAGA and Srb mediator by transcriptional activator Gcn4p. Mol Cell Biol *25*, 3461-3474.

Ricci, A. R., Genereaux, J., and Brandl, C. J. (2002). Components of the SAGA histone acetyltransferase complex are required for repressed transcription of ARG1 in rich medium. Mol Cell Biol *22*, 4033-4042.

Roark, D. E., Geoghegan, T. E., Keller, G. H., Matter, K. V., and Engle, R. L. (1976). Histone interactions in solution and susceptibility to denaturation. Biochemistry *15*, 3019-3025.

Sprague, E. R., Redd, M. J., Johnson, A. D., and Wolberger, C. (2000). Structure of the C-terminal domain of Tup1, a corepressor of transcription in yeast. Embo J *19*, 3016-3027.

Sterner, D. E., Belotserkovskaya, R., and Berger, S. L. (2002). SALSA, a variant of yeast SAGA, contains truncated Spt7, which correlates with activated transcription. Proc Natl Acad Sci U S A *99*, 11622-11627.

Strahilevitz, J., Onodera, Y., and Hooper, D. C. (2005). An improved expression plasmid for affinity purification of Staphylococcus aureus gyrase A subunit. Protein Expr Purif.

Takahata, S., Ryu, H., Ohtsuki, K., Kasahara, K., Kawaichi, M., and Kokubo, T. (2003). Identification of a novel TATA element-binding protein binding region at the N terminus of the Saccharomyces cerevisiae TAF1 protein. J Biol Chem *278*, 45888-45902.

Tan, S., Hunziker, Y., Pellegrini, L., and Richmond, T. J. (2000). Crystallization of the yeast MATalpha2/MCM1/DNA ternary complex: general methods and principles for protein/DNA cocrystallization. J Mol Biol *297*, 947-959.

ter Haar, E., Harrison, S. C., and Kirchhausen, T. (2000). Peptide-in-groove interactions link target proteins to the beta-propeller of clathrin. Proc Natl Acad Sci U S A *97*, 1096-1100.

Vassilev, A., Yamauchi, J., Kotani, T., Prives, C., Avantaggiati, M. L., Qin, J., and Nakatani, Y. (1998). The 400 kDa subunit of the PCAF histone acetylase complex belongs to the ATM superfamily. Mol Cell *2*, 869-875.

Vaughan, M. (1998). Signaling by heterotrimeric G proteins minireview series. J Biol Chem *273*, 667-668.

Wall, M. A., Coleman, D. E., Lee, E., Iniguez-Lluhi, J. A., Posner, B. A., Gilman, A. G., and Sprang, S. R. (1995). The structure of the G protein heterotrimer Gi alpha 1 beta 1 gamma 2. Cell *83*, 1047-1058.

Winston, F., Dollard, C., Malone, E. A., Clare, J., Kapakos, J. G., Farabaugh, P., and Minehart, P. L. (1987). Three genes are required for trans-activation of Ty transcription in yeast. Genetics *115*, 649-656.

Wu, P. Y., and Winston, F. (2002). Analysis of Spt7 function in the Saccharomyces cerevisiae SAGA coactivator complex. Mol Cell Biol *22*, 5367-5379.

Chapter 4

Characterization of the bromodomain of yeast Gcn5

4.1 Abstract

The bromodomain has the ability to bind to an acetylated histone tail. In addition, it has been shown to play a role in nucleosome acetylation by the SAGA complex. However, the latter role of the bromodomain is not well characterized. In this chapter, I analyzed the role of the bromodomain of yeast Gcn5 on the nucleosomal HAT activity. In the context of the yeast Ada3/Ada2/Gcn5, I found that this function of the bromodomain is not dependent on the peptide binding pocket but instead, lies within the three basic residues on the surface of the bromodomain. Amino acid substitutions in any of these three residues that change a positive charge confer a similar effect to a bromodomain deletion mutant. In addition to the *in vitro* analysis, the bromodomain of Gcn5 is required for full, global acetylation of histone H3. I hypothesize that the same three basic residues that are required for the Ada3/Ada2/Gcn5 nucleosomal HAT activity are also required for the global histone H3 acetylation by the SAGA complex.

4.2 Introduction

The evolutionarily conserved bromodomain is a small domain, comprising of roughly 110 amino acids. The bromodomain binds to an acetylated protein or histone tail (Yang, 2004), and consists of a left-handed four-helix bundle with a hydrophobic cavity formed by the loops that link the helixes on one end of the structure (Hudson et al., 2000; Owen et al., 2000). Interestingly, the bromodomain is found only in the type A nuclear HAT enzyme (Kleff et al., 1995). The bromodomain is involved in regulation of transcription

of genes and can be found in many transcription factors including yeast Gcn5, the only HAT catalytic subunit of the SAGA complex.

A subset of the SAGA complex, Ada3/Ada2/Gcn5 is the smallest subcomplex that is sufficient to modify histone tails in nucleosomes (Balasubramanian et al., 2002). Gcn5 alone is capable of acetylating a core histone but not a nucleosome substrate (Balasubramanian et al., 2002). Ada2 interacts and enhances the core histone acetylation function of Gcn5 (unpublished data), whereas Ada3, which only interacts with Ada2 in the Ada2/Gcn5 complex, confers a nucleosomal HAT function to the Ada3/Ada2/Gcn5 trimeric complex (Balasubramanian et al., 2002; Horiuchi et al., 1995). While a structure and a mechanism of the HAT domain of Gcn5 that acetylates the histone H3 tail have been well characterized (Berndsen and Denu, 2005; Rojas et al., 1999; Trievel et al., 1999), the mechanism whereby Gcn5 in the context of Ada3/Ada2/Gcn5 complex acetylates a nucleosome substrate is less well understood. It has been shown *in vitro* that the SAGA complex harboring a bromodomain deleted Gcn5 shows a significant decrease in the nucleosomal HAT activity.

In this work, I characterized the role of bromodomain in the nucleosomal HAT activity. In the context of the purified yeast Ada3/Ada2/Gcn5 complex, I found that the peptide binding pocket of the bromodomain of Gcn5 is not required for the nucleosomal HAT activity tested. Instead, I have identified the specific residues in the bromodomain structure: K412, R419, and K422, which are important for the overall nucleosomal HAT activity of the complex. In addition, I addressed the role of the bromodomain in the global histone H3 acetylation *in vivo*. Similar to the deletion of Gcn5, deletion of the bromodomain of Gcn5 affects the overall H3 acetylation *in vivo*. I hypothesize that those three basic residues might play a role in the global histone H3 acetylation. Future experiment will need to be performed in order to test the hypothesis.

4.3 Results

4.3.1 Deletion of the Gcn5 bromodomain affects the nucleosomal HAT activity of the Ada3/Ada2/Gcn5 complex

I set out to determine whether the deletion of the bromodomain of Gcn5 would affect the nucleosomal HAT activity of the Ada3/Ada2/Gcn5 complex. This work was previously done by Adam Barrios, a former graduate student in the laboratory. Gcn5 with bromodomain deletion (Gcn5Δ6, 2-368) was created by PCR amplification and subcloned into a polycistronic vector containing Ada3 and Ada2 genes in the first and second cassette of the pST44 expression vector (Tan et al., 2005). In this plasmid, the Ada3 gene was truncated at the N-terminus and was shown to have no effect on the nucleosomal HAT activity of Ada3/Ada2/Gcn5 complex (Adam Barrios's unpublished result). All three proteins were coexpressed and partially purified with a metal affinity resin (Figure **4-1** C). Fractions from the resin were diluted and used for HAT assays. The HAT activity reported in this study was the ratio between the chicken long oligo nucleosomes (LON) and chicken core histones relative to the wild type complex (v37), which was set to a value of 1.0. The HAT assay ratio reported here emphasized the ability of the Ada3/Ada2/Gcn5 complexes to acetylate nucleosomes. This HAT assay ratio also allows the comparison among different sets of data. It should be noted that there were some variations among different sets of the chicken LON used for the HAT assay. For example, the LON activity of the wild type v37 in Figure **4-1** was 870 ± 232 whereas it was 3952 ± 227 in Figure **4-5**. I noticed that some of the chicken LON aliquots may contain precipitation of histones. This could contribute to variations of LON HAT activity among different experiments. The discrepancy in the HAT activity among the chicken LON was also observed by Adam Barrios. However, the HAT assay results reported in each figure was always performed concomitantly with the wild type v37. Thus, the relative LON/core HAT ratio of each mutant version can be made directly

to the activity of the wild type v37 from the same experiment, eliminating the problem with variations in the LON HAT activity.

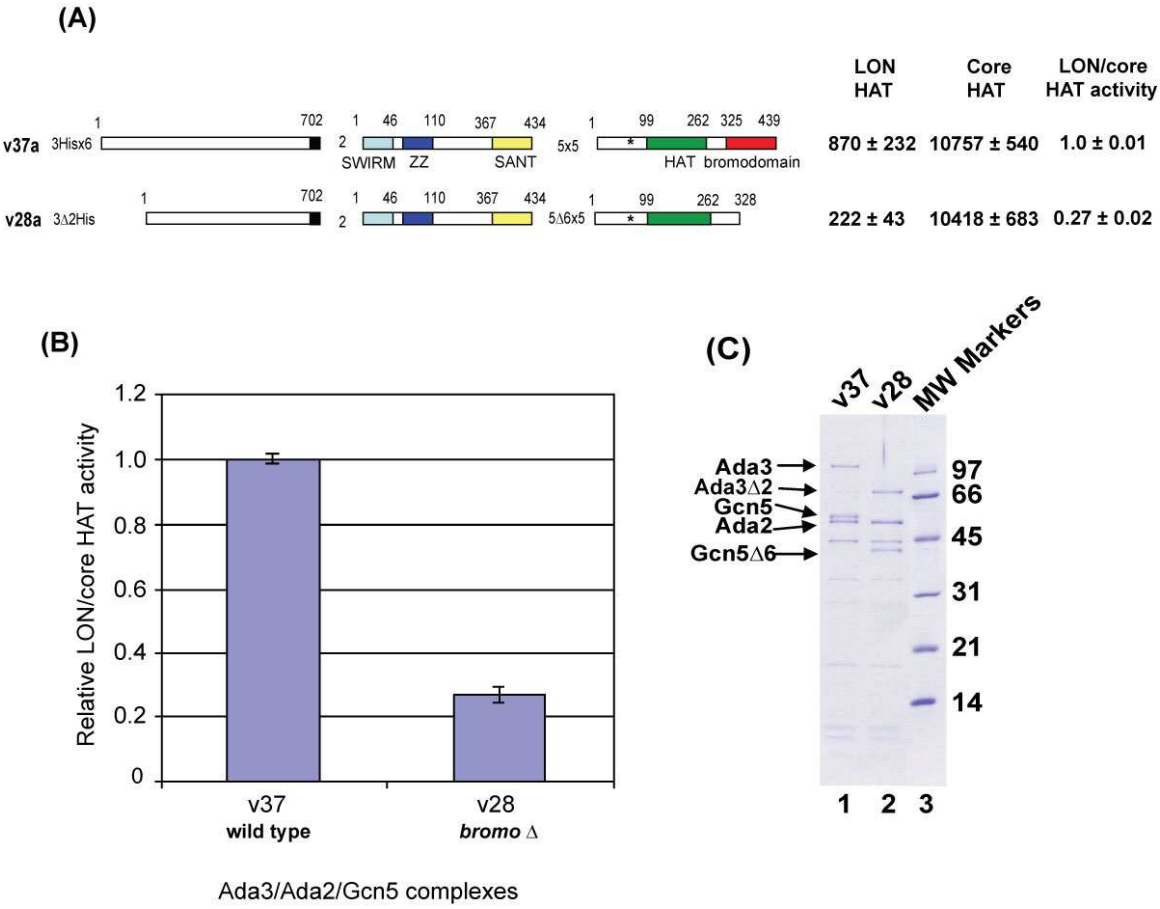

Figure **4-1**: Bromodomain is required for the nucleosomal HAT activity of the Ada3/Ada2/Gcn5 complex.

(A) This panel shows the schematic representations and the relative HAT activity of the wild type (v37) and bromodomain deletion (v28) Ada3/Ada2/Gcn5 complexes. A star within the Gcn5 indicates a silent mutation to eliminate a cryptic Shine Dalgado start site from Val66. (B) A bar chart compares the relative HAT activity of v28 Ada3/Ada2/Gcn5 complex with the wild type complex (v37). The HAT activity shown is the average, and the error bars represent the standard deviations of 3 measurements. (C) A Coomassie stained gel shows the partially purified wild type (v37) and bromodomain deletion (v28) Ada3/Ada2/Gcn5 complexes.

The bromodomain deletion (v28) did not display any defect in the core histone HAT activity. As shown in Figure **4-1** B, the HAT activity of v28 was approximately 25% of the wild type complex, higher than the previous result (10%) obtained by Adam Barrios. This was probably due to a different set of the chicken LON substrate. Therefore, these results suggest that bromodomain is required for the proper nucleosomal HAT activity of the Ada3/Ada2/Gcn5 complex.

4.3.2 The binding pocket of the acetylated histone H4 tail is not required for nucleosomal HAT activity of the Ada3/Ada2/Gcn5 complex

The deletion of the bromodomain of Gcn5 affects the nucleosomal HAT activity of the trimeric Ada3/Ada2/Gcn5 complex. The goal is to identify the residues of the bromodomain that play a role in the nucleosomal HAT function. The first area of the bromodomain to analyze is the peptide binding pocket, which recognizes an acetylated histone tail (Ornaghi et al., 1999; Owen et al., 2000). To test whether the residues within the peptide binding pocket of the bromodomain is important for nucleosomal HAT activity of the complex, I performed site-directed mutagenesis to mutate specific residues within the area (Figure **4-2** A). These residues: Y364, N407, and Y413 make contacts with the acetylated lysine 16 of histone H4 that inserts itself within the peptide binding pockets of the bromodomain (Figure **4-2** A). The alanine substitution was introduced into each of these amino acids of the bromodomain. The Ada3, Ada2, and mutated Gcn5 were coexpressed and purified with a metal affinity resin (Figure **4-2** D). Previous work by Adam Barrios showed that a single point mutation within the peptide binding pocket did not affect the nucleosomal HAT activity (data not shown). It was possible that those residues might have redundant functions. Thus, I created double and triple mutations within the peptide binding pocket and assayed the nucleosomal HAT activity. As shown in Figure **4-2** A, B and C, those complexes: Y364A;N407A (v84), Y364A;Y413A (v85), and Y364A;N407A;Y413A (v86) still retained approximately 80%-85% of the wild type HAT activity (Figure **4-2** B and C), indicating that the nucleosomal HAT activity was not

affected by those mutations. The relative LON/core HAT activity of the mutant complex v86 was reproducible when the HAT assays with v86 were conducted together with other mutant complexes (Figure **4-3**). Therefore, I conclude that the peptide binding pocket of bromodomain is not important for the nucleosomal HAT activity *in vitro*.

4.3.3 Point mutations on the surface of bromodomain affect nucleosomal HAT activity of the complex

If the peptide binding pocket of the bromodomain is dispensable for the *in vitro* nucleosomal HAT activity of the Ada3/Ada2/Gcn5 complex, then other features of the bromodomain must be required for this function. I reexamined the crystal structure of the bromodomain of Gcn5 and noticed three clusters of residues that might be interacting with nucleosomes or other proteins. Those three clusters are 1) the K415, R419, and K422 residues; 2) the E378, I 379, and E382 residues; and 3) the K380 and K385 residues (Figure **4-3** A). Therefore, I created three additional mutations: K415A;R419A;K422A (v87), E378A;I379A;E382A (v88), and K380A;K385A (v89) (Figure **4-3** A and B). I found that mutations in the three basic residues (v87 but not v89) decreased the nucleosomal HAT activity to roughly 20% of the wild type complex (Figure **4-3** C). Interestingly, the other two mutations had different effects: v88 mutant conferred a significant increase in the nucleosomal HAT activity by 50% of the wild type while v89 mutant did not have any effect (Figure **4-3** C).

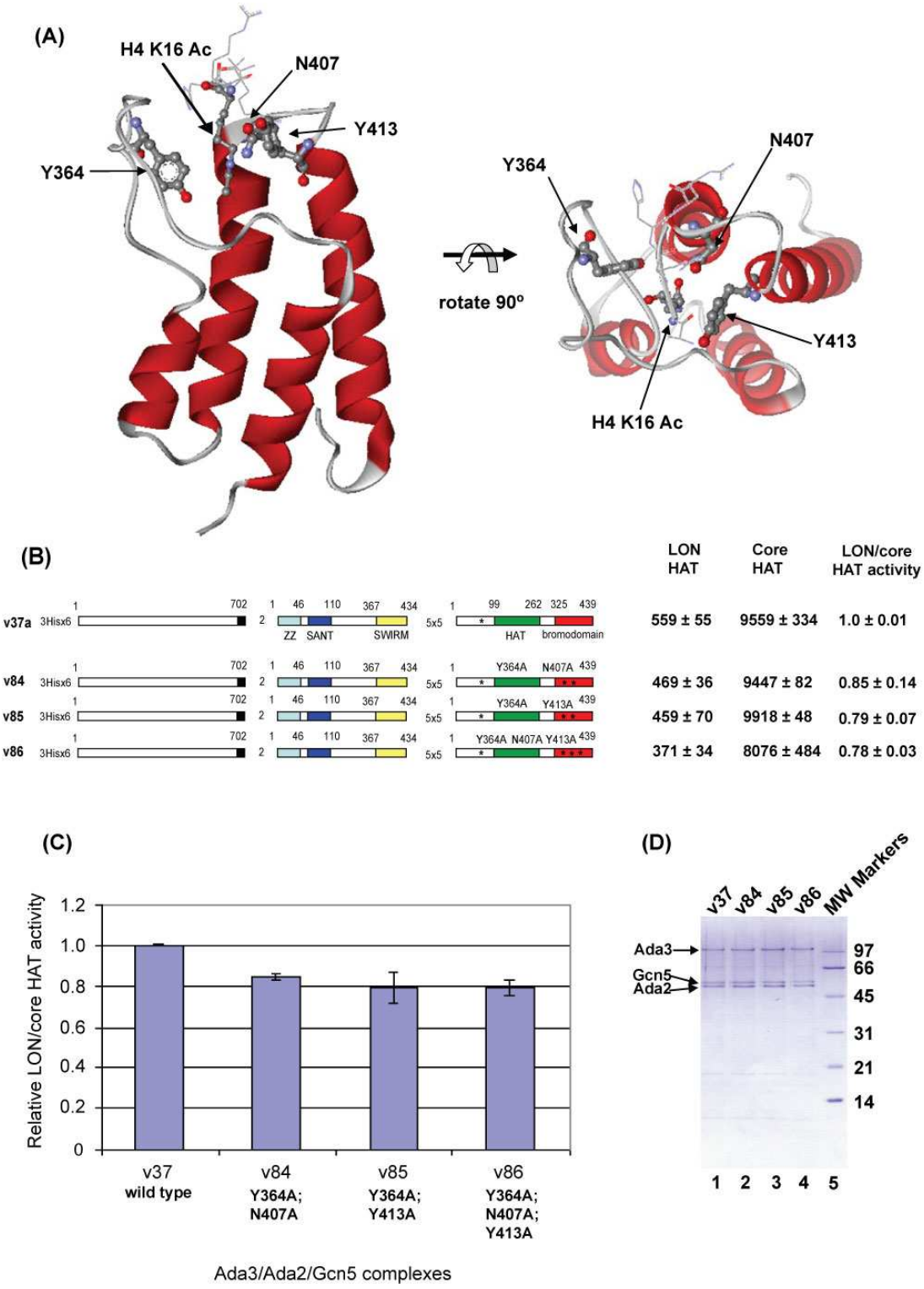

Figure **4-2**: The peptide binding pocket of the bromodomain is not essential for nucleosomal HAT activity of the Ada3/Ada2.Gcn5 complex.

(A) Structure of the bromodomain (Owen et al., 2000). The residues shown in the structure: Y364, N407, and Y413 are the amino acids, which are located within the peptide binding pocket of the bromodomain and interact with the acetylated lysine 16 of histone H4. Each of these residues was subject to alanine substitution, which will disrupt the acetylated peptide binding ability of the bromodomain (PDB Id: 1E61, using the WebLab ViewerLite program to manipulate the structure). (B) The schematic representations and the relative HAT activity of the wild type complex (v37), the Y364A;N407A mutant (v84), the Y364A;Y413A mutant (v85), and the Y364A;N407A;Y413A mutant (v86) Ada3/Ada2/Gcn5 complexes. A star within the Gcn5 indicates a silent mutation to eliminate a cryptic Shine Dalgado start site from Val66. (C) A bar chart compares the relative HAT activity among the wild type (v37) and the mutant complexes. The HAT activity shown is the average of at least 3 measurements. The error bars represent the standard deviations. (D) A Coomassie stained gel shows the partially purified Ada3/Ada2/Gcn5 complexes.

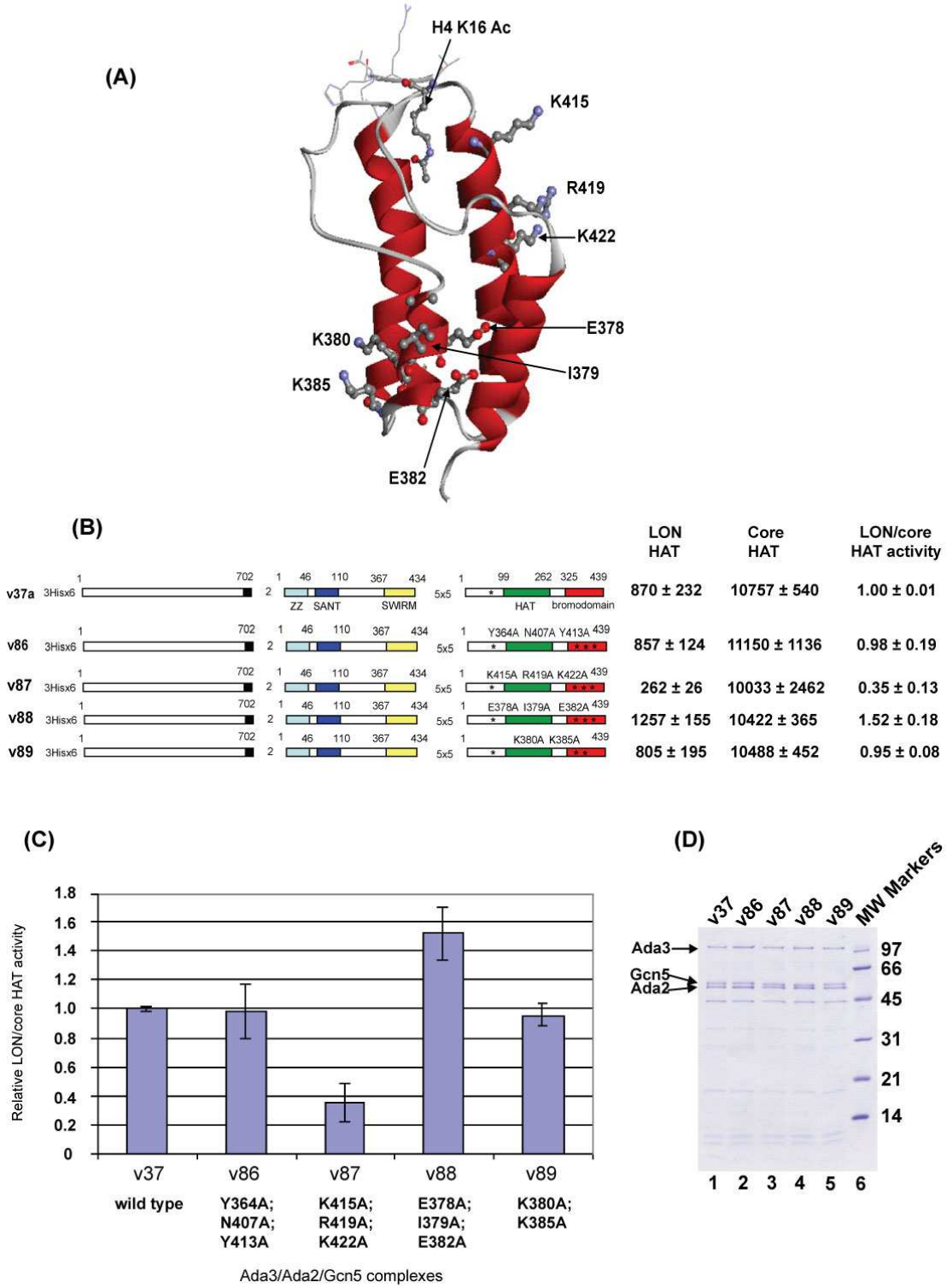

Figure **4-3**: Surface of bromodomain that requires for the nucleosomal HAT activity of the Ada3/Ada2/Gcn5 complex.

(A) Structure of the bromodomain (Owen et al., 2000) and the residues which were mutated (PDB Id: 1E61, using the WebLab ViewerLite program to manipulate the structure). (B) The schematic representations and the relative HAT activity of the wild type complex (v37), the K415A;R419A;K422A mutant (v87), the Y364A; N407A; Y413A mutant (v86); the E378A;I379A;E382A mutant (v88), and the K380A;K385A mutant (v89) Ada3/Ada2/Gcn5 complexes. A star within the Gcn5 indicates a silent mutation to eliminate a cryptic Shine Dalgado start site from Val66. (C) A bar chart compares the relative HAT activity among the wild type (v37) and the mutant complexes. The HAT activity shown is the average, and the error bars represents the standard deviations of 3 measurements. (D) A Coomassie stained gel shows the partially purified Ada3/Ada2/Gcn5 complexes.

I further created a single point mutation for each amino acid residue in the basic cluster to test whether or not individual mutations in those residues would have any effect and to what level compared with the triple mutation. Three additional mutations: K415A (v92), R419A (v93), and K422A (v94) were created (Figure **4-4** B). As shown in Figure **4-4** C, a single alanine substitution in any of those residues conferred a similar effect to the bromodomain deletion (v28) or the triple mutations (v87), suggesting an equal requirement of each residue in the nucleosomal HAT activity of the trimeric complex. The relative LON/core HAT activity of v87 in Figure **4-4** was consistent with that from Figure **4-3**. It is possible that the overall positive charge of the cluster rather than a specific interaction with each residue is important for the nucleosomal HAT activity. To test this idea, I further created three additional mutants: K415R;K422R (v95), K415D (v96), and K415D;K419D;K422D (v97) (A and B). If the overall positive charge is important for the nucleosomal HAT activity, then the K415D and K415D;K419D;K422D but not the K415R;K422R mutants would show an effect. In contrast, if a specific interaction with each of those residues is important, then those three mutant complexes should show some effect on the nucleosomal HAT activity. As shown in Figure **4-5** C, the K415D (v96) and K415D;K419D;K422D (v97) but not the K415R;K422R (v95) mutants had about 30% of the nucleosomal HAT activity of the wild type version. Therefore, I conclude that the overall positive charge in this region of the bromodomain plays a role in the nucleosomal HAT activity of the Ada3/Ada2/Gcn5 complex.

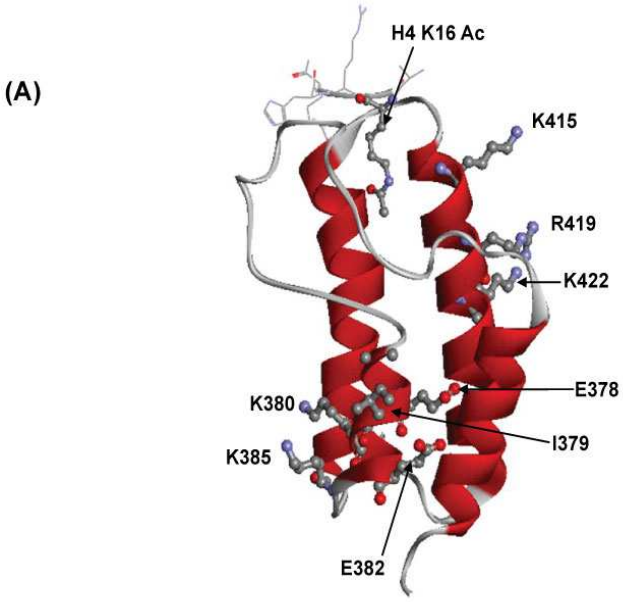

(B)

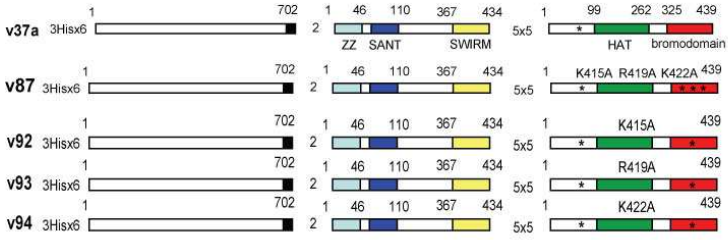

	LON HAT	Core HAT	LON/core HAT activity
v37a	1336 ± 255	9666 ± 598	1.00 ± 0.02
v87	292 ± 155	10299 ± 326	0.20 ± 0.07
v92	488 ± 45	10153 ± 533	0.32 ± 0.03
v93	365 ± 141	10276 ± 633	0.25 ± 0.06
v94	406 ± 50	10085 ± 520	0.295 ± 0.03

(C)

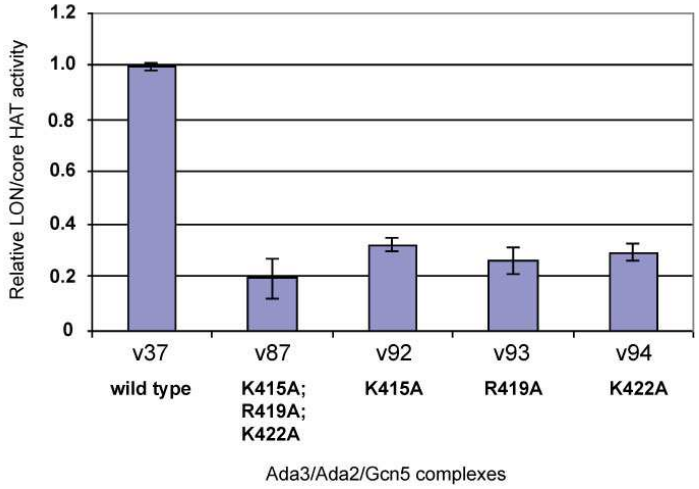

(D)

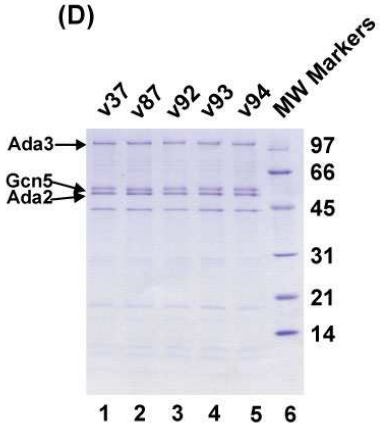

Figure **4-4**: K415, R419, or K422 is equally important for nucleosomal HAT activity of the Ada3/Ada2/Gcn5 complex

(A) Structure of the bromodomain (Owen et al., 2000) and the residues that were mutated (PDB Id: 1E61, using the WebLab ViewerLite program to manipulate the structure). (B) The schematic representations and the relative HAT activity of the wild type complex (v37), the K415A;K419R;K422A mutant (v87), the K415A mutant (v92), the R419A mutant (v93), and the K422A mutant (v94) Ada3/Ada2/Gcn5 complexes. A star within the Gcn5 indicates a silent mutation to eliminate a cryptic Shine Dalgado start site from Val66. (C) A bar chart compares the relative HAT activity among the wild type (v37) and the mutant complexes. The HAT activity shown is the average, and the error bars represent the standard deviations of 3 measurements. (D) A coomassie stained gel shows the partially purified Ada3/Ada2/Gcn5 complexes.

4.3.4 Recombinant core histones and nucleosome substrates do not change the relative HAT activity of the Ada3/Ada2/Gcn5 mutant complexes

All the HAT assays in this study involved chromatin substrates extracted from chicken erythrocytes, which could potentially contain some post-translationally modified histones. As discussed in **1.1.3**, a modification on histone tails could potentially affect another histone modification: a concept of the histone code hypothesis. One could also argue that the results from the mutations in the bromodomain of the Ada3/Ada2/Gcn5 complexes might have been different when unmodified nucleosomes are used in the HAT assay. To test this possibility, I carried out additional HAT assays, using recombinant *Xenopus laevis* core histones and reconstituted nucleosomes as the HAT substrates for the trimeric complexes v28, v84, and v87, respectively. As shown in Figure **4-6**, the HAT assay results from the trimeric complexes v28, v84, and v87 from the recombinant core histones and nucleosomes mirrored those from the chicken chromatin substrates. These results suggest that the existence of post-translational modifications on the chicken

histones (if any) is not relevant to the HAT activity of the Ada3/Ada2/Gcn5 complex *in vitro*.

4.3.5 The bromodomain of Gcn5 is required for the global acetylation of histone H3

It was quite interesting that an alanine substitution at any of the basic residues on the surface of the bromodomain produced the same effect as the bromodomain deletion in an *in vitro* HAT assay. Therefore, I set out to test whether or not mutations in these residues would affect the global histone H3 acetylation. To address this issue, I created different yeast strains from the *gcn5*Δ background yeast. The Gcn5 deleted yeast strain (*gcn5*Δ) was a gift from the Pugh Lab. Yeast was transformed with either vector only (no *GCN5*), wild type *GCN5*, Y364A; N407A; Y413A (YNY) *gcn5* mutant, K415A; R419A; K422A (KRK) *gcn5* mutant, or the bromodomain deletion (*bromo* Δ) *gcn5* mutant containing plasmid. Yeast extract were made and the Western blots were performed using anti-histone H3 and anti-histone H3 K9&K14 acetylated antibodies since these two residues have been shown to be the main target of SAGA acetylation (Balasubramanian et al., 2002; Eberharter et al., 1998).

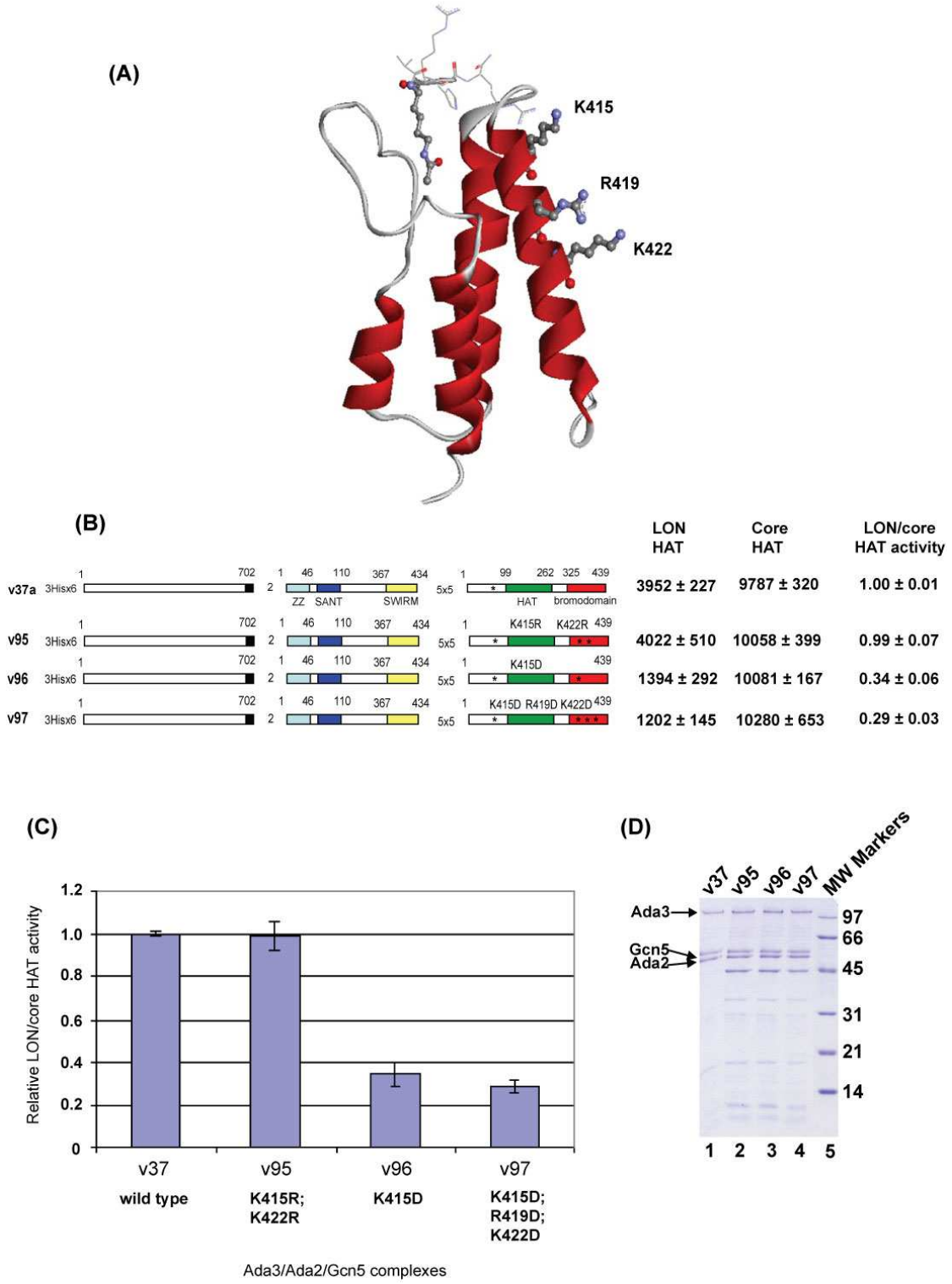

Figure **4-5**: Positive charges of bromodomain residues 415, 419, and 422 are important for the nucleosomal HAT activity of the Ada3/Ada2/Gcn5 complex.

(A) Structure of the bromodomain (Owen et al., 2000) and the residues that were mutated (PDB Id: 1E61, using the WebLab ViewerLite program to manipulate the structure). (B) The schematic representations and the relative HAT activity of the wild type complex (v37), the K415R;K422R mutant (v95), the K415D mutant (v96), and the K415D;R419D;K422D mutant (v97) Ada3/Ada2/Gcn5 complexes. A star within the Gcn5 indicates a silent mutation to eliminate a cryptic Shine Dalgado start site from Val66. (C) A bar chart compares the relative HAT activity among the wild type (v37) and the mutant complexes. The HAT activity shown is the average, and the error bars represent the standard deviations of at least 3 measurements. (D) A coomassie stained gel shows the partially purified Ada3/Ada2/Gcn5 complexes.

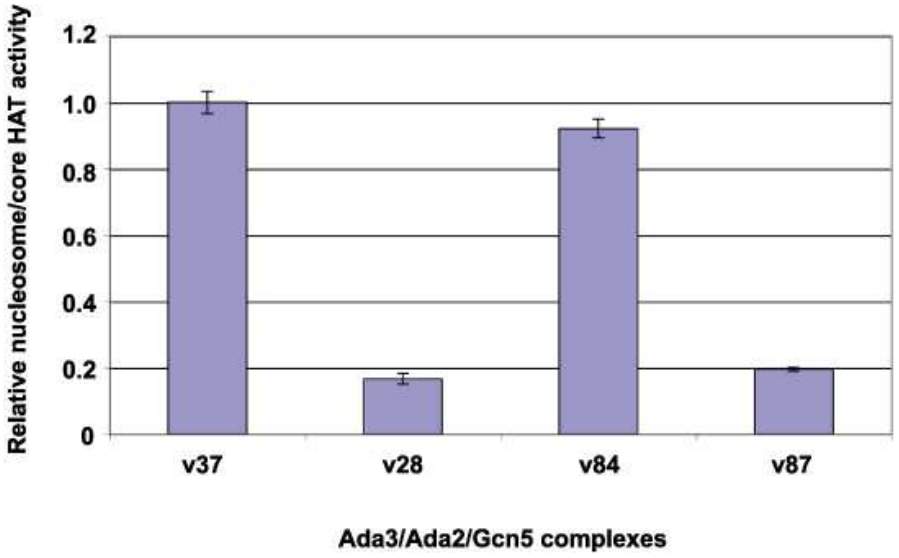

Figure **4-6**: HAT assays of the Ada3/Ada2/Gcn5 complexes with the recombinant core histones and nucleosomes.

After subtracted from blanks, the average HAT activity of each complex calculated is the ratio between the nucleosome to the core histone HAT activity relative to the wild type complex (v37). The averages and the standard deviations were calculated from 3 measurements.

Results from the Western blot with anti-histone H3 K9&K14 acetylated antibodies were normalized based on the signals from the anti-histone H3 antibodies. As shown in Figure **4-7**, my preliminary data showed that the cell has lost the global histone H3 acetylation in the *gcn5* deleted mutant. In contrast to my data, many reports in the

literature have suggested that the global histone H3 acetylation in *gcn5*Δ deleted strains was significantly reduced but not completely abolished because other histone H3 HAT, such as Sas3, also functions to acetylate histone H3 on the same residues as SAGA (Howe et al., 2001; Kristjuhan et al., 2002). It is possible that histone H3 acetylation in my *gcn5*Δ strain was not lost but the acetylation level was too low to be detected by the antibodies. In addition, the global histone H3 acetylation was affected in all mutations. The global histone H3 acetylation effect observed in the KRK mutations are consistent with my analysis of the Ada3/Ada2/Gcn5 complex. However, it appeared that mutations within the peptide binding pocket of the bromodomain (YNY mutant) conferred a more severe effect than the KRK mutations. These residues are located on the side surface of the bromodomain. These results suggest that the peptide binding pocket is more important for SAGA acetylation than the Ada3/Ada2/Gcn5 complex.

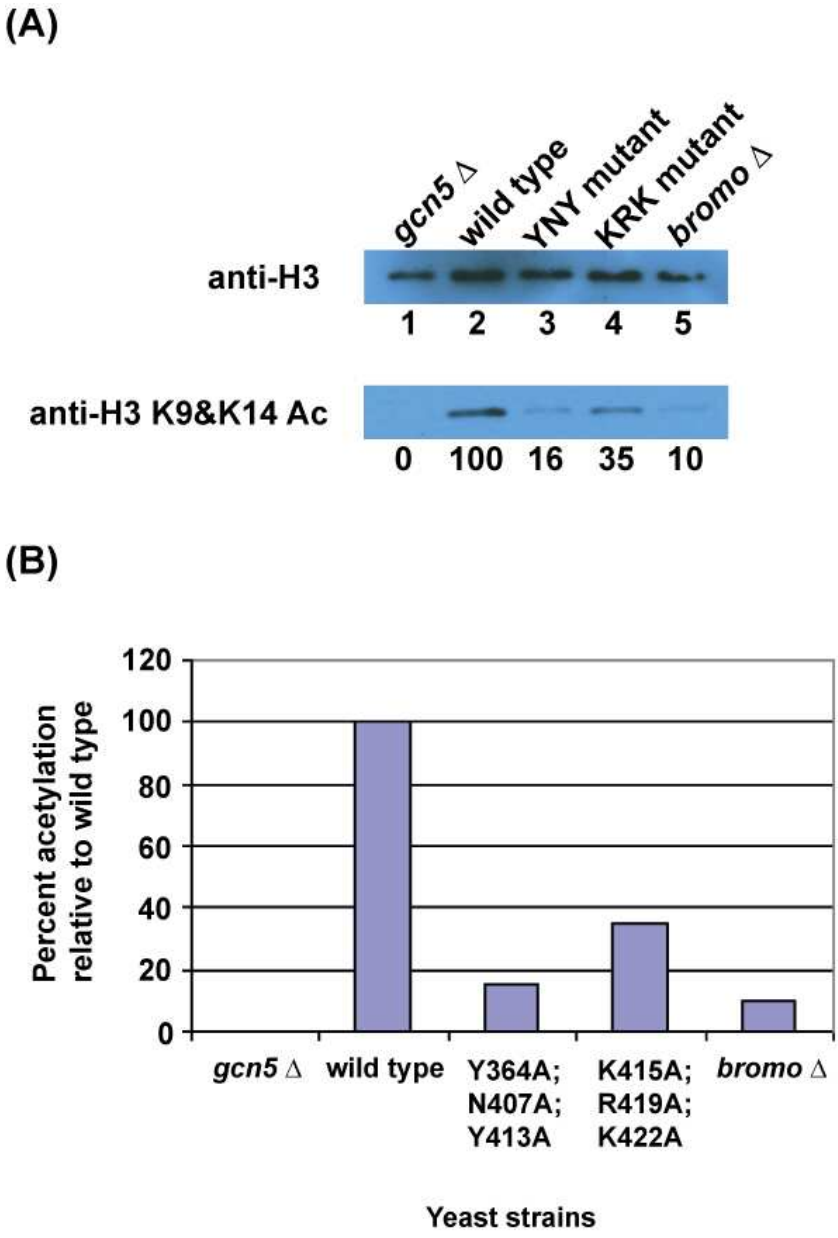

Figure **4-7**: Bromodomain of Gcn5 is required for the global histone H3 acetylation.

The figure shows preliminary data for global histone H3 acetylation in yeast. (A) Western blot analysis shows histone H3 and the acetylation of the histone H3 at K9&K14. The numbers in the bottom of the lower panel indicate the relative intensity of histone H3 K9&K14 acetylation relative to the wild type after normalization with signals from the histone H3 antibodies. (B) Data from (A) is plotted into a bar chart that shows percent acetylation relative to the wild type, which is set to 100%.

4.4 Discussion

4.4.1 The role of the bromodomain of Gcn5 in the HAT function of the isolated Ada3/Ada2/Gcn5 complex

I was interested in determining how the bromodomain of Gcn5 plays a supporting role in the nucleosome acetylation function of the Ada3/Ada2/Gcn5 complex since the bromodomain deletion affects the nucleosomal but not the core histone HAT activity. Because it has been shown *in vitro* that the bromodomain of Gcn5 can bind to acetylated histone H3 and H4 tails, I tested if mutations in the peptide binding pocket of this protein would affect the HAT activity of the Ada3/Ada2/Gcn5 complex. However, I found that this was not the case because those mutations in the peptide binding pocket caused very little effect on the nucleosomal HAT activity. The bromodomain of Gcn5 is well conserved among the bromodomain of other proteins such as the human PCAF. The invariant tyrosine 413 of the Gcn5 corresponds to the conserved tyrosine 809 in the bromodomain of the human PCAF. It has been shown that the alanine substitution mutation at the tyrosine 809 (Y809A mutation) in the human PCAF bromodomain completely abolished the binding of an acetylated peptide to the bromodomain of PCAF (Dhalluin et al., 1999). Moreover, alanine substitution mutations at other residues within the peptide binding pocket of the PCAF's bromodomain significantly affect the peptide binding by almost 30 fold (Dhalluin et al., 1999). Thus, mutations in the conserved residues in the peptide binding pocket of the Gcn5's bromodomain are likely to disrupt the peptide binding ability of the bromodomain. From this, I conclude that the peptide binding pocket of the bromodomain is not needed by the Ada3/Ada2/Gcn5 complex to acetylate a nucleosome substrate *in vitro*.

My study shows that deletion of the bromodomain severely affects the nucleosome acetylation of the Ada3/Ada2/Gcn5 complex. In contrast, a previous study shows that deletion of the bromodomain of Gcn5 decreases the nucleosome acetylation of isolated

SAGA complex but not the ADA complex (Sterner et al., 1999). The basic for why the deletion of the bromodomain does not affect the HAT activity of the ADA complex is not clear. However, the ADA complex is not identical to the Ada3/Ada2/Gcn5 complex because it contains some additional subunits such as the Ahc1 (Eberharter et al., 1999). It is quite possible that Ahc1 has some functional redundancy with the bromodomain of the Gcn5, although this protein does not contain a bromodomain.

The substrates used for the HAT assays in this study were core histones and the LON extracted from chicken erythrocyte cells, which might contain some pre-acetylated histone that could help the binding of the Ada3/Ada2/Gcn5 complex. This would suggest that the peptide binding ability of the Ada3/Ada2/Gcn5 complex might play a role in substrate recognition of the complex and contribute to overall acetylation. I showed that both chicken LON and HeLa cell LON were better HAT substrates than the recombinant nucleosomes, which lack pre-modifications. However, the mononucleosomes from HeLa cells created by the micrococcal nuclease digestion of the HeLa cell LON conferred a lower HAT activity by the SAGA complex, as low as that of recombinant nucleosomes (Figure **B-3**). These results suggest that at least for these nucleosome substrates used in my HAT assays, pre-existing histone modifications do not play a major role in nucleosomal HAT activity of the SAGA complex. The most likely explanation for better HAT activity on LON than mononucleosome is that a HAT complex can acetylate multiple nucleosomes in an array without having to dissociate and rebind to a different nucleosome. Furthermore, I have shown that similar effects on the HAT activity resulting from mutations in the Ada3/Ada2/Gcn5 complexes v28, v84, and v87 on the chicken LON were also observed when the recombinant core histone and nucleosome were used as the HAT substrates. These data suggest that nucleosome HAT activity of the Ada3/Ada2/Gcn5 complex is not influenced by pre-existing histone modifications in the chicken LON used in HAT assays. In addition, recombinant nucleosomes can at least function as well as the chicken LON.

The role of the bromodomain in the nucleosomal HAT activity of the Ada3/Ada2/Gcn5 complex is not involved to peptide binding. I find that any combination of mutations that eliminate the positive charge of amino acid positions 415, 419, or 422 in v87, v92, v93, v94, v96 and v97 severely affects the HAT activity of the Ada3/Ada2/Gcn5 complex to the same level as the loss of the bromodomain in v28. These results suggest a new function of the bromodomain which might involve interaction with nucleosomes. Kinetic studies by Berndsen, CE and Denu, JM from University of Wisconsin-Madison, using our recombinant nucleosomes as a substrate for the HAT assay with the Ada3/Ada2/Gcn5 complexes v37, v87, and v28, suggest that the bromodomain plays a role in substrate recognition as well as the efficiency of Gcn5 to acetylate histone H3 at all possible sites in nucleosomes (data not shown). To address the possibility of an interaction between the bromodomain of Gcn5 and nucleosomes, I have isolated the bromodomain that was fused to the GST tag and performed a pull down experiment with nucleosomes. I observed no interaction between the two entities (data not shown). This result suggests that the bromodomain itself is not sufficient for interaction with nucleosomes. How the bromodomain interacts with nucleosomes is not yet understood. It is possible that a negatively charged area on the nucleosome, which could be the DNA, may interact with the bromodomain in the Ada3/Ada2/Gcn5 complex.

Previous results from Adam Barrios have suggested that domains in Ada2 and Ada3 are required for the nucleosomal HAT function of the Ada3/Ada2/Gcn5 complex. It would be interesting to understand how they are required for the nucleosome HAT function of the complex. Adam Barrios has shown that in addition to the bromodomain, the ZZ domain of Ada2 is required for the proper HAT activity of the Ada3/Ada2/Gcn5 complex. As for Ada3, deletion from the N-terminus to codon 336 severely affects the nucleosomal HAT activity of the Ada3/Ada2/Gcn5 complex (Adam Barrios's unpublished data). Perhaps the complex missing the first 336 amino acids of the Ada3 is unable to interact with the nucleosome. In addition, the SANT domain has been reported to facilitate both core histones and nucleosomal HAT activities of the SAGA complex (Sterner et al., 2002b). The SANT domain probably interacts with histones or mediates

nucleosome recognition by the SAGA complex. It is possible that the N-terminal region of Ada3, the ZZ and SANT domains of Ada2, and the HAT domain and bromodomain of Gcn5 make simultaneous contacts with a nucleosome. The collaborative nucleosome binding and the spatial arrangement of the bromodomain in relation to the SANT, HAT and N-terminal region of Ada3 remain an interesting future study.

4.4.2 The role of the bromodomain of Gcn5 in the context of the SAGA complex

Here I show that the bromodomain of Gcn5 plays an important role in the global histone H3 acetylation. This function of the bromodomain is dependent on both the basic side surface residues (K415, R419, and K422) and the peptide binding pocket residues (Y364, N407, and Y413). While the basic residues, but not the peptide binding pocket residues of the bromodomain, are required for nucleosome HAT activity of the Ada3/Ada2/Gcn5 complex, all of the residues are important for global acetylation function of SAGA. Importantly, the conserved residues within the peptide binding pocket of the bromodomain appear to be more important for the global histone H3 acetylation than those basic residues of the bromodomain.

My preliminary data suggest an interesting relationship between the acetylated peptide binding ability and the global acetylation function of the SAGA complex. This direct relationship has not been suggested, although a previous study has shown a connection between the bromodomain of Gcn5 and nucleosome acetylation function of the SAGA complex (Sterner et al., 1999). It has been shown that the bromodomain of Gcn5 binds to an acetylated histone H4 K16 *in vitro* (Ornaghi et al., 1999; Owen et al., 2000). Hassan et al. showed that activator recruited SAGA complex can be anchored to an acetylated nucleosomal array via the bromodomain of Gcn5, but not that of Spt7, suggesting the role of the Gcn5 bromodomain at promoter regions (Hassan et al., 2002). Another study has shown that histone H3 acetylation is mostly concentrated at promoter of the SAGA

dependent genes such as *PHO5* gene (Vogelauer et al., 2000). Upon recruitment by an activator, the SAGA complex may utilize the Gcn5 bromodomain to bind acetylated histone H4 K16 then acetylate nucleosomes at H3 K9 and K14 residues. The basic residues of the bromodomain (K415, R419, and K422) may facilitate nucleosome acetylation by the SAGA complex but do not play a major role in the context of the SAGA complex. Additional research will be required to test whether the SAGA complex can better acetylate a nucleosomes array that has previously been modified by other HAT complexes such as the NuA4 or Piccolo complex. In addition, it would be interesting to test whether the histone H3 acetylation at promoter regions is reduced when the peptide binding pocket residues are mutated.

The bromodomain of Gcn5 has been shown to mediate transcriptional activation. For example, a deletion of the bromodomain of Gcn5 affects the kinetics of expression of the *PHO5* gene (Barbaric et al., 2003), and causes an intermediate effect on the transcription of the *HIS3* genes (Sterner et al., 1999). In addition, two previous studies show that the deletion of the bromodomain creates a reduced ability to complement a *gcn5*Δ under transcriptional activation by Gcn4 protein (Georgakopoulos et al., 1995; Marcus et al., 1994). Thus, a defect in the global histone H3 acetylation observed in the *bromo*Δ, and the YNY mutant yeast strains may reflect the inability of the SAGA complex to respond to a transcriptional activation. Additional research should also be performed to further examine how gene expression in yeast is affected in the Y364A, N407A, and Y413A substitution mutations.

The existence of another bromodomain in the Spt7 SAGA subunit raised the possibility that it has a redundant function in the global histone H3 acetylation with the bromodomain of Gcn5. However, deletion of the bromodomain of Spt7 did not cause transcription, cell growth defects, or Spt- phenotypes, while the deletion of Spt7 affected gene transcriptions and cell growth (Gansheroff et al., 1995). This study suggests that the bromodomain of Spt7 is not required for the function of the protein itself. Deletion of the bromodomain of Spt7 did not affect the ability of the SAGA complex to bind to a pre-

acetylated nucleosome array *in vitro* (Hassan et al., 2002). Moreover, the deletion of the bromodomain of Spt7 did not appear to play a role in the *in vitro* HAT function of the SAGA complex (Sterner et al., 1999). Together, these results suggest that the bromodomain of Spt7 is unlikely to play a redundant role with the bromodomain of Gcn5, or to participate in the global histone H3 acetylation.

4.5 Materials and methods

4.5.1 Plasmids, expression, and metal affinity purification of the Ada3/Ada2/Gcn5 complex

pST50Trc3-yGcn5x5, a transfer vector that contains yeast Gcn5, encoding for a wild type protein was used as a template for a PCR-mediated site-directed mutagenesis to mutate specific residues in the bromodomain. The x5 indicates the conservative mutation Val66 codon changed from GTG to GTT to eliminate the alternative start site at this position. A desired yeast Gcn5 mutant was subcloned into a polycistronic vector pST44 that contains a full length C-terminal His-tagged yeast Ada3 and yeast Ada2 in the first and second cassette, respectively (Tan et al., 2005). For the bromodomain deletion construct, yGcn5 was truncated after codon 328 by PCR mediated amplification and the gene was subcloned into another pST44 vector that had the C-terminal His-tagged yeast, Ada3Δ2 (187-702) and a full length yeast Ada2 at the first and second cassette, respectively (Tan et al., 2005). A list of oligo nucleotides used for site-directed mutagenesis of Gcn5 is provided in Table **4-1**. A pST44 plasmid that carries yAda3, yAda2, and yGcn5 mutant was transformed into *Escherichia coli* BL21(DE3)Codon+ cells and plated on a TYE plate (1.0% bacto tryptone, 0.5% yeast extract, 0.8% NaCl, and 1.5% agar) that contained 100 µg/ml Ampicillin and 25 µg/ml chloramphenicol. After overnight incubation at 37°C, a few colonies were selected to inoculate a 500 ml flask containing 100 ml 2xTY medium (1.6% bacto tryptone, 1.0% yeast extract, and 0.5% NaCl) with 100 µg/ml

Ampicillin and 25 µg/ml chloramphenicol added in a 37°C shaking incubator. Once the optical density (OD_{600}) of the cells reached between 0.1-0.2, the flask was transferred to an 18°C shaking incubator. Cells continued to grow and were induced by adding 100 µl 0.2 M IPTG when the OD_{600} became 0.4-0.6. After 12-16 hours of induction, cells from 50 ml cultures were collected in a 50 ml Falcon tube, resuspended with 10 ml P300 buffer (50 mM sodium phosphate pH 7.0, 100 mM NaCl, 1 mM benzamidine, and 5 mM 2-mercaptoethanol), and kept frozen at -20°C until ready for a metal affinity batch purification.

A metal affinity batch purification of the complex was performed with P300 buffer using the same procedures described in chapter 4. The E2 and E3 fractions were combined and used directly for the HAT assay.

4.5.2 HAT assay

Partially purified Ada3/Ada2/Gcn5 complexes were normalized against the wild type v37 on a coomassie stained SDS PAGE gel. Each HAT assay was performed in parallel with the sample from the wild type (v37) as a control. Talon E2 and E3 pooled fractions of each complex were further diluted 5 fold with P300 buffer and used for the HAT assay, which was performed as described previously (Eberharter et al., 1998). Briefly, 2 µl of diluted pooled fractions were mixed into a 30 µl reaction that contains 6 µl 5x HAT buffer (250 mM Tris-Cl pH 8.0, 25% glycerol, 0.5 mM EDTA, 250 mM KCl, and 62.5 µl/ml PSC-protector solution (Roche)), 1 mM DTT, 10 mM sodium butyrate, 1 mM Pefabloc SC (Roche), 1 µg chicken core histones, and 0.125 µCi tritiated acetyl-CoA. The HAT assay with chicken long-oligo nucleosomes (LON) reaction was prepared the same way but 1µg chicken core histones were substituted for 1 µg LON per reaction. The reaction mixture was incubated at 30°C for 30 minutes. After incubation, the reaction mix was placed on ice to stop the reaction. Then, 15 µl reaction samples were spotted onto P81 phosphocellulose filters (Whatman) cut in half and allowed to

completely air-dry. Dried filters were washed 4x 50 ml 1x wash buffer (50 mM $NaHCO_3$-$NaCO_3$, pH ~9.2), rinsed in 50 ml acetone, and dried. The filters were placed in scintillation vials which contain 4 ml scintillation fluid (ScintiSafe Econo F, FisherChemical). Each vial was counted in a scintillation counter for 1 minute.

HAT assay results were obtained by calculating the ratio between the CPM of LON and the core histone HAT activities. Results from the mutant complexes were calculated in relation to the wild type set (v37).

4.5.3 Plasmids and yeast strains

yGcn5x13 (K415A, R419A, and K422A substitution mutations), yGcn5x12 (Y364A, N407A, and Y413A substitution mutations), and yGcn5x24 (which has codon 326 changed to a stop codon) were created by a PCR-mediated site-directed mutagenesis method and subcloned into a pRS316 vector, which was a gift from the Pugh lab at Penn State. The plasmids, pRS316 (vector), pRS316-yGcn5 (R419G), pRS316-yGcn5x13 (KRK mutant), and pRS316-yGcn5x24 (bromodomain deletion) were transformed into *gcn5*Δ BY4742 yeast, and plated on CSM-URA plates. Yeast *gcn5*Δ BY4742 was also a gift from the Pugh lab. A colony from each strain was selected and further restreaked for a single colony isolation which was used to prepare a -80°C glycerol stock.

Cells from glycerol stocks were restreaked on URA- plates before culturing in URA- minimum media. Cells were grown at 30°C and approximately 10 ml culture was harvested when OD_{600} reached 0.8-1.0. A cell pellet was collected in a 1.7 ml eppendorf tube and frozen at -20°C.

Table **4-1**: Primers used for creating Gcn5 bromodomain point mutants

Name	Sequence	Purpose
STO1753	ATTGCCGAATGTATGCTGGCGAGAATACGTC	Forward PCR primer to create yGcn5 N407A bromodomain point mutation
STO1754	GACGTATTCTCGCCAGCATACATTCGGCAAT	Reverse PCR primer to create yGcn5 N407A bromodomain point mutation
STO1755	GCGAGAATACGTCGGCTTACAAGTATGCTA	Forward PCR primer to create yGcn5 Y413A bromodomain point mutation
STO1756	TAGCATACTTGTAAGCCGACGTATTCTCGC	Reverse PCR primer to create yGcn5 Y413A bromodomain point mutation
STO1757	AGGAGGTCCCCGACGCTTATGATTTTATCA	Forward PCR primer to create yGcn5 Y364A bromodomain point mutation
STO1758	TGATAAAATCATAAGCGTCGGGGACCTCCT	Reverse PCR primer to create yGcn5 Y364A bromodomain point mutation
STO1759	CCCGACTATTATGATGCTATCAAAGAGCCAAT	Forward PCR primer to create yGcn5 F367A bromodomain point mutation
STO1760	ATTGGCTCTTTGATAGCATCATAATAGTCGGG	Reverse PCR primer to create yGcn5 F367A bromodomain point mutation
STO1806	CGTCGTATTACGCTTATGCTAATGCTCTAGAGGCCTTCTTCAATA	Forward PCR primer to create yGcn5 K415A;R419A;K422A bromodomain point mutations
STO1807	TATTGAAGAAGGCCTCTAGAGCATTAGCATAAGCGTAATACGACG	Reverse PCR primer to create yGcn5 K415A;R419A;K422A bromodomain point mutations
STO1808	CTTGAGCACCATGGCTGCAAAATTAGCTAGCAACAAATATC	Forward PCR primer to create yGcn5 E378A;I379A'E382A bromodomain point mutations
STO1809	GATATTTGTTGCTAGCTAATTTTGCAGCCATGGTGCTCAAG	Reverse PCR primer to create yGcn5 E378A;I379A'E382A bromodomain point mutations
STO1810	GCACCATGGAAATAGCTTTAGAGAGCAACGCTTATCAGAAGATGG	Forward PCR primer to create yGcn5 K380A;K385A bromodomain point mutations
STO1811	CCATCTTCTGATAAGCGTTGCTCTCTAAAGCTATTTCCATGGTGC	Reverse PCR primer to create yGcn5 K380A;K385A bromodomain point mutations
STO1824	AATACGTCGTATTACGCATATGCTAATAGGCTAG	Forward PCR primer to create yGcn5 K415A bromodomain individual point mutation
STO1825	TAGCCTATTAGCATATGCGTAATACGACGTATTC	Reverse PCR primer to create yGcn5 K415A bromodomain individual point mutation
STO1826	TACAAGTATGCTAATGCTCTAGAGAAATTCTTC	Forward PCR primer to create yGcn5 R419Abromodomain individual point mutation
STO1827	GAAGAATTTCTCTAGAGCATTAGCATACTTGTA	Reverse PCR primer to create yGcn5 R419Abromodomain individual point mutation
STO1828	GCTAATAGGCTAGAGGCCTTCTTCAATAATAAA	Forward PCR primer to create yGcn5 K422A bromodomain individual point mutation
STO1829	TTTATTATTGAAGAAGGCCTCTAGCCTATTAGC	Reverse PCR primer to create yGcn5 K422A bromodomain individual point mutation

Name	Sequence	Purpose
STO1837	CGTCGTATTACCGGTATGCTAATAGGCTAGAGAGATTCTTCAATA	Forward PCR primer to create yGcn5 K415R;K422R bromodomain point mutations
STO1838	TATTGAAGAATCTCTCTAGCCTATTAGCATACCGGTAATACGACG	Reverse PCR primer to create yGcn5 K415R;K422R bromodomain point mutations
STO1839	CGTCGTATTACGACTATGCTAATGATCTAGAGGATTTCTTCAATA	Forward PCR primer to create yGcn5 K415D;R419D;K422D bromodomain point mutations
STO1840	TATTGAAGAAATCCTCTAGATCATTAGCATAGTCGTAATACGACG	Reverse PCR primer to create yGcn5 K415D;R419D;K422D bromodomain point mutations
STO1841	CGTCGTATTACGACTATGCTAATAGGC	Forward PCR primer to create yGcn5 K415D bromodomain point mutation
STO1842	GCCTATTAGCATAGTCGTAATACGACG	Reverse PCR primer to create yGcn5 K415D bromodomain point mutation
STO1843	CGTCGTATTACGACTATGCTAATGATCTAGAGGATTTCTTCAATAATAAA	Forward PCR primer to create yGcn5 K415D;R419D;K422D bromodomain point mutations, revised design
STO1844	TTTATTATTGAAGAAATCCTCTAGATCATTAGCATAGTCGTAATACGACG	Reverse PCR primer to create yGcn5 K415D;R419D;K422D bromodomain point mutations, revised design
STO1895	GATGCGTTGGCATAACGTCCCAAGC	Forward PCR mutagenesis primer to mutate codon 327 of yGcn5 to a stop codon
STO1896	GCTTGGGACGTTATGCCAACGCATC	Reverse PCR mutagenesis primer to mutate codon 327 of yGcn5 to a stop codon

The pellet was resuspended in 200 µl HG400 (40 mM HEPES pH 7.5, 400 mM NaCl, 10% glycerol, 0.1% Tween 20, 1 mM benzamidine, 2 µg/ml leupeptin, 2 µg/ml pepstatin, 1 mM PMSF, and 5 mM 2-mercaptoethanol) and vortexed with 200 µl glass beads, which were washed with the same buffer, 2x 30 seconds with a 1 minute break. The tube was vortexed again for 45 minutes at 4°C. Vortexed cells were extracted and directly mixed 1:1 with 2x protein gel loading buffer 2xPGLB (1.25 M Bis-Tris pH 6.8, 20% glycerol, 4% SDS, 2.16 M 2-mercaptoethanol, and 0.4 mg/ml bromophenol blue), boiled and electrophoresed with an 18% SDS PAGE gel for western blot analysis.

4.5.4 Western blots

Protein samples on an SDS PAGE gel were transferred to a nitrocellulose membrane (Hybond ECL, Amersham pharmacia biotech). The membrane was blocked by incubating with 50 ml 5% milk in 1xTBST (25 mM Tris-Cl pH 8.0, 150 mM NaCl, and 0.005% Tween 20) for 45 minutes. The membrane was subsequently washed 3x 5 minutes with 50 ml 1xTBST buffer before incubating with 5 ml anti-H3 antibodies (Abcam) at 1:2000 dilutions in 1xTBST for 1 hour at room temperature. The membrane was subsequently washed in the same way, with 1xTBST and incubated with 10 ml anti-rabbit Ig HRP linked (Amersham Biosciences) at 1:10,000 dilutions with 1xTBST for 1 hour at room temperature. The membrane was washed 3 more times with 1xTBST, chemiluminiscent substrate (SuperSignal West Pico, Pierce) added, and exposed to an X-ray film. The film was developed, and the western blot signal on the X-ray film was scanned with a Personal Densitometer SI, Molecular Dynamics and quantified with the ImageQuant program. A Western blot with anti-H3 K9&K14 Ac antibodies, which was a gift from the Pugh lab, was also performed the same way, except that the antibodies were used at 1:5000 dilutions.

4.6 Acknowledgements

I am grateful for the help and suggestions from the Pugh lab, especially from Melissa Durant. I would like to thank Joe Reese for critical and valuable advice on this project, and to all the members of the Reese Lab for so much help and friendship. I would also like to thank Adam Barrios, a former graduate student from the Tan Lab for discussion about the project, and to all the Tan Lab members for their help and encouragement.

4.7 Bibliography

Allard, S., Utley, R. T., Savard, J., Clarke, A., Grant, P., Brandl, C. J., Pillus, L., Workman, J. L., and Cote, J. (1999). NuA4, an essential transcription adaptor/histone H4 acetyltransferase complex containing Esa1p and the ATM-related cofactor Tra1p. Embo J *18*, 5108-5119.

Balasubramanian, R., Pray-Grant, M. G., Selleck, W., Grant, P. A., and Tan, S. (2002). Role of the Ada2 and Ada3 transcriptional coactivators in histone acetylation. J Biol Chem *277*, 7989-7995.

Barbaric, S., Reinke, H., and Horz, W. (2003). Multiple mechanistically distinct functions of SAGA at the PHO5 promoter. Mol Cell Biol *23*, 3468-3476.

Berndsen, C. E., and Denu, J. M. (2005). Assays for mechanistic investigations of protein/histone acetyltransferases. Methods *36*, 321-331.

Dhalluin, C., Carlson, J. E., Zeng, L., He, C., Aggarwal, A. K., and Zhou, M. M. (1999). Structure and ligand of a histone acetyltransferase bromodomain. Nature *399*, 491-496.

Eberharter, A., John, S., Grant, P. A., Utley, R. T., and Workman, J. L. (1998). Identification and analysis of yeast nucleosomal histone acetyltransferase complexes. Methods *15*, 315-321.

Eberharter, A., Sterner, D. E., Schieltz, D., Hassan, A., Yates, J. R., 3rd, Berger, S. L., and Workman, J. L. (1999). The ADA complex is a distinct histone acetyltransferase complex in Saccharomyces cerevisiae. Mol Cell Biol *19*, 6621-6631.

Gansheroff, L. J., Dollard, C., Tan, P., and Winston, F. (1995). The Saccharomyces cerevisiae SPT7 gene encodes a very acidic protein important for transcription in vivo. Genetics *139*, 523-536.

Georgakopoulos, T., Gounalaki, N., and Thireos, G. (1995). Genetic evidence for the interaction of the yeast transcriptional co-activator proteins GCN5 and ADA2. Mol Gen Genet *246*, 723-728.

Hassan, A. H., Prochasson, P., Neely, K. E., Galasinski, S. C., Chandy, M., Carrozza, M. J., and Workman, J. L. (2002). Function and selectivity of bromodomains in anchoring chromatin-modifying complexes to promoter nucleosomes. Cell *111*, 369-379.

Horiuchi, J., Silverman, N., Marcus, G. A., and Guarente, L. (1995). ADA3, a putative transcriptional adaptor, consists of two separable domains and interacts with ADA2 and GCN5 in a trimeric complex. Mol Cell Biol *15*, 1203-1209.

Howe, L., Auston, D., Grant, P., John, S., Cook, R. G., Workman, J. L., and Pillus, L. (2001). Histone H3 specific acetyltransferases are essential for cell cycle progression. Genes Dev *15*, 3144-3154.

Hudson, B. P., Martinez-Yamout, M. A., Dyson, H. J., and Wright, P. E. (2000). Solution structure and acetyl-lysine binding activity of the GCN5 bromodomain. J Mol Biol *304*, 355-370.

Kleff, S., Andrulis, E. D., Anderson, C. W., and Sternglanz, R. (1995). Identification of a gene encoding a yeast histone H4 acetyltransferase. J Biol Chem *270*, 24674-24677.

Kristjuhan, A., Walker, J., Suka, N., Grunstein, M., Roberts, D., Cairns, B. R., and Svejstrup, J. Q. (2002). Transcriptional inhibition of genes with severe histone h3 hypoacetylation in the coding region. Mol Cell *10*, 925-933.

Ornaghi, P., Ballario, P., Lena, A. M., Gonzalez, A., and Filetici, P. (1999). The bromodomain of Gcn5p interacts in vitro with specific residues in the N terminus of histone H4. J Mol Biol *287*, 1-7.

Owen, D. J., Ornaghi, P., Yang, J. C., Lowe, N., Evans, P. R., Ballario, P., Neuhaus, D., Filetici, P., and Travers, A. A. (2000). The structural basis for the recognition of acetylated histone H4 by the bromodomain of histone acetyltransferase gcn5p. Embo J *19*, 6141-6149.

Rojas, J. R., Trievel, R. C., Zhou, J., Mo, Y., Li, X., Berger, S. L., Allis, C. D., and Marmorstein, R. (1999). Structure of Tetrahymena GCN5 bound to coenzyme A and a histone H3 peptide. Nature *401*, 93-98.

Sterner, D. E., Grant, P. A., Roberts, S. M., Duggan, L. J., Belotserkovskaya, R., Pacella, L. A., Winston, F., Workman, J. L., and Berger, S. L. (1999). Functional organization of the yeast SAGA complex: distinct components involved in structural integrity, nucleosome acetylation, and TATA-binding protein interaction. Mol Cell Biol *19*, 86-98.

Sterner, D. E., Wang, X., Bloom, M. H., Simon, G. M., and Berger, S. L. (2002). The SANT domain of Ada2 is required for normal acetylation of histones by the yeast SAGA complex. J Biol Chem *277*, 8178-8186.

Tan, S., Kern, R. C., and Selleck, W. (2005). The pST44 polycistronic expression system for producing protein complexes in Escherichia coli. Protein Expr Purif *40*, 385-395.

Trievel, R. C., Rojas, J. R., Sterner, D. E., Venkataramani, R. N., Wang, L., Zhou, J., Allis, C. D., Berger, S. L., and Marmorstein, R. (1999). Crystal structure and mechanism of histone acetylation of the yeast GCN5 transcriptional coactivator. Proc Natl Acad Sci U S A *96*, 8931-8936.

Vogelauer, M., Wu, J., Suka, N., and Grunstein, M. (2000). Global histone acetylation and deacetylation in yeast. Nature *408*, 495-498.

Yang, X. J. (2004). Lysine acetylation and the bromodomain: a new partnership for signaling. Bioessays *26*, 1076-1087.

Zhang, W., Bone, J. R., Edmondson, D. G., Turner, B. M., and Roth, S. Y. (1998). Essential and redundant functions of histone acetylation revealed by mutation of target lysines and loss of the Gcn5p acetyltransferase. Embo J *17*, 3155-3167.

Chapter 5

Summary and future directions

5.1 Summary

The coactivator model for transcriptional activation has been proposed for over a decade ago (Dynlacht et al., 1991; Pugh and Tjian, 1990; Tanese et al., 1991). Coactivators usually exist as a multiprotein complex that is recruited by a specific activator to assist transcriptional activation. Coactivators can be classified into several classes based on their function. The work described in this thesis mainly describes the functions of the SAGA coactivator complex that 1) recruits TBP to a promoter and 2) acetylates nucleosomes to activate gene transcription.

My work in chapter 2 describes different methods for purification of the SAGA complex, the problems of using the CBP tag for pull down experiments, and how I determine the components of SAGA that interact with TBP. By utilizing a photo-cross-linking assay and pull down technique, I find Spt8 and possibly Ada1 as the SAGA subunits that interact with TBP. The interaction between Spt8 and TBP has been previously illustrated (Warfield et al., 2004). Spt3, which has strong genetic interaction with TBP (Eisenmann et al., 1992), is not sufficient for interaction with TBP. Spt3 does not appear to cross-link with TBP, suggesting that Spt3 in the SAGA complex may not directly interact with TBP. However, Spt3 somehow interacts with TBP since the deletion of this protein affects the SAGA-TBP interaction.

Interestingly, Ada1 in SAGA can also cross-link to TBP independent of the presence of Spt8 in the complex, suggesting that Ada1 in the SAGA complex also makes a contact

with TBP. The role of Ada1 in interacting with TBP has not been suggested in literature. One of the reasons is that deletion of Ada1 disintegrates the SAGA complex (Sterner et al., 1999; Wu and Winston, 2002); thus, the effects on TBP recruitment or phenotypes observed in the *ada1*Δ yeast strain are consequences of the loss of the SAGA complex. In addition, recombinant Ada1 expressed in *E. coli* by itself is highly insoluble. While my data indicate a possible interaction between Ada1 and TBP, future experiments will be required to determine this interaction.

I further analyzed the TBP-Spt8 and TBP-SAGA interactions as I describes in Chapter 3. My pull down experiment with the R171E TBP mutant led us to a better understanding of how the SAGA complex regulates TBP recruitment *in vivo*. Known as a mutation that stabilizes the TBP dimer, the R171E TBP mutant is defective in the interaction with Spt8 or the SAGA complex. Thus, perhaps Spt8 or the SAGA complex binds to TBP and competes with TBP dimerization. My results from the competition experiment support this hypothesis. I have also investigated the binding of TATA box DNA to TBP-Spt8 or TBP-SAGA complexes. I also find that the TATA box DNA had to compete with Spt8 or the SAGA complex in order to bind to TBP. Based on these results, I propose a hand off model as a mechanism of gene activation by the SAGA complex.

The simple hand off model can explain many behaviors of the SAGA complex observed *in vivo*. The SAGA complex represses transcription in a non-inducing condition but activates transcription when cells are induced. In this hand off model, Spt8 and possibly Ada1 subunits of the SAGA complex associate with a TBP monomer, possibly by binding to the underside surface of the saddle-like structure to prevent TBP from binding to a promoter. This is why the SAGA complex in the absence of Spt8 derepresses its target genes such as HIS3, TRP3 and ARG1 (Belotserkovskaya et al., 2000; Ricci et al., 2002). However, the situation is reversed in an inducing condition because the SAGA complex is required for TBP recruitment to the core promoter. But because the SAGA complex also prevents the TBP from binding to the TATA box DNA (Belotserkovskaya et al., 2000), the only way that the TATA element can bind to TBP is by a competing

with the SAGA complex, breaking the TBP-SAGA contact. Thus, the SAGA complex does not physically bridge an activator and TBP that binds to the core promoter. This model explains why the SAGA complex is never observed at the core promoter but is always associated at the upstream activating sequence (UAS) (Bhaumik and Green, 2001; Larschan and Winston, 2001; van Oevelen et al., 2005).

Because Spt8 in the SAGA complex provides an interaction with TBP and inhibits TBP binding to DNA, I investigated the structural properties of Spt8. Sequence alignment and a secondary structure prediction suggest that Spt8 contains a putative WD40 domain, which is found in many eukaryotic cells and serves as an interaction module with other proteins (Lodowski et al., 2003; Sprague et al., 2000). My results in chapter 3 suggest that the putative WD40 domain of Spt8 is sufficient for the interaction with TBP. Chapter 3 also describes strategies for purifying the putative domain of Spt8. Although the WD40 domain is highly expressed in bacteria, it is insoluble. However, I am able to overcome this obstacle by purifying this domain in the presence of a 3 M urea.

In addition to the ability to interact and recruit TBP to promoters, the SAGA complex is capable of acetylating histone H3 in nucleosomes. An acetylated histone tail can be recognized by a bromodomain which is found in many transcription factors including Gcn5. Work in Chapter 4 describes the analysis of the role of the bromodomain in nucleosomal HAT activity of the Ada3/Ada2/Gcn5 and the SAGA complexes. I show that deletion of the bromodomain causes a significant decrease in the nucleosomal HAT activity of the Ada3/Ada2/Gcn5 complex. Furthermore, the bromodomain plays an essential role in the global histone H3 acetylation *in vivo*. I define the three basic residues: K415, R419, and K422, but not the residues in the peptide binding pocket, necessary for the nucleosomal HAT function of the Ada3/Ada2/Gcn5 trimeric complex. This also suggests the role of these three basic residues in the global histone H3 acetylation. However, I am unable to address the role of those three residues in the global histone H3 acetylation since the original Gcn5 plasmid contains the R419G point

mutation. Therefore, the experiment will need to be repeated together with the correct wild type Gcn5 plasmid.

Overall, the work in this thesis advances our understanding of how the SAGA coactivator complex functions in a living cell. In brief, the SAGA complex is recruited to a UAS element by a specific DNA bound activator. With help from the bromodomain, Gcn5 subunit in the SAGA complex can acetylate nucleosomes to activate gene transcription. The SAGA complex can also recruit TBP to a promoter in which TBP binding to a promoter occurs through a competition with the TATA box DNA. Future experiments are still required to explore some unanswered questions, such as how precisely Spt8 binds to TBP, or how Spt3 in SAGA contributes to the overall TBP-SAGA interaction.

5.2 Future directions and experiments

5.2.1 Analysis of the role of TFIIA in TATA box-SAGA competitive binding with TBP

Transcription factor IIA (TFIIA) is a general transcription factor specific for the RNA polymerase II (Kang et al., 1995). TFIIA consists of two subunits, Toa1a and Toa2, which bind to the TBP/DNA complex (Tan et al., 1996). An *in vitro* experiment has suggested that the TFIIA complex induces TBP dimer dissociation, stabilizes the binding of TBP or TFIID to the TATA box, and enhances transcription by transcriptional activators (Coleman et al., 1999; Weideman et al., 1997; Yokomori et al., 1994). In addition, TFIIA has the ability to overcome the repressive effect of the negative cofactor 2 (NC2) *in vitro* (Xie et al., 2000). Those studies together suggest the positive role of TFIIA in gene transcription.

An *in vitro* cross-linking study shows that the N-terminal domain (NTD) of TFIIA is in a close proximity to Spt8 and Taf4, and yet, TFIIA does not make physical contact with Spt8 (Warfield et al., 2004). Moreover, the same study also shows that Spt8 binds to TBP in competition with the TFIIA. Nonetheless, both Spt8 and TFIIA play a positive role in gene regulation (Bhaumik and Green, 2002; Qiu et al., 2005). With respect to my discovery, it would be interesting to test if TFIIA is involved in the SAGA-TBP-TATA box relationship. I have to objectives: 1) to determine whether or not TFIIA physically interacts with the TBP/SAGA complex and 2) to investigate if TFIIA affects the TBP-SAGA interaction.

5.2.1.1 Determining if TFIIA interacts with TBP/SAGA complex

Although it has been shown that TFIIA competes with Spt8 to bind to TBP (Warfield et al., 2004), it is unknown whether TFIIA associates with the TBP/SAGA complex that contains Spt8. To test whether TFIIA associates with the TBP/SAGA complex, I could perform a simple pull down experiment. I have STR-tagged TBP which can pull down the SAGA complex. I could incubate TFIIA with the TBP/SAGA complex and perform a Western blot analysis to detect the presence of TFIIA in the beads and supernatant. Since TFIIA could also bind to TBP by itself, I could determine whether the binding of TFIIA is enriched in the beads that have SAGA complex bound to TBP. I could attach a small affinity tag to the N-terminus of the Toa2 subunit for Western blot analysis since this terminal is pointing away from the TFIIA/TBP/DNA structure (Tan et al., 1996).

5.2.1.2 Testing the effect of TFIIA in TBP-SAGA interaction

Regardless of the outcome of the pull down experiment, I can investigate the role of TFIIA in the SAGA-DNA competition to the binding with TBP. Because there exists evidence that TFIIA stabilizes the binding of TBP to the TATA box DNA (Weideman et

al., 1997), I propose that the presence of TFIIA might increase the rate of TBP-SAGA dissociation and stabilize the binding of TBP to the TATA box. To test this hypothesis, I could perform a competition assay similar to that described in Chapter 3. As illustrated in Figure **5-1**, SAGA is indirectly bound to the Protein A Sepharose through the antibodies that recognize the CBP tag. I would try to avoid using the Calmodulin Affinity Matrix because I observed non-specific binding of this resin with the TBP (data not shown). The tagged TBP, such as STRNyTBPcore, would be added to the system to create a TBP/SAGA complex. Then, I would manipulate the system by adding increasing amounts of TATA box DNA or TFIIA and observing the changing amount of TBP binding to TATA box DNA in the supernatant.

Figure **5-2** shows possible outcomes of a Western blot analysis to detect TBP in the supernatant. (a) and (b) are the expected results from the experiments with either TATA box DNA or non-TATA box DNA, respectively. If TFIIA helps TBP to dissociate from the SAGA complex, then I would predict the result shown in (c). If TFIIA has no effect on the competition, then the amount of TBP in the supernatant shown in (d) will be comparable to (a). If TFIIA binds and stabilizes the TBP/SAGA complex, then less TBP will be observed in the supernatant (e). For (f), a fixed amount of TATA box DNA would be added to compete for TBP binding for a short period of time; thus, the amount of TBP detected in supernatant should be constant in all lanes. If TFIIA does not induce TBP dissociation from SAGA, then the amount of TBP in the supernatant represented in (g) would be comparable to (f). However, if TFIIA induces TBP dissociation, one would expect to see the results shown in (h). For a negative control, the TBP mutant that does not interact with TFIIA should yield the result shown in (i).

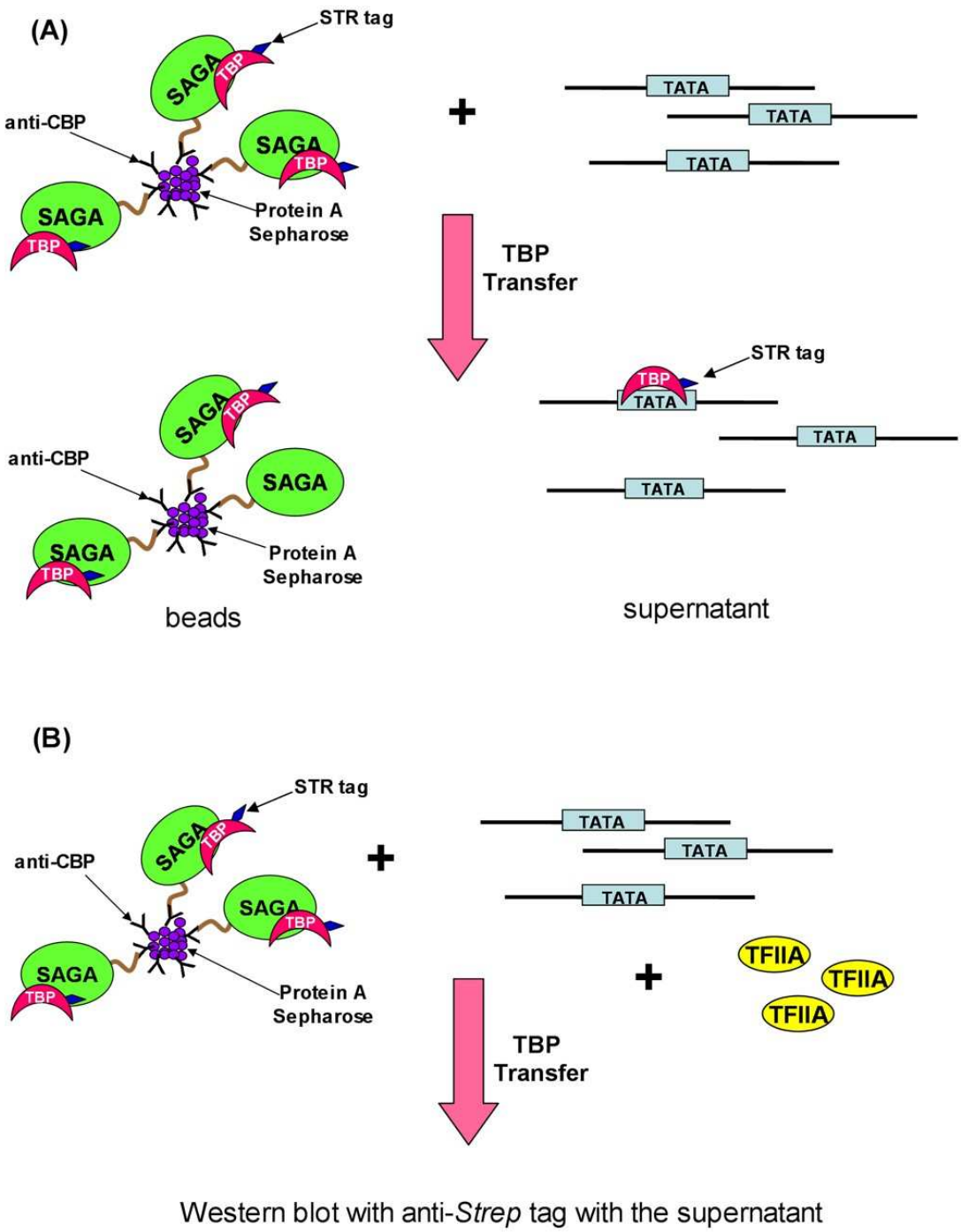

Figure **5-1**: Testing the effect of TFIIA in TBP-SAGA interaction.

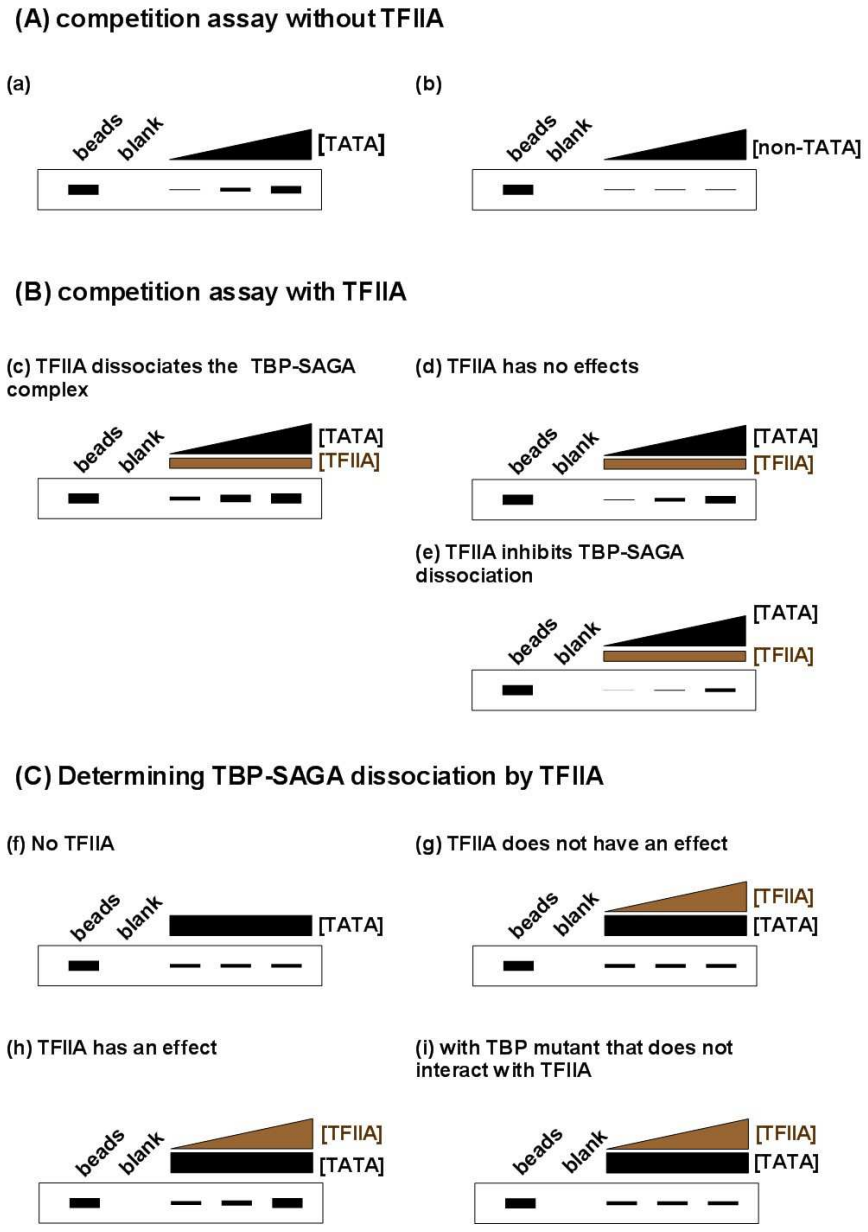

Figure **5-2**: Possible outcomes of the competition experiment with TFIIA.

(A) Competition experiment without TFIIA. (B) Competition experiment with the presence of TFIIA. The supernatant that contains TBP could be analyzed by Western blot with the anti-*Strep* tag monoclonal antibody. The bands in the boxes are the Western blot results using the anit-*Strep* monoclonal antibody to detect the STR-tagged TBP in the supernatant after the competition experiment. (C) Similar experiments as in (B) except that the concentration of TFIIA is increased.

TBP that binds to DNA in the supernatant could be analyzed by a Western blot method using the appropriate antibody. Alternatively, I could utilize a gel-shift assay to detect the TFIIA/TBP/DNA complex since TFIIA preferentially binds to the TBP/DNA complex rather than TBP itself (Tan et al., 1996). However, the latter method might require a radiolabeling of the DNA, which could be done by using the T4 DNA kinase.

5.2.2 Developing the *in vitro* hand off assay

The hand off model I propose is based on the competition assays between the TATA box DNA and the SAGA complex. However, the mechanism by which SAGA hands off TBP to a promoter requires that the SAGA complex indirectly binds to the UAS via an activator protein. Thus, I would like to imitate the actual hand off action happening *in vivo* by performing an *in vitro* hand off assay. The idea of the assay is simple: the assay will test whether or not the TBP that binds to the SAGA complex can be transferred to the TATA box core promoter by the SAGA complex which associates with an activator bound UAS element (Figure **5-3** A).

5.2.2.1 Testing the *in vitro* hand off model

It is imperative to check and make sure that the assay could be working properly as expected before applying the experiment to other analyses. The assay requires an activator protein, SAGA complex, N-terminal 3x Flag-tagged TBP, and the DNA from the actual promoter element of a selected system.

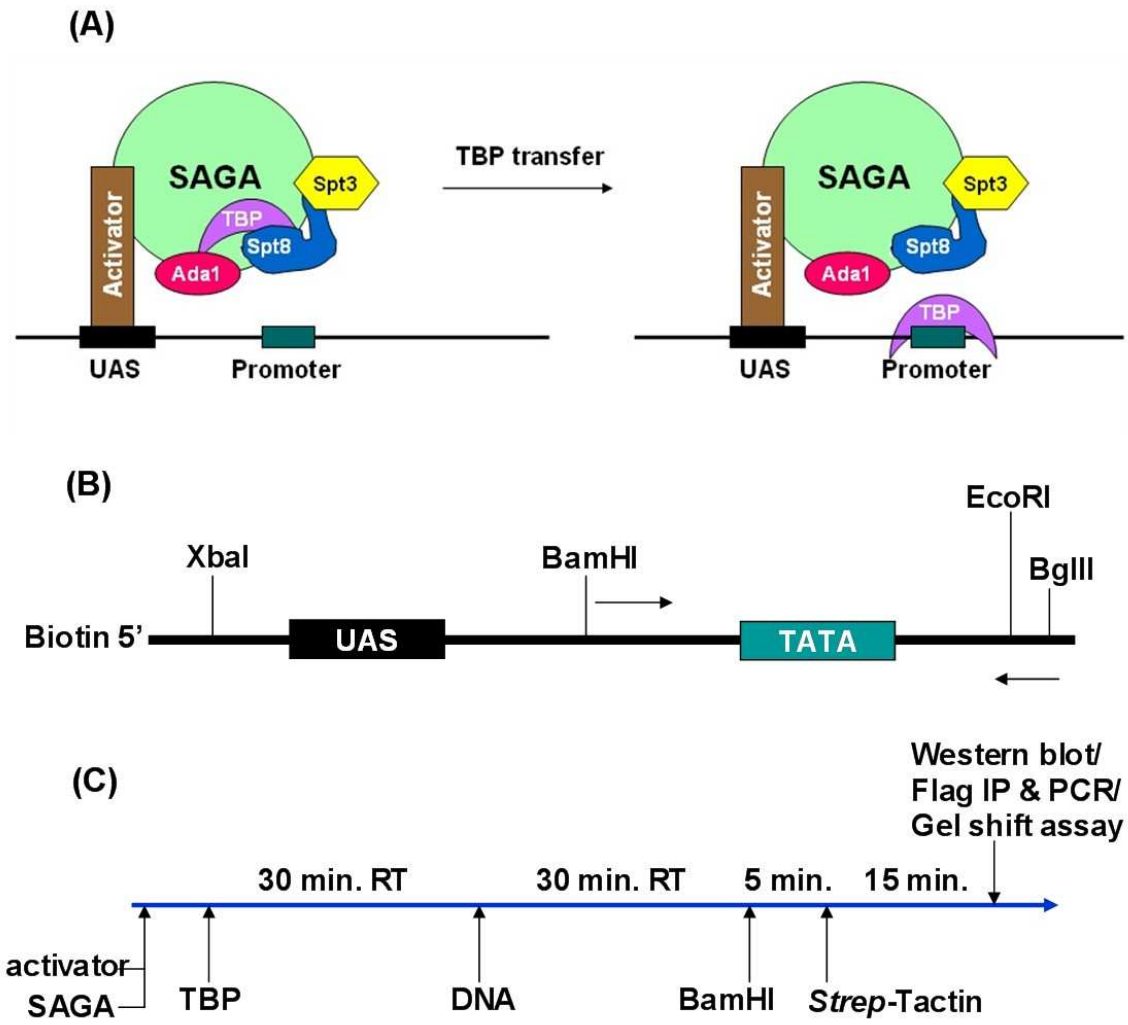

Figure **5-3**: Developing the *in vitro* hand off assay.

(A) The hand off model for TBP recruitment by the SAGA complex. (B) The schematic representation of the DNA constructs used for the *in vitro* hand off assay. XbaI-BglII sites allow cloning of the sequence in a plasmid. BamHI allows the separation between the UAS and the TATA box. In addition, it can be used to insert a DNA sequence to lengthen the distance between the two elements. EcoRI can be used for radiolabeling the DNA. The two arrows represent primers used for PCR amplification. (C) The proposed procedures for the *in vitro* hand off assay.

The key question is which promoter of choice could be used for the experiment. Two of the SAGA dependent promoters Gcn4-ARG1 and Gal4-GAL1 have been very well characterized. Gcn4 controls the expression of ARG genes including ARG1 (Ricci et al.,

2002). It has been shown that both Spt3 and Spt8 are involved in the TBP recruitment of this promoter (Qiu et al., 2004; Qiu et al., 2005; Ricci et al., 2002). Similarly, the Gal4 activator recruits the SAGA complex to the GAL1 promoter. However, deletion of Spt8 does not have an effect on TBP recruitment to the GAL1 promoter (Bhaumik and Green, 2002). Although it may seem that the ARG1 promoter may have an advantage because it is dependent on both Spt8 and Spt3 in the SAGA complex, the experiment in the *in vitro* context should not matter. An initial experiment could be performed with the ARG1 promoter. The promoter would be modified to create some additional restriction sites as illustrated in Figure **5-3** B. If the system works as expected, I could use the Gal4-GAL1 promoter to compare with the Gcn4-ARG1 system.

The activator (Gcn4) should be added before the SAGA complex, TBP, and DNA, respectively. In addition, the concentration of the activator should not be limited, to ensure the binding of the SAGA complex to the activator. The concentration of the SAGA complex should be at least two times higher than the concentration of TBP to ensure that SAGA binds to the activator. The concentration of the DNA should be similar to that of TBP; too high a concentration of DNA will force TBP to form a complex with DNA. Lastly, DNA would be added in the last step to ensure that TBP forms a complex with SAGA before being transferred to the DNA.

The *in vitro* hand off experiment would be done as shown in Figure **5-3** C. Each component would be added in order. After incubation, BamHI would be added to separate the TATA element from the UAS while the *Strep*-Tactin resin would be added to capture biotinylated DNA that contains the UAS element. If TBP is handed off by the SAGA complex and the TBP/TATA complex did not associate with SAGA, then I should be able to detect the presence of TBP by Western blot analysis with the anti-Flag monoclonal antibody.

The prediction for the hand off assay is summarized in Figure **5-4**. (a)-(f) serve as the control while (g) is the actual experimental set. All the experimental sets contain the

DNA template. In the presence of TBP without SAGA complex as in (d) and (f), I expect to observe the maximum binding of TBP to the TATA box. Thus, these two sets should yield the strongest signal on the Western blot. However, in the presence of the SAGA complex without the activator (e), very little or no TBP should bind to the DNA since I have a higher concentration of SAGA than DNA. As for the experimental set (g), I should observe a level of TBP binding greater than that of (e), but lower than that of (d) and (f). The reason is simple: after TBP is handed off to the TATA box by the SAGA complex, it is possible that SAGA competitively takes the TBP back from the TATA box. Thus, TBP might be in the binding equilibrium with both the SAGA complex and the TATA box element. Although this is a premature thought, I hypothesize that in cells, once TBP is handed off by the SAGA complex, a positive factor (See **1.2.4.3**) such as TFIIA would stabilize the TBP binding to the TATA box, thereby preventing the SAGA complex from taking TBP back from the core promoter.

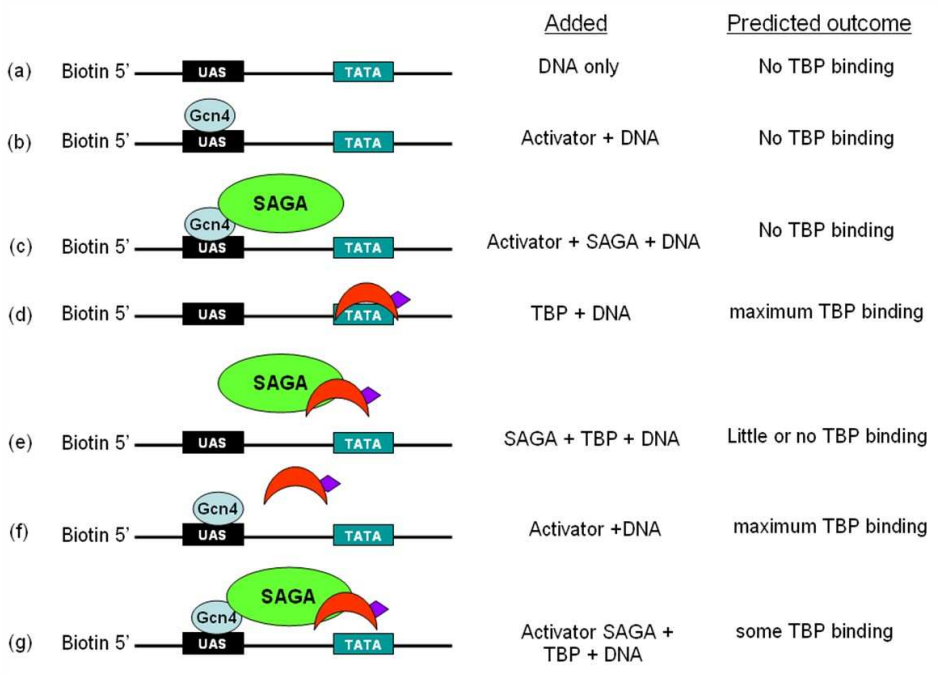

Figure **5-4**: Predictions of the in vitro hand off assay.

The key for the prediction is that TBP binds to the TATA box in the absence of SAGA complex. SAGA complex prevents the TBP binding to the TATA box unless linked to the UAS by an activator protein

One problem that could arise from the experiment is the detection limit of TBP. In my experience, a 9-liter yeast culture yields approximately 300 µl of about 100 nM or about 54 µg of a highly purified SAGA complex. Since it is important to have a higher concentration of SAGA complex than TBP, the final concentration of the complex and TBP in the reaction would be in a nanomolar range. To detect TBP, I would utilize a Western blot analysis with the anti-Flag monoclonal antibody with a very sensitive chemiluminescent substrate such as SuperSignal Femto Maximum Sensitivity from Pierce as the first method of choice to detect TBP. The three tandem copies of the Flag tag on TBP will help by increasing the detection limit. It would be important to determine the detection limit of the Western blot system with the 3x Flag tagged TBP before starting the actual experiment. Besides the Western blot technique, I also propose two additional methods: PCR with the Flag IP and gel shift assay with radiolabeled DNA (see description for Figure **5-3** C). The anti-Flag monoclonal antibody could be used to immunoprecipitate the Flag-tagged TBP. If the TATA element is bound by the TBP, those PCR primers could be used to amplify the DNA fragment, as an indication of TBP handed off. In addition, the DNA template could be radiolabeled at the EcoRI site for the gel shift assay, in which the TATA fragment as a result of BamHI digestion will have a slower mobility if it is bound by TBP.

The ability of SAGA to nonspecifically interact with DNA has been reported (Lee et al., 2005a). In this case, the TATA box DNA fragment from the BamHI digestion could possibly bind nonspecifically to the SAGA complex. Another possibility is that TBP interacts with both Spt8 and DNA to form a trimeric SAGA/TBP/DNA complex, which would be inconsistent with my predicted hand off model. To differentiate the two possibilities, I could include non-TATA box DNA in the reaction. If the BamHI fragment only interacts nonspecifically with the SAGA, then the presence of the DNA competitor will elute the TBP/TATA box complex. However, if TBP interacts with both SAGA and TATA box DNA, the BamHI digested fragment will associate with the beads but not in the supernatant.

5.2.2.2 Additional experiments based on the *in vitro* hand off assay

I am aware of the possibility of the failure of the assay, which would require troubleshooting steps. However, if I am able to show that the assay worked as expected, I can use it for more experiments to test: 1) the role of TFIIA in TBP handed off by SAGA complex; 2) the role of Spt3 in the TBP recruitment; 3) the role of the TATA element on TBP recruiting and binding to the core promoter; and 4) the effect of increasing the distance between the UAS and the core promoter on TBP binding to the core promoter.

The TFIIA experiment would be similar to what is described in **5.2.1.** I would compare the effect of having or not having TFIIA in the hand off reaction. If the presence of TFIIA enhances the TBP hand off and stabilizes the TBP/DNA complex, then the level of TBP detected in the set with TFIIA would be higher than another set which does not have TFIIA.

I have hypothesized that Spt3 might play a role in discarding TBP from the SAGA complex. If this is true, then the SAGA complex without Spt3 should have a slower kinetic on the TBP delivery than the wild type SAGA complex. This would explain why the deletion of Spt3 universally affects TBP recruitment to all SAGA dependent promoters tested (Bhaumik and Green, 2002). If my hypothesis is incorrect, then the SAGA complex should still be able to deliver TBP to the promoter. In addition to using the *spt3*Δ SAGA complex, I could create a SAGA complex that contains the *spt3*-401 (E240K) mutant to test in the hand off assay, since this mutant is a strong suppressor of *spt15*-21 (G174E) (Eisenmann et al., 1992). I would be interested to evaluate the effect of this Spt3 mutation on the TBP hand off mechanism. If there is an effect, I could use the same SAGA with *spt3*-401 mutation with the *spt15*-21 TBP mutant in the assay. My prediction is that the *spt15*-21 would reverse or suppress the effect of the *spt3*-401 mutation.

In addition to determining the role of Spt3 in the SAGA complex, I could mutate the TATA element from the promoter and test whether TBP would bind to the promoter, or still remain bound to the SAGA complex at the UAS. Deletion of the TATA element causes a significant reduction of TBP binding to the core promoter and severely impairs the pre-initiation complex (PIC) formation at the ARG1 ARG4 and SNZ1 promoters (Qiu et al., 2004). In this case, I hypothesize that the TBP would still recruited to the SAGA complex and should be localized to the UAS.

Lastly, I would test whether or not the distance between the UAS and the core promoter element would have an effect on TBP binding to the promoters. The distance between the two promoter elements is approximately 200 basepairs for several SAGA dependent promoters such as ARG1 and GAL1 (Larschan and Winston, 2001; Qiu et al., 2004). If the distance between the two elements does not affect TBP binding, then increasing the length between the two elements will not affect the TBP transfer. On the other hand, if the distance is important, lesser amount of TBP transfer will be observed as the distance between the two elements increases.

5.2.3 Characterization of Spt8-TBP interaction

The interaction between TBP and Spt8 is very interesting since I have shown that Spt8 contains a putative WD40 repeat domain, which is sufficient for interaction with TBP. Objectives of this study are: 1) determining the structural features of Spt8, especially within the WD40 repeat domain that interacts with TBP, 2) determining the structural features of TBP that make contact with Spt8, and 3) determining *in vivo* effects of Spt8 mutants that fail to interact with TBP.

5.2.3.1 Determining the structural features of Spt8 that interact with TBP

I would like to determine the structural features of Spt8 that interact with TBP. There are several possible ways to tackle this problem. The first method is to perform an *in vitro* photo-cross-linking between a purified recombinant Spt8 and TBP. TBP could be conjugated with a chemical cross-linker such as Sulfo-SBED which would transfer biotin label to a cross-linked protein (See chapter 2 for photo-cross-linking). The Spt8 interface, which is located in close proximity to TBP, can be identified by Mass Spec analysis (Alley et al., 2000; Ishmael et al., 2001). In addition to the first method, TBP could be conjugated with another reagent: Fe(III) (*S*)-1-(*p*-Bromoacetamido-benzyl)ethylene diamine tetraacetic acid, which is referred to as FeBABE (Datwyler and Meares, 2000; Traviglia et al., 1999a; Traviglia et al., 1999b). In the presence of ascorbic acid and hydrogen peroxide, Fe(III) is activated and will nonspecifically cleave peptide bonds of a protein target (i.e. Spt8) that locates within 12 Å from the conjugated protein. The resulting Spt8 fragment could be analyzed by Western blot analysis, protein sequencing or Mass Spec analysis. To determine the specific site of cleavage, I could create Spt8 markers by cleaving a recombinant purified Spt8 with different chemicals such as Cyanogen Bromide (CNBr) that cleaves at methionine residues, or 2-(2'-nitrophenylsulfenyl)-3-methyl-3'-bromoindolenine, which is also known as BNPS-skatole, to cleave the protein at tryptophan residues (Ishmael et al., 2001; Swamy et al., 2000) (Figure **5-5**). An alternative method of creating the markers would be to design different PCR primers to amplify different fragments of Spt8 and express them in bacteria (Figure **5-5**). The anti-Spt8 antibodies recognize at the N-terminal part of Spt8 and could be used directly for Western blot analysis of the Spt8 cleavage. Additionally, I could attach a C-terminal His tag to Spt8 to use for the Western blot. Using FeBABE reagent, I could conduct the cleavage experiment with both recombinant Spt8 and the purified SAGA complex to compare the cleavage pattern between the two (Figure **5-5**). I reason that TBP could possibly interact with some regions of Spt8 which are hidden or protected within the SAGA complex.

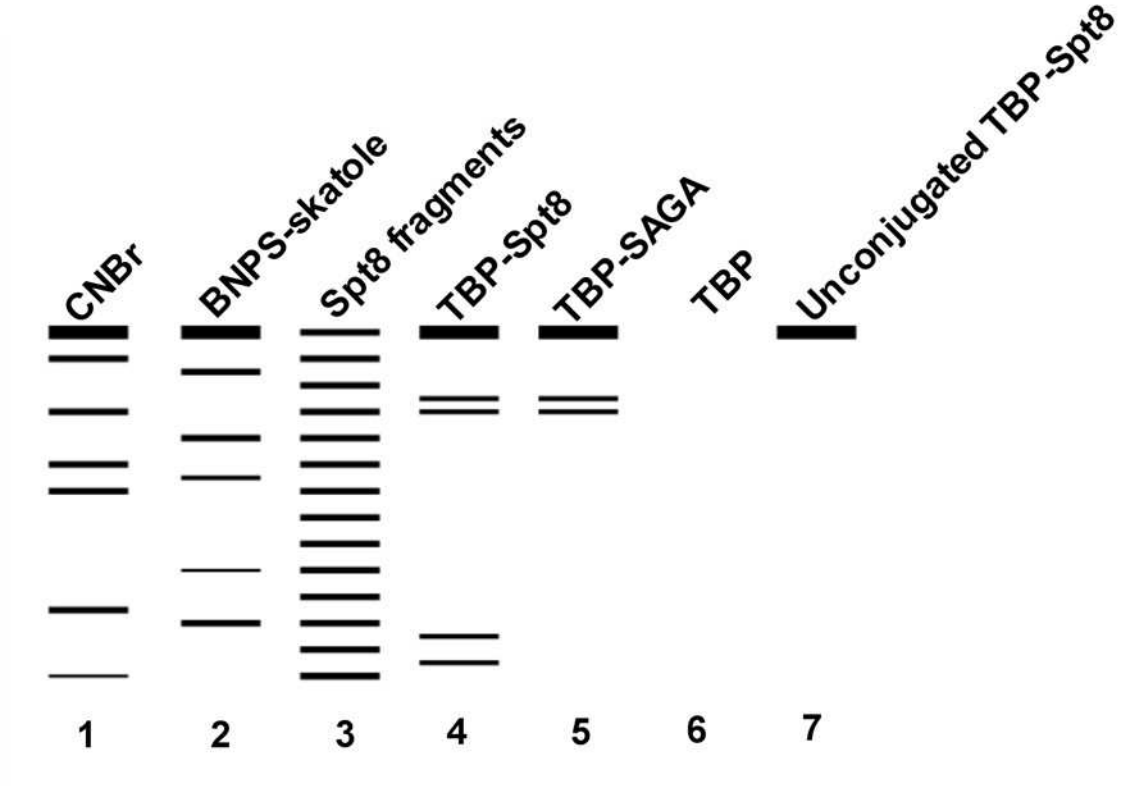

Figure **5-5**: A simplified diagram to illustrate the use of the FeBABE to map the region of interaction.

A picture shows a prediction of Western blot analysis with anti-Spt8 antibodies or with anti-His tag antibodies which recognizes the C-terminal His tag of Spt8 (if applicable). Lanes 1 and 2 are the markers from the Spt8 protein itself created by chemical cleavages using CNBr or BNPS-Skatole, which cleaves at methionine and tryptophan residues, respectively. The protocols for using CNBr and BNPS-Skatole to cleave proteins have been described (Ishmael et al., 2001; Swamy et al., 2000) Lane 3 is a serial deletion of Spt8 expressed in bacteria. Lanes 4 and 5 are the experiment performed with purified Spt8 and the SAGA complex, respectively. Lanes 6 and 7 are negative control in which lane 5 only has TBP while lane 6 is the reaction with unconjugated TBP.

Conjugation of TBP with FeBABE requires a sulfhydryl group on the protein. Sulfhydryl groups on TBP could be created by performing a site-directed mutagenesis to change a specific residue to a cysteine, or by converting an available lysine into a sulfhydryl group with Traut's reagent (2-iminothiolane, Pierce) (Traut et al., 1973; Wower et al., 1981). Each method has an advantage and disadvantage. For example, the site directed

mutagenesis specifically controls where I conjugate the TBP molecule, which may or may not yield the cleavage product. On the other hand, Traut's reagent would preserve the positive charge of the lysine residues, which might be important for interaction with Spt8, but the presence of FeBABE on the TBP molecules would be random.

It is possible that TBP which has been conjugated with FeBABE might fail to cleave Spt8. The first experiment would be to identify whether FeBABE has been coupled to TBP by testing with Ellman reagent (Pierce), which can determine free sulfhydryl groups in proteins. If the FeBABE has been conjugated with TBP but the TBP fails to cleave Spt8, it is possible that the FeBABE is not present within the area of interaction or it is pointing away from the contact site. The problem may be fixed by using Traut's reagent before conjugation or mutating some other residues in TBP into cysteines. A positive control experiment might be useful. For instance, TBP interacts with Mot1, TFIIA and TFIIB (Geisberg and Struhl, 2004; Nikolov et al., 1995; Warfield et al., 2004). The same experiment could be performed with those factors to test whether or not they can be cleaved by TBP conjugated with FeBABE.

In case the cleaving experiment with FeBABE fails to reveal a valuable insight into Spt8-TBP interaction regions, another experiment could be performed. I have predicted the secondary structure of the WD40 repeat domain of Spt8 (Figure **3-3**). Based on literature, residues on the loops that connect beta strands of the WD40 propeller usually make contact with another protein, as seen in the case of G protein β subunit interacting with G protein receptor kinase (GRK) (Lodowski et al., 2003). Thus, I could mutagenize some of the Spt8 residues and perform pull down experiments with TBP to determine specific Spt8 mutants that have a defect on this interaction. While this experiment could be performed, it may be very time-consuming because it might require a combination of mutations to observe an effect.

Regions on Spt8 that contact TBP identified from the cross-linking or the Fe(BABE) reagents would need to be verified for the interaction. Because the Sulfo-SBED or

FeBABE does not necessarily cross-link or cleave Spt8 exactly where it interacts with TBP, further mutagenesis within or around those regions would need to be performed. Those Spt8 mutants would need to be expressed and purified to test their interaction with TBP.

5.2.3.2 Determining the structural features of TBP which are required for the interaction with Spt8

To achieve this goal, the same experimental technique used for the first objective could be applied. I could conjugate a purified Spt8 with FeBABE and perform a cleavage reaction to identify specific residues of TBP that interact with Spt8. The similar analysis which was done in the first objective would be applied. In addition, my data in Chapter 3 indicate that TBP may utilize its residues within (or close to) the concave surface of the saddle-like structure to interact with Spt8. Thus, I could perform site-directed mutagenesis to mutate TBP residues within the concave surface, or residues that would affect TBP dimerization besides the R171 residue, to use for pull down experiments with Spt8 protein. Alternatively, I can also ask for TBP mutants from the Pugh lab since the Pugh lab have generated a series of TBP mutants to analyze their interactions with other transcription factors (Kou et al., 2003). Analyzing TBP mutants is more feasible than using FeBABE reagent to conjugate the Spt8 since 1) my data suggest that TBP may utilize its concave surface to bind to Spt8 and 2) using FeBABE requires a certain concentration of the bait protein which is difficult to do with low-yield purified recombinant Spt8 (See Chapter 4).

5.2.3.3 Determining *in vivo* effects of Spt8 mutants that fail to interact with TBP

Identification of Spt8 mutants that do not interact—or interact weakly—with TBP will be more meaningful if they have *in vivo* phenotypes. Because I have created the *spt8*Δ yeast strain, I could transform plasmids that contain different mutations on the SPT8 to the cells and test for phenotypes. First, I would analyze the association of those Spt8 mutants with the SAGA complex with Western blotting. I would also analyze the transcription of some SAGA dependent genes such as HIS3, TRP3 and ARG1 under both non-inducing and inducing conditions. A method for total RNA isolation and transcription assay has been described (Iyer and Struhl, 1996). In addition, I would investigate the genetic interaction of those Spt8 mutants with Spt15 (TBP) and Spt3 mutants such as spt15-21 (G174E) and spt3-401 (E240K) (Eisenmann et al., 1992; Eisenmann et al., 1994).

5.3 Bibliography

Alley, S. C., Ishmael, F. T., Jones, A. D., and Benkovic, S. J. (2000). Mapping Protein-Protein Interactions in the Bacteriophage T4 DNA Polymerase Holoenzyme Using a Novel Trifunctional Photo-cross-linking and Affinity Reagent. J Am Chem Soc *122*, 6126-6127.

Belotserkovskaya, R., Sterner, D. E., Deng, M., Sayre, M. H., Lieberman, P. M., and Berger, S. L. (2000). Inhibition of TATA-binding protein function by SAGA subunits Spt3 and Spt8 at Gcn4-activated promoters. Mol Cell Biol *20*, 634-647.

Bhaumik, S. R., and Green, M. R. (2001). SAGA is an essential in vivo target of the yeast acidic activator Gal4p. Genes Dev *15*, 1935-1945.

Bhaumik, S. R., and Green, M. R. (2002). Differential requirement of SAGA components for recruitment of TATA-box-binding protein to promoters in vivo. Mol Cell Biol *22*, 7365-7371.

Coleman, R. A., Taggart, A. K., Burma, S., Chicca, J. J., 2nd, and Pugh, B. F. (1999). TFIIA regulates TBP and TFIID dimers. Mol Cell *4*, 451-457.

Datwyler, S. A., and Meares, C. F. (2000). Protein-protein interactions mapped by artificial proteases: where sigma factors bind to RNA polymerase. Trends Biochem Sci *25*, 408-414.

Dynlacht, B. D., Hoey, T., and Tjian, R. (1991). Isolation of coactivators associated with the TATA-binding protein that mediate transcriptional activation. Cell *66*, 563-576.

Eisenmann, D. M., Arndt, K. M., Ricupero, S. L., Rooney, J. W., and Winston, F. (1992). SPT3 interacts with TFIID to allow normal transcription in Saccharomyces cerevisiae. Genes Dev *6*, 1319-1331.

Eisenmann, D. M., Chapon, C., Roberts, S. M., Dollard, C., and Winston, F. (1994). The Saccharomyces cerevisiae SPT8 gene encodes a very acidic protein that is functionally related to SPT3 and TATA-binding protein. Genetics *137*, 647-657.

Geisberg, J. V., and Struhl, K. (2004). Cellular stress alters the transcriptional properties of promoter-bound Mot1-TBP complexes. Mol Cell *14*, 479-489.

Ishmael, F. T., Alley, S. C., and Benkovic, S. J. (2001). Identification and mapping of protein-protein interactions between gp32 and gp59 by cross-linking. J Biol Chem *276*, 25236-25242.

Iyer, V., and Struhl, K. (1996). Absolute mRNA levels and transcriptional initiation rates in Saccharomyces cerevisiae. Proc Natl Acad Sci U S A *93*, 5208-5212.

Kang, J. J., Auble, D. T., Ranish, J. A., and Hahn, S. (1995). Analysis of the yeast transcription factor TFIIA: distinct functional regions and a polymerase II-specific role in basal and activated transcription. Mol Cell Biol *15*, 1234-1243.

Kou, H., Irvin, J. D., Huisinga, K. L., Mitra, M., and Pugh, B. F. (2003). Structural and functional analysis of mutations along the crystallographic dimer interface of the yeast TATA binding protein. Mol Cell Biol *23*, 3186-3201.

Larschan, E., and Winston, F. (2001). The S. cerevisiae SAGA complex functions in vivo as a coactivator for transcriptional activation by Gal4. Genes Dev *15*, 1946-1956.

Lee, D., Ezhkova, E., Li, B., Pattenden, S. G., Tansey, W. P., and Workman, J. L. (2005). The proteasome regulatory particle alters the SAGA coactivator to enhance its interactions with transcriptional activators. Cell *123*, 423-436.

Lodowski, D. T., Pitcher, J. A., Capel, W. D., Lefkowitz, R. J., and Tesmer, J. J. (2003). Keeping G proteins at bay: a complex between G protein-coupled receptor kinase 2 and Gbetagamma. Science *300*, 1256-1262.

Nikolov, D. B., Chen, H., Halay, E. D., Usheva, A. A., Hisatake, K., Lee, D. K., Roeder, R. G., and Burley, S. K. (1995). Crystal structure of a TFIIB-TBP-TATA-element ternary complex. Nature *377*, 119-128.

Pugh, B. F., and Tjian, R. (1990). Mechanism of transcriptional activation by Sp1: evidence for coactivators. Cell *61*, 1187-1197.

Qiu, H., Hu, C., Yoon, S., Natarajan, K., Swanson, M. J., and Hinnebusch, A. G. (2004). An array of coactivators is required for optimal recruitment of TATA binding protein and RNA polymerase II by promoter-bound Gcn4p. Mol Cell Biol *24*, 4104-4117.

Qiu, H., Hu, C., Zhang, F., Hwang, G. J., Swanson, M. J., Boonchird, C., and Hinnebusch, A. G. (2005). Interdependent recruitment of SAGA and Srb mediator by transcriptional activator Gcn4p. Mol Cell Biol *25*, 3461-3474.

Ricci, A. R., Genereaux, J., and Brandl, C. J. (2002). Components of the SAGA histone acetyltransferase complex are required for repressed transcription of ARG1 in rich medium. Mol Cell Biol *22*, 4033-4042.

Sprague, E. R., Redd, M. J., Johnson, A. D., and Wolberger, C. (2000). Structure of the C-terminal domain of Tup1, a corepressor of transcription in yeast. Embo J *19*, 3016-3027.

Sterner, D. E., Grant, P. A., Roberts, S. M., Duggan, L. J., Belotserkovskaya, R., Pacella, L. A., Winston, F., Workman, J. L., and Berger, S. L. (1999). Functional organization of the yeast SAGA complex: distinct components involved in structural integrity, nucleosome acetylation, and TATA-binding protein interaction. Mol Cell Biol *19*, 86-98.

Swamy, N., Xu, W., Paz, N., Hsieh, J.-C., Haussler, M. R., Maalouf, G. J., Mohr, S. C., and Ray, R. (2000). Molecular Modeling, Affinity Labeling, and Site-Directed Mutagenesis Define the Key Points of Interaction between the Ligand-Binding Domain of the Vitamin D Nuclear Receptor and 1α,25-Dihydroxyvitamin D_3. Biochemistry *39*, 12162-12171.

Tan, S., Hunziker, Y., Sargent, D. F., and Richmond, T. J. (1996). Crystal structure of a yeast TFIIA/TBP/DNA complex. Nature *381*, 127-151.

Tanese, N., Pugh, B. F., and Tjian, R. (1991). Coactivators for a proline-rich activator purified from the multisubunit human TFIID complex. Genes Dev *5*, 2212-2224.

Traut, R. R., Bollen, A., Sun, T. T., Hershey, J. W., Sundberg, J., and Pierce, L. R. (1973). Methyl 4-mercaptobutyrimidate as a cleavable cross-linking reagent and its application to the Escherichia coli 30S ribosome. Biochemistry *12*, 3266-3273.

Traviglia, S. L., Datwyler, S. A., and Meares, C. F. (1999a). Mapping protein-protein interactions with a library of tethered cutting reagents: the binding site of sigma 70 on Escherichia coli RNA polymerase. Biochemistry *38*, 4259-4265.

Traviglia, S. L., Datwyler, S. A., Yan, D., Ishihama, A., and Meares, C. F. (1999b). Targeted protein footprinting: where different transcription factors bind to RNA polymerase. Biochemistry *38*, 15774-15778.

van Oevelen, C. J., van Teeffelen, H. A., and Timmers, H. T. (2005). Differential requirement of SAGA subunits for Mot1p and Taf1p recruitment in gene activation. Mol Cell Biol *25*, 4863-4872.

Warfield, L., Ranish, J. A., and Hahn, S. (2004). Positive and negative functions of the SAGA complex mediated through interaction of Spt8 with TBP and the N-terminal domain of TFIIA. Genes Dev *18*, 1022-1034.

Weideman, C. A., Netter, R. C., Benjamin, L. R., McAllister, J. J., Schmiedekamp, L. A., Coleman, R. A., and Pugh, B. F. (1997). Dynamic interplay of TFIIA, TBP and TATA DNA. J Mol Biol *271*, 61-75.

Wower, I., Wower, J., Meinke, M., and Brimacombe, R. (1981). The use of 2-iminothiolane as an RNA-protein cross-linking agent in Escherichia coli ribosomes, and the localisation on 23S RNA of sites cross-linked to proteins L4, L6, L21, L23, L27 and L29. Nucleic Acids Res *9*, 4285-4302.

Wu, C., and Travers, A. (2004). A 'one-pot' assay for the accessibility of DNA in a nucleosome core particle. Nucleic Acids Res *32*, e122.

Xie, J., Collart, M., Lemaire, M., Stelzer, G., and Meisterernst, M. (2000). A single point mutation in TFIIA suppresses NC2 requirement in vivo. Embo J *19*, 672-682.

Yokomori, K., Zeidler, M. P., Chen, J. L., Verrijzer, C. P., Mlodzik, M., and Tjian, R. (1994). Drosophila TFIIA directs cooperative DNA binding with TBP and mediates transcriptional activation. Genes Dev *8*, 2313-2323.

Appendix A

Gel Shift assay

Gel shift assay was performed to test the ability of TBP to interact with TFIIA. A total of 2 µM DNA (16 bp double-stranded oligonucleotide DNA: 5'-TGTATGTATATAAAAC-3') was incubated with different concentrations of TBP and TFIIA whose concentrations were ranged from 0.5-4.0 µM in the DNA binding buffer (20 mM HEPES pH 7.5, 5 mM $MgCl_2$, 60 mM KCl, and 5% glycerol) in a 20 µl reaction volume. After 25 minute incubation at 4ºC, 4 µl of 6xGLB (10 mM HEPES pH 7.5, 0.1% bromophenol blue, 0.1% xylene cyanol, and 30% glycerol) was added to the reaction. Samples were analyzed by gel electrophoresis with a 10% native polyacrylamide gel (10% of 30%/0.5% acrylamide/bis-acrylamide, 5% Tris-boric acid (TBE), 3 mM $MgCl_2$, 0.1% Ammonium persulfate, and 0.1% TEMED), which was previously pre-electrophoresed at 100 volts for 1 hour at 4ºC, while the actual sample was electrophoresed at 160 volts for 30-45 minutes at 4ºC. The gel shift result is shown in Figure **A-1**

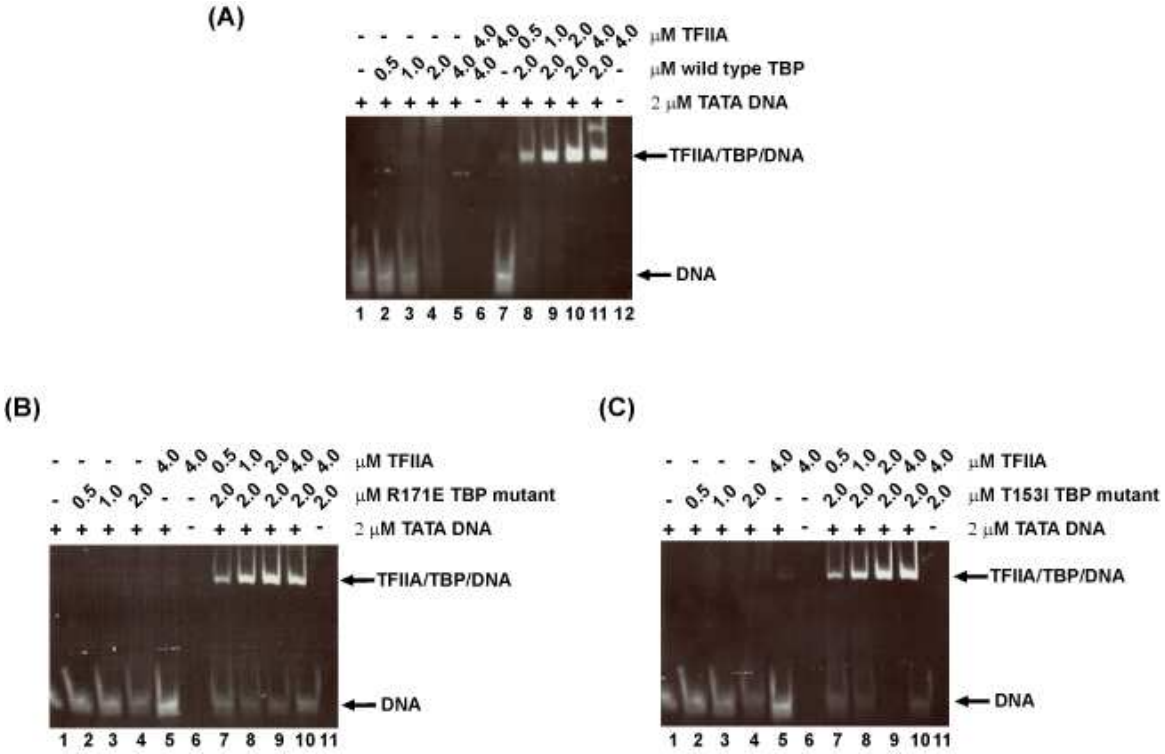

Figure **A-1**: Gel-shift assay of TBP/TFIIA/DNA complexes**.**

Like the wild type TBP (A), both R171E (B) and T153I (C) are able to form a complex with TFIIA and DNA.

Appendix B

Purification of the core histones and long oligo nucleosomes from HeLa cells

Purification of the core histones and long oligo nucleosomes (LON) from HeLa cells involves several steps which include 1) preparation of HeLa cell nuclei and 2) preparation of nuclei pellet. The resulting chromatin from HeLa nuclei is used to extract the core histones and prepare the LON.

B.1 Preparation of HeLa cell nuclei

This protocol is adapted from the National Cell Culture Center (NCCC), adjusted from the protocol previously described (Desjardins et al., 1963). All steps were performed at 4°C or on ice. Five liters of HeLa-S3 cells, which is equal to roughly 8 to 10 ml of cell pellet, were purchased from the National Cell Culture Center (NCCC). Briefly, five volumes of cold nuclear extract buffer A with protease inhibitors (10 mM HEPES pH 7.8, 1.5 mM $MgCl_2$, 10 mM KCl, 2 µg/ml leupeptin, 2 µg/ml pepstatin, and 0.2 mM PMSF) were added to the cell pellet. Cells were gently resuspended and incubated on ice for 20 minutes, swirling once or twice. With a pre-chilled dounce homogenizer (type B pestle), cells were subsequently homogenized slowly with 20 up and down strokes. Cells were centrifuged at 1706xg force for 10 minutes to precipitate the nuclei. The supernatant, which contains cytosol extract, was discarded. The pellet was resuspended with 2 or 3 volumes of 0.25 M sucrose solution (0.25 M sucrose and 0.01 M $MgCl_2$) and centrifuged at 1430xg force for 5 minutes. The resulting nuclei pellet from the centrifugation can be stored at -80°C. The entired nuclei pellet from this step was used in **B.2**.

B.2 Preparation of nuclei pellet

A method for nuclei extraction was previously described (Abmayr and Workman, 1993). All steps were performed at 4°C. Approximately 2.5 ml of the packed nuclei were resuspended with 2.5 ml low salt buffer (20 mM HEPES pH 7.5, 25% glycerol, 1.5 mM $MgCl_2$, 20 mM KCl, 0.2 mM EDTA, 0.5 mM DTT, 0.2 mM PMSF, 2 µg/ml leupeptin, 2 µg/ml pepstatin, 1 mM Pefabloc SC (Roche), and 0.8 µl/ml PSC-protector solution (Roche)). With constant stirring, approximately 2.5 ml high salt buffer (20 mM HEPES pH 7.5, 25% glycerol, 1.5 mM $MgCl_2$, 1500 mM KCl, 0.2 mM EDTA, 0.5 mM DTT, 0.2 mM PMSF, 2 µg/ml leupeptin, 2 µg/ml pepstatin, 1 mM Pefabloc SC (Roche)), and 0.8 µl/ml PSC-protector solution (Roche)) was added drop wise to the nuclei, which were subsequently homogenized two to five times in a glass Dounce homogenizer (type B pestle). The final KCl concentration should be about 300 mM. After homogenization, nuclei were constantly and gently stirred for 30 minutes before centrifugation at ~25,000xg force for 30 minutes. The supernatant is the nuclear extract which contains transcription factors but not chromatin and can be stored at -80°C for other applications. The pellet, which contains chromatin, was used immediately.

The resulting nuclei pellet from centrifugation was resuspended in 25 ml H400 (20 mM HEPES pH 7.5, 400 mM NaCl, 1 mM EDTA, 10% glycerol, 1 mM 2-mercaptoethanol, 0.5 mM PMSF, 2 µg/ml leupeptin, 2 µg/ml pepstatin, 1 mM Pefabloc SC (Roche), and 0.8 µl/ml PSC-protector solution (Roche)). The pellet can be homogenized with a glass Dounce homogenizer for 1 or 2 strokes to help with resuspension. The resuspended pellet was centrifuged at 20,000xg force for 5 minutes. Resuspension of the pellet with H400 and centrifugation were repeated for 4 additional times. Then, the pellet was resuspended with 25 ml H400 with 0.2% NP40 added and centrifuged at 20,000xg force for 5 minutes. The resuspension step was repeated one more time in which the total prep was split into two sets before centrifugation so that each half could be used for core histone and long oligo nucleosome preparations, respectively. The supernatant can be discarded and the pellet can be used immediately or stored at -80°C.

B.3 Purification of HeLa core histones

The procedures for extracting core histones was previously described (Grant et al., 1997). Nuclei pellet from the previous procedure (**B.2**) was washed twice with 25 ml HAP400 buffer (50 mM sodium phosphate pH 6.8, 400 mM NaCl, 1 mM 2-mercaptoethanol, 0.5 mM PMSF, 2 g/ml leupeptin, 2 µg/ml pepstatin, 1 mM Pefabloc SC (Roche), and 0.8 µl/ml PSC-protector solution) (Roche)), and centrifuged at 20,000xg force for 5 minutes at 4°C. The pellet was subsequently resuspended in 25 ml HAP600 buffer (50 mM sodium phosphate pH 6.8, 600 mM NaCl, 1 mM 2-mercaptoethanol, 0.5 mM PMSF, 2 g/ml leupeptin, 2 µg/ml pepstatin, 1 mM Pefabloc SC (Roche), and 0.8 µl/ml PSC-protector solution) (Roche)) and Dounce homogenized for 10 up and down strokes. 600 mM NaCl lyses the nuclei which will increase viscosity of the extract.

The chromatin extract was sonicated in 15 second pulses for 4 times with 70% power output with a 30 second rest on ice (Branson Digital Sonifier). Sonication should produce chromatin fragments no larger than 2 kbp, which can be analyzed with gel electrophoresis using a 1% agarose gel. Briefly, 100 µl sonicated product was digested with 20 µg protease K at 55°C for 30 minutes. Then, the DNA was extracted by a phenol/CIA extraction method, and concentrated by ethanol precipitation. 20 µg glycogen can be added to the extracted DNA before ethanol precipitation to help capturing any small DNA fragments.

Core histones can be extracted with 5 grams Hydroxyapatite resin (DNA grade Bio-gel HTP gel, Bio-RAD). The sonicated chromatin was incubated with the resin equilibrated with HAP600 buffer for 30 minutes at 4°C. After incubation, the resin was centrifuged at 3,000xg force for 5 minutes to get rid of the supernatant which contains histone H1. The resin was subsequently resuspended twice with 125 ml HAP600 buffer. Two volumes of HAP2000 (50 mM sodium phosphate pH 6.8, 2000 mM NaCl, 1 mM 2-mercaptoethanol, 0.5 mM PMSF, 2 g/ml leupeptin, 2 µg/ml pepstatin, 1 mM Pefabloc SC (Roche), and 0.8 µl/ml PSC-protector solution) (Roche)) was added to the resin to extract histone octamers

from the resin bound chromatin. An additional 5 M NaCl was added drop wise with constant shaking to bring the final NaCl concentration to 2.0 M. The supernatant was separated from the resin by centrifugation and saved. The resin pellet can be extracted twice with the same buffer. Core histones which remain in the supernatant can be quantified using absorption at 230 nM UV wavelength. The A230 absorption value at 3.3 is roughly equal to 1 mg/ml of core histones. The core histones can be aliquoted and stored at -80°C.

B.4 Purification of long oligo nucleosomes (LON)

Owens-Hughes et al also describes the purification of long oligo nucleosomes (Grant et al., 1997). The nuclei pellet from the previous procedure (**B.2**) was washed twice with H400 buffer (20 mM HEPES pH 7.5, 400 mM NaCl, 1 mM EDTA, 1 mM 2-mercaptoethanol, 0.5 mM PMSF, 2 µg/ml leupeptin, 2 µg/ml pepstatin, 1 mM Pefabloc Sc (Roche), and 0.8 µl/ml PSC-protector solution (Roche)). The nuclei pellet was resuspended in 10 ml H600 buffer (20 mM HEPES pH 7.5, 600 mM NaCl, 1 mM EDTA, 1 mM 2-mercaptoethanol, 0.5 mM PMSF, 2 µg/ml leupeptin, 2 µg/ml pepstatin, 1 mM Pefabloc Sc (Roche), and 0.8 µl/ml PSC-protector solution (Roche)) which will lyse the nuclei. A Dounce homogenizer may be used to help resuspension of the pellet.

The chromatin extract was sonicated in 15 second pulses for 4 times with 70% power output with 30 second incubation on ice (Branson Digital Sonifier) to obtain chromatin at about 4 kbp fragments. The size of the DNA fragment can be analyzed with gel electrophoresis using a 1% agarose gel, using the same method described in the purification of HeLa core histones. After sonication, the fragmented chromatin was dialyzed against H100 buffer (20 mM HEPES pH 7.5, 100 mM NaCl, 1 mM EDTA, 1 mM 2-mercaptoethanol, 0.5 mM PMSF, 2 µg/ml leupeptin, 2 µg/ml pepstatin, 1 mM Pefabloc Sc (Roche), and 0.8 µl/ml PSC-protector solution (Roche)). After dialysis, 0.03

volume of 0.1 M $CaCl_2$ was added to the dialyzed chromatin before digesting with the MNase enzyme.

A small amount of the samples was tested by digestion with a 0.1 or 0.01 Unit/µl MNase for different times ranging from 0 to 10 minutes. The digestion reaction was stopped by adding 50 mM EDTA, and the size of digested nucleosomes was analyzed by gel electorphoresis with a 1% agarose gel, using the same procedure described in the purification of HeLa core histones. The preferred size of the digested chromatin is in an average of 400 bp. Once the time and concentration of MNase were determined, bulk digestion of the chromatin can be performed and checked with 1% agarose gel. For this experiment, 15 ml of the dialyzed chromatin was digested with 0.3 Units of MNase for 1 minute at 37°C. The size of the digested chromatin from the bulk digestion was analyzed with a gel electrophoresis using a 1% agarose gel.

Subsequently, NaCl was added to a final concentration of 0.6 M to separate histone H1 from chromatin. The sample was centrifuged at 20,000xg force for 15 minutes before loading onto a 300 ml Sepharose CL-6B gel filtration column (Pharmacia XK 26/70) which was previously equilibrated with HB600 (20 mM HEPES pH 7.5, 600 mM NaCl, 1 mM EDTA, 10% glycerol, 0.2% NP40, 1 mM 2-mercaptoethanol, 0.5 mM PMSF, 2 µg/ml leupeptin, 2 µg/ml pepstatin, 1 mM benzamidine, 1 mM Pefabloc Sc (Roche), and 0.8 µl/ml PSC-protector solution (Roche)). The column was run at a flow rate of 0.4 ml/minute with a total of 425 ml HB600 buffer while collecting 4 ml fractions. The size of nucleosomes and the presence of histones in the peak fractions were analyzed on 1% agarose and 18% SDS PAGE gels, respectively. Peak fractions were pooled and dialyzed against H600 buffer (20 mM HEPES pH 7.5, 600 mM NaCl, 0.1% Tween 20, 1 mM benzamidine and 1 mM 2-mercaptoethanol), concentrated to approximately 1.2 mg/ml of the histone content, aliquoted, flash frozen with liquid nitrogen, and stored at -80°C.

B.5 Quality control

In order to test whether my core histones and LON could function correctly, I compared my HAT substrates with those from the Workman Lab. To do the experiment, I used the SAGA complex to acetylate the core histones from my purification, the Workman Lab, and our chicken core histones. As shown in Figure **B-1**, my purified HeLa cell core histones yielded approximately the same HAT activity obtained from the Workman Lab's HeLa cell core histones, both of which are better substrates for SAGA acetylation than our chicken core histones. Thus, I concluded that my purified HeLa cell core histones are at the same quality as the core histones from the Workman Lab. In addition, I applied a similar analysis on the long oligo nucleosome (LON) I purified. As shown in Figure **B-2**, my purified HeLa LON has a slightly higher in HAT activity than that from the Workman Lab. This might be due to a slight difference in the amount of the LON between the two sources.

I also noticed that while the SAGA complex acetylates the HeLa cell core histones better than the chicken core histones (Figure **B-1**), the complex prefers the chicken LON to the HeLa cell LON (Figure **B-2**). The paradoxical observations between the HAT assay results from both kinds of substrates complicate the conclusion using the histone code hypothesis, in which one type of histone modification could affect another (See **1.3.3**). In other words, either core histones from chicken or LON from HeLa cells has some existing covalent modifications which might disfavor or enhance SAGA acetylation. Thus, if the SAGA complex acetylates HeLa cell core histones better than chicken core histones, then the complex should acetylate HeLa LON better than chicken LON, and vise versa. I speculate that the difference between the chicken LON and the HeLa LON is due to the different salt concentrations in both substrates. The chicken LON was purified with zero salt, whereas the HeLa LON was kept in 600 mM NaCl. Because the SAGA acetylation ability could be affected by salt concentration, this could explain why the chicken LON is a preferred substrate for the SAGA complex. In addition, I consistently observed a high HAT activity in the blank of the chicken core histones,

where the SAGA complex was omitted. This high background might be the result of some contaminations, which also decrease the HAT activity. Therefore, this might explain why the chicken core histones are not a good HAT substrate for the SAGA complex.

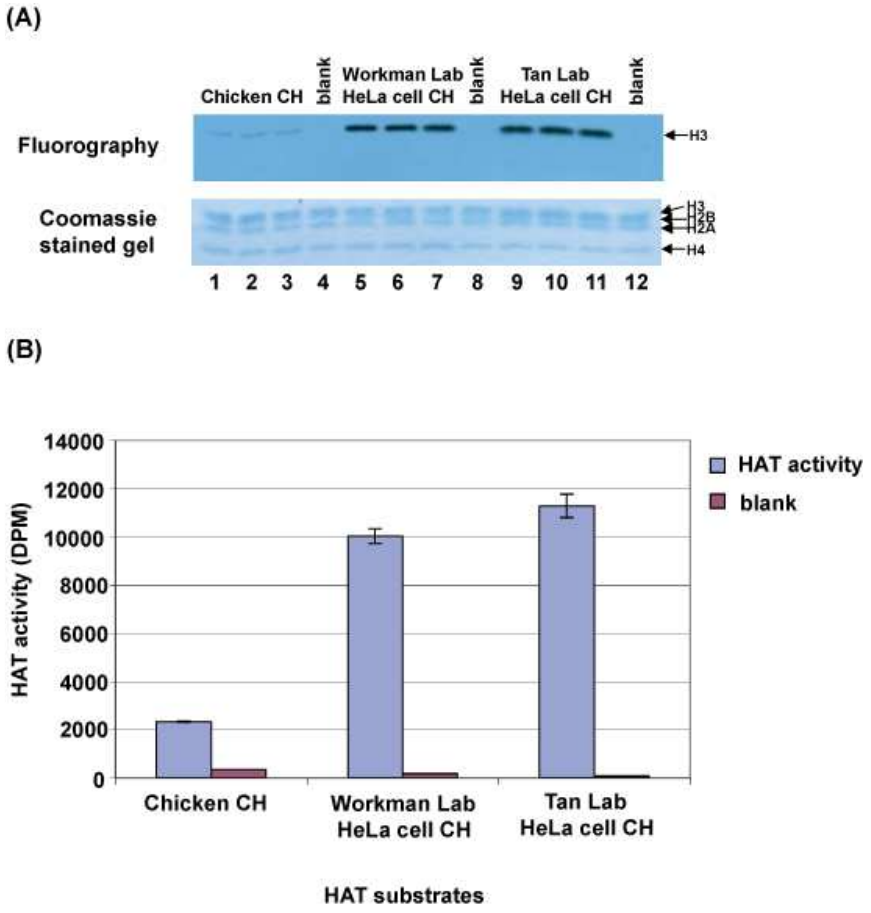

Figure **B-1**: SAGA HAT assays using core histones as the enzyme substrate.

(A) The top panel is a fluorography that shows the relative SAGA acetylation on our chicken core histones (lanes 1-3), HeLa cell core histones from Workman Lab (lanes 5-7) and my purified HeLa cell core histones (Tan Lab; lanes 9-11), respectively. Lanes 4, 8, and 12 are the blanks of each core histones type. The bottom panel shows the equal amount of core histones among the three sources. Each of the core histones has 3 repeat sets. (B) The same HAT assays from (A) but represented as a bar chart. The SAGA HAT activity on each histone substrate was the average from 3 measurements, and was obtained by liquid scintillation counting. The error bars represent the standard deviations from the measurements.

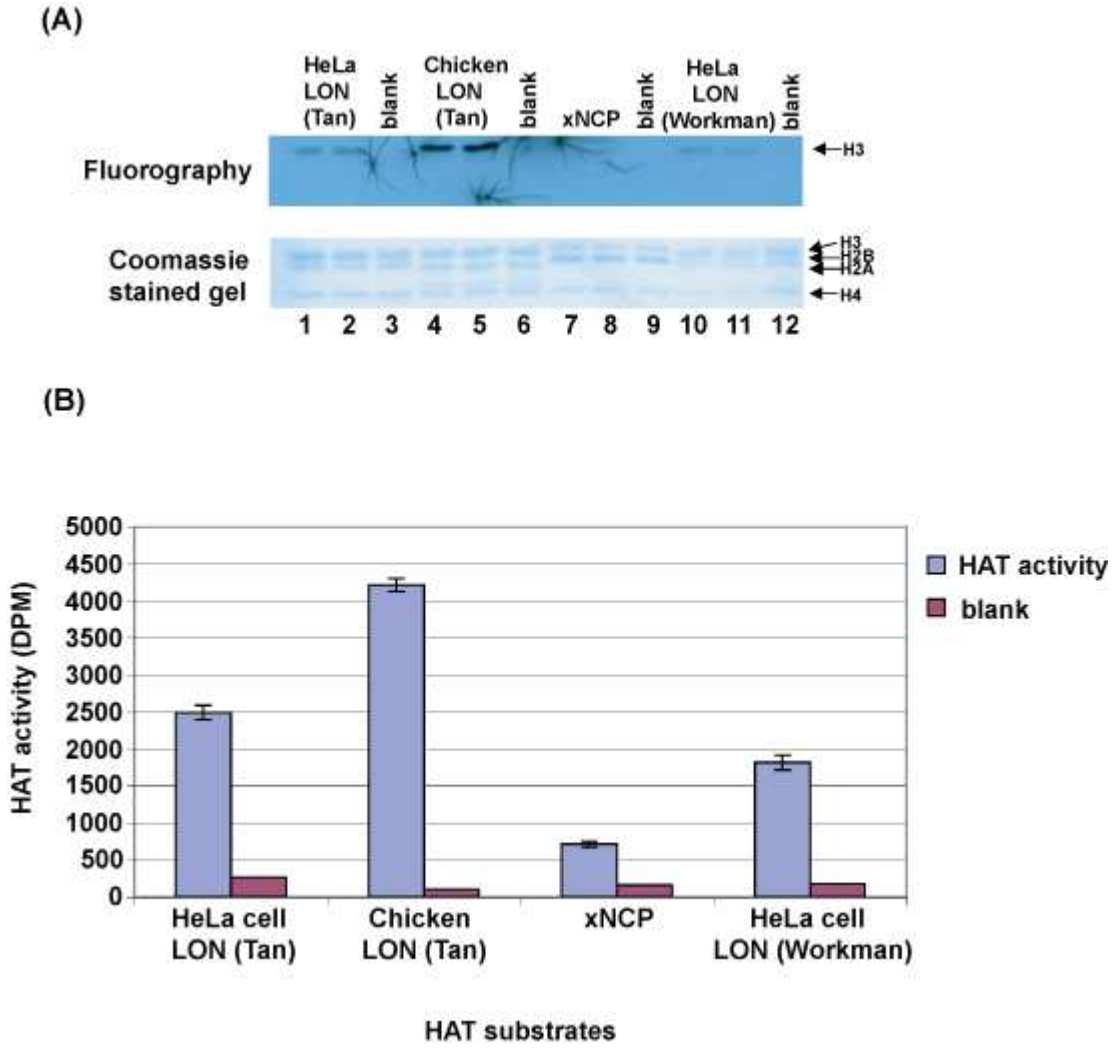

Figure **B-2**: SAGA HAT assays using LON as the enzyme substrate.

(A) The top panel is a fluorography that shows the relative SAGA acetylation on my purified HeLa cell LON (Tan Lab; lanes 1-2), our chicken LON (lanes 4-5), the reconstituted nucleosomes with the recombinant histones from *Xenopus laevis* (lanes 7-8), and the HeLa cell LON from Workman Lab (lanes 10-11). Lanes 3, 6, 9, and 12 are the blank from each LON substrate. The bottom panel shows the amount of histones proteins from each LON. Only two out of three HAT results of each LON are shown. (B) The same HAT assays from (A) but represented as a bar chart. The SAGA HAT activity on each histone substrate was the average from 3 measurements, and was obtained by liquid scintillation counting. The error bars represent the standard deviations from the measurements.

Interestingly, the *in vitro* reconstituted mono nucleosomes using the recombinant core histones from *Xenopus laevis* and the 146 bp DNA sequence from the Mouse Mammary Tumor Virus (MMTV) promoter (xNCP) were found to be the least preferred substrate for the SAGA acetylation. It is possible that the high HAT activity observed in both HeLa cell and chicken LON is due to the array of nucleosomes rather than the presence of other modifications on those LON substrates that might influence SAGA acetylation (see **1.3.3**). To test this hypothesis, I further digested the HeLa cell LON with the micrococcal nuclease to create mono nucleosomes from the HeLa cells. If the array of nucleosomes helps SAGA acetylation, then the mono nucleosomes from the HeLa cells should exhibit the same level of HAT activity as the xNCP. In contrast, if the presence of histone modifications plays a role, then the mono nucleosomes from HeLa cells should confer the same HAT activity as the HeLa cell LON. As shown in Figure **B-3**, the HeLa cell mono nucleosomes exhibit a similar HAT activity to that of the xNCP. Thus, I conclude that the histone modifications do not contribute to the different HAT activity observed between the HeLa cell LON and the xNCP, but it is the presence of the array of nucleosomes that counts.

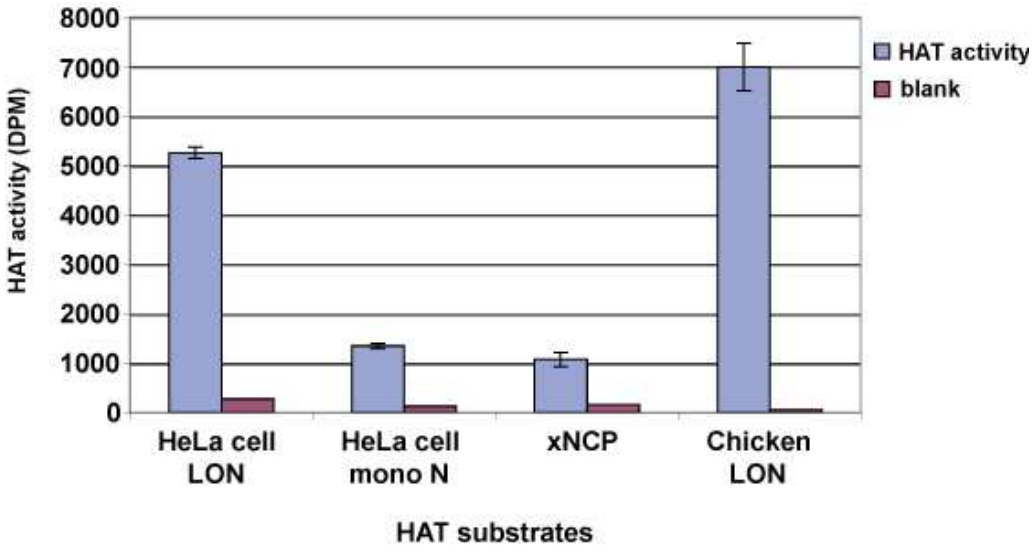

Figure **B-3**: The number of nucleosomes per unit length within the LON enhances the acetylation by the SAGA complex.

The bar chart represents the average of the 3 measurements of the HAT activity from each nucleosome substrates obtained by liquid scintillation counting. The error bars are the standard deviations from the measurements.

B.6 Bibliography

Abmayr, S. M., and Workman, J. L. (1993). Preparation of Nuclear and Cytoplasmic Extracts from Mammalian Cells. In Current Protocols In Molecular Biology, F. M. Ausubel, R. Brent, R. E. Kingston, D. D. Moore, J. G. Seidman, J. A. Smith, and K. Struhl, eds. (New York, Wieley Interscience), pp. 12.1.1-12.1.7.

Desjardins, R., Smetana, K., Steele, W. J., and Busch, H. (1963). Isolation of Nucleoli of the Walker Carcinosarcoma and Liver of the Rat Following Nuclear Disruption in a French Pressure Cell. Cancer Res *23*, 1819-1823.

Owen-Hughes, T., Utley, R. T., Steger, D. J., West, J. M., John, S., Cote, J., Havas, K. M., and Workman, J. L. (1999). Analysis of nucleosome disruption by ATP-driven chromatin remodeling complexes. Methods Mol Biol *119*, 319-331.

Appendix C

Nucleosome footprinting by the Piccolo NuA4 complex

C.1 Introduction

The yeast Piccolo NuA4 complex is the smallest NuA4 subcomplex that can acetylate nucleosomes. Like the yeast Ada3/Ada2/Gcn5 SAGA subcomplex, the Piccolo NuA4 complex is comprised of three subunits: Esa1, Yng2, and Epl1 (Boudreault et al., 2003; Selleck et al., 2005). Esa1, a HAT enzyme in the MYST family, is the catalytic subunit of the Piccolo and NuA4 complexes. This enzyme is essential for the cell viability and the cell cycle progression of yeast, as a deletion of the Esa1 causes slow growth defects and cell cycle arrested phenotype at G2/M stage (Allard et al., 1999). Yng2 shares homology with the human suppressor Ing1, which is involved in DNA repair, apoptosis, and nucleosome remodeling (Feng et al., 1995; Garkavtsev et al., 1998; Loewith et al., 2000). The sequence homology lies within the conserved C-terminal plant homeodomain (PHD). We have found that the conserved PHD is dispensable for the nucleosomal HAT activity of the Piccolo NuA4 complex, while the N-terminus region of the Yng2 is required for the nucleosomal HAT activity (Selleck et al., 2005). Lastly, the Enhancer of Polycomb Like-1 (Epl1) is the yeast homologue of the Drosophila Enhancer of Polycomb, E(Pc), which is a suppressor of the position-effect variegation in flies (Sinclair et al., 1998). Strong sequence conservation is found within the Enhancer of Polycomb A (EPcA) domain throughout many eukaryotic organisms (Stankunas et al., 1998). This conserved EPcA is found to be important for the ability of the Piccolo NuA4 complex to acetylate nucleosomes (Selleck et al., 2005).

Aside from the fact that both the Piccolo NuA4 and the Ada3/Ada2/Gcn5 complexes acetylate nucleosomes, they share some similarities and differences. Like the Ada3/Ada2/Gcn5 complex, the Piccolo NuA4 complex does not interact with an activator protein but rather plays a role in the global histone H4 and H2A acetylation (Boudreault et al., 2003). Just as Gcn5 depends on both Ada3 and Ada2 proteins to recognize and acetylate nucleosomes, Esa1 requires both Yng2 and Epl1 in its nucleosomal HAT function (Selleck et al., 2005). However, unlike the Ada3/Ada2/Gcn5 and the SAGA complexes, which prefer core histones to nucleosome acetylation, both Piccolo and the NuA4 complex display a strong acetylation preference toward the nucleosome substrate, especially at the histone H4 and H2A (Boudreault et al., 2003; Selleck et al., 2005). I speculate that the strong, preferential nucleosome acetylation of the Piccolo NuA4 complex reflects a high binding affinity of the complex relative to the Ada3/Ada2/Gcn5 complex (See discussion in **2.4.2**).

Esa1 and Gcn5 represent the HAT enzymes from two different families which utilize a different HAT mechanism (See **1.3.3.1**). Additionally, Esa1 contains a chromodomain (Allard et al., 1999), while Gcn5 has a bromodomain (Marcus et al., 1994). The chromodomain binds to a methylated histone tail, as in the case of the chromodomain of HP1 (Jacobs and Khorasanizadeh, 2002), whereas the bromodomain of Gcn5 recognizes an acetylated histone tail (Ornaghi et al., 1999). Deletion of the chromodomain of Esa1 substantially reduces the ability of the Piccolo NuA4 complex to acetylate nucleosomes (Selleck et al., 2005). By the same token, deletion of the bromodomain of Gcn5 affects the nucleosomal HAT activity of the Ada3/Ada2/Gcn5 complex (Chapter 4). A single point mutation within the peptide binding pocket of the chromodomain of Esa1 (Y56A, E65K, or E65L) causes a severe effect on the Piccolo nucleosomal HAT function (Selleck et al., 2005). Furthermore, the chromodomain is not required for the ability of the Piccolo NuA4 complex to interact with a nucleosome, suggesting that the chromodomain might play a role in a catalytic step of nucleosomal acetylation by the Piccolo NuA4 complex. In contrast, point mutations within the conserved residues within the acetylated peptide binding pocket of the bromodomain of Gcn5 only cause a

minimal effect on nucleosome acetylation by the Ada3/Ada2/Gcn5 complex (Chapter 4). The discussion and speculation of how bromodomain contributes to the nucleosomal acetylation function of the Ada3/Ada2/Gcn5 complex is provided in Chapter 4.

I am interested in understanding how the Piccolo NuA4 complex interacts with the nucleosome core particle. I show the interaction between the Piccolo NuA4 complex and the nucleosome core particle by a gel shift assay. It has been shown that the Piccolo NuA4 complex associates with the nucleosome in a 1:1 stoichiometric fashion, and the complex binds tightly (K_d is approximately 10 nanomolar concentrations; Will Selleck's unpublished results). I observe some nucleosome protection by the Piccolo NuA4 complex in a DNase I footprinting assay. I estimate those locations to be either around the dyad or approximately 4 helical turns from the dyad. In addition, I performed the 'One-pot' assay with the Piccolo-NCP complex. However, the 'One-pot' assay results are negative: I am unable to observe any nucleosomal protection conferred by the Piccolo NuA4 complex. I will discuss problems associated with those assays as well as suggest some future directions toward understanding how these two complexes interact with each other.

C.2 Results

C.2.1 The Piccolo NuA4 complex confers nucleosome footprinting.

It has been shown that the Piccolo NuA4 complex interacts with nucleosomes through gel filtration chromatography, pull down and gel shift assays (Boudreault et al., 2003; Selleck et al., 2005) but how they interact with each other still remains unclear. It has been shown that the Piccolo NuA4 complex interacts with free DNA and nucleosomes in a gel shift assay, suggesting that some interaction is mediated through the DNA (Boudreault et al., 2003). Therefore, I investigate the interaction by performing a DNase

I footprinting analysis. The basic principle of the assay is that if the Piccolo NuA4 complex binds to a certain location of the DNA on a nucleosome, that DNA region will be protected from the nuclease activity of the DNase I enzyme. Because the DNA that wraps around the histone octamer turns an average of 10.2 basepairs away from the proteins (Luger et al., 1997), almost every 10.2 basepairs of DNA is accessible by the DNase I. In fact, a study using 1-nucleotide resolution gel has shown that the DNase I enzyme cuts approximately every 10.4 nucleotides apart (Prunell et al., 1979). A simplified cartoon comparing DNase I digestion on both naked DNA and a nucleosome is illustrated in Figure **C-1**.

DNase I footprinting assay was performed with either free DNA or the nucleosome core particle (NCP) in the presence or an absence of the Piccolo NuA4 complex. The DNA fragment that was used in the nucleosome reconstitution assay was from the nucleosome B (NucB) DNA sequence of the mouse mammary tumor virus (MMTV) (See **C.4.3**). While keeping the concentration of the free DNA or the NCP constant, I increased the amount of the Piccolo NuA4 complex in the reaction from a 1:1 ratio to 1:3, and 1:10 ratios (free DNA or NCP per Piccolo NuA4 complex). The Piccolo NuA4 complex was allowed to bind to either free DNA or NCP prior to the actual DNase I footprinting experiment. As a control for the experiment, I aliquoted the reaction mixture for the gel shift assay to confirm the interaction between the two complexes. As shown in Figure **C-2**, the Piccolo NuA4 complex appeared to gel shift both free DNA and the NCP, indicating that the Piccolo NuA4 complex interacts with both substrates. Since the Piccolo NuA4 complex gel shifted the free DNA, the complex might also interact with the NCP through the DNA.

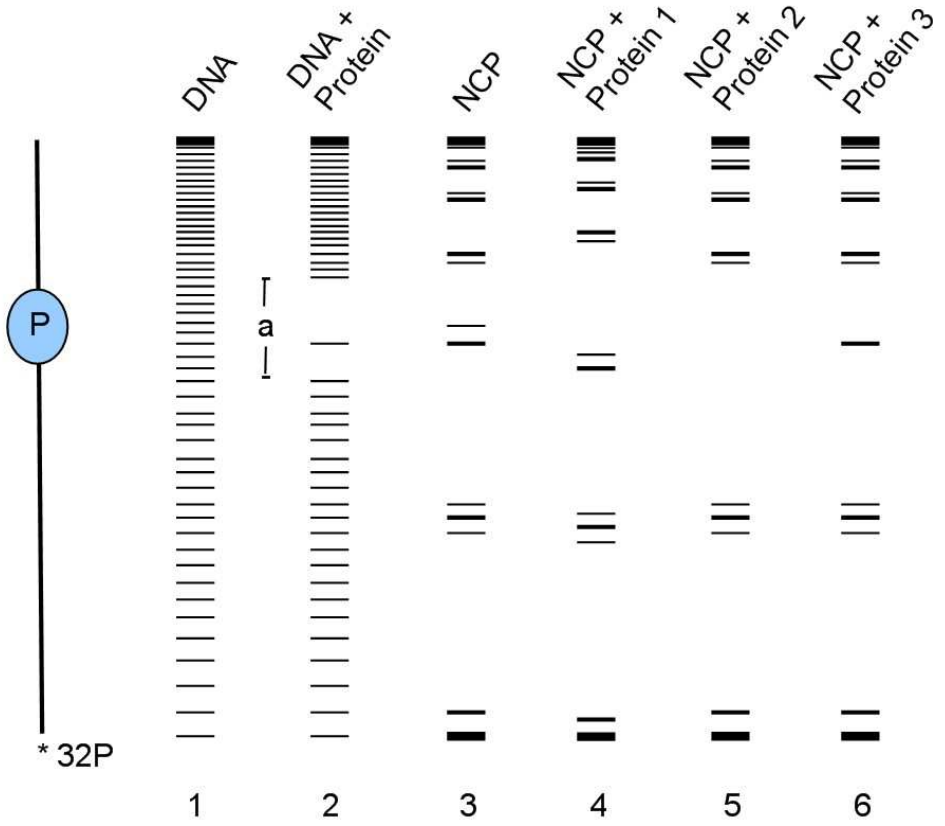

Figure **C-1**: An illustration of the expected outcomes of the DNase I digestion assay with radiolabeled free DNA or nucleosome core particle (NCP).

The image on the left is a cartoon of a double stranded DNA (represented as a vertical line) being occupied by a protein (P). The labeled end is marked by the asterisk. Lane 1 to lane 6 illustrate results from the DNAse I digestion of the free DNA (lanes 1 and 2) or the nucleosomes (lanes 4 and 5). Lane 1 is free DNA without a protein bound, while lane 2 shows the footprinted area (a) that is void of the DNase I nuclease activity because area (a) is occupied by a protein (P). In the context of the nucleosomes (lane 3), DNase I digestion is expected to digest approximately every 10 basepairs because the average of 10.2 DNA basepairs faces outward. When a nucleosome is bound by a protein, three possible outcomes may be observed. First, protein 1 does not change the number of the digested bands but rather changes the helical turns of the DNA, which changes the digestion pattern (lane 4). Second, the binding of protein 2 protects a minor groove in the NCP from being digested by the DNAse I. As a result, one major digested band is missing (lane 5). Lastly, protein 3 might bind to a major groove of the helix, which is not the major target of the DNase I enzyme (lane 6). In this case, the digestion pattern might remain similar to the results in lane 3, and only some minor digested bands are protected.

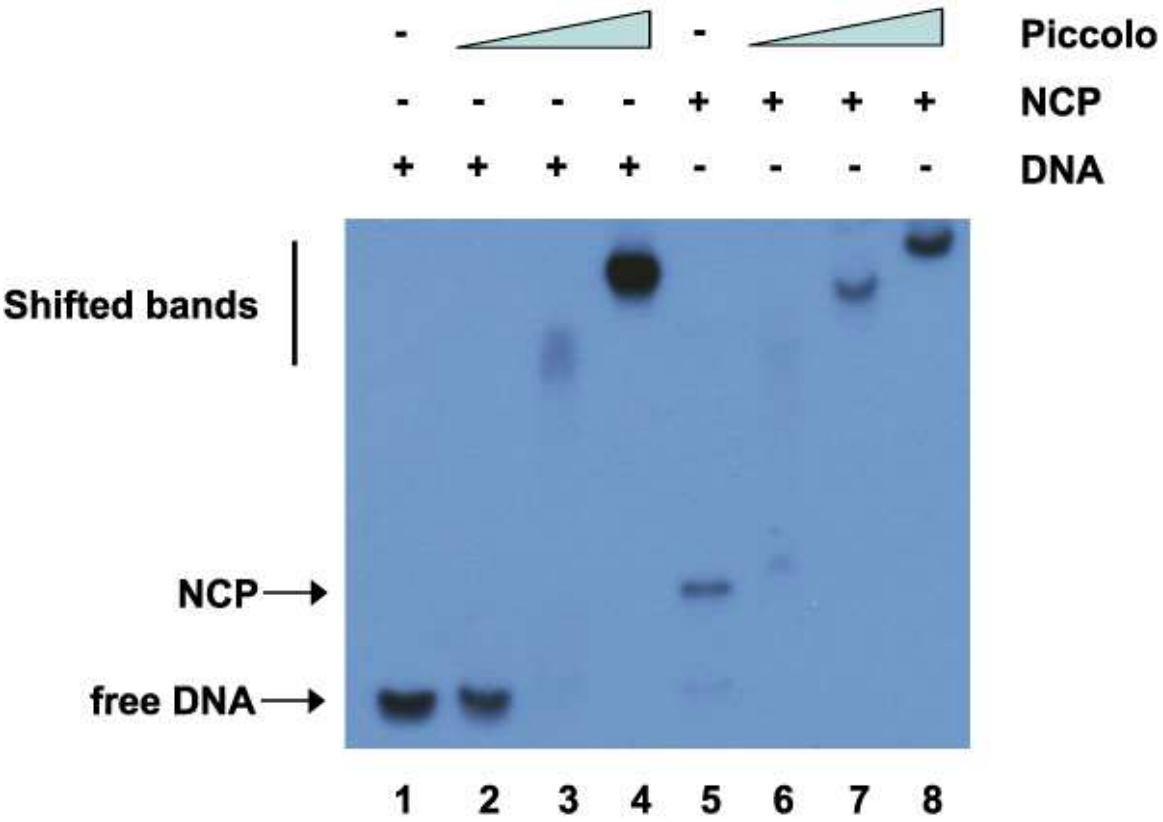

Figure **C-2**: The Piccolo NuA4 complex gel shifts both free DNA and nucleosomes.

The gel shift experiment performed with free DNA (lanes 1-4) and the NCP (lanes 5-8). The ratios between the Piccolo NuA4 complex to NCP or to DNA were increased from 1:1 to 3:1 and 10:1. The sample was electrophoresed with a 5% native polyacrylamide gel, dried, and exposed to an X-ray film.

The results of the DNase I footprinting experiment are shown in Figure **C-3**. I utilized Sac I digestion of the 165-basepair NucB DNA sequence and the actual sequencing by the Maxum-Gilbert chemical degradation at G residues (Maxam and Gilbert, 1980) as the markers (Figure **C-3** lane 1 and 2). However, the G-tracking results did not match the locations of all G residues in the sequence (See **C.4.3** for the DNA sequence); thus, they cannot be used as the markers. Because the SacI enzyme digests the DNA once at 105 basepairs away from the radiolabeled end, I used SacI digestion as the marker for that position. The numbers of nucleotide bands appearing below the 105 basepair positions were counted, and listed on the left column of Figure **C-3**. I also made an assumption

that the dyad of the nucleosomes used in the DNase I footprinting experiment falls at the basepair position 83. Thus, the nucleotide at that position was referred to as the dyad or 0, while a position approximately every 10 nucleotides away from the dyad was translated into the number of the helical turns relative to 0 as shown on the right column of Figure **C-3**.

First, I found that the digestion pattern of the free DNA and the NCP are different, especially at the regions above the 105 nucleotide position (Figure **C-3** lanes 7, 11 and 15). These results gave me some confidence that I analyzed the DNase I footprinting of the NCP, but not DNA that was dissociated from the histones. Second, the DNase I digestion on the free DNA itself appeared to be a little over digested (Figure **C-3** lanes 7 and 8), judging by the disappearance of the bands below the 60 nucleotide position. Because the Piccolo NuA4 complex binds to the free DNA in the gel shift assay (Figure **C-2** lanes 2-4), those DNA sequences should be protected from degradation by the DNase I nuclease. However, no Piccolo NuA4 footprint on free DNA was observed on the gel, but rather the digestion of free DNA was more apparent at the highest concentration of the Piccolo NuA4 complex (Figure **C-3** lanes 11 and 14). Perhaps this could be explained by the heterogeneity of the Piccolo-DNA complex. In other words, the Piccolo NuA4 complex did not recognize a specific location on the DNA. That is why all the locations of free DNA had an equal chance to be digested by the DNase I enzyme. Thus, I conclude that the Piccolo NuA4 complex randomly binds to free DNA.

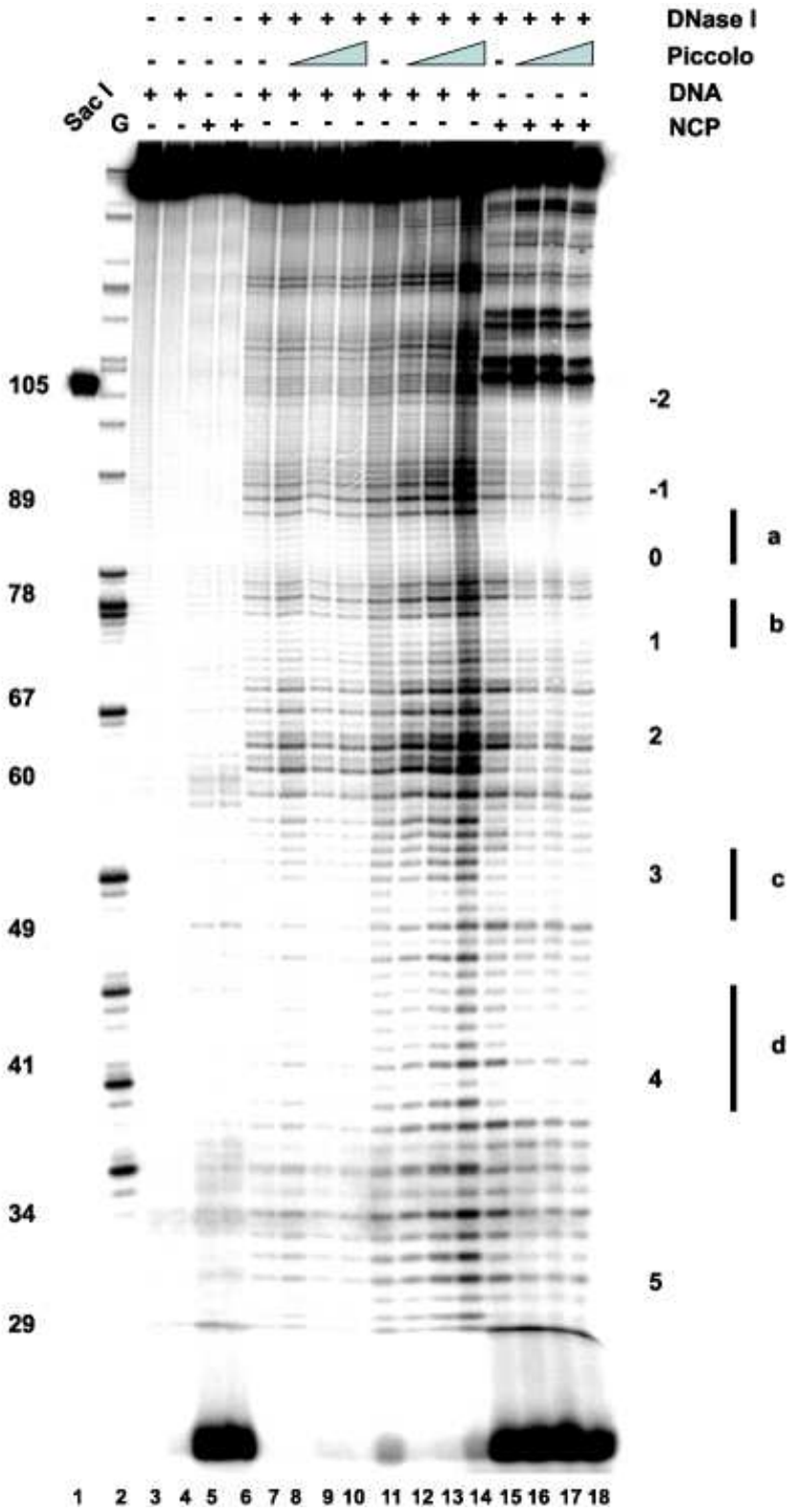

Figure **C-3**: DNase I footprinting assay with the Piccolo NuA4 complex.

Markers in lanes 1 and 2 are the Sac I digested of the radiolabeled free DNA and the G-tracking, respectively. For the DNase I footprinting with free DNA, samples in lanes 7-10 were digested with 0.05 Units DNase I enzyme, while lanes 11-15 were digested with 0.1 Units DNase I. The DNase I footprinting experiment in the context of the NCP was performed with 1.0 Unit DNase I per reaction (lanes 15-18). The molar ratios between the Piccolo NuA4 complex and the sample (DNA or NCP) were 1:1, 3:1, and 10:1, respectively. The numbers listed on the left column of the gel picture are nucleotide positions related to the marker in lane 1, while the numbers on the right are the helical turns relative to the dyad at nucleotide position 83. The footprinted areas are marked with vertical lines, which are labeled as a, b, c, and d.

Lastly, the Piccolo NuA4 complex conferred some nucleosome protection in the DNase I footprinting assay. DNase I footprinting results performed in the context of the NCP are shown in Figure **C-3** lanes 15 to 18. Comparing DNase I digestion on the NCP itself (lane 15) and the NCP digestion in the presence of the Piccolo NuA4 complex (lanes 16 to 18), I noticed that the presence of the Piccolo NuA4 complex altered the digestion pattern of DNase I digestion on the nucleosome. Some minor nucleosome protections, which were located between the major digested bands, can be observed at 85-80 (a), 76-72 (b), 53-49 (c), and 46-39 (d) (Figure **C-3**). The nucleosome protection at the nucleotide positions 76-72 (b) appeared to be the weakest, while protection at the nucleotide positions 46-39 (d)—with an exception of one nucleotide band in the area—seems to be the strongest footprinted area (Figure **C-3**). By counting the number of nucleotide bands relative to the Sac I digested band at the basepair position 105, I estimated those two regions, a and d, to be at around the dyad (0) and the 4^{th} helical turn, respectively (Figure **C-3**). To help locating the helical turn positions of those regions within the NCP, the counted nucleotide positions were placed in the context of the DNA that wraps around the histone octamer (Figure **C-4**). My results in Figure **C-3** lanes 16-18 suggest those footprinted areas might be positioned within major grooves of the DNA because those protected areas were weakly digested by the DNase I. Moreover, it has been shown that the DNase I enzyme positions to a minor groove of the B form DNA (Suck et al., 1988). Thus, minor grooves of the DNA should be prominent targets of the DNase I enzyme. However, based on my estimated nucleotide locations, it appeared that those protected areas were positioned within the minor grooves (Figure **C-3** and

Figure **C-5**). It is possible and very likely that the positions determined from the counting method were inaccurate. Nonetheless, my DNase I footprinting results suggest that the Piccolo NuA4 complex might bind to either around the dyad or the approximately four helical turns away from the dyad where the N-terminal tail of H2A is located (Figure **C-5**).

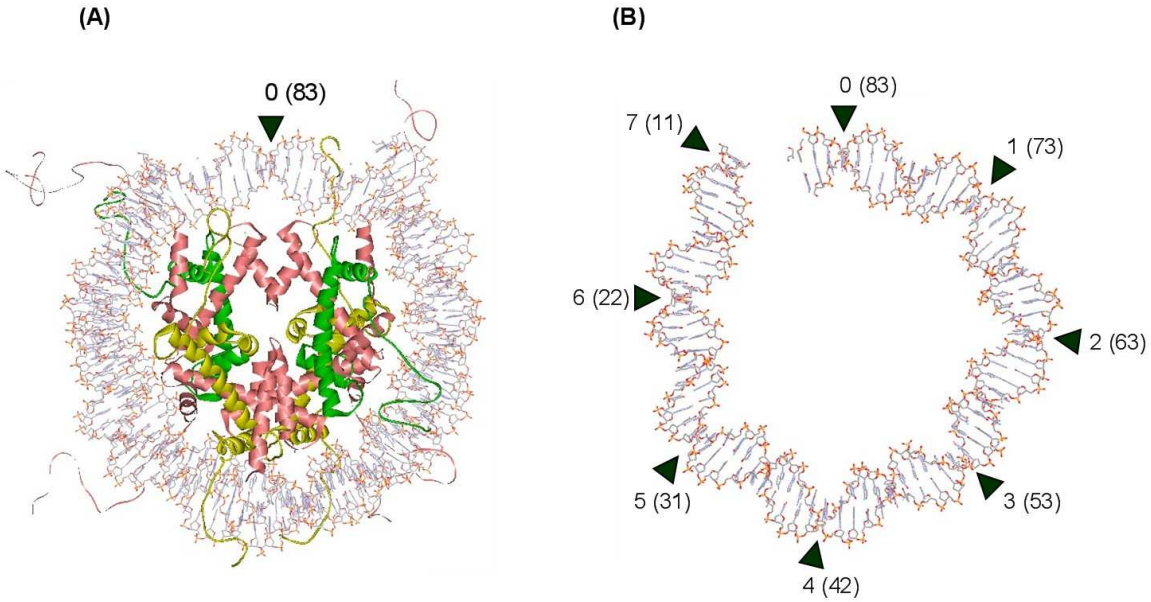

Figure **C-4**: Estimated nucleotide positions in the nucleosome core particle (NCP).

(A) The structure of the NCP (Davey et al., 2002) shows the position of the dyad (0), which would be in equivalent to the basepair position 83 in the NucB nucleosomal DNA sequence used for the nucleosome reconstitution. Histone H2A is shown in yellow, while histone H4 is shown in green. (B) Half of the DNA from (A) is shown. The number from 0 to 7 in the clockwise direction refers to the number of helical turns from the dyad, and the number in parenthesis indicates the number of basepair position in the 165 NucB nucleosomal DNA sequence. The WebLab ViewerLite program was used to manipulate the structure (1KX5).

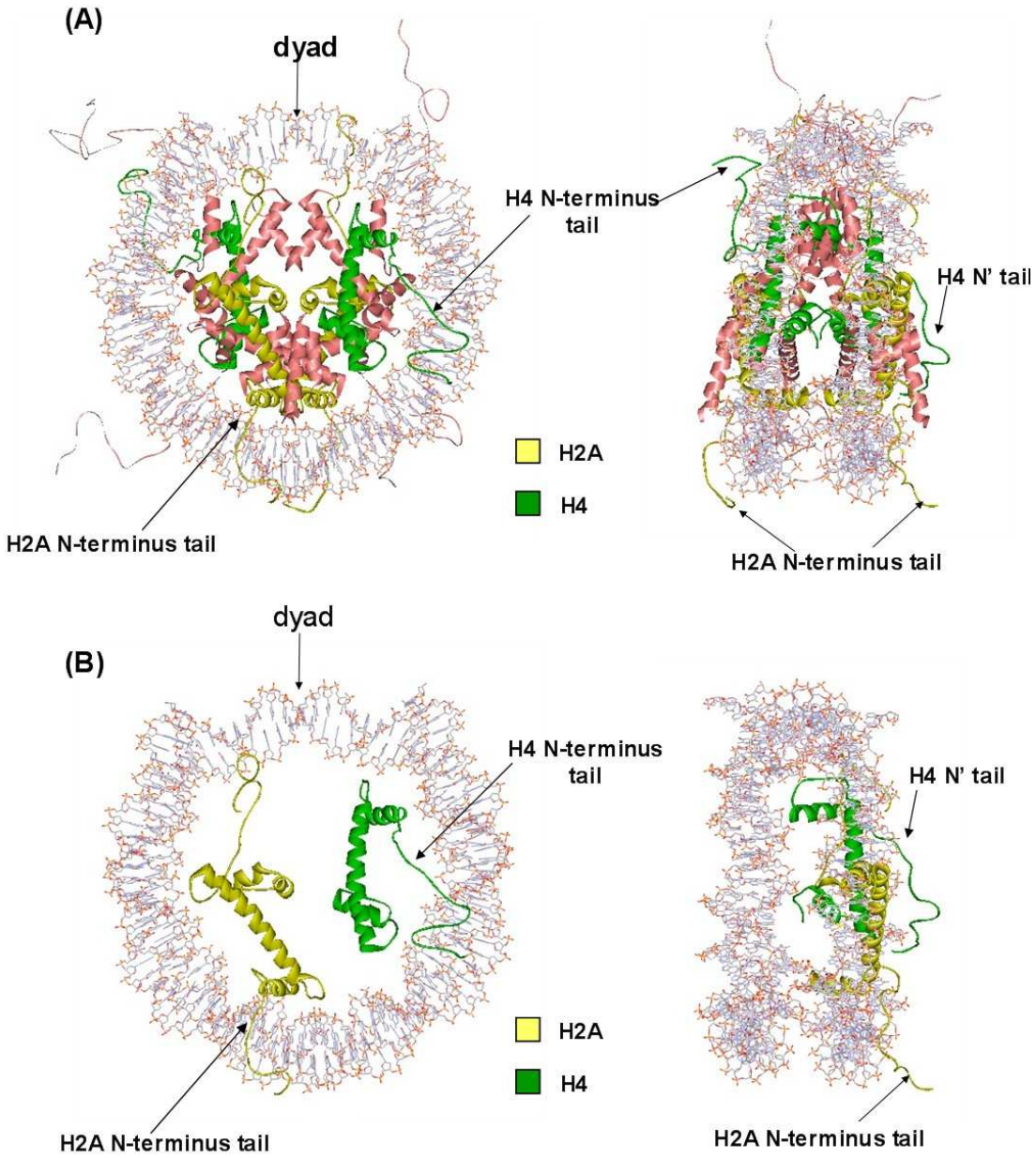

Figure **C-5**: Locations of the N-termini of histone H2A and H4 in the nucleosome core particle.

(A) Structure of the nucleosome core particle at 1.9 Å (Davey et al., 2002) and the positions of the N-termini of histone H2A (yellow) and H4 (green). Other core histones are shown in red. The right panel is the same structure but rotated 90° horizontally. (B) The same structure as (A) but showing only the locations of one histone H2A and H4 in relative to the DNA. The structure of the nucleosome (1KX5) was manipulated with the WebLab ViewerLite program.

C.2.2 The ‘One-pot’ assay

Although the results from the DNase I footprinting assay were interesting, most of the interpretations were made based on assumption and speculation. Therefore, a different assay would be needed to support the data from the DNase I footprinting assay. The group of Travers has developed the ‘One-pot’ assay as a tool to determine the accessibility of the DNA at various positions on the nucleosome structure (Wu and Travers, 2004). This assay has both similarities to, and differences from, the DNase I footprinting assay. In both assays, the accessibility of the DNA is determined by the ability of an endonuclease to digest the DNA. However, the ‘One-pot’ assay relies on the use of a certain restriction enzyme, rather than a general nuclease like the DNase I enzyme. Wu and Travers utilized an artificial, well positioning nucleosomal DNA sequence, called the 601.2 sequence, which was developed by the group of Widom (Anderson et al., 2002), to analyze the accessibility of the DNA. The nucleosomal 601.2 DNA sequence is shown in **C.4.9**. In this technique, the HaeIII restriction digestion site was created by the PCR mutagenesis at various positions related to the dyad of the nucleosome structure. Eight different plasmids, each contains a HaeIII site at the dyad, -1, -2, -3, -4, -5, -6, or -7 helical turns away from the dyad. All eight plasmids were simultaneously amplified by the same primer pair to create a heterogeneous mixture 601.2 dyad sequences, which were further reconstituted into nucleosomes. Those nucleosomes were digested by the HaeIII restriction enzyme, which digests each of the nucleosomes at a single position where the engineered HaeIII site is located. As a result, the 8-ladder digested bands can be observed in a sequencing gel. The scheme of how this ‘One-pot’ assay works is summarized in Figure **C-6**.

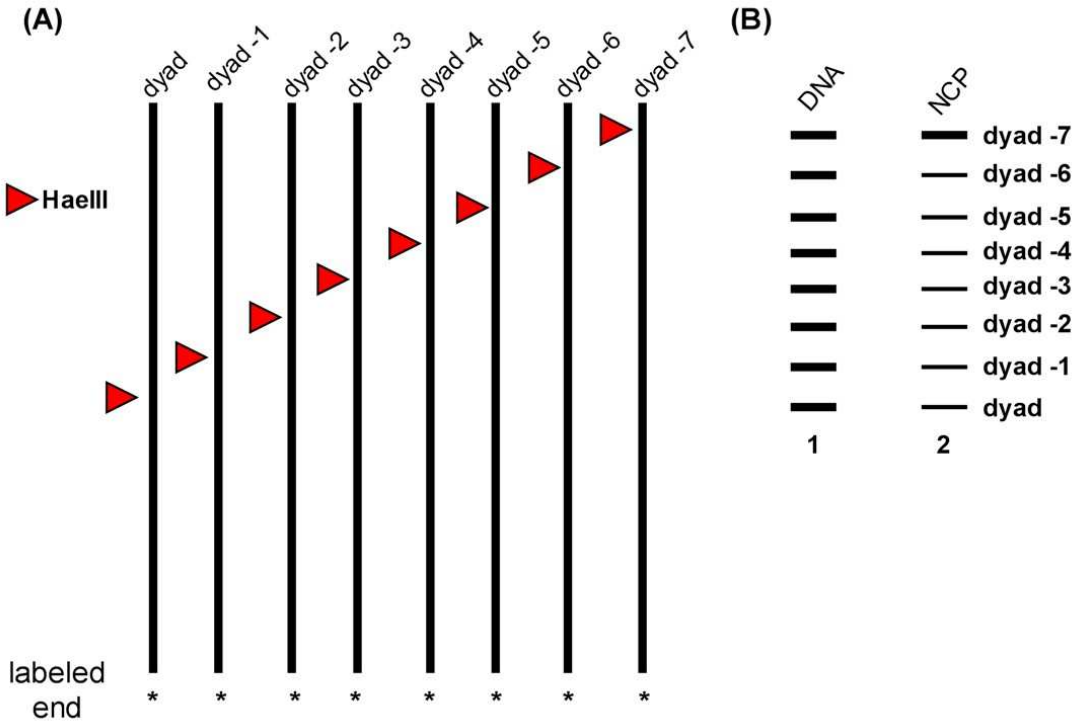

Figure **C-6**: Cartoon to show how the 'One-pot' assay works.

(A) Each DNA is radiolabeled with the PCR mediated method (the labeled end is marked by the asterisk). Each of them has one HaeIII site at different positions from the dyad of the 601.2 nucleosomal DNA sequence. Thus, the HaeIII enzyme will digest each DNA piece at a different position. (B) Expected results from digestion of those 8 PCR products and a mixture of nucleosome reconstituted with those PCR products are shown in lane 1 and lane 2, respectively. HaeIII digestion results of DNA on the nucleosomes are expected to be in a lesser intensity than that from the free DNA since the overall accessibility of the DNA is limited by the presence of the histone octamer.

The 'One-pot' assay was performed similarly to what was described for the DNase I footprinting assay. Either free DNA or NCP was incubated with an increasing concentration of the Piccolo NuA4 complex. An aliquot of the reaction mixture was subjected to a gel shift assay to confirm the interaction between the Piccolo NuA4 complex and the free DNA or NCP. As shown in Figure **C-7**, the Piccolo NuA4 complex was able to gel shift either free DNA or the NCP, consistent with the results in Figure **C-2**.

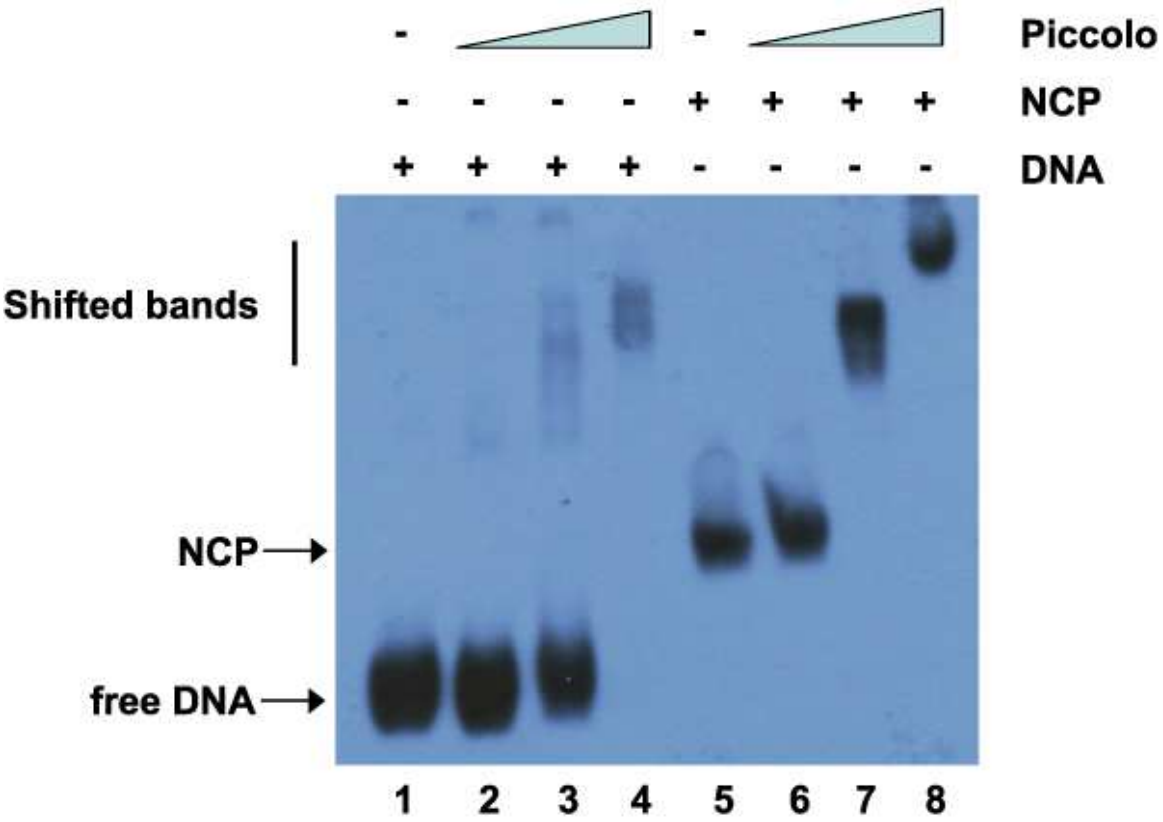

Figure **C-7**: Gel shift of the reaction mixtures for the 'One-pot' assay.

The gel shift samples were prepared as part of the 'One-pot' assay. The gel shift experiment was performed with free DNA (lanes 1-4) and NCP (lanes 5-8). The ratios between the Piccolo NuA4 complex to NCP or to DNA were increased from 1:1 to 3:1 and 6:1. The sample was electrophoresed with a 5% native polyacrylamide gel, dried, and exposed to an X-ray film.

For the 'One-pot' assay, I added 1 µl of the 50 Units/µl HæIII restriction enzyme to a 10-µl reaction to digest the free DNA or NCP at room temperature for 10 minutes. The digestion time with the HaeIII enzyme should be minimized to reduce the chances of nucleosome-Piccolo NuA4 complex dissociation and re-association. Based on optimization, the 10-minute digestion was found to be the least amount of time required for the assay. Like the DNase I footprinting assay, the digestion was terminated by the addition of 50 µM EDTA. Then, 10 µl of Formamide dye were added to each sample, which was subsequently boiled for 2 minutes. Samples were electrophoresed on a 6%

denaturing polyacrylamide gel. In the free DNA set, one should expect to see an 8- band ladder on the gel as a result of the digestion of different DNA fragments that contain different positions of the HaeIII sites. In the NCP set, the same pattern of the ladder should be expected with a lesser intensity since the DNA was being protected by the histone octamers within the nucleosomes.

The results from the 'One-pot' assay are illustrated in Figure **C-8**. Although the five digested bands from the bottom (dyad, dyad -1, dyad -2, dyad -3, and dyad -4) could clearly be seen, the rest of the digested bands were clouded by smudges in the gel. The locations of dyad -5, dyad -6, and dyad -7 bands were predicted based on a different gel (Figure **C-8** B). I speculate that the smudge and some higher molecular weight bands were the results of non-specific PCR products, which I could not observe from the exposure with the X-ray film (Figure **C-7** lane 1).

The results from the 10 and 30 minute digestions at room temperature did not confer a clear nucleosomal protection by the Piccolo NuA4 complex. However, these results were not necessary inconsistent with the DNase I footprinting results because I observed only minor protections from the Piccolo NuA4 complex in the DNase I footprinting assay. The Piccolo NuA4 complex still bound to the NCP (Figure **C-8**), and allowed the HaeIII restriction enzyme to gain access to the DNA. Thus, for this aspect, the 'One-pot' assay might not be the best technique to determine the accessibility of the DNA in the NCP complex. On the other hand, the fact that I was not able to obtain clean digestion results suggests that optimization of the technique is required. However, considering the results I obtained from the DNase I footprinting experiment, I speculate that the results would not have been changed even with the best optimized 'One-pot' assay.

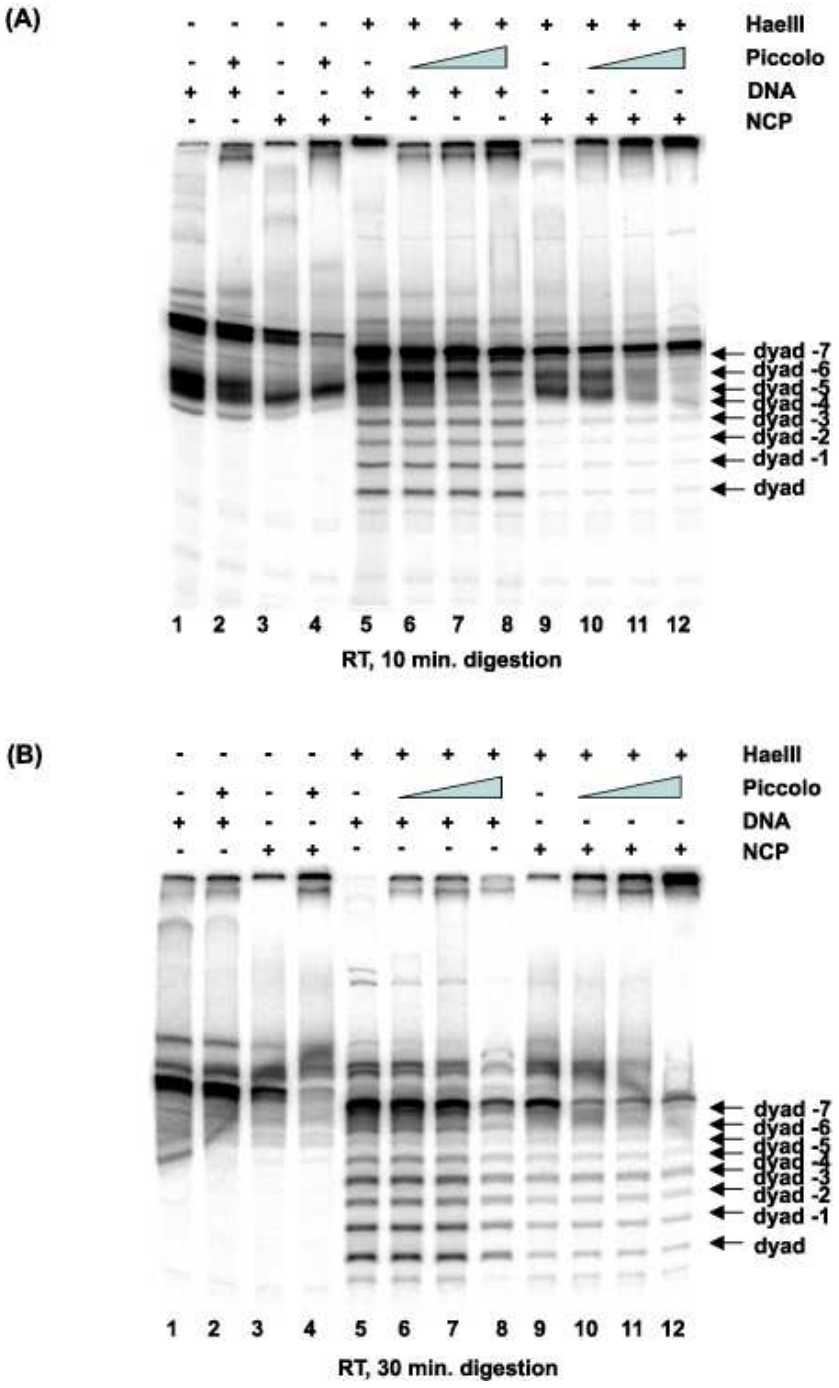

Figure **C-8**: The 'One-pot' assay does not reveal nucleosomal protection by the Piccolo NuA4 complex.

(A) The digestion with 50 Units HaeIII restriction enzyme per reaction was performed at room temperature for 10 minutes. (B) Same as (A) but the digestion time was 30 minutes at room temperature.

C.3 Discussion

C.3.1 Features of the nucleosomes that might interact with the Piccolo NuA4 complex

We have shown by the Sedimentation ultracentrifugation that the Piccolo NuA4 complex and the nucleosome associate in a 1:1 stoichiometry (Will Selleck's unpublished results). In other words, only one molecule of the Piccolo NuA4 complex binds to one molecule of the nucleosome complex at a given time. My data suggest two strongest nucleosomal locations where the interactions with the Piccolo NuA4 complex might take place: the DNA at a location near the dyad and the 4^{th} helical turn from the dyad. The Piccolo NuA4 complex might interact with the nucleosome in either of those locations. In addition, my data also suggest that the interaction appears to be located at the major grooves where the DNase I is less accessible compared with the minor grooves. It is important to note that these locations were based on estimation, which itself contains errors. Moreover, I assumed that the dyad of this nucleosome passed through the basepair position 83. If the actual dyad were shifted, the interpretation of the data would definitely be changed.

My DNase I footprinting analysis suggests possible regions on the NCP which are occupied by the Piccolo NuA4 complex. Although the Piccolo NuA4 complex can nonspecifically interact with free DNA, this does not mean that all the interaction that occurs in the context of nucleosomes is only mediated through the DNA. At least some direct contacts with the histone tails are made by Piccolo NuA4 subunits, such as a direct contact between the HAT domain of the Esa1 and the histone H4 and H2A tails. Because the Piccolo NuA4 complex in yeast plays a role in the global histone H4 and H2A acetylation (Boudrealut et al., 2003), it can be inferred that the Piccolo NuA4 complex does not employ a specific DNA sequence for the nucleosome interaction. But one could speculate that the relative position of histones dictates the binding orientation and

positions of the Piccolo NuA4 complex. Figure **C-4** illustrates the positions of the N-terminal tails of both histone H4 and H2A, which are the targets of the Piccolo NuA4 acetylation. It is possible that the H4/H2A core histones mediate the binding orientation of the Piccolo NuA4 complex. It is important to note that the region of the DNA on nucleosomes where the Piccolo NuA4 complex makes contact is not necessarily the region where the acetylation occurs. The Esa1 subunit of the Piccolo NuA4 complex functions as a catalytic subunit, but by itself does not acetylate or interact with nucleosomes (Boudreault et al., 2003; Selleck et al., 2005). The DNA interaction seems to be at least conferred by the Epl1 subunit (Boudreault et al., 2003). In addition, the Esa1 and the Yng2 subunits do not physically interact (Selleck et al., 2005). Together, I propose a model to explain how the Piccolo NuA4 complex might possibly interact with a nucleosome, and only the structural information of the nucleosome complex is available (Figure **C-9**). In this model, the Epl1 subunit of the Piccolo NuA4 complex makes a direct contact with the DNA. The HAT domain of the Esa1 subunit that directly interacts with the Epl1 through the conserved EPcA is positioned toward the histone H4 tail of a nucleosome (Figure **C-9**). In contrast, the N-terminal tails of the histone H2A that are located near the 4^{th} helical turn from the dyad (the Piccolo footprinting site) can only be acetylated when the Piccolo NuA4 complex binds at around the dyad area (Figure **C-9**).

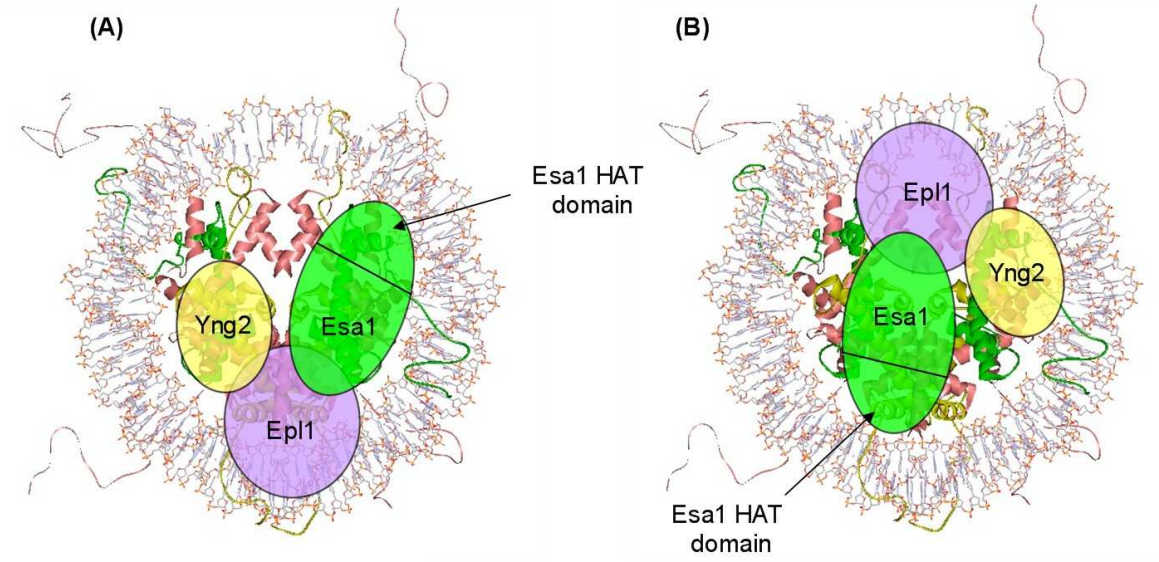

Figure **C-9**: A model of how the Piccolo NuA4 complex might bind to a nucleosome to acetylate histone H2A and H4.

(A) Through the Epl1 subunit, which was shown to be sufficient for the interaction with nucleosomes (Boudreault et al., 2003), the Esa1 subunit is able to "reach" the H4 tail for acetylation. In this picture, the Epl1 makes contact with the DNA at approximately 4 helical turn position from the dyad. (B) The same Piccolo NuA4 complex is turned upside down so that the Piccolo NuA4 complex footprints the nucleosome at around the dyad position. In this case, the Esa1 in the Piccolo NuA4 complex can acetylate the histone H2A tail. This model does not depict the protein-protein interactions between the Piccolo NuA4 complex and the nucleosome, or the accurate size of the Piccolo NuA4 subunits. In addition, it does not explain why the binding of the Piccolo NuA4 complex to the nucleosome is in 1:1 stoichiometry. The WebLab ViewerLite program was used to manipulate the nucleosome structure (1KX5).

This model should be further tested. If one of the Piccolo NuA4 binding sites could somehow be blocked by the presence of certain protein factors or molecules, then the Piccolo NuA4 complex should lose its ability to acetylate certain histones. For example, if the binding site near the N-terminal tails of histone H2A is blocked, then the Piccolo NuA4 complex may lose the ability to acetylate histone H4. This model, however, does not explain why the Piccolo NuA4 complex associates with the nucleosome in a 1:1 stoichiometric fashion. The binding of a Piccolo NuA4 complex might interfere with the binding of a second Piccolo NuA4 complex on the same nucleosome. Understanding the

precise mechanisms by which the Piccolo NuA4 complex binds to a nucleosome remains an interesting task.

C.3.2 Problems associated with the DNase I footprinting assay

Although my DNase I footprinting study suggests the locations on the nucleosome which might be in contact with the Piccolo NuA4 complex, many problems from the assay and the experimental procedures do exist and cannot be denied. I will discuss some of the problems which have or have not been solved such as the problem with some non-specific nuclease activity and the problem with the G-tracking technique. In addition, purification of the reconstituted nucleosomes might be important to obtain cleaner results. I will also discuss some additional ideas that could be use to further contribute to our understanding of how the Piccolo NuA4 complex interacts with the nucleosome.

First, I did observe some nuclease activity in a negative control set without DNase I. Levels of non-specific degradation were low but significant enough to be observed in the phosphorimager scan. Degraded DNA could potentially interfere with interpretation of the results. Experiments using autoclaved tips and previously heated solution, which should eliminate some contaminated nuclease activity, were unable to reduce non-specific degradation of free DNA. Perhaps these non-specific nuclease activities were associated with the Formamide dye solution. I found that the non-specific nuclease activity was maximized if no EDTA was added prior to the addition of the Formamide dye. Furthermore, a low concentration of the EDTA (i.e. at 10 or 20 mM) was not sufficient to eliminate non-specific nuclease activities. However, if the concentration of the EDTA was 50 mM, much of the non-specific nuclease activity was diminished or minimized. Therefore, I utilized the 50 mM EDTA concentration to stop the DNase I footprinting reaction and improve the background in my negative controls.

Besides the problem with the non-specific nuclease, I experienced an unrelated problem associated with the markers. The Maxum-Gilbert cleavage at G-residues (G-tracking) was inaccurate and ambiguous. As discussed in **C.2.1**, I was not able to match the G-tracking results with the accurate locations of all G residues within the DNA sequence. There may have been many problems with the procedures. For example, if the DNA methylation by dimethyl sulfate (DMS) was not completed, this would result in an incomplete digestion of all available G residues. In order to obtain more accurate DNA markers, other degradations of the Maxum-Gilbert such as A+G or C the G-tracking should be performed in parallel with the G-tracking. In addition, the more accurate enzyme-based DNA sequencing technique, the dideoxy-mediated chain-termination method (Sanger and Coulson, 1975), could be performed. This way, a more accurate position of the protected areas could be determined.

The two problems listed above (non-specific nuclease activity and the problem with the markers) could easily be solved. However, one very important experimental procedure that I have not performed was the purification of the reconstituted nucleosomes from the excess radiolabeled free DNA. Because the nucleosome reconstitution was performed on a small scale and without further purification, some free radiolabeled DNA could have contaminated the reconstituted nucleosomes. And because the radiolabeled free DNA is more accessible to the DNase I enzyme, any nucleosomal protection conferred by the Piccolo NuA4 complex might not be observed since the footprinted area might be masked by the digestion of naked DNA. This problem might not be a concern to my experiment since I observed some nucleosomal protection from the Piccolo NuA4 complex. However, the nucleosome purification might improve the quality of the results—I might be able to observe a better 10 basepairs bands ladder from the DNase I digestion on the nucleosome itself. The nucleosome purification could be conducted with glycerol gradient centrifugation (Perlmann and Wrange, 1988) or with a preparative gel electrophoresis (Luger et al., 1997).

Future experiments could be performed to help the understanding of how the Piccolo NuA4 complex interacts with nucleosomes. As mentioned above, the purification of the reconstituted nucleosomes may be necessary for a better result. Furthermore, changing a DNA piece used for nucleosome reconstitution might confer a better result. For example, it has been shown that 146 basepair DNA derived from the 5 S RNA gene produces a well positioned nucleosomes and well defined 10 basepairs bands ladders (Luger et al., 1997). In addition to the 5 S RNA gene sequence, the artificial 601.2 sequence (Anderson et al., 2002), which has a strong preference toward a nucleosome formation, should also be tested.

In addition, the protein-protein interaction between the histones and the Piccolo NuA4 complex should also be considered. To analyze the protein-protein interaction, certain cross-linking assays might be performed. The idea of these experiments would be similar to the cross-linking experiment between the TBP and the SAGA complex described in Chapter 2. The experimental design involves using one complex as a bait (i.e. the nucleosome complex) to catch a prey within the other complex (the Piccolo NuA4 complex). The bait (i.e. the nucleosome complex) has to be labeled by a specific cross-linker molecule such as a cross-linking agent specific to the sulfhydryl (-SH) group of the cysteine. This way, the cross-linking reaction on the prey complex (the Piccolo NuA4 complex) can be performed. Because the Piccolo NuA4 complex contains too many cysteine residues, a conjugation on this complex might not be feasible. On the other hand, there exists one cysteine residue within the histone fold domain of the histone H3 peptide. However, it appears that this cystenie residue is hidden and inaccessible within the structure. Therefore, a site-specific mutagenesis to convert some surface residues on the histones to cysteine might be required. A site-specific mutated histone protein can be purified and reconstituted into nucleosomes. Conjugation of this residue can be performed and purified. A cross-linking reaction between the modified nucleosome and the Piccolo NuA4 complex can be conducted and determined which of the Piccolo NuA4 subunits is in a close proximity to the specific nucleosome position.

C.3.3 Problem associated with a 'One-pot' assay

The 'One-pot' assay does not reveal insight into how the Piccolo NuA4 and nucleosome complexes interact. I reason that the Piccolo NuA4 only binds to a small region of the DNA on nucleosomes which are not sufficient to confer a protection from the HaeIII restriction enzyme. One significant contrast between this assay and the DNase I footprinting assay is that the 'One-pot' assay relies on a certain endonuclease (the HaeIII in the assay), which digests at a very specific site. While the specificity could be useful for some applications, the amount of time required for the 'One-pot' assay reaction is approximately ten times longer than that in the DNase I footprinting assay. It is possible that during the digestion with the HaeIII, the Piccolo NuA4 complex dissociates from one nucleosome and re-associates with another. Thus, the protection pattern might not be observed even though the Piccolo NuA4 complex protects a nucleosome at a precise location.

The problem associated with smudges as well as some high molecular weight DNA contaminants should be considered. After the PCR reaction, the PCR products were purified only with the phenol/CIA and CIA extractions, followed by a spun column with the G-25 medium resin. Although these purification steps could eliminate much of the free nucleotides and the DNA polymerase, they did not purify away some non-specific PCR products. I have optimized the PCR reactions and did not observe non-specific PCR products upon exposure to an X-ray film. However, those non-specific PCR products might still be present at an intensity too low to be detected by limited exposure to an X-ray film. An additional gel purification of the PCR products might be a necessary step which improves the purity of the DNA. Gel purification of the PCR product should eliminate many of those contaminants observed in the denaturing gel. One drawback of gel purification is that some PCR product could have been lost during purification procedures. However, better quality results outweigh the loss of some DNA.

C.4 Materials and methods

C.4.1 Purification of core histones from the *Xenpous laevis*

Each recombinant core histone from *Xenopus laevis* was overexpressed and purified as described (Luger et al., 1999). Transformation and overexpression of the core histone proteins procedures were performed in the BL21(DE3)pLysS *Escherichia coli* cells in the same manner described in **2.5.1**. Cells expressing a core histone protein from a 6-liter culture were resuspended in 150 ml T100 buffer (20 mM Tris-Cl pH 8.0, 100 mM NaCl, 0.5 mM EDTA, 1 mM benzamidine, and 10 mM 2-mercaptoethanol) and stored at -80°C.

A 1670-ml Sephacryl S300 column (XK 50/100, Amersham Pharmarcia Biotech) was pre-equilibrated with 2 liters of AU200 buffer (20 mM NaAc pH 5.2, 0.5 mM EDTA, 10 mM 2-mercaptoethanol, 200 mM NaCl, and 8 M Urea). Column chromatography was executed at a flow rate of 3 ml/minute overnight. The next day, cells expressing a core histone were thawed, and equally divided among four 100 ml sized glass beakers. Cells were sonicated at 70% power output for 3 repeats of 14 pulses (0.5 second on and 0.5 second off) using the Branson Digital Sonifier (450D). The sonicated cells were centrifuged at 18,000 rpm in a SS34 rotor for 30 minutes at room temperature. The pellet, which contains the histone protein in inclusion bodies, was resuspended in a total of 180 ml TRITON buffer (20 mM Tris-Cl pH 8.0, 0.5 mM EDTA, 100 mM NaCl, 10 mM 2-mercaptoethanol, 1 mM benzamidine, and 1% TRITON X-100). The resuspended pellet was centrifuged at 15,000 rpm in a SS34 rotor for 10 minutes at room temperature. The resuspension of the pellet was repeated for additional 3 times. Finally, the pellet was resuspended in a total of 50 ml WASH buffer (20 mM Tris-Cl pH 8.0, 0.5 mM EDTA, 100 mM NaCl, 10 mM 2-mercaptoethanol, and 1 mM benzamidine) and centrifuged at 15,000 rpm for 10 minutes. The supernatant was discarded, and the pellet was mixed with 1 ml dimethyl sulfoxide (DMSO) and incubated for 30 minutes at room temperature. Then, the pellet was homogenized with a dounce homogenizer (type B glass pestle) in 30

ml TG0 buffer (20 mM Tris-Cl pH 8.0, 10 mM DTT, and 7 M Guanidine-HCl). 20 ml of additional TG0 was added to the homogenized pellet and mixed. The sample was centrifuged at 15,000 rpm in a SS34 rotor for 20 minutes to separate the insoluble portion before loading onto the pre-equilibrated Sephacryl S300 gel filtration column. The chromatography over the Sephacryl S300 column was performed at a flow rate of 3 ml/minute. The histone protein was fractionated with approximately 2 liters of AU200 buffer while 15 ml fractions were collected. Peak fractions were analyzed by the Sodium dodecyl sulphate Polyacrylamide Gel Electrophoresis (SDS PAGE).

The histone protein containing fractions having the fewest contaminants were combined and further purified with the cationic exchange Source S10 HPLC column (Pharmacia Biotech) on the BioCAD Sprint HPLC System (PerSeptive Biosystems, Inc). The overall histone concentration was estimated by measuring the absorption at 280 nm UV. Typically, 100-200 mg of a histone protein is obtained from a 6-liter culture. For purification with the Source S10 HPLC column, no more than 50 mg of histone was loaded onto the column per chromatographic run. Each core histone was purified with a different salt gradient made with buffer A, AU200 pH 5.2 and buffer B, AU600 pH 5.2. For example, histone H3 was eluted with a 14 column volume (CV) linear gradient from 0% B to 70% B. Histone H2A was eluted with a 17.6CV linear gradient from 16% B to 60% B. Histone H2B was eluted with a 18CV linear gradient from 5% B to 50% B. Lastly, histone H4 was eluted with a 15CV linear gradient from 21% B to 77% B. HPLC fractions were analyzed by SDS PAGE. Peak fractions were pooled and dialyzed against at least 4 changes of 2 liters of 5 mM 2-mercaptoethanol to eliminate the urea. Histone protein was lyophilized to completeness, which would usually take a few days. The lyophilized histone protein was re-dissolved in a total of 10 ml MilliQ water. The overall concentration of the histone was determined by measuring the 276 nm UV absorption of 1:25 diluted histone in AU200 buffer. Approximately 4-4.5 mg of histone protein was aliquoted in 2 ml sized cryotubes, which were lyophilized before storing at -80°C.

C.4.2 Histone octamer preparation.

Each lyophilized core histone protein was dissolved in 600 µl unfolding buffer (20 mM Tris-Cl pH 7.5, 10 mM DTT, and 7 M guanidine-HCl) and incubated at room temperature for 15 minutes. After incubation, an additional 600 µl unfolding buffer was added, followed by a 20-minute incubation at room temperature to let the histone protein fully dissolved. Then, the last aliquot of 600 µl unfolding buffer was added again to each core histone. The final concentration of each histone was determined by the UV absorption. Then, an equal molar of each core histone was added to a 15 ml Falcon tube, and the overall concentration of the histone proteins was adjusted to 1 mg/ml with an unfolding buffer. The histone proteins mixture was dialyzed in a 7 kDa cutoff dialysis tubing against 2 liters of cold refolding buffer (10 mM Tris-Cl pH 7.5, 1 mM EDTA, 5 mM 2-mercaptoethanol, and 2 M NaCl) for 3 hours at 4°C to allow for histone octamer formation. The refolding buffer was changed twice for two additional dialyses: one for 3 hours and another for at least 12-hour dialysis or over night.

A 125-ml HiLoad 16/60 Superdex 200 gel filtration column was equilibrated with 130 ml refolding buffer at a flow rate of 1 ml/minute. The reconstituted histone octamer was centrifuged at 15,000 rpm in a SS34 rotor for 20 minutes at 4°C. The sample was subsequently concentrated to about 1 ml using 10,000 kDa cutoff Vivaspin (Vivascience) and loaded onto the HiLoad Superdex 200 gel filtration column at 1 ml/minute flow rate. The histone octamer was fractionated at a flow rate of 1 ml/minute with a total of 130 ml refolding buffer while collecting 1 ml fractions. Peak fractions were analyzed with the SDS PAGE. The fractions containing histone octamer were combined, and the concentration determined by measuring the absorption at 276 nm UV. (1 A_{276}=0.45 $(mg/ml)^{-1}cm^{-1}$). The histone octamer was mixed with 20% glycerol, aliquoted, and stored at -80°C.

C.4.3 Nucleosome reconstitution

The DNA fragment that was used in the DNAse I footprinting assay contains 165 basepairs of the nucleosome B (NucB) sequence of the mouse mammary tumor virus (MMTV) that had been digested with EcoRI and BspEI enzymes. The EcoRI (GAATTC) and BspEI (TCCGGA) sites are located at the 5' and 3' ends of the sequence, respectively. The sequence of the NucB DNA is shown below.

5'-**GAATTC**GATATCAGTAAGTTTTTGGTTACAAACTGTTCTTAA
AACGAGGATGTGAGACAAGTGGTTTCCTGACTTGGTTTGGTATC
AAAGGTTCTGATCTGAGCTCTGAGTGTTCTATTTTCCTATGTTCT
TTTGGAATTTATCCAAATCTTAGATATC**TCCGGA-3'**

A 100-µl reconstitution mixture (3 µM NucB DNA, 3.3 µM histone octamer, 2 M KCl, 10 mM Tris-Cl pH 7.5, and 0.5 mM DTT) was prepared. Typically, the concentration between the DNA and the histone octamer should be at 1:1 molar ratio. Based on a titration experiment, the 1:1 DNA per histone octamer molar ratio yielded no precipitation but had some excess free DNA after reconstitution, while the 1:1.1 DNA per histone octamer molar ratio has the least precipitation and the lowest amount of free DNA after reconstitution. Therefore, I used this 1:1.1 DNA per octamer molar ratio. The reconstitution mixture was dialyzed to decrease the salt concentration in consecutive 2-hour steps against refolding buffers (20 mM Tris-Cl pH 7.5, 1 mM DTT, and 1 mM EDTA) that contain 2 M, 0.85 M, 0.65 M, and 0.5 M KCl, respectively. The last dialysis was performed with the buffer without KCl (20 mM Tris-Cl pH 7.5, 0.1 mM DTT, and 0.1 mM EDTA) for 8-12 hours or over night. Any precipitation resulting from dialysis can be removed from the reconstituted nucleosomes by centrifugation. The concentration of the reconstituted nucleosome core particle (NCP) obtained from dialysis was calculated, and the NCP was stored at -80°C with glycerol added to 20%.

C.4.4 Radiolabeling of free DNA and NCP

Because the 165-basepair NucB DNA had been previously digested with the EcoRI and BspEI enzymes, it contained the 5' overhang sequence, which could be used for the specific end labeling with the Klenow polymerase. The end labeling was performed with α-^{32}P dATP, which was incorporated into the EcoRI site. For labeling the NCP, a 100-µl reaction mixture that contains 1x NEBuffer 2 (BioLabs), 1 mM DTT, 0.33 mM dCTP, 0.33 mM dGTP, 0.33 mM dTTP, 50 µCi α-^{32}P dATP, 0.7 µM NCP, and 5 units Klenow enzyme (BioLabs) was incubated at room temperature for 15 minutes. Labeling of the free DNA was also performed with 0.7 µM 165-basepair NucB DNA with the same ingredients and procedures. After a 15-minute incubation, cold (non-radioactively labeled) dATP was added to the reaction mix to a final concentration of 0.33 mM and further incubated for 5 minutes. To stop the labeling reaction for the NCP, the sample was incubated at 60°C for 30 minutes and subsequently purified with a Sephadex G-25 Medium (Amersham Pharmacia Biotech) spun column. As for the free DNA, one extraction of the Phenol/CIA (1:1 mixture of TE (10 mM Tris pH 8.0 and 0.1 mM EDTA)-equilibrated phenol and CIA) and another with the CIA (a mixture of 24 volumes chloroform with 1 volume of isoamyl alcohol) was performed to remove the Klenow enzyme. To check the labeling, an aliquot of free DNA and the NCP was analyzed with a 5% native DNA polyacrylamide gel (5% of 60:1 acrylamide:bis-acrylamide and 0.25x Tris-boric acid-EDTA or TBE). The gel was pre-electrophoresed at 10 Watts for 20 minutes before the actual electrophoresis of the samples at 5 watts for 10 minutes. The gel was fixed with a fix solution (45% ethanol and 10% acetic acid) and subsequently dried for 1 hour at 90°C before exposing to an X-ray film.

C.4.5 Limited cleavage at G-residues (G-tracking)

With a screwed-capped Eppendorf tube, 5 µl of end-labelled DNA fragment was added to 200 µl of DMS reaction buffer (50 mM sodium cacodylate pH 8.0, 0.1 mM EDTA).

Then, 1 µl of Dimethyl sulfate (DMS) was added to the sample and incubated at room temperature for 10 minutes. The reaction was stopped by the sequential addition of 50 µl MGS2 solution (1 M NaAc and 1 M 2-mercaptoethanol), 2 µl of 2.5 mg/ml sonicated calf thymus DNA, and 750 µl ethanol. The sample was vortexed briefly and centrifuged for 10 minutes at room temperature. The supernatant was discarded in a waste bottle while the DNA pellet was resuspended in 250 µl 0.3 M NaAc (no pH adjusted), followed by the addition of 750 µl ethanol. The sample was vortexed and centrifuged to isolate the pellet. The resulting pellet was subsequently resuspended in 100 µl of 1.0 M freshly diluted piperidine, and incubated in a 90°C water bath for 30 minutes. After incubation, the sample was centrifuged for 1 minute to remove any precipitates, and the supernatant was transferred into a new tube. DNA in the solution was precipitated by the addition of 10 µl 3 M NaAc pH 5.2 and 275 µl ethanol. The tube was vortexed briefly and centrifuged for 10 minutes at room temperature to pellet the precipitated DNA. The DNA pellet was washed with 300 µl cold 70% ethanol and air dried. The DNA was finally resuspended in an appropriate volume of Formamide dye and typically contained between 1000 to 5000 cpm/µl of the Formamide dye.

C.4.6 DNAse I footprinting

The DNase I footprinting experiment was performed with the free DNA only, the free DNA with a titration of the Piccolo NuA4 complex, the NCP only, or the NCP with a titration of the Piccolo NuA4 complex. The experiment with the radiolabeled free DNA (NucB DNA) was done as following. A 25-µl reaction mixture which contained 0.11 µM radiolabeled DNA, 25 mM Tris-Cl pH 7.5, 50 mM NaCl, 2 mM $MgCl_2$, and the Piccolo NuA4 complex at 0, 0.11, 0.33, or 1.1 µM was incubated for 1 hour at 4°C. After the incubation, 1 µl of the DNase I enzyme at 0.05 or 0.1 Unit/µl in 25 mM Tris-Cl pH 7.5 was added to a 9-µl aliquot of the reaction mixture. The rest of the reaction mixture was subjected to a gel shift analysis (**C.4.7**). The DNase I digestion reaction proceeded for 1 minute at room temperature, and was terminated by the addition of 50 µM EDTA, which

chelates the Mg^{2+} ions. Subsequently, 10 µl Formamide dye (deionized formamide solution, 50 mg/ml xylene cyanol, 50 mg/ml Bromophenol blue, and 10 mM EDTA) was added to the stopped reaction, and the samples were boiled for 2 minutes at 90°C before loading onto a sequencing gel. In addition, the experiment involving the NCP was conducted the same way except that 1) the NCP concentration was at 0.28 µM; 2) the Piccolo NuA4 complex in the reaction was 0, 0.28, 0.84, or 2.8 µM, and 3) the amount of the DNase I enzyme was 1.0 Unit per reaction.

The sequencing gel (8% of 20:1 acrylamide: bis-acrylamide, 1x TBE, and 8 M Urea) in a 21 x 50 cm Sequi-Gen GT (Bio-Rad), using 0.25 mm spacers and a regular comb was pre-electrophoresed at 40 Watts for 45 minutes. The electrophoresis of the samples was performed at 40 Watts for 2 hours and 30 minutes. The gel was fixed with a fix solution (10% acetic acid and 10% methanol) for 15 minutes, and dried to completeness for 2 hours at 90°C. Dried gel was exposed to a Phosphorimager cassette (Molecular Dynamics) for at least 3-4 hours or over night. The screen was scanned with the Typhoon 8600 (Molecular Dynamics) and the scanned image was analyzed with the ImageQuant 5.2 program.

C.4.7 Gel shift analysis

A 10-µl aliquot of the reaction mixture of each sample was mixed with 2 µl of 30% sucrose and loaded onto a 5% native polyacrylamide gel, which was previously electrophoresed at 10 Watts for 20 minutes. The gel electrophoresis of the sample was performed at 5 Watts for 10 minutes. The gel was fixed in a fix solution (45% ethanol and 10% acetic acid) and subsequently dried for 1 hour at 90°C before exposing to an X-ray film.

C.4.8 Labeling a primer with the γ-^{32}P ATP

A reverse primer, STO1805 (5'- TACATGCACAGGATGTATATATCTG-3'), used for amplifying the 601.2 nuleosomal DNA sequence (See **C.4.9**), was subjected to radiolabeling with the γ-^{32}P ATP. The 100-µl labeling reaction mixture (1x T4 PNK buffer, 5 mM DTT, 1 µM STO1805, 50 µCi γ-^{32}P ATP, and 25 Units T4 Polynucleotide kinase (BioLabs)) was incubated at 37°C for 30 minutes. After incubation, the primer was purified with two extractions of the Phenol/CIA mixture, one extraction with the CIA, and with a Sephadex G-25 Medium (Amersham Pharmacia Biotech) spun column.

C.4.9 PCR mediated radiolabeling of the 601.2 nucleosomal DNA sequence

Eight different plasmids (pGem-3Z dyad 0 to pGem-3Z dyad -7) that carry the modified 601.2 nucleosomal DNA sequence, which has a HaeIII site introduced by PCR mutagenesis, were gifts from Dr. Andrew Travers, the MRC Laboratory of Molecular Biology, UK (Wu and Travers, 2004). The numbering of the plasmids (0 to -7) describes the position of the helical turns of the HaeIII site from the dyad. The original synthetic 601.2 is shown below:

5'-GGACCCTATACGCGGCCGCCCTGGAGAATCCCGGTGCCGAG
GCCGCTCAATTGGTCGTAGCAAGCTCTAGCACCGCTTAAACGC
ACGTACGCGCTGTCCCCCGCGTTTTAACCGCCAAGGGGATTACT
CCCTAGTCTCCAGGCACGTGTCAGATATATACATCCTGTGCATG
TA-3'

The modified 601.2 nucleosomal DNA sequence that contains the HaeIII site (bold and underlined) at different location is represented below:

5'-GGACCCTATACGCGGCCGCC**<u>GGCC</u>**$_{(-7)}$AGAAGC**<u>GGCC</u>**$_{(-6)}$TC
CCGG**<u>GGCC</u>**$_{(-5)}$GCTCAA**<u>GGCC</u>**$_{(-4)}$TCGTAG**<u>GGCC</u>**$_{(-3)}$CTCTGG
<u>GGCC</u>$_{(-2)}$GCTTGA**<u>GGCC</u>**$_{(-1)}$ACGTACG**<u>GGCC</u>**$_{(0)}$GTCCCCCGCGTTT
TAACCGCCAAGGGGATTACTCCCTAGTCTCCAGGCACGTGTCA
GATATATACATCCTGTGCATGTA-3'

All eight plasmids at approximately 10 ng/µl each were mixed and used for the PCR reactions with STO1804 (5'-GGACCCTATACGCGGCCGCCC-3') and radiolabeled STO1805 (5'- TACATGCACAGGATGTATATATCTG-3') to amplify and radiolabel the modified 601.2 nucleosomal DNA sequences. A 100-µl PCR reaction contained 1x Thermopol buffer (Bio-Labs), 250 mM dNTP, 1 µl of the mixed plasmid, 0.05 µM STO1804, 0.03 µM radiolabeled STO1805, 25 µM $MgSO_4$, and 1 Unit Vent DNA polymerase (Bio-Labs). The reaction was performed with 26 cycles of a 95°C, 30-second denaturing step, a 55°C, 30-second annealing step, and a 75°C, 25-second extension step. The PCR product was purified with two extractions of the Phenol/CIA mixture, one extraction with the CIA, and with a Sephadex G-25 Medium (Amersham Pharmacia Biotech) spun column. After purification, the PCR product was analyzed with a 5% native polyacrylamide gel using the same procedures described in **C.4.4**.

C.4.10 Nucleosome reconstitution with the radiolabeled 601.2 nucleosomal DNA

Since the labeling procedure of the 601.2 DNA sequence was performed with the PCR reaction, the amount of the DNA obtained was not sufficient for nucleosome reconstitution. Thus, to reconstitute nucleosomes with the radiolabeled 601.2 DNA, cold (unlabeled) DNA from another source was included together with the labeled DNA in the reconstitution reaction. A 100-µl reconstitution mixture and the nucleosome reconstitution procedures were similar to the procedures described in "nucleosome reconstitution" except that 10 µl of the radiolabeled PCR product and 3 µM unlabeled 147-basepair NucB DNA were included in the reaction mixture. The product of the nucleosome reconstitution was analyzed with a 5% native polyacrylamide gel.

C.4.9 'One-pot' assay

This protocol was adapted from the literature (Wu and Travers, 2004). The procedures for the 'One-pot' assay were similar to that described for the DNase I footprinting experiment, except that the reaction required the HaeIII restriction enzyme instead of the DNase I endonuclease. Like the DNase I footprinting experiment, the 'One-pot' assay was performed with either the free DNA, the free DNA incubated with a titration of the Piccolo NuA4 complex, the NCP by itself, or the NCP incubated with a titration of the Piccolo NuA4 complex. Because the nucleosome reconstitution product contains both labeled and unlabeled DNA, the free DNA sets in the 'One-pot' assay should contain the same amount of the labeled versus unlabeled DNA. The 'One-pot' assay for free DNA and NCP was conducted as follows. 1 µM of the DNA mixture or the NCP (refers to the concentration of the cold DNA or nucleosomes, and assumes a low concentration of the Hot, radiolabeled DNA or nucleosomes) was incubated with the Piccolo NuA4 complex at the concentration of 0, 1, 3, or 6 µM in a 22.5 µl reaction mixture containing 1x NEBuffer 2 (Bio-Labs), 50 mM NaCl, and 20 µg/ml BSA. The incubation was performed at room temperature for 30 minutes. After incubation, 1 µl of the 50 Units/µl HaeIII restriction enzyme was added to a 9-µl aliquot of the reaction mixture to allow the DNA digestion by the HaeIII enzyme. The rest of the reaction mixture was used for a gel shift assay (**C.4.7**). The digestion was performed at room temperature for 10 minutes and was terminated by the addition of 50 mM EDTA. 10 µl Formamide dye was added to each sample, which was subsequently boiled for 2 minutes at 90°C. The samples were analyzed with a 6% denaturing polyacrylamide gel (6% of 20:1 acrylamide: bis-acrylamide, 0.5x TBE, and 8 M urea) in a Protean II xi Cell (Bio-Rad)), which was pre-electrophoresed at 20 watts for 30 minutes. The actual electrophoresis of the samples was performed at 12 watts for 60 to 65 minutes. The gel was fixed with a fix solution (10% methanol and 10% acetic acid), and subsequently dried for 2 hours at 90°C. Dried gel was exposed to a Phosphorimager cassette (Molecular Dynamics) for 3-4 hours or over night. The screen was scanned with the Typhoon 8600 (Molecular Dynamics) and the scanned image was processed with the ImageQuant 5.2.

C.5 Bibliography

Allard, S., Utley, R. T., Savard, J., Clarke, A., Grant, P., Brandl, C. J., Pillus, L., Workman, J. L., and Cote, J. (1999). NuA4, an essential transcription adaptor/histone H4 acetyltransferase complex containing Esa1p and the ATM-related cofactor Tra1p. Embo J *18*, 5108-5119.

Anderson, J. D., Thastrom, A., and Widom, J. (2002). Spontaneous access of proteins to buried nucleosomal DNA target sites occurs via a mechanism that is distinct from nucleosome translocation. Mol Cell Biol *22*, 7147-7157.

Boudreault, A. A., Cronier, D., Selleck, W., Lacoste, N., Utley, R. T., Allard, S., Savard, J., Lane, W. S., Tan, S., and Cote, J. (2003). Yeast enhancer of polycomb defines global Esa1-dependent acetylation of chromatin. Genes Dev *17*, 1415-1428.

Clarke, A. S., Lowell, J. E., Jacobson, S. J., and Pillus, L. (1999). Esa1p is an essential histone acetyltransferase required for cell cycle progression. Mol Cell Biol *19*, 2515-2526.

Davey, C. A., Sargent, D. F., Luger, K., Maeder, A. W., and Richmond, T. J. (2002). Solvent mediated interactions in the structure of the nucleosome core particle at 1.9 a resolution. J Mol Biol *319*, 1097-1113.

Feng, K., Mahdavi-Anary, F., Partch, R. E., and Li, Y. (1995). Photochemical reactions of azidocoumarins. Photochem Photobiol *62*, 813-817.

Garkavtsev, I., Grigorian, I. A., Ossovskaya, V. S., Chernov, M. V., Chumakov, P. M., and Gudkov, A. V. (1998). The candidate tumour suppressor p33ING1 cooperates with p53 in cell growth control. Nature *391*, 295-298.

Jacobs, S. A., and Khorasanizadeh, S. (2002). Structure of HP1 chromodomain bound to a lysine 9-methylated histone H3 tail. Science *295*, 2080-2083.

Loewith, R., Meijer, M., Lees-Miller, S. P., Riabowol, K., and Young, D. (2000). Three yeast proteins related to the human candidate tumor suppressor p33(ING1) are associated with histone acetyltransferase activities. Mol Cell Biol *20*, 3807-3816.

Luger, K., Mader, A. W., Richmond, R. K., Sargent, D. F., and Richmond, T. J. (1997). Crystal structure of the nucleosome core particle at 2.8 A resolution. Nature *389*, 251-260.

Luger, K., Rechsteiner, T. J., and Richmond, T. J. (1999). Expression and purification of recombinant histones and nucleosome reconstitution. Methods Mol Biol *119*, 1-16.

Marcus, G. A., Silverman, N., Berger, S. L., Horiuchi, J., and Guarente, L. (1994). Functional similarity and physical association between GCN5 and ADA2: putative transcriptional adaptors. Embo J *13*, 4807-4815.

Maxam, A. M., and Gilbert, W. (1980). Sequencing end-labeled DNA with base-specific chemical cleavages. Methods Enzymol *65*, 499-560.

Ornaghi, P., Ballario, P., Lena, A. M., Gonzalez, A., and Filetici, P. (1999). The bromodomain of Gcn5p interacts in vitro with specific residues in the N terminus of histone H4. J Mol Biol *287*, 1-7.

Perlmann, T., and Wrange, O. (1988). Specific glucocorticoid receptor binding to DNA reconstituted in a nucleosome. Embo J *7*, 3073-3079.

Prunell, A., Kornberg, R. D., Lutter, L., Klug, A., Levitt, M., and Crick, F. H. (1979). Periodicity of deoxyribonuclease I digestion of chromatin. Science *204*, 855-858.

Sanger, F., and Coulson, A. R. (1975). A rapid method for determining sequences in DNA by primed synthesis with DNA polymerase. J Mol Biol *94*, 441-448.

Selleck, W., Fortin, I., Sermwittayawong, D., Cote, J., and Tan, S. (2005). The Saccharomyces cerevisiae Piccolo NuA4 histone acetyltransferase complex requires the Enhancer of Polycomb A domain and chromodomain to acetylate nucleosomes. Mol Cell Biol *25*, 5535-5542.

Sinclair, D. A., Clegg, N. J., Antonchuk, J., Milne, T. A., Stankunas, K., Ruse, C., Grigliatti, T. A., Kassis, J. A., and Brock, H. W. (1998). Enhancer of Polycomb is a suppressor of position-effect variegation in Drosophila melanogaster. Genetics *148*, 211-220.

Stankunas, K., Berger, J., Ruse, C., Sinclair, D. A., Randazzo, F., and Brock, H. W. (1998). The enhancer of polycomb gene of Drosophila encodes a chromatin protein conserved in yeast and mammals. Development *125*, 4055-4066.

Suck, D., Lahm, A., and Oefner, C. (1988). Structure refined to 2A of a nicked DNA octanucleotide complex with DNase I. Nature *332*, 464-468.

Wu, C., and Travers, A. (2004). A 'one-pot' assay for the accessibility of DNA in a nucleosome core particle. Nucleic Acids Res *32*, e122.

VITA

Decha Sermwittayawong

Education

Ph.D. in Biochemistry, Microbiology, and Molecular Biology. The Pennsylvania State University (PSU), August 2006

B.A. in Molecular, Cellular, and Developmental Biology with *Magna Cum Laude*. The University of Colorado at Boulder (CU Boulder)

Publications

Sermwittayawong, D and Tan, S. SAGA binds TBP via its Spt8 subunit in competition with DNA: a handoff model for SAGA recruitment of TBP to the core promoter (accepted).

Selleck, W., Fortin, I., **Sermwittayawong, D**., Cote, J., and Tan, S. (2005). The Saccharomyces cerevisiae Piccolo NuA4 histone acetyltransferase complex requires the Enhancer of Polycomb A domain and chromodomain to acetylate nucleosomes. Mol Cell Biol 25, 5535-5542.

Presentations

Sermwittayawong, D and Tan, S. Identification of TBP interacting subunits in the yeast SAGA coactivator HAT complex. Poster. Cold Spring Harbor Laboratory: Mechanisms of Eukaryotic Transcription, August 31st-September 4th, 2005

Sermwittayawong, D and Tan, S. Transcriptional regulation in yeast: How SAGA coactivator complex recruits TATA-binding protein (TBP). Poster. 20th Graduate Exhibition, The Pennsylvania State University, March 20th, 2005

Honors and awards

2005 Paulberg Travel Fund, Dept. of Biochem. & Mol. Biol., PSU.
2001 Honorable mention for the Althouse Outstanding TA Teaching Award, Dept. of Biochem. & Mol. Biol., PSU
2000 Braddock Graduate Fellowship, Dept. of Biochem. & Mol. Biol., PSU